



HAL
open science

Nonperturbative renormalization group approach to polymerized membranes

Karim Essafi

► **To cite this version:**

Karim Essafi. Nonperturbative renormalization group approach to polymerized membranes. Chemical Physics [physics.chem-ph]. Université Pierre et Marie Curie - Paris VI, 2012. English. NNT : 2012PAO66501 . tel-00828639

HAL Id: tel-00828639

<https://theses.hal.science/tel-00828639>

Submitted on 31 May 2013

HAL is a multi-disciplinary open access archive for the deposit and dissemination of scientific research documents, whether they are published or not. The documents may come from teaching and research institutions in France or abroad, or from public or private research centers.

L'archive ouverte pluridisciplinaire **HAL**, est destinée au dépôt et à la diffusion de documents scientifiques de niveau recherche, publiés ou non, émanant des établissements d'enseignement et de recherche français ou étrangers, des laboratoires publics ou privés.

*Nonperturbative Renormalization Group Approach to
Polymerized Membranes*

by

Karim Essafi

Thesis presented in fulfilment of
the degree of Doctor in Theoretical Physics
of the University Pierre & Marie Curie

Doctoral supervisor: **Dominique Mouhanna**

Laboratoire de Physique Théorique de la Matière Condensée
Ecole Doctorale de Physique de la Région Parisienne

November 16th 2012

Jury:

Prof. Vladimir Dotsenko	(Examineur)
Prof. Nils Hasselmann	(Examineur)
Prof. Malte Henkel	(Rapporteur)
Prof. Dominique Mouhanna	(Directeur)
Prof. Gunnar Pruessner	(Rapporteur)

"All too often in physics familiarity is a substitute for understanding"

Analysis, Manifolds and Physics, Y. Choquet-Bruhat, C. DeWitt-Morette, M. Dillard-Bleick

Abstract

In this thesis, we study the long-range behaviour of polymerized membranes using a non-perturbative renormalization group (NPRG) approach. We start by presenting the NPRG after which we introduce membranes systems.

In our work, we concentrate on polymerized membranes of different types: homogeneous, anisotropic and quench disordered. Moreover as a side project, we work on Lifshitz critical behaviour (LCB) in magnetic systems. Our results, both for polymerized membranes and LCB, compare well with weak-coupling, low-temperature and large- d (or large- n for LCB) perturbative results in the limiting cases. But more importantly the need of a non-perturbative approach is justified by the fact that the physically interesting have been difficult to compute.

A long-standing question in homogeneous membranes is the order of the transition between the crumpled and flat phases. Although we do not have a definite answer, our results seem to indicate that the transition is first order in agreement with recent Monte Carlo simulations. An interesting feature of homogeneous membranes is the existence of the flat phase at low-temperature with a non-trivial behaviour. This flat phase has shown to correctly describe the behaviour of graphene although the electronic degrees of freedom are not taken into account. Another long-standing problem is the negative value of the anomalous dimension for anisotropic membranes at the crumpled-tubule transition. This negativeness is in contradiction with what is expected from physical grounds. This problem is solved in our approach and we obtain a positive anomalous dimension.

In LCB, huge technical difficulties due to the anisotropy has plagued the perturbative approaches and limit their computations to lowest order. We show that our approach is free of these difficulties and being systematically improvable we can control the convergence of successive approximations and thus to get reliable physical quantities in $d = 3$ for Heisenberg spins $n = 3$.

: Membranes; Non-perturbative renormalization group; Phase transitions; Symmetry breaking; Geometry; Anisotropic scale invariance; Lifshitz critical behaviour; Quench disorder.

Résumé

Dans cette thèse, nous étudions le comportement à longue distance des membranes polymérisées en utilisant une approche de groupe de renormalisation non-perturbative (NPRG). Après une présentation du NPRG, nous introduisons les membranes.

Dans notre travail, nous nous concentrons sur différents types de membranes polymérisées: homogène, anisotrope et avec du désordre gelé. De plus, nous avons aussi étudié les points de Lifshitz dans les systèmes magnétiques. Nos résultats, aussi bien pour les membranes que pour Lifshitz, se comparent bien aux résultats perturbatifs dans les différents cas limites: couplages faibles, basse température et large- d (ou large- n pour Lifshitz). Mais, en utilisant le NPRG, nous pouvons aller au-delà de ces cas limites et atteindre les cas qui sont physiquement intéressants.

La question de l'ordre de la transition entre la phase froissée et la phase plate dans les membranes homogènes est depuis longtemps sans une réponse définitive. Malgré que nos résultats ne permettent pas encore de lever cette question, ils semblent indiquer que la transition est du premier ordre en accord avec des simulations récentes. Une propriété importante des membranes polymérisées est l'existence d'une phase plate à basse température avec un comportement non-trivial. Cette phase décrit correctement le comportement du graphène malgré que les degrés de liberté électroniques ne soient pas pris en compte. Une autre problématique qui date depuis de nombreuses années est celui de la valeur négative de la dimension anormale dans les membranes anisotropes dans la transition entre la phase froissée et la phase tubulaire. Cette valeur négative est en contradiction avec les arguments physiques. Dans notre approche de NPRG, nous parvenons à résoudre ce problème et nous obtenons une dimension anormale positive.

Dans les systèmes de Lifshitz, les approches perturbatives se sont confrontées à de grandes difficultés à cause de l'anisotropie et ceci à limiter les calculs aux plus bas ordres. Nous montrons que notre approche est libre de ces difficultés et étant améliorable de façon systématique nous pouvons contrôler la convergence et obtenir des résultats satisfaisants en $d = 3$ pour les spins de Heisenberg $n = 3$.

: Membranes; Groupe de renormalisation non-perturbative; Transitions de phase; Brisure de symétrie; Géométrie; Invariance d'échelle anisotrope; Comportement critique de Lifshitz; Désordre trempé.

Acknowledgements

First I would like to thank my PhD advisor, Dominique Mouhanna, for giving me the chance to work with him on this interesting subject. I have learned many things from him both on the technical and physical aspects. I would also like to thank Jean-Philippe Kownacki with whom I have collaborated during these three years.

I would like to thank Malte Henkel and Gunnar Pruessner who have accepted to write a report on my thesis. And I also thank Vladimir Dotsenko and Nils Hasselmann for being part of my jury.

I would like to thank all the members of the LPTMC and its director Pascal Viot. It has been a pleasure to work in this lab. The discussions during the coffee and lunch breaks have always been pleasure. A special thanks to the administrative staff of the lab Sylvie Dalla-Foglia, Liliane Cruzel and Diane Domand who have always been helpful.

I am also grateful to Julien Vidal for his help with mathematica and his advice in general. I also would like to thank all the persons that have given me advice and with whom I had some nice discussions during these three years: Claude Aslangul, Nicolas Sator, Jean-Marie Maillard, Bertrand Delamotte, Mathieu Tissier, Rémy Mosseri, Richard Kerner, Annie Lemarchand, H el ene Berthoumieux, Jean-Marc Victor, Philippe Sindzingre...

A great thanks to all the members of the study group on NPRG: Bertrand Delamotte, Nicolas Dupuis, Mathieu Tissier, Gilles Tarjus, Maxime Baczyk, Federico Benitez, Damien Gredat, Adam Rancon. I would particularly want to thank Bertrand who has always been available when I had any question oh physics in general and on the renormalization group in particular.

During these three years, I had the chance to teach with Claude Aslangul and Jean-Bernard Zuber. It was really a pleasure to work with them and to learn from their experience. I would like to thank them as well as the rest of the teaching staff.

I would like to thank all the youngsters of the lab for some very pleasant discussions: Pascal Carrivain, Michael Kamfor, Marc Schulz, Jean-Fran ois Rupprecht, Jules Morand, Axel Cournac and Fabien Paillusson.

I would like to thank all my friends and particularly those with whom I have studied physics at the university: Maxime Goguet, Emmanuel Jolibois, Demian Levis and Charles-Alexandre Marillier.

Last but not least, I would like to thank all my whole family for encouraging me during my studies. Most importantly I would like to thank my wife St ephanie who has always been present by my side and who has encouraged me during all these years.

Contents

Abstract	ii
Acknowledgements	v
Chapter 1 Introduction	I
Chapter 2 Non-Perturbative Renormalization Group	5
2.1 A Brief Historical Introduction	5
2.2 Wilson Renormalization Group	7
2.2.1 Kadanoff's Block Spin	7
2.2.2 Wilson Momentum Shell Integration	10
2.2.3 Polchinski and Proof of Renormalizability	12
2.3 Wetterich Renormalization Group	13
2.3.1 Effective Average Action	13
2.3.2 The Wetterich Equation	17
2.3.3 Approximations	21
2.3.3.1 Derivative Expansion	22
2.3.3.2 Field Expansion	23
2.3.3.3 Combination of the Derivative Expansion and the Field Expansion	23
2.3.3.4 Blaizot-Mendez-Wschebor Approximation	24
2.3.4 Optimisation and Cut-off Function Choice	25
2.3.5 The $O(n)$ -model	27
2.3.5.1 Propagator	28
2.3.5.2 Definitions of the Coupling Constants	28

2.3.5.3	Derivation of the Flow Equations	29
2.3.5.4	Weak-coupling Expansion	31
2.3.5.5	Low-Temperature Expansion	33
2.3.5.6	Large- n Expansion	34
2.3.6	Conclusion	35
Appendix Chapter A Threshold Functions		37
Chapter 3 Membranes		39
3.1	Introduction	39
3.2	Differential Geometry of Membranes	50
3.2.1	Basic Definitions and Some Fundamental Properties	50
3.2.2	Monge Parametrization	59
3.3	Deformations	61
3.4	Long-Range Behaviour of Fluid Membranes	61
3.4.1	The Model	61
3.4.2	Fluid Membranes in Monge Parametrization	64
3.5	Polymerized Membranes	65
3.5.1	The Model	65
3.5.2	Mean Field Theory	67
3.5.3	Perturbative RG for the Crumpled-to-Flat Transition	69
3.5.4	The normal-normal Correlation Function in the Harmonic Approx- imation	69
3.5.5	Self-Consistent Screening Approximation (SCSA)	72
3.5.6	Conclusion	75
3.6	NPRG Approach to Polymerized Membranes	76
3.6.1	The propagator in Fourier Space	78
3.6.2	The Minimum Configuration ζ	80
3.6.3	The Flow Equations of u and v and the Anomalous Dimension η_k	82
3.6.4	Derivation of the Flow Equations	85
3.6.4.1	The Effective Action	85
3.6.4.2	The Configuration Λ	87
3.6.4.3	Propagator at the minimum	91
3.6.4.4	Flow Equations of u and v	94
3.6.4.5	Flow of ζ^2	96

3.6.4.6	Definitions of the Coupling Constants	97
3.6.5	Crumpled to Flat Transition	99
3.6.6	Symmetry Breaking, Goldstone Bosons and Flat Phase	100
3.7	Conclusion	105
Appendix Chapter B	Cayley-Hamilton Theorem and Faddeev-Leverrier Algorithm	107
Appendix Chapter C	Derivatives of the Flow of U_{eff}	111
C.1	Derivative of the Propagator	113
Appendix Chapter D	New Definition of the Minimum Configuration ζ	115
Appendix Chapter E	Threshold Functions	119
Chapter 4	Anisotropic Membranes	121
4.1	Introduction	121
4.2	Anisotropic Scaling Behaviour	122
4.3	Perturbative RG	124
4.4	Non-Perturbative Approach	125
4.4.1	The propagator	126
4.4.2	Flow equation of ζ_y	127
4.4.3	Flow equations	128
4.5	Physical Results	130
4.6	Conclusion	132
Appendix Chapter F	Threshold Functions	135
Chapter 5	Lifshitz Critical Behaviour	137
5.1	Introduction	137
5.2	The Model	138
5.3	Anisotropic Scale Invariance	140
5.4	Critical Dimensions	142
5.5	Perturbative RG	142
5.5.1	Weak-Coupling ϵ -Expansion	142
5.5.2	Large- n Expansion	144
5.6	NPRG Approach	145

5.6.1	Lowest Order of the Derivative Expansion	145
5.6.2	Flow Equations	146
5.6.3	Upper Critical Dimension $d_{uc} = 4 + \frac{m}{2}$	148
5.6.4	Lower Critical Dimension $d_{lc} = 2 + \frac{m}{2}$	151
5.7	Higher Order Expansion and Physical Results	155
5.8	Conclusion	158
Appendix Chapter G Threshold Functions		161
Chapter 6 Disordered Membranes		163
6.1	Introduction	163
6.2	Replica Formalism	163
6.3	The Model	165
6.4	Perturbative RG	168
6.5	NPRG	170
6.5.1	Effective Action	170
6.5.2	Propagator	171
6.5.3	Flow Equations	174
6.5.4	Conclusion	179
Conclusion		181

I would like to dedicate this thesis to my loving parents ...
to my brothers, Soufian and Samir...
and to my wife Stéphanie

Chapter 1

Introduction

A scientific truth does not triumph by convincing its opponents and making them see the light, but rather because its opponents eventually die and a new generation grows up that is familiar with it.

Max Planck (1948)

A key concept in physics is that of *phase transition*. A phase transition is an abrupt change in the macroscopic behaviour of a system. It is a phenomenon present in different areas of physics such as condensed matter, particle physics or cosmology.

An example of phase transition that one observes in everyday life is when water is heated to 100°C. At this temperature and at atmospheric pressure the water boils and changes its state from liquid to gas. Moreover at a certain *critical temperature* and pressure the water starts to look milky and the distinction between liquid and gas states becomes impossible. At this *critical point* fluctuations are present at all length scales which means that the characteristic scale called the *correlation length* ξ diverges and as a consequence light is strongly scattered. This phenomenon is called *critical opalescence*. It was first observed by the French physicist Charles Cagniard de la Tour in 1822 [2, 3, 4] while working on alcohol in a sealed glass cell. The term *critical point* was introduced by the Irish chemist and physicist Thomas Andrews in 1869 when he observed critical opalescence in carbon dioxide at 31°C and 73 atmospheres pressure [1].

Although the observation that matter can change state has been known for centuries, our understanding of the mechanism behind this phenomena was lacking until the end of nineteenth century and the works of Maxwell and Boltzmann. The description of collective phenomena using statistical physics has brought great insight to our understanding of phase transitions and critical phenomena. All the properties of a system can be obtained from the partition function or its logarithm the free energy. For a finite system, the free energy is always an analytic function. As a consequence a singularity in the free energy can only appear at the thermodynamic limit, *i.e.* for infinite systems.

From this simple example of water phase transition one can see that there are two types of transitions. First-order transitions, such as the usual liquid-gas transition, where the correlation length ξ remains finite and the fluctuations are of order ξ^d where d is the space dimension. The other type called second-order, or more exactly continuous, transitions occur at a critical point and the correlation length diverges.

The divergence of the correlation length ξ is the signature that an infinite number of degrees of freedom are in interaction which leads to scale invariance. The consequence of scale invariance can be seen on the two-point correlation function $\langle \phi(r)\phi(0) \rangle = G(r)$:

$$G(r) = \frac{e^{-r/\xi}}{r^\lambda} \quad (1.1)$$

where λ is a power that depends on the system under study. At criticality the correlation length diverges and as a consequence one obtains a power-law behaviour for the correlation function:

$$G(r) \sim \frac{1}{r^\lambda}. \quad (1.2)$$

Other physical quantities such as the heat capacity C or the magnetization M will also obey power laws: $C \propto |T - T_c|^{-\alpha}$ and $M \propto |T - T_c|^{-\beta}$ where T_c is the critical temperature and α and β are called the *critical exponents*. Moreover completely different systems can have the exact same value for the critical exponents. This is the phenomenon of *universality* and the systems are said to belong to the same universality class. Each universality class, except when marginal operators are present, is determined by the space dimension, the symmetries of the system and the range of the interactions.

The presence of an infinite number of interacting degrees of freedom makes the study of critical phenomena very difficult and almost impossible by analytical methods except in some

special cases like the Onsager solution for the two-dimensional Ising model. New mathematical methods had to be developed. Kadanoff proposed a way of integrating of the degrees of freedom step by step. This idea was later enriched by Wilson and led to the renormalization group in critical phenomena. This approach brought new insight to phase transitions and critical phenomena. It led to important results such as solving the Kondo problem and the computation of the critical exponents for various different systems. However although Wilson derived an exact flow equation it has been mainly used in perturbative expansions which is not satisfying when the couplings are not small or when the phenomena is genuinely non-perturbative. A new non-perturbative approach based on Kadanoff's and Wilson's has been formulated by Wetterich in the early nineties which does not rely on the smallness of a coupling. This non-perturbative renormalization group offers a more adapted theoretical approach to critical phenomena far from the *upper critical dimension* which is the dimension above which mean field theory is exact. Moreover it gives a direct connection to the usual perturbative approaches such as the weak-coupling, the low-temperature and large- d expansions.

In this thesis we present our work on the statistical physics of polymerized membranes. These systems are fascinating both theoretically and experimentally and they have wide range of applications. Before presenting membranes and their thermodynamical behaviour, we start by introducing the non-perturbative renormalization group which is the approach we have used in our work. Then in the third chapter we present our work on homogeneous polymerized membranes and in the following chapter we see how the behaviour of the membranes changes when modifications are made on its homogeneity: inclusion of anisotropy and disorder.

Chapter 2

Non-Perturbative Renormalization Group

I would say that mathematics is the science of skilful operations with concepts and rules invented just for this purpose. The principal emphasis is on the invention of concepts.

Eugene P. Wigner (1959)

2.1 A Brief Historical Introduction

In modern theoretical physics the *renormalization group* occupies a central role in our understanding of physical phenomena where many degrees of freedom interact. Before discussing the technical aspects of the renormalization group (RG), I will start by a small historical introduction of the RG (see [5, Part VII] for an interesting discussion on the ideas underlying the RG).

The need for renormalization arose from the problem of infinities encountered in field theory in the formal computation of observable quantities. The problem of infinities is not new to modern physics. It is already present in classical electrodynamics in J. J. Thomson's

model of the electron when taking the limit of vanishing radius a in the electric field E :

$$E = \frac{e^2}{2a} \xrightarrow{a \rightarrow 0} \infty. \quad (2.1)$$

But if a stays finite one obtains an unstable configuration. Poincaré's suggestion to solve this problem is the existence of a non-electromagnetic energy that compensates the Coulomb force and stabilizes the electron. This idea inspired others such as Ernst Stückelberg (1938), Fritz Bopp (1940), Abraham Pais (1945), Shoichi Sakata (1947) for their study of the problem of the electron self-energy.

In the hydrogen atom the orbitals $S_{1/2}$ and $P_{1/2}$ should be degenerate, *i.e.* have the same energy, according to the Dirac equation. But an experimental measurement in 1947 by Willis Lamb and Robert Retherford showed that there is an energy shift between the two levels. This shift is due to quantum *fluctuations* which are induced by the interaction of the electron with the electromagnetic field of the vacuum which is ignored by the Dirac equation. Theoretically these fluctuations lead to divergences. Including this interaction as a perturbation of the hydrogen theory leads to a divergent Lamb shift. To solve this problem Hans Bethe introduced an upper limit to the energy equal to the electron mass, or precisely equal to $m_e c^2$, for the integral involved in the Lamb shift calculation to suppress the shift of the free electron. The interpretation of this trick is that the observable mass is different from the “bare mass” the electron would have if there were no fluctuations. This was the beginning of the *renormalization*. However the renormalization group as we know it today started with the works of Stückelberg & Petermann [6] and Gell-Mann & Low [7]. The starting point was the idea that physical parameters should depend on the energy scale in quantum field theory whereas physics is scale independent as suggested by Freeman Dyson in 1951 [8]. Stückelberg & Petermann [6] introduced a group transformation to suppress the divergences in particle physics by transforming the physical quantities from bare to renormalized ones. This group transformation shows that the physics is self-similar when the scale is changed. Independently, Gell-Mann & Low developed a similar approach and they derived a differential equation with respect to the energy scale for the interaction coupling, the fine-structure constant α in quantum electrodynamics (QED).

In critical phenomena the divergences have their origin in the existence of thermal fluctuations at all length scales which are the classical counterpart of quantum fluctuations. Near a critical point the size of the fluctuations is proportional to the correlation length up to some

power: $\sim \xi^d$ where d is the space dimension. And at the critical point the correlation length diverges ($\xi \rightarrow \infty$) which leads to an infinite number of interacting degrees of freedom. To reduce the number of degrees of freedom Kadanoff introduced a scale transformation called block spin technique which leads to *scaling laws*. The Kadanoff transformation maps the Hamiltonian to an effective Hamiltonian at a different scale. While working on continuous phase transitions Wilson implemented in an infinitesimal manner the Kadanoff idea of eliminating degrees of freedom. This led to the derivation of an evolution equation for the Hamiltonian which can have a *fixed-point*. The existence of a fixed-point was the missing link to the explanation why different systems had the same critical exponents at a second order phase transition which is the signature of *universality*, *i.e.* different systems described by the same critical behaviour.

The renormalization group has shown to be a powerful method for dealing with some very difficult problems in statistical and quantum field theory such as quantum electrodynamics, the unification of electromagnetic and weak interactions, the Kondo problem or second order phase transition. Albeit the Wilson RG is non-perturbative, for a long time it has shown to be hard to implement in a non-perturbative manner. Several attempts to overcome the technical difficulties of the Wilson RG were unsuccessful until the mid 90's with the approach of Wetterich which I present in this chapter.

2.2 Wilson Renormalization Group

The Wilsonian RG is a classic in modern lectures in theoretical physics (see [9, 10, 11, 12]). Nevertheless, we recall the basic concepts and ideas of this technique essentially because it serves as a basis for the non-perturbative renormalization group as implemented by Wetterich [13].

2.2.1 Kadanoff's Block Spin

The starting point of the renormalization group is the block spin idea introduced by Leo Kadanoff [14] to eliminate degrees of freedom of small length scales. The Kadanoff transformation consists in dividing the system into blocks and doing a local average (*coarse-graining*). Kadanoff's idea arises from the fact that since the correlation length is very large near the critical point, neighbouring spins are strongly correlated and one can locally average over them and obtain effective spins.

In his seminal paper, Leo Kadanoff [14] was the first to see the connection between rescaling and scaling properties of a critical point. Kadanoff proved the existence of the scaling laws postulated by Benjamin Widom and others [15]. Although the block spin idea was introduced independently by Buckingham a year earlier, Kadanoff was the first to introduce a practical computational scheme.

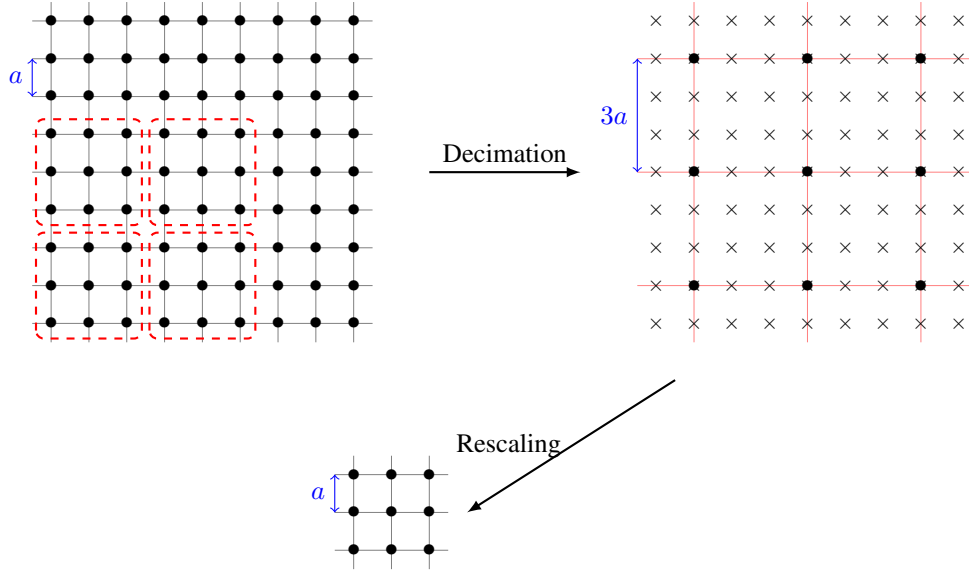


FIGURE 2.1: Kadanoff bloc spin procedure. As an example in this figure, we take a square lattice with Ising spins $S_i = \pm 1$ and lattice spacing a . The initial lattice is divided into blocks of size 9 ($b = 3$ and $d = 2$ in the figure). After the first transformation, we end up with a new square lattice but with a lattice spacing $3a$ and a effective spin S_A that is the average of the previous 9 spins. And to recover the original lattice, we must perform a rescaling: $3a \rightarrow a$.

As an example we take an Ising spin system on a two-dimensional lattice (see fig. 2.1). The partition function which encode the thermodynamical behaviour reads:

$$\mathcal{Z} = \sum_{\{S_i\}} e^{-\beta\mathcal{H}[S_i]} \quad (2.2)$$

where $\beta = 1/(k_B T)$, with k_B the Boltzmann constant and T the temperature. Starting with a lattice size a , we divide it into blocks of size b^d where d is the space dimension (here

$d = 2$) and b the *spatial rescaling factor*. Then we average out the spins of each block. The new system has N/b^d sites and a new lattice size ba . To recover the initial lattice, we must perform a rescaling $ba \rightarrow a$:

$$S_A = b^{-d} \sum_{i \in A} S_i \quad (2.3)$$

where S_A is the average value of the spins in the block A . After summing over the spins in a block one obtains an effective Hamiltonian related to the original one by:

$$e^{-\mathcal{H}_{\text{eff}}[S_A]} = \sum_{\{S_i\}} \prod_A \delta \left(S_A - b^{-d} \sum_{i \in A} S_i \right) e^{-\mathcal{H}[S_i]} \quad (2.4)$$

with:

$$\sum_{\{S_A\}} \prod_A \delta \left(S_A - b^{-d} \sum_{i \in A} S_i \right) = 1 \quad (2.5)$$

which keeps the partition function unchanged:

$$\mathcal{Z} = \sum_{\{S_A\}} e^{-\beta \mathcal{H}_{\text{eff}}[S_A]} = \sum_{\{S_i\}} e^{-\beta \mathcal{H}[S_i]}. \quad (2.6)$$

This new effective Hamiltonian eff describes the same long-range physics as the initial one.

The renormalization group (RG) consists of iterating this procedure an infinite number of times. After each step, the Hamiltonian is mapped into a new Hamiltonian at larger scales and the iteration $\mathcal{H}^{(0)} \rightarrow \mathcal{H}^{(1)} \rightarrow \dots \rightarrow \mathcal{H}^{(n)}$ generates a flow of Hamiltonians. At a critical point the system is scale invariant and the RG transformation has a fixed-point Hamiltonian, *i.e.* $\lim_{n \rightarrow \infty} \mathcal{H}^{(n)} = \mathcal{H}^*$, which explains the scale law behaviour at the second order phase transition [16]. The existence of a fixed-point is the signature of scale invariance. An important remark is that the rescaling is necessary in order to find a fixed-point.

The correlation function, which measures how different regions of the system are correlated, changes with the scale. After each RG-step, the correlation length ξ is reduced by a factor b : $\xi' = \xi/b$. Therefore at a fixed point ξ can either vanish or diverge because of the scale invariance. This means that not all fixed-points are critical. If $\xi \rightarrow 0$, the system is either in the

high- or low-temperature phase and if $\xi \rightarrow \infty$, the system is at its critical point:

$$\begin{cases} \xi \rightarrow \infty: \text{critical fixed-point} \\ \xi \rightarrow 0: \text{trivial fixed-point.} \end{cases} \quad (2.7)$$

If we start at the critical point, the system will remain critical after any number of iterations but if we start slightly above or below the critical point, the system will be driven to the high- or in the low-temperature phase respectively.

This decimation method introduced by Kadanoff¹ is hard to use in practice except for one-dimensional systems. Even if a system has only one interaction over neighbouring spins like in the Ising model each RG-step introduces new interactions over next-neighbouring spins and so on. To overcome this difficulty Wilson introduced an new approach in a continuous theory implemented in the Fourier space.

2.2.2 Wilson Momentum Shell Integration

In critical phenomena, we are interested in low-momentum or long wave-length fluctuations and it is more convenient to work in momentum space. We can write the Hamiltonian in Fourier space and carry out the block spin transformation over the momentum. Wilson's approach is to work with a continuous theory where the partition functions reads:

$$\mathcal{Z} = \int \mathcal{D}\phi e^{\mathcal{H}_\Lambda[\phi]} \quad (2.8)$$

where the sum has been replaced by a functional integral, ϕ is the microscopic field and \mathcal{H}_Λ the Hamiltonian which is also called the Landau-Ginzburg-Wilson action at the lattice scale Λ . Since the approach is based on a continuous theory of a lattice model the momenta must be lower than the inverse lattice size $\Lambda = a^{-1}$. We separate the field into slow modes with momenta lower than Λ/b and rapid modes² with momenta between Λ/b and Λ : $\phi = \phi_{<} + \phi_{>}$ (see figure 2.2). Then we integrate over the rapid modes and we are left with an effective

¹There are other ways of performing the block spin transformation such as the Niemeijer and van Leeuwen majority rule which was derived for a triangular lattice [17], [18] but they will not be presented here.

²Here slow and rapid stand respectively for long and short distance or equivalently for low and high momentum.

action $\mathcal{H}_{\Lambda/b}$ which depend only on the slow modes:

$$e^{-\mathcal{H}_{\Lambda/b}[\phi_{<}]} = \int \mathcal{D}\phi_{>} e^{\mathcal{H}_{\Lambda}[\phi_{<} + \phi_{>}]}. \quad (2.9)$$

This is called the Wilson momentum shell integration [19].

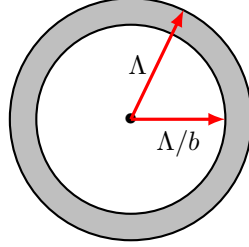


FIGURE 2.2: Wilson momentum shell integration. The inner zone corresponds to the slow modes $\phi_{<}$ and the outer region to the rapid modes $\phi_{>}$.

The Wilson momentum shell is well suited for carrying out the RG procedure with an infinitesimal transformation. We take $\Lambda/b = \Lambda - \delta k$ and now the momenta of the rapid modes lay between Λ and $\Lambda - \delta k$ and the momenta of the slow modes are lower than $\Lambda - \delta k$ with $\delta k \ll 1$ (see fig. 2.2). This way of separating the modes with a sharp boundary induces non-analyticities that one would like to avoid³ and one prefers to avoid this by introducing smooth boundaries through some smooth cut-off function (which is introduced below). With this in hand one derives the Wilson equation [19] for the effective action \mathcal{H}_k :

$$\partial_t \mathcal{H}_k = \int_p \partial_t \alpha_t(p) \left[\frac{\delta^2 \mathcal{H}_k}{\delta \phi(-p) \delta \phi(p)} - \frac{\delta \mathcal{H}_k}{\delta \phi(-p)} \frac{\delta \mathcal{H}_k}{\delta \phi(p)} + \phi(p) \frac{\delta \mathcal{H}_k}{\delta \phi(p)} \right] \quad (2.10)$$

where t is the RG-“time” $t = \ln k/\Lambda$, $\alpha_t(p)$ a cut-off function that separates the rapid modes from the slow ones in a smooth manner. In [20] Wilson and Kogut used a cut-off function of the form $\alpha_t(p) = p^2(e^{2t} - 1) + \rho(t)$ with $\rho(0) = 0$. The function $\rho(t)$ allows to impose a normalization condition on the kinetic term of the effective action and thus to define the anomalous dimension η . The last term on the right hand side of (2.10) is present since we are working with dimensionless quantities. This is the equivalent of the rescaling step in the Kadanoff procedure.

³sharp boundaries result in non-local interactions in position space.

In addition to this formulation of the RG in the continuum limit and the derivation of a differential equation (2.10) another of Wilson's great contribution is the introduction of the anomalous dimension. This is a crucial point if one wants to obtain any fixed-point [19, 21]. The anomalous dimension is an exponent responsible for the change of the dimension of the field from its canonical value obtained by simple dimensional analysis.

Conceptually this approach is of great importance in critical phenomena. However it has been hard to implement except in specific cases: numerically to solve the Kondo problem [20] or with perturbative approximations such as the weak-coupling [22], the large- n and the low-temperature approximations at leading order of the ϵ -expansion.

One of the origins of the difficulties is that the second term in the r.h.s of eq. (2.10) makes this equation very hard use. This is a *non-local* term in direct space which means that it is difficult to compute the field renormalization or equivalently the anomalous dimension.

The problem with this equation (2.10) is that the effective Hamiltonian \mathcal{H}_k does not have any direct physical meaning since it is the Hamiltonian of modes that have not been integrated out $\phi_<$ and these modes completely disappear in the limit $k \rightarrow 0$, *i.e.* when all fluctuations have been integrated out. As a consequence, some of the information on the high-momentum degrees of freedom is lost. However this equation is useful to compute critical exponents at a given fixed-point.

Various formulation of the Wilson RG have been developed such as the Wegner-Houghton RG [23] using a sharp cut-off or the Migdal-Kadanoff direct space RG which is difficult to perform when dealing with more than one dimension because of the accuracy of the approximation one has to make are difficult to estimate.

2.2.3 Polchinski and Proof of Renormalizability

A regain of interest in the Wilson RG appeared when Polchinski used Eq. (2.10) to prove the perturbative renormalizability of the ϕ^4 field theory in four dimensions [24]. Since then the Wilson equation has been mainly used to prove the renormalizability of different theories ([25], [26], [27]). Note that the Wilson equation (2.10) is often incorrectly referred to as the Wilson-Polchinski or simply the Polchinski equation.

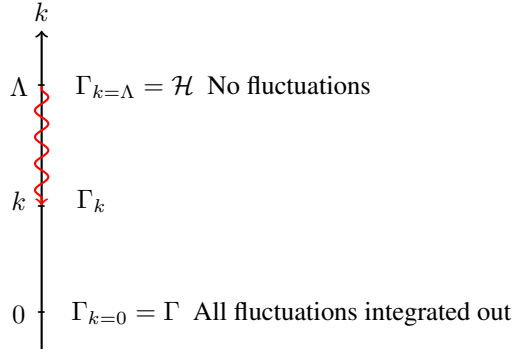


FIGURE 2.3: Continuous Interpolation of the Effective Average Action Γ_k between the Classical Action \mathcal{H} and the Effective Action Γ .

2.3 Wetterich Renormalization Group

2.3.1 Effective Average Action

To overcome the problems of the Wilson RG it is preferable to work with quantities with more physical meaning. Christof Wetterich's idea [13] was to work with the Legendre transform Γ of the free energy $\ln \mathcal{Z} = W$. More precisely he has introduced a new quantity called the effective average action Γ_k which depends on the coarse-grained scale k . This effective average action interpolates continuously between the Hamiltonian or classical action \mathcal{H} when all the fluctuations are frozen at $k = \Lambda$ and the effective action Γ , *i.e.* the Gibbs free energy or the generating functional of the one particle irreducible (1PI) Green functions, when all the fluctuations have been integrated out at $k = 0$ (see fig. 2.3). This scheme is still a Wilsonian type of RG but now we construct running effective actions rather than running Hamiltonians. Therefore the Kadanoff block spin idea continues to be applicable here and one still separates the fields into rapid and slow modes. The effective average action generically depends on a scale k that makes the interpolation between the Hamiltonian and the effective action possible. This scale also separates the rapid modes with momentum $q > k$ from the slow modes with $q \leq k$.

To decouple the slow modes from the rapid modes in the partition function, a large mass is given to the slow modes and an almost vanishing one to the rapid modes. Thus we modify

the partition function by adding a scale dependent mass term $\Delta\mathcal{H}_k$:

$$\mathcal{Z}_k[B] = \int \mathcal{D}\phi \exp \left[-\mathcal{H}[\phi] - \Delta\mathcal{H}_k[\phi] + \int_q B(-q)\phi(q) \right] \quad (2.11)$$

where B is an external field, $\int_q = \int d^d q / (2\pi)^d$ and $\Delta\mathcal{H}_k[\phi] = \frac{1}{2} \int_q R_k(q)\phi(q)\phi(-q)$ where R_k is dimensioned like a mass. This cut-off R_k prevents the propagation of fluctuations with momenta $q < k$. A typical behaviour of the cut-off function R_k is given by:

$$\begin{cases} R_k(q) \underset{q \rightarrow 0}{\sim} k^2 \\ R_k(q) \underset{q \rightarrow \infty}{\sim} 0. \end{cases} \quad (2.12)$$

Since the effective average action interpolates between the Hamiltonian and the effective action, some constraints are imposed to the behaviour of the cut-off function R_k . It must vanish in the limit of vanishing k and it must diverge when the scale k is equal to the inverse lattice scale Λ :

$$\begin{cases} k = 0 \rightarrow R_{k=0}(q) = 0, \forall q \implies \mathcal{Z}_{k=0}[B] = \mathcal{Z}[B] \\ k = \Lambda \rightarrow R_{k=\Lambda}(q) = \infty, \forall q \implies \text{all the fluctuations are frozen} \end{cases}$$

which must lead to:

$$\begin{cases} \tilde{\Gamma}_{k=0} = \Gamma \\ \tilde{\Gamma}_{k=\Lambda} = \mathcal{H}. \end{cases}$$

This said, we can now begin constructing the effective average action Γ_k . From the partition function $\mathcal{Z}_k[B]$, we can construct the Helmholtz free energy:

$$W_k[B] = \ln \mathcal{Z}_k[B] \quad (2.13)$$

where we have dropped the minus sign, the temperature T and the Boltzmann constants k_B . The effective average action, *i.e.* the Gibbs free energy, is defined as the Legendre transform

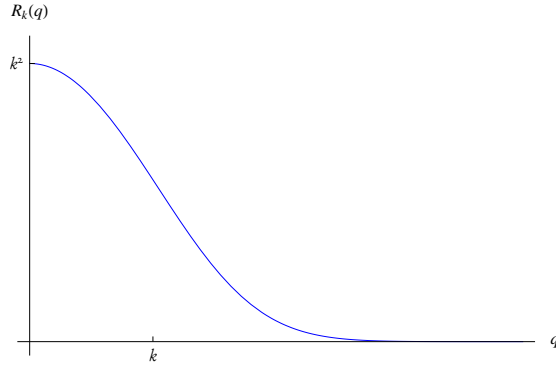


FIGURE 2.4: Typical cut-off function.

of the free energy:

$$\tilde{\Gamma}_k[M] + W_k[B] = \int_x B(x)M(x) \quad (2.14)$$

where $M(x) = \frac{\delta W_k}{\delta B(x)}$.

Having defined the effective average action, let us see if we recover the required asymptotic behaviour. When $k \rightarrow 0$, the mass term R_k vanishes and the free energy $W_{k=0}$ is equal to W and hence $\tilde{\Gamma}_{k=0} = \Gamma$. Now let us see what happens in the other limit $k \rightarrow \Lambda$. By definition of the Legendre transform the external field is given by:

$$B(x) = \frac{\delta \tilde{\Gamma}_k}{\delta M(x)}. \quad (2.15)$$

Therefore substituting this definition in eq. (2.14) we obtain:

$$\tilde{\Gamma}_k[M] = \int_x \frac{\delta \tilde{\Gamma}_k}{\delta M(x)} M(x) - W_k[B]. \quad (2.16)$$

Now we take the exponential of $\tilde{\Gamma}_k$:

$$e^{-\tilde{\Gamma}_k[M]} = e^{W_k[B]} e^{-\int_x \frac{\delta \tilde{\Gamma}_k}{\delta M(x)} M(x)} \quad (2.17)$$

and using $e^{W_k} = Z_k$ we find:

$$\begin{aligned} e^{-\tilde{\Gamma}_k[M]} &= \int \mathcal{D}\phi(x) e^{-\mathcal{H}[\phi] - \Delta\mathcal{H}_k[\phi] + \int_x B(x)\phi(x)} e^{-\int_x \frac{\delta\tilde{\Gamma}_k}{\delta M(x)} M(x)} \\ &= \int \mathcal{D}\phi(x) e^{-\mathcal{H}[\phi] - \frac{1}{2} \int_{x,y} \phi(x) R_k(x,y) \phi(y) + \int_x \frac{\delta\tilde{\Gamma}_k}{\delta M(x)} (\phi(x) - M(x))}. \end{aligned} \quad (2.18)$$

If we take a cut-off that diverges when $k \rightarrow \Lambda$ for all momentum:

$$\exp\left[-\frac{1}{2} \int_{x,y} \phi_x R_{k=\Lambda}(x,y) \phi_y\right] \sim \delta(\phi) \quad (2.19)$$

which leads to:

$$\tilde{\Gamma}_{k=\Lambda}[M] = \mathcal{H}[\phi = 0] + \int_x \frac{\delta\tilde{\Gamma}_k}{\delta M(x)} M(x). \quad (2.20)$$

This is not the result we wanted since $\tilde{\Gamma}_{k=\Lambda}[M] \neq \mathcal{H}[\phi = M]$. One solves this problem by subtracting the term $\frac{1}{2} \int_{x,y} M(x) R(x,y) M(y)$ in eq. (2.14) which leads to a modified Legendre transform:

$$\Gamma_k[M] = \int_x B(x)M(x) - \frac{1}{2} \int_{x,y} M(x) R_k(x,y) M(y) - W_k[B]. \quad (2.21)$$

With this change in the definition, the limit $k \rightarrow 0$ remains unchanged. And after the same computation as before, we have:

$$e^{-\Gamma_k[M]} = \int \mathcal{D}\phi(x) e^{-\mathcal{H}[\phi] + \int_x \frac{\delta\Gamma_k}{\delta M(x)} (\phi_x - M(x))} e^{-\frac{1}{2} \int_{x,y} (\phi_x - M(x)) R_k(x,y) (\phi_y - M(y))}. \quad (2.22)$$

Taking the limit $k = \Lambda$ we find:

$$\exp\left[-\frac{1}{2} \int_{x,y} (\phi_x - M(x)) R_{k=\Lambda}(x,y) (\phi_y - M(y)) \phi_y\right] \sim \delta(\phi - M) \quad (2.23)$$

and this equation with eq. (2.22) lead to:

$$\Gamma_{k=\Lambda}[M] = \mathcal{H}[\phi = M]. \quad (2.24)$$

If the cut-off R_k does not diverge in this limit but is only very large then $\Gamma_{k=\Lambda} \sim \mathcal{H}$. This shows that the form of the cut-off has an influence on the flow at the beginning of the integration process. However the critical behaviour in principle remains unchanged. Therefore for critical phenomena we can take a finite cut-off for $k = \Lambda$ but if we are interested in non-universal behaviour we must use have $\lim_{k \rightarrow \Lambda} R_k = \infty$ (see [28]).

A main difference between the Wilson and the Wetterich pictures is the role played by k . It is an ultraviolet cut-off in the Wilson approach whereas it is an infra-red one in Wetterich approach.

2.3.2 The Wetterich Equation

In this section, we derive the Wetterich equation which is the exact evolution equation of the effective average action. We start by deriving an evolution equation for the partition function \mathcal{Z}_k :

$$\begin{aligned} \partial_k \mathcal{Z}_k &= -\frac{1}{2} \int \mathcal{D}\phi \left(\int_{x,y} \phi_x \partial_k R_k(x-y) \phi_y \right) \\ &\quad \exp \left[-\mathcal{H}[\phi] - \frac{1}{2} \int_{x,y} \phi_x R_k(x-y) \phi_y + \int_x B(x) \phi_x \right] \\ &= \frac{1}{2} \left(\int_{x,y} \partial_k R_k(x-y) \frac{\delta}{\delta B(x)} \frac{\delta}{\delta B(y)} \right) e^{W_k} \end{aligned} \quad (2.25)$$

from which we deduce the evolution equation of the free energy W_k :

$$\partial_k W_k = -\frac{1}{2} \int_{x,y} \partial_k R_k(x-y) \left(\frac{\delta^2 W_k}{\delta B(x) \delta B(y)} + \frac{\delta W_k}{\delta B(x)} \frac{\delta W_k}{\delta B(y)} \right). \quad (2.26)$$

Note that this equation is equivalent of the Wilson-Polchinski equation (2.10) and therefore has the same non-locality problems.

Now we have the evolution equation for W_k , we can easily derive the equivalent one for Γ_k . But first we must recall that the derivation ∂_k is taken at fixed B . And we need to change this at some point to derivations at fixed magnetization M . The relation between the two derivatives is:

$$\partial_{k|M} = \partial_{k|B} + \int_x \partial_k M(x)|_B \frac{\delta}{\delta M(x)}. \quad (2.27)$$

Taking the derivation of the Legendre transform (2.21) with respect to k we find:

$$\begin{aligned} \partial_k \Gamma_{k|_B} + \partial_k W_{k|_B} &= \int_x B(x) \partial_k M(x)|_B - \frac{1}{2} \int_{x,y} M(x) \partial_k R_k(x-y)|_B M(y) \\ &\quad - \int_{x,y} M(x) R_k(x-y) \partial_k M(y)|_B. \end{aligned} \quad (2.28)$$

Substituting $\partial_k W_k$ by its result (2.26) together with eq. (2.27) we obtain:

$$\begin{aligned} \partial_k \Gamma_{k|M} + \int_x \partial_k M(x)|_B \frac{\delta \Gamma_k}{\delta M(x)} - \frac{1}{2} \int_{x,y} \partial_k R_k(x-y) \left(\frac{\delta^2 W_k}{\delta B(x) \delta B(y)} \right. \\ \left. + \frac{\delta W_k}{\delta B(x)} \frac{\delta W_k}{\delta B(y)} \right) &= \int_x B(x) \partial_k M(x)|_B - \frac{1}{2} \int_{x,y} M(x) \partial_k R_k(x-y)|_B M(y) \\ &\quad - \int_{x,y} M(x) R_k(x-y) \partial_k M(y)|_B. \end{aligned} \quad (2.29)$$

Replacing $B(x)$ by its expression $\frac{\delta \Gamma_k}{\delta M(x)} + \int_y R_k(x-y) M(y)$ in the previous equation, we obtain:

$$\begin{aligned} \partial_k \Gamma_{k|M} &= \frac{1}{2} \int_{x,y} \partial_k R_k(x-y) \left(\frac{\delta^2 W_k}{\delta B(x) \delta B(y)} + \frac{\delta W_k}{\delta B(x)} \frac{\delta W_k}{\delta B(y)} \right) \\ &\quad - \frac{1}{2} \int_{x,y} M(x) \partial_k R_k(x-y)|_B M(y) \end{aligned} \quad (2.30)$$

and using $\frac{\delta W_k}{\delta B(x)} = M(x)$ we find:

$$\partial_k \Gamma_{k|M} = \frac{1}{2} \int_{x,y} \partial_k R_k(x-y) \frac{\delta^2 W_k}{\delta B(x) \delta B(y)}. \quad (2.31)$$

We are close to the final expression. We just need to express the second functional derivative of W_k as a function of Γ_k and therefore we again use $\frac{\delta W_k}{\delta B(x)} = M(x)$ and derive it with respect to M :

$$\frac{\delta^2 W_k}{\delta B(x) \delta M(z)} = \int_y \frac{\delta^2 W_k}{\delta B(x) \delta B(y)} \frac{\delta B(y)}{\delta M(z)} \quad (2.32)$$

which is also given by:

$$\frac{\delta^2 W_k}{\delta B(x) \delta M(z)} = \frac{\delta M(x)}{\delta M(z)} = \delta(x - z). \quad (2.33)$$

The field B can be expressed in terms of Γ_k :

$$B(x) = \frac{\delta \Gamma_k}{\delta M(x)} + \int_y R_k(x - y) M(y) \quad (2.34)$$

and taking its functional derivative with respect to $M(z)$ we obtain:

$$\frac{\delta B(x)}{\delta M(z)} = \frac{\delta^2 \Gamma_k}{\delta M(x) \delta M(z)} + R_k(z - y). \quad (2.35)$$

Replacing this equation into eq. (2.33) we find:

$$\delta(x - z) = \int_y \frac{\delta^2 W_k}{\delta B(x) \delta B(y)} \left(\frac{\delta^2 \Gamma_k}{\delta M(x) \delta M(z)} + R_k(z - y) \right) \quad (2.36)$$

which means that $W_k^{(2)}$ is the inverse of $\Gamma_k^{(2)} + R_k$:

$$W_k^{(2)}(x, y) = \left(\Gamma_k^{(2)} + R_k \right)^{-1}(x, y) \quad (2.37)$$

which is slightly different from the usual relation $W^{(2)} = (\Gamma^{(2)})^{-1}$. Injecting this into eq. (2.31) we finally obtain the *Wetterich equation*:

$$\partial_k \Gamma_k[M] = \frac{1}{2} \int_{x,y} \partial_k R_k(x - y) \left(\Gamma_k^{(2)} + R_k \right)^{-1}(x, y) \quad (2.38)$$

which reads in Fourier space:

$$\partial_k \Gamma_k[M] = \frac{1}{2} \int_q \partial_k R_k(q) \left(\Gamma_k^{(2)} + R_k \right)^{-1}(q, -q). \quad (2.39)$$

A remarkable feature of this equation is that it does not have the non-local term that plagued

the Wilson-Polchinski equation (2.10). This evolution equation is an *exact functional integro-differential* equation which makes it impossible to solve in general without any approximation. Before talking about the approximations that one can make while preserving the non-perturbative character, let us review the properties of this flow equation. Albeit having a *one-loop structure* since it involves only one integral which can be seen from a diagrammatic representation it is an exact equation:

$$\partial_t \Gamma_k = \frac{1}{2} \textcircled{\bullet} \quad (2.40)$$

where t is the RG-“time” $t = \ln k/\Lambda$ and the dot represents $\partial_t R_k$. This one-loop structure gives a direct connection with perturbative RG both in the vicinity of the upper and lower critical dimension as well as with the large- n expansion at lowest orders (one-loop).

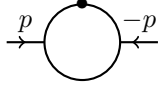
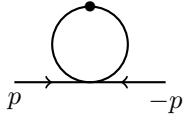
The flow equations for the Green functions are straightforward to derive. We simply need to take the functional derivatives of the Wetterich equation. The flow equations of $\Gamma^{(1)}$ and $\Gamma^{(2)}$ are given by:

$$\partial_t \Gamma_k^{(1)}(p) = -\frac{1}{2} \int_{q_i} \partial_t R_k(q) G_k(q_1, -q_2) \Gamma_k^{(3)}(q_2, -q_3, p) G_k(q_3, -q_1) \quad (2.41)$$

$$\begin{aligned} \partial_t \Gamma_k^{(2)}(p_1, p_2) &= \int_{q_i} \partial_t R_k(q) G_k(q_1, -q_2) \Gamma_k^{(3)}(q_2, -q_3, p_1) G_k(q_3, -q_4) \Gamma_k^{(3)}(q_4, -q_5, p_2) \\ &\times G_k(q_5, -q_1) - \frac{1}{2} \int_{q_i} \partial_t R_k(q) G_k(q_1, -q_2) \Gamma_k^{(4)}(q_2, -q_3, p_1, p_2) G_k(q_3, -q_1) \end{aligned} \quad (2.42)$$

where G_k is the propagator $(\Gamma_k^{(2)} + R_k)^{-1}$. The diagrammatic forms of $\partial_t \Gamma_k^{(1)}$ and $\partial_t \Gamma_k^{(2)}$ show that the one-loop structure is preserved:

$$\partial_t \Gamma_k^{(1)} = -\frac{1}{2} \overrightarrow{p} \textcircled{\bullet} \quad (2.43)$$

$$\partial_t \Gamma_k^{(2)} = -\frac{1}{2} \left[\text{Diagram 1} \right] - \left[\text{Diagram 2} \right] \quad (2.44)$$



where $p_1 = -p_2 = p$. Note that these equations are not closed. In particular we see that the flow of $\Gamma_k^{(1)}$ involves $\Gamma_k^{(2)}$ and $\Gamma_k^{(3)}$ and the flow of $\Gamma_k^{(2)}$ involves $\Gamma_k^{(3)}$ and $\Gamma_k^{(4)}$. More generally the flow of $\Gamma_k^{(n)}$ involves $\Gamma_k^{(n+1)}$ and $\Gamma_k^{(n+2)}$.

2.3.3 Approximations

In general the effective average action Γ_k involves an infinite number of couplings but since the Wetterich equation (2.39) cannot be solved exactly some approximations must be made to close the system and perform actual calculations. However, as the approximations used do not rely on the smallness of a usual parameter, the approach remains non-perturbative in essence. In particular, it is not confined to weak-coupling regimes or to the vicinity of critical dimensions and is therefore suitable to overcome the limitations of perturbative RG schemes.

In the following, I shall present the most used approximations which transform the Wetterich equation (2.39) from a functional differential equation to a set of ordinary differential equations:

- the derivative expansion where the effective action is expanded in power of the derivatives of the fields
- the field expansion, where the effective action is expanded in power of the fields
- the Blaizot-Mendez-Wschebor or BMW approximation where the full momentum dependence is kept.

These approximations are presented with the $O(n)$ -model in mind, which we discuss below as an example, but the generalization to systems with more than one field or with different symmetries does not pose any conceptual problem.

The choice of the approximations is a very complicated question which depends on the system at hand.

2.3.3.1 Derivative Expansion

The derivative expansion is a series expansion in the derivatives of the field and equivalently, in Fourier space it is an expansion in powers of the momenta. Therefore it is well suited for the study of phase transitions and critical phenomena where we are interested in the long-distance, low-momentum, physics. In this approximation the effective average action Γ_k reads:

$$\Gamma_k[\vec{\phi}] = \int d^d x \left\{ \frac{Z_k(\vec{\phi})}{2} (\partial\vec{\phi})^2 + \frac{Y_k(\vec{\phi})}{4} (\partial\rho)^2 + U_k(\vec{\phi}) + o(\partial^4) \right\} \quad (2.45)$$

where $\vec{\phi}$ is a n -vector field, $\rho = \vec{\phi}^2/2$, $Z_k(\vec{\phi})$ and $Y_k(\vec{\phi})$ are the field dependent kinetic terms and $U_k(\vec{\phi})$ the potential part of $\Gamma_k[\vec{\phi}]$. This equation can be further simplified by taking $Z_k = 1$ and neglecting the function Y_k :

$$\Gamma_k^{LPA}[\vec{\phi}] = \int d^d x \left\{ \frac{1}{2} (\partial\vec{\phi})^2 + U_k(\vec{\phi}) \right\}. \quad (2.46)$$

This is called the *local potential approximation* (LPA) since no field renormalization is included and thus the anomalous dimension vanishes $\eta = 0$.

One can improve this approximation by taking into account the field renormalization constant Z_k and get the LPA':

$$\Gamma_k^{LPA'}[\vec{\phi}] = \int d^d x \left\{ \frac{Z_k}{2} (\partial\vec{\phi})^2 + U_k(\vec{\phi}) \right\} \quad (2.47)$$

where we note that Z_k depend only on the scale k but not on the field ϕ . This will give a non trivial anomalous dimension since $Z_k \sim k^{-\eta}$.

This truncation is well suited to the study for the long distance physics. The derivative expansion has been successfully applied in statistical physics where in the study of critical phenomena we are only interested in the long wave-length physics: $O(n)$ -model [29], the Gross-Neveu models [30], [31], frustrated magnets [32] and see [33] for other examples.

2.3.3.2 Field Expansion

In the field expansion we keep all the derivatives but expand the effective average action in powers of the field:

$$\Gamma_k[\phi] = \sum_{n=0}^{\infty} \frac{1}{n!} \int \left(\prod_{i=1}^n d^d x_i \phi(x_i) \right) \Gamma_k^{(n)}(x_1, \dots, x_n). \quad (2.48)$$

From convergence studies it has been shown ([34], [35]) that expanding the effective average action around the minimum configuration ϕ_0 of Γ improves the convergence properties when one is interested in the critical behaviour. With this Γ_k reads:

$$\Gamma_k[\phi] = \sum_{n=0}^{\infty} \frac{1}{n!} \int \left(\prod_{i=1}^n d^d x_i (\phi(x_i) - \phi_0) \right) \Gamma_k^{(n)}(x_1, \dots, x_n). \quad (2.49)$$

2.3.3.3 Combination of the Derivative Expansion and the Field Expansion

We can of course combine both the derivative and the field expansions. This is probably the most used truncations and it is the one we have used in our work. The effective potential with this double truncation reads

$$U_k(\rho) = \sum_{n=0}^m a_{n,k} (\rho - \kappa)^n \quad (2.50)$$

where $\rho = \phi^2/2$ and $\kappa = \phi_0^2/2$ which correspond to the minimum of the potential $U'_k(\rho = \kappa) = 0$. The functions Z_k and Y_k read:

$$\begin{cases} Z_k(\rho) = \sum_{n=0}^m Z_k^{(n)} (\rho - \kappa)^n \\ Y_k(\rho) = \sum_{n=0}^m Y_k^{(n)} (\rho - \kappa)^n. \end{cases} \quad (2.51)$$

Within this expansion we select the couplings depending on their canonical dimension. Now the flow equation of Γ_k becomes a set of ordinary differential equations which considerably simplifies the integration. Although the derivative and field expansion have many advantages, it still has some drawbacks. The momentum dependence of the Green functions $\Gamma^{(n)}$ is badly

truncated at the transition. Moreover the independence of the physical quantities on the cut-off choice is not preserved and there is no general theorem on the convergence of the derivative expansion. However, it has been noticed and it is physically reasonable that if there is convergence, hence the dependence upon the cut-off R_k decreases with the order of the expansion.

Note that an interesting modification to this approximation was been made by Braghin and Hasselmann [36, 37] where the full momentum dependence of the coupling constants is kept. This approximation yields closed coupled integro-differential equations which are solve self-consistently and it allows for investigation beyond the asymptotic $q \approx 0$ regime.

2.3.3.4 Blaizot-Mendez-Wschebor Approximation

The BMW approximation, developed by Blaizot, Mendez-Galain and Wschebor [38], starts with the exact equation on the Green functions. In this method one considers that most of the relevant information is encoded in the two-point correlation function $\Gamma_k^{(2)}$ taken in a uniform field M . The flow equation of $\Gamma_k^{(2)}$ reads:

$$\begin{aligned} \partial_k \Gamma_k^{(2)}(p; M) = & \int_q \partial_k R_k(q) G(p; M)^2 \left(-\frac{1}{2} \Gamma_k^{(4)}(p, -p, q, -q; M) \right. \\ & \left. + \Gamma_k^{(3)}(p, q, -p - q; M) G(p + q; M) \Gamma_k^{(3)}(-p, -q, p + q; M) \right) \end{aligned} \quad (2.52)$$

which is slightly different from the one written previously, because we used the fact that there are Dirac δ -functions in the G 's and $\Gamma^{(n)}$'s. To close this evolution equation we need approximations on $\Gamma_k^{(3)}$ and $\Gamma_k^{(4)}$. The BMW-approximation consists in taking a vanishing dependence over the internal momenta q and by performing the following replacement:

$$\left\{ \begin{array}{l} \Gamma_k^{(4)}(p, -p, q, -q; M) \rightarrow \Gamma_k^{(4)}(p, -p, 0, 0; M) = \frac{\partial^2 \Gamma_k^{(2)}}{\partial M^2}(p; M) \\ \Gamma_k^{(3)}(p, q, -p - q; M) \rightarrow \Gamma_k^{(3)}(p, 0, -p; M) = \frac{\partial \Gamma_k^{(2)}}{\partial M}(p; M) \\ \Gamma_k^{(3)}(-p, -q, p + q; M) \rightarrow \Gamma_k^{(3)}(-p, 0, p; M) = \frac{\partial \Gamma_k^{(2)}}{\partial M}(p; M) \end{array} \right. \quad (2.53)$$

which leads to:

$$\begin{aligned} \partial_k \Gamma_k^{(2)}(p; M) = \int_q \partial_k R_k(q) G_k(p; M)^2 \left\{ -\frac{1}{2} \frac{\partial^2 \Gamma_k^{(2)}}{\partial M^2}(p; M) \right. \\ \left. + G(p+q; M) \left(\frac{\partial \Gamma_k^{(2)}}{\partial M}(p; M) \right)^2 \right\} \end{aligned} \quad (2.54)$$

where the q momentum dependence is kept only in the Green functions G . This is a closed equation since the functions G are equal to $(\Gamma_k^{(2)} + R_k)^{-1}$. Finally one solves this equation numerically or analytically if possible.

2.3.4 Optimisation and Cut-off Function Choice

After performing approximations, a crucial question is that 1) of the convergence of the results when the approximation is enriched and 2) the choice of the cut-off function R_k . Normally the physical results must be independent on the choice of R_k . But since approximations are made, this independence of the results obtained is broken. Therefore, an important question is how to choose the optimal cut-off? To answer this question one must establish which optimisation criteria are the most relevant: the speed of convergence of the physical quantities with the order of the expansion (derivatives and fields), the sensitivity of the results at each order to the cut-off variation, the accuracy of the results . . . Following Canet et. al [39], we concentrate on the two latter criteria.

Taking a family of cut-off function R_k^α parametrized by α and since the untruncated results are independent of α we seek a region where the results are less sensitive to the variation of the parameter α at all orders of the truncation: this is called the principle of minimum sensitivity (PMS). This criterion reads:

$$\frac{dQ(\alpha)}{d\alpha} \Big|_{\alpha_{\text{PMS}}} = 0 \quad (2.55)$$

where Q can be a critical exponent or any another physical quantity of interest.

Canet et. al [39] computed the correlation length exponent ν for the Ising model in three dimensions. In figure 2.5, we can see the results at different orders of the field expansion where

two cut-off functions were used, an exponential $R_{k,\text{exp}}^{(\alpha)}$ [40] and a theta cut-off $R_{k,\theta}^{(\alpha)}$ [41]:

$$\begin{aligned} R_{k,\text{exp}}^{(\alpha)} &= \frac{\alpha q^2}{e^{q^2/k^2} - 1} \\ R_{k,\theta}^{(\alpha)} &= \alpha (k^2 - q^2) \theta(1 - q^2/k^2). \end{aligned} \quad (2.56)$$

The difference between the results corresponding to the two cut-off functions taken at their PMS value α_{PMS} is less than 5% when the field expansion is converged (see fig. 2.5).

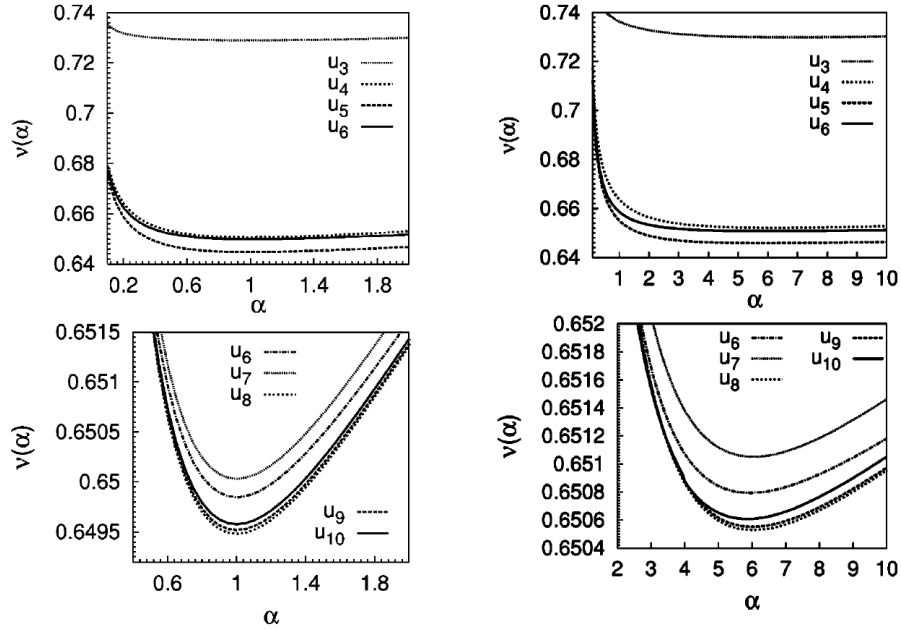


FIGURE 2.5: The correlation length exponent ν for different order of the field expansion from Canet et. al [39]. On the left, we have the results with the theta cut-off and on the right with the exponential cut-off. The lower figures correspond to a magnification for the higher orders.

The choice of the cut-off will depend on the physical system under consideration. And since the approximations break the cut-off independence, one needs to optimize the cut-off choice and see how the exponents vary when the cut-off changes.

2.3.5 The $O(n)$ -model

To illustrate the ideas we have introduced in this chapter we use the $O(n)$ -model as an example. The $O(n)$ -model describes systems with a n -vectorial field $\vec{\phi}$ with $O(n)$ rotational invariance in the symmetric high-temperature phase. Lowering the temperature a phase transition occurs at the critical temperature T_c and the symmetry is broken into $O(n - 1)$.

The $O(n)$ -model is probably the most studied model in theoretical physics because of its simplicity which is related to the maximal $O(n)$ symmetry but its importance is also related to the wide range of systems it describes going from the paramagnetic-ferromagnetic transition in magnetic systems to superfluidity and superconductivity:

- $n = 0$: polymers
- $n = 1$: Ising model
- $n = 2$: XY-model
- $n = 3$: Heisenberg model

We consider the effective average action with the combination of the derivative and field expansions and to the lowest order it reads:

$$\Gamma_k[\vec{\phi}] = \int d^d x \left\{ \frac{Z_k}{2} (\partial\vec{\phi})^2 + \frac{\lambda}{2} \left(\frac{\vec{\phi}^2}{2} - \kappa \right)^2 \right\} \quad (2.57)$$

where Z_k , λ and κ are the running coupling constants. The coupling κ is defined as the configuration that minimizes the potential. At the critical temperature the field renormalization Z_k has a power law behaviour:

$$Z_k \sim k^{-\eta_k} \quad (2.58)$$

where η_k is the anomalous dimension.

From the Wetterich equation (2.39) we see that the flow equations depend on the propagator $(\Gamma_k^{(2)} + R_k)^{-1}$. Therefore it is the first quantity that we compute.

2.3.5.1 Propagator

The two-point correlation function $\Gamma_k^{(2)}$ is computed by taking the second functional derivative of eq. (2.57) and expressing it in one minimum configuration $\phi_i = \sqrt{2\kappa}\delta_{1i}\delta(p)$:

$$\Gamma_k^{(2)}(p_1, i, p_2, j) \Big|_{\min} = \delta(p_1 + p_2) \{ Z_k p_1^2 \delta_{ij} + 2\lambda \kappa \delta_{1i} \delta_{1j} \} \quad (2.59)$$

which is diagonal both in momentum and component space. Therefore the propagator \mathcal{P} is straightforward:

$$\mathcal{P}(p_1, i, p_2, j) \Big|_{\min} = \delta(p_1 + p_2) \{ G_0(p_1)(1 - \delta_{i1}) + G_1(p_1)\delta_{i1} \} \delta_{ij} \quad (2.60)$$

where the functions G_i are given by:

$$\begin{cases} G_0(p) &= (Z_k p^2 + R_k(p))^{-1} \\ G_1(p) &= (Z_k p^2 + R_k(p) + 2\lambda\kappa)^{-1}. \end{cases} \quad (2.61)$$

These functions describe to the different modes of the system. At the transition the $O(n)$ symmetry is broken into $O(n-1)$ therefore in the low-temperature symmetry broken phase G_0 correspond to the $n-1$ massless Goldstone modes and G_1 to the radial massive mode with mass $2\lambda\kappa$.

2.3.5.2 Definitions of the Coupling Constants

Now we must express the coupling constants in terms of derivatives of the effective average action in order to find their flow equation. We start with the coupling κ which by definition of the minimum of Γ_k is given by:

$$\lim_{p \rightarrow 0} \Gamma_k^{(1)}(p, 1) \Big|_{\min} = \lim_{p \rightarrow 0} \frac{\delta \Gamma_k}{\delta \phi_1(p)} \Big|_{\min} = 0 \quad (2.62)$$

The coupling λ is given by:

$$\lambda = \frac{1}{2\kappa} \lim_{p \rightarrow 0} \Gamma_k^{(2)}(p, 1; -p, 1) \Big|_{\min} \quad (2.63)$$

and last but not least the field renormalization Z_k is defined by:

$$Z_k = \lim_{p \rightarrow 0} \frac{d}{dp^2} \Gamma_k^{(2)}(p, 2; -p, 2) \Big|_{\min}. \quad (2.64)$$

2.3.5.3 Derivation of the Flow Equations

For the derivation of the flow equations it is more convenient to use a different form for the Wetterich equation (2.39):

$$\partial_t \Gamma_k[\phi] = \frac{1}{2} \tilde{\partial}_t \text{Tr} \int_q \ln \left(\Gamma_k^{(2)} + R_k \right) (q, -q) \quad (2.65)$$

where $\tilde{\partial}_t$ acts only on R_k .

The flow of κ is obtained by deriving eq. (2.62) with respect to t :

$$\begin{aligned} \lim_{p \rightarrow 0} \partial_t \left(\Gamma_k^{(1)}(p, 1) \Big|_{\min} \right) &= \lim_{p \rightarrow 0} \left\{ \partial_t \Gamma_k^{(1)}(p, 1) + \frac{1}{\sqrt{2\kappa}} \partial_t \kappa \Gamma_k^{(2)}(p, 1; -p, 1) \right\} \Big|_{\min} \\ &= 0 \end{aligned} \quad (2.66)$$

which leads to:

$$\partial_t \kappa = - \lim_{p \rightarrow 0} \frac{\sqrt{2\kappa}}{\Gamma_k^{(2)}(p, 1; -p, 1) \Big|_{\min}} \partial_t \Gamma_k^{(1)}(p, 1) \Big|_{\min}. \quad (2.67)$$

Deriving eq. (2.63) the flow of λ reads:

$$\begin{aligned} \partial_t \lambda &= \partial_t \kappa \lim_{p \rightarrow 0} \left\{ -\frac{1}{2\kappa^2} \Gamma_k^{(2)}(p, 1; -p, 1) + \frac{1}{(2\kappa)^{3/2}} \Gamma_k^{(3)}(p, 1; -p, 1; 0, 1) \right\} \Big|_{\min} \\ &\quad + \frac{1}{2\kappa} \lim_{p \rightarrow 0} \Gamma_k^{(2)}(p, 1; -p, 1) \Big|_{\min} \end{aligned} \quad (2.68)$$

and the flow of the field renormalization (2.64) reads:

$$\partial_t Z_k = \lim_{p \rightarrow 0} \frac{d}{dp^2} \left\{ \partial_t \Gamma_k^{(2)}(p, 2; -p, 2) + \frac{\partial_t \kappa}{(2\kappa)^{1/2}} \Gamma_k^{(3)}(p, 2; -p, 2; 0, 1) \right\} \Big|_{\min}. \quad (2.69)$$

Computing the functional derivative of the effective action and replacing them in eq. (2.67) the flow of κ reads:

$$\partial_t \kappa = -\frac{1}{2} \tilde{\partial}_t \int_q \left\{ \frac{n-1}{Z_k q^2 + R_k(q)} + \frac{3}{Z_k q^2 + R_k(q) + 2\lambda \kappa} \right\}. \quad (2.70)$$

Similarly from eq. (2.68) we find:

$$\partial_t \lambda = -\frac{\lambda^2}{2} \tilde{\partial}_t \int_q \left\{ \frac{n-1}{(Z_k q^2 + R_k(q))^2} + \frac{9}{(Z_k q^2 + R_k(q) + 2\lambda \kappa)^2} \right\} \quad (2.71)$$

and from eq. (2.69) the flow of the field renormalization Z_k is given by:

$$\partial_t Z_k = -2\kappa \lambda^2 \lim_{p \rightarrow 0} \frac{d}{dp^2} \tilde{\partial}_t \int_q \frac{1}{(Z_k q^2 + R_k(q)) (Z_k (p+q)^2 + R_k(p+q) + 2\lambda \kappa)}. \quad (2.72)$$

In order to find a fixed-point we must work with dimensionless coupling. We recall that this step is equivalent of the rescaling step in the Kadanoff transformation:

$$\begin{cases} y & = q^2/k^2 \\ R_k(q) & = Z_k q^2 r(y) = Z_k k^2 y r(y) \\ \tilde{\kappa} & = Z_k k^{2-d} \kappa \\ \tilde{\lambda} & = Z_k^{-2} k^{d-4} \lambda \end{cases} \quad (2.73)$$

and the running anomalous dimension η_k is given by:

$$\eta_k = -\frac{1}{Z_k} \partial_t Z_k. \quad (2.74)$$

The flow equations of the dimensionless couplings read:

$$\begin{aligned} \partial_t \tilde{\kappa} &= -(d-2+\eta) \tilde{\kappa} + 2v_d \left((n-1) l_1^d(0) + 3 l_1^d(2\tilde{\lambda} \tilde{\kappa}) \right) \\ \partial_t \tilde{\lambda} &= (d-4+2\eta) \tilde{\lambda} + 2v_d \tilde{\lambda}^2 \left((n-1) l_2^d(0) + 9 l_2^d(2\tilde{\lambda} \tilde{\kappa}) \right) \end{aligned} \quad (2.75)$$

and from the flow of the field renormalization together with eq. (2.74) we find:

$$\eta_k = \frac{16v_d}{d} \tilde{\kappa} \tilde{\lambda}^2 m_{2,2}^d(2\tilde{\lambda} \tilde{\kappa}) \quad (2.76)$$

where $v_d = 2^{-d-1}\pi^{d/2}\Gamma[d/2]$ and the threshold functions l_a^d and $m_{a,b}^d$ are given by:

$$\left\{ \begin{array}{l} l_a^d(w) = -\frac{1}{4v_d}\tilde{\partial}_t \int_q \frac{1}{(Z_k q^2 + R_k(q) + w)^a} \\ m_{a,b}^d(w) = -\frac{1}{8v_d} \lim_{p \rightarrow 0} \frac{d}{dp^2} \tilde{\partial}_t \int_q \frac{1}{(Z_k q^2 + R_k(q))^a} \\ \quad \times \frac{1}{(Z_k(p+q)^2 + R_k(p+q) + w)^b} \end{array} \right. \quad (2.77)$$

These functions encode the non-perturbative content of the approach. The argument w correspond to the squared masses of the radial and the Goldstone modes which are $2\lambda\kappa$ and 0 respectively.

From these equations (2.75-2.76) we can find the fixed-points and by linearising in the vicinity of the fixed-points we find the correlation critical exponent ν . The anomalous dimension is given by eq. (2.76) at the fixed-point. From the one-loop structure of the Wetterich equation (2.39) one can recover the weak-coupling ϵ -expansion and the low-temperature expansion as well as the large- n expansion. The other critical exponents can be obtained from the following scaling relations:

$$\left\{ \begin{array}{l} \alpha = 2 - d\nu \\ \beta = \frac{\nu}{2}(d - 2 + \eta) \\ \gamma = \nu(2 - \eta) \\ \delta = \frac{d+2-\eta}{d-2+\eta} \end{array} \right. \quad (2.78)$$

2.3.5.4 Weak-coupling Expansion

In the vicinity of the upper critical dimension $d_{uc}=4$ the coupling $\tilde{\lambda}$ is of order $\epsilon = 4 - d$ and the anomalous dimension η_k is vanishing at order ϵ . Therefore to recover the weak-coupling results we expand the flow equations (2.75) in the first non-trivial order of $\tilde{\lambda}$. We start by expanding the threshold function with non vanishing mass entering the flow of $\tilde{\kappa}$:

$$l_1^4(w) \approx l_1^{d=4}(0) - 2\tilde{\lambda}\tilde{\kappa}. \quad (2.79)$$

Replacing this in eq.(2.75) we find:

$$\partial_t \tilde{\kappa} = -(2 - \epsilon) \tilde{\kappa} + \frac{(n+2)}{16\pi^2} l_1^{d=4}(0) - \frac{3}{8\pi^2} \tilde{\lambda} \tilde{\kappa} \quad (2.80)$$

where the last term is only relevant for the calculation of the correlation exponent and not for the fixed-point coordinate. For the coupling $\tilde{\lambda}$ we consider the threshold $l_2^{d=4}(2\tilde{\lambda}\tilde{\kappa})$ in the limit of vanishing mass at the lowest order in λ since it is multiplied $\tilde{\lambda}^2$ term:

$$l_2^{d=4}(2\tilde{\lambda}\tilde{\kappa}) \rightarrow l_2^{d=4}(0). \quad (2.81)$$

Moreover the threshold $l_2^{d=4}(0)$ has a universal cut-off independent value which equals to 1:

$$\begin{aligned} l_2^{d=4}(0) &= - \int_0^\infty dy \frac{2r'(y)}{(1+r(y))^3} = \int_0^\infty dy \frac{d}{dy} \left[\frac{1}{(1+r(y))^2} \right] \\ &= \left[\frac{1}{(1+r(y))} \right]_0^\infty = 1 \end{aligned} \quad (2.82)$$

since $\lim_{y \rightarrow \infty} r(y) = 0$ and $\lim_{y \rightarrow 0} r(y) = \infty$ for any cut-off. With this $\partial_t \tilde{\lambda}$ is given by:

$$\partial_t \tilde{\lambda} = -\epsilon \tilde{\lambda} + \frac{(n+8)}{16\pi^2} \tilde{\lambda}^2. \quad (2.83)$$

The coordinates of the fixed-point are given by:

$$\begin{cases} \tilde{\kappa}^* &= \frac{(n+2)}{32\pi^2} l_1^{d=4}(0) \\ \tilde{\lambda}^* &= \frac{16\pi^2}{n+8} \epsilon. \end{cases} \quad (2.84)$$

The correlation exponent is obtained by linearising the flow equations in the vicinity of the fixed-point and we find:

$$\nu = \frac{1}{2} + \frac{(n+2)}{4(n+8)} \epsilon \quad (2.85)$$

which corresponds to the perturbative result at one-loop order. The anomalous dimension at this order is vanishing: $\eta = o(\epsilon)$.

2.3.5.5 Low-Temperature Expansion

The lower-critical dimension d_{lc} corresponds to the dimension below which the ordered phase disappears for finite temperature and for the $O(n)$ -model it is equal to 2 for $n \geq 2$. At d_{lc} the critical exponent ν diverges which justifies a low-temperature expansion in the vicinity of d_{lc} . At low-temperatures the massive modes contribution is vanishing at all order of the expansion in powers of the temperature T . Therefore the physics is completely governed by the Goldstone modes.

In our approach where the temperature dependence is implicit the low-temperature expansion is equivalent to an expansion in powers of $1/\tilde{\kappa}$. This means that we must expand the threshold functions with non-vanishing mass at dominant order in $1/\tilde{\kappa}$. However the contribution of the lowest order in the massive threshold functions entering the flows of $\tilde{\kappa}$ and $\tilde{\lambda}$ is vanishing and in the vicinity of $d = 2$ these equations read:

$$\partial_t \tilde{\kappa} = -(\epsilon + \eta_k) \tilde{\kappa} + 2v_2(n-1)l_1^{d=2}(0) \quad (2.86)$$

$$\partial_t \tilde{\lambda} = (\epsilon - 2)\tilde{\lambda} + 2v_2\tilde{\lambda}^2(n-1)l_2^{d=2}(0) \quad (2.87)$$

and for the anomalous dimension the threshold $m_{2,2}^{d=2}$ is taken in the infinite mass limit:

$$\eta_k = \frac{2v_2}{\kappa} m_{2,2}^{d=2}(\infty). \quad (2.88)$$

The threshold functions $l_1^{d=2}(0)$ and $m_{2,2}^{d=2}(\infty)$ have universal behaviour given by:

$$l_1^{d=2}(0) = 1 \quad (2.89)$$

$$m_{2,2}^{d=2}(\infty) = 1. \quad (2.90)$$

Replacing this in the flow equations we find:

$$\eta_k = \frac{1}{4\pi\tilde{\kappa}} \quad (2.91)$$

$$\partial_t \tilde{\kappa} = -\epsilon\tilde{\kappa} + \frac{(n-2)}{4\pi} \quad (2.92)$$

$$\partial_t \tilde{\lambda} = (\epsilon - 2)\tilde{\lambda} + \frac{(n-1)}{4\pi} l_2^{d=2}(0). \quad (2.93)$$

Since $\tilde{\kappa} \sim 1/T$ the flow of the temperature is identical to the one found in perturbative theory. The coordinates of the fixed-point are given by:

$$\begin{cases} \tilde{\kappa}^* &= \frac{n-2}{4\pi\epsilon} \\ \tilde{\lambda}^* &= \frac{8\pi}{(n-1)l_2^{d=2}(0)}. \end{cases} \quad (2.94)$$

The anomalous dimension at this fixed-point is given by:

$$\eta^* = \frac{\epsilon}{n-2} \quad (2.95)$$

and the correlation exponent is obtained from the linearisation of the flow equation near the fixed-point:

$$\nu = \frac{1}{\epsilon} \quad (2.96)$$

which agrees with the result of the non-linear σ -model.

2.3.5.6 Large- n Expansion

From the NPRG approach we can also recover the result from the large- n expansion. From the fixed-points of the two previous perturbative approaches eqs. (2.84) and (2.94) we suppose that $\tilde{\kappa}^*$ and $\tilde{\lambda}^*$ are respectively of order n and $1/n$ and in the end we verify that this is coherent. At the dominant order of the expansion in powers of $1/n$ the anomalous dimension is vanishing and the flow equations read:

$$\partial_t \tilde{\kappa} = -(d-2)\tilde{\kappa} + 2n v_d l_1^d(0) \quad (2.97)$$

$$\partial_t \tilde{\lambda} = (d-4)\tilde{\lambda} + 2n v_d \tilde{\lambda}^2 l_2^d(0) \quad (2.98)$$

from which we deduce the coordinates of the fixed-point:

$$\begin{cases} \tilde{\kappa}^* &= \frac{2n v_d l_1^d(0)}{d-2} \\ \tilde{\lambda}^* &= \frac{4-d}{2n v_d l_2^d(0)} \end{cases} \quad (2.99)$$

and the result is coherent with the initial assumption. The correlation exponent ν is again obtained from the linearisation around the fixed-point and we find:

$$\nu = \frac{1}{d-2} \quad (2.100)$$

which agrees with the one-loop perturbative result.

2.3.6 Conclusion

A remarkable property of the NPRG approach is that we can recover the one-loop perturbative results of the weak-coupling, low-temperature and large- n expansions with truncations at lowest orders. This is a unique property. There is no other approach that we know of that provides a connection between the various different perturbative results. Moreover the NPRG allows for an investigation of the physics at any given dimension d and any number of field components n .

An important result of the NPRG is that one finds accurate results for the XY-model. At the Berezinskii-Kosterlitz-Thouless transition [42, 43] one finds for the anomalous dimension $\eta = 0.24$ at lowest order of the field and derivative expansion [44] and $\eta = 0.287$ with higher orders [45] which compare well with the exact result $\eta = 0.25$. The variation of the value of η between the two NPRG calculations means that the expansion has not converged yet. These results show that without an explicit investigation of the vortex configuration the NPRG seems to automatically include these configurations and therefore seems to correctly describe the topological excitations.

For the three dimensional Ising model, using a derivative expansion at order ∂^2 together with a field expansion to order ϕ^{10} Canet *et al.* [39] computed the anomalous dimension $\eta = 0.04426$ and the correlation exponent $\nu = 0.6281$. These results are in good agreement with the 7-loop results [46]: $\eta = 0.0335(25)$ and $\nu = 0.6304(13)$; and with Monte Carlo simulations [47]: $\eta = 0.0362(8)$ and $\nu = 0.6297(5)$.

The BMW method has been used to compute both universal and non-universal quantities for the $O(n)$ -model in two and three dimensions [48]. For instance the anomalous dimension for $n = 2$ in $d = 3$ equals $\eta = 0.041$ which is in good agreement with Monte Carlo result $\eta = 0.0381(2)$ [46].

The power of this approach is that one can compute non-universal quantities such as the critical temperature. Using a local potential approximation Machado and Dupuis [49] computed the critical temperature for the Ising, XY and Heisenberg models in three dimensions which are respectively given by 4.48, 2.18 and 1.42 and are in very good agreement with Monte Carlo results to an accuracy of 1%: 4.51 [50], 2.20 [51] and 1.44 [52].

It has been applied with great success to a wide number of systems and situations by several teams. It is now recognized as a very efficient method that has shown its ability to go beyond the perturbative approaches and to replace them favorably when they fail to correctly describe the critical physics. Among many situations we mention the case of frustrated magnets [32], membranes ([53], [54]), disordered systems [55]), out of equilibrium systems including KPZ equation [56], Bose systems ([57], [38]), gravity [58], see [59] and [60] for reviews. In all these situations the NPRG has clarified a confused perturbative situation and, in several case, has revealed intrinsic nonperturbative aspects necessary for a clear understanding of the physics.

Appendix A

Threshold Functions

To find a fixed-point we must use dimensionless quantities. For the momenta we perform the change of variable:

$$y = \frac{q^2}{k^2} \tag{A.1}$$

and the flow derivation ∂_t is taken at constant q . Thus we must express it in terms of the variable y :

$$\partial_{t|q^2} = \partial_{t|y} - 2y \partial_y \tag{A.2}$$

This relation serves to calculate explicitly the flow of the cut-off R_k in terms of r :

$$\partial_{t|q^2} R_k(q) = -Z_k k^2 (-\eta_k y r(y) - 2y^2 r'(y)) \tag{A.3}$$

where we have used $\partial_t Z_k = -\eta_k Z_k$ and $r'(y) = \partial_y r(y)$. With this at hand we can express the threshold functions in a dimensionless form:

$$\left\{ \begin{array}{l} l_a^d(w) = -\frac{a + \delta_{a,0}}{2} \int_0^\infty dy \frac{y^{d/2-1} (\eta_k y r(y) + 2y^2 r'(y))}{(y(1+r(y)) + w)^{a+1}} \\ m_{a,b}^d(w) = \frac{1}{2} \int_0^\infty \frac{y^{d/2} (1+r(y) + y r'(y))^2}{(y + y r(y))^a (y + y r(y) + w)^b} \\ \quad \times \left\{ (\eta_k y r(y) + y^2 r'(y)) \left(\frac{a}{(y + y r(y))} + \frac{b}{(y + y r(y) + w)} \right) \right. \\ \quad \left. - 2 \frac{(\eta_k r(y) + y r'(y)(\eta_k + 4) + 2y^2 r''(y))}{(1+r(y) + y r'(y))} \right\} \end{array} \right. \quad (\text{A.4})$$

Chapter 3

Membranes

Geometry, which should always follow physics when used to describe nature, sometimes commands it.

Jean-Baptiste Le Rond D'Alembert (1752)

3.1 Introduction

One may consider that the first observation of a membrane goes way back to Babylon in the eighth century B.C. when an oil droplet was put in water (fig. 3.1). But the interest in membranes has its origin in the seventeenth century microscopic observations. In 1665, the English natural philosopher Robert Hooke made the first observation of a cell (see Fig. 3.2) while studying cork under a compound microscope [61]. He also observed similar cells in other plants and animals. But the chemical nature and the structure of these cells was a complete mystery. It was not until the nineteenth century that new experimental techniques and more powerful microscopes gave new insight into the nature of membranes. The surgeon and histologist Sir William Bowman gave the first representation of a membrane when he discovered and described cells of transverse and longitudinal striae of voluntary muscles in 1840 [62]. Sir William Bowman is better known for the Bowman's membrane which is a smooth layer in the eye.

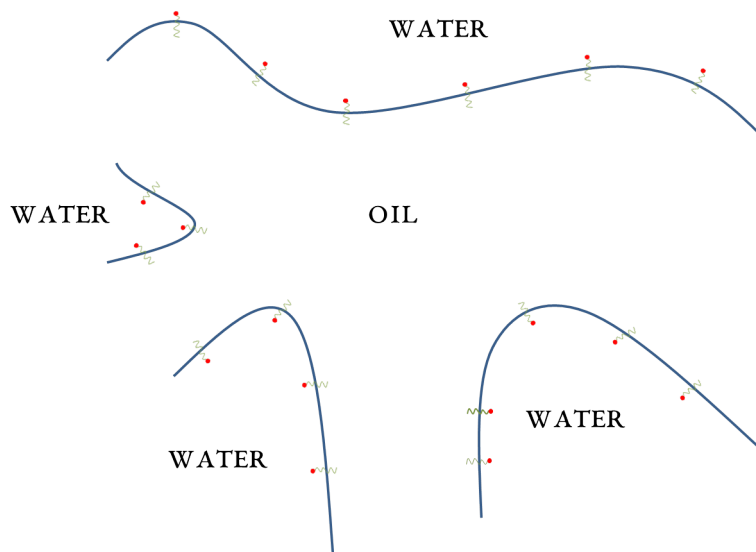


FIGURE 3.1: Water-oil interface.



FIGURE 3.2: Observation of cork by Robert Hooke in 1665 [61].

A couple of decades later, the German surgeon and internist Heinrich Quincke observed how a spherical cell in water forms two separate parts of the same spherical shape when broken in half. From this observation, he postulated the lipid nature of these cells by analogy to the behaviour of oil in water. In the 1890's, this lipid nature was confirmed by the independent works of Hans Meyer and Ernest Overton [63]. During the same period of time, Ernest Overton also discovered that cells are encapsulated within a selectively permeable layer while

studying cells of plant root hairs. This can be considered as the first observation of a membrane separating the cell's contents from the environment.

In 1905, the American chemist and physicist Irving Langmuir dissolved phospholipids in benzene and then spread them on a water surface and then evaporated the benzene. He discovered that the molecules of phospholipid membranes have a polar head and tails made of hydrocarbon chains. He also found that the typical area occupied by a lipid molecule is 50 \AA^2 .

In the 1920's, Fricke [64] measured the capacitance of a cell-membrane. This measurement indicated that the membrane was only 4 nm thick. A couple of years later, Gorter & Grendel [65] applied a pressure measurement method developed by Irving Langmuir in 1917 [66], to lipid extracts of erythrocyte (red blood cell) membranes. They compared the area occupied by the lipid extracts and the area of the whole erythrocyte and they concluded that plasma membranes had a bilayer structure (see Fig. 3.3). Albeit Gorter & Grendel made some mistakes in their experiment, luckily the different errors cancelled out and their conclusion was correct. Although other experiments confirmed the bilayer structure of plasma membranes and more generally of all cell-organelle membranes, this bilayer nature was not widely accepted until X-ray diffraction [67] and new evidence on the physical state of membrane lipids [68] settled this once and for all.

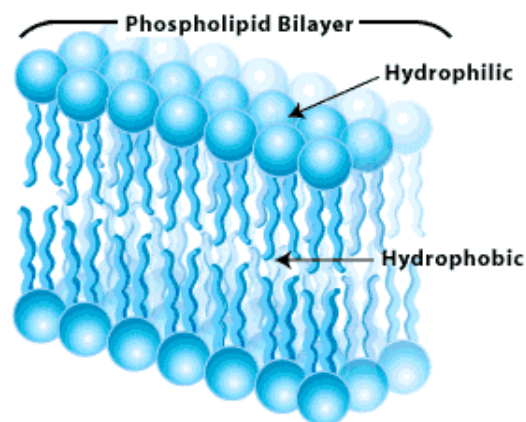


FIGURE 3.3: Phospholipid bilayer.

In the early membrane models, the membrane was made only of lipids. But experiments showed that membranes absorbed water faster than a pure phospholipid membrane should. In 1935, Danielli & Davson's [69] proposed a membrane model where globular proteins lay

on the surface of the phospholipid bilayer (Fig. 3.4), since proteins are water absorbent. This model excludes transmembrane proteins based on the previously shown hydrophilic surface of globular proteins. The Danielli-Davson model suggests that all the membranes are alike and that the proteins are homogeneously distributed.

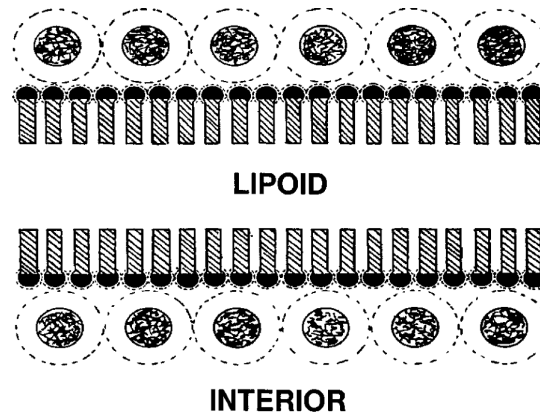


FIGURE 3.4: Original drawing of the Davson-Danielli cell membrane model. The lipids are sandwiched between two layers of globular proteins [69].

In the 1970's, work from laboratories of Harden McConnell and by Dennis Chapman (see [70] for review) mentioned the possibility that bilayer lipids are asymmetrically distributed, *i.e.* that the two membrane layers or leaflets have different lipid composition and fluidity.

The first images of a membrane with an electron micrograph 3.5 showed that the membrane had a three layer structure and this was taken incorrectly as a confirmation of the Davson-Danielli model until the 1970's. But advances in biology and chemistry were incompatible with the Davson-Danielli model. A better understanding of proteins showed that most of them were not hydrophilic as previous thought but rather lipophilic and hydrophobic. In 1972, a new model by S.J. Singer & G.L. Nicolson came into light [71]. This model takes into account some of the complexity of the membrane which was not the case in the Davson-Danielli model. One or more types of lipids may form the bilayer like a mosaic. And the proteins are inserted within the fluid bilayer in which one can also find cholesterol. Both the proteins and the cholesterol can diffuse freely within the membrane. This model was named the fluid mosaic model for obvious reasons.

In all that we have discussed above, we have never mentioned the underlying forces that hold the bilayer together. The main force that shapes membrane bilayers is the hydrophobic

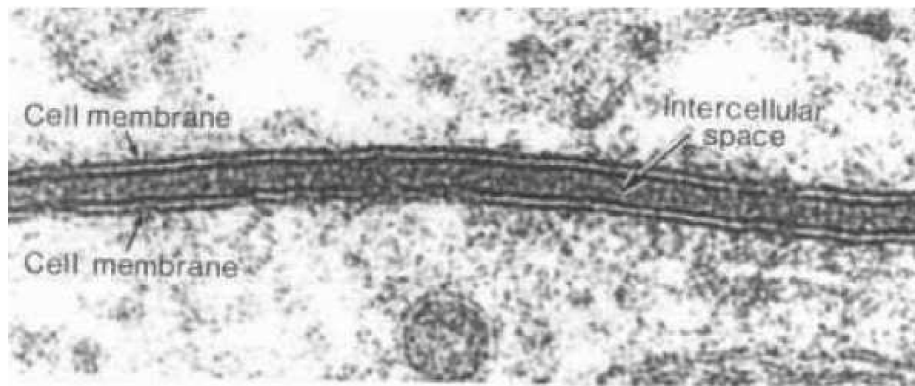


FIGURE 3.5: Electron micrograph of a cell [72]. The cell membrane has three layers, a light layer sandwiched between two dark layers.

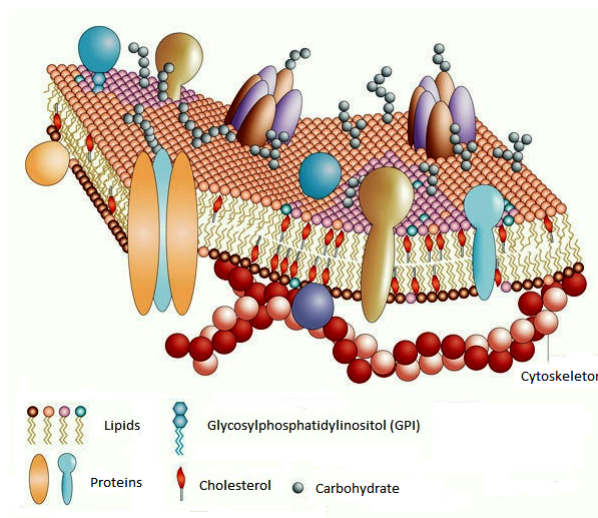


FIGURE 3.6: Fluid Mosaic Model [73]. Like a mosaic, the cell membrane is a complex structure made up of many different parts, such as proteins, phospholipids and cholesterol. The relative amounts of these components vary from membrane to membrane, and the types of lipids in membranes can also vary.

force [74]. The lipid molecules are made of a head and one or more tails. The head is made of glycerol and phosphates and the tail of fatty acid chains which are respectively hydrophilic (head) and hydrophobic (tail). Therefore, in aqueous solutions the lipids organise so that the arrangement minimizes its contact with water which explains why the bilayer structure formation. This principle also applies to the insertion of membrane proteins into the bilayer. The

proteins are usually arranged so that their hydrophobic surfaces are buried in the lipid.

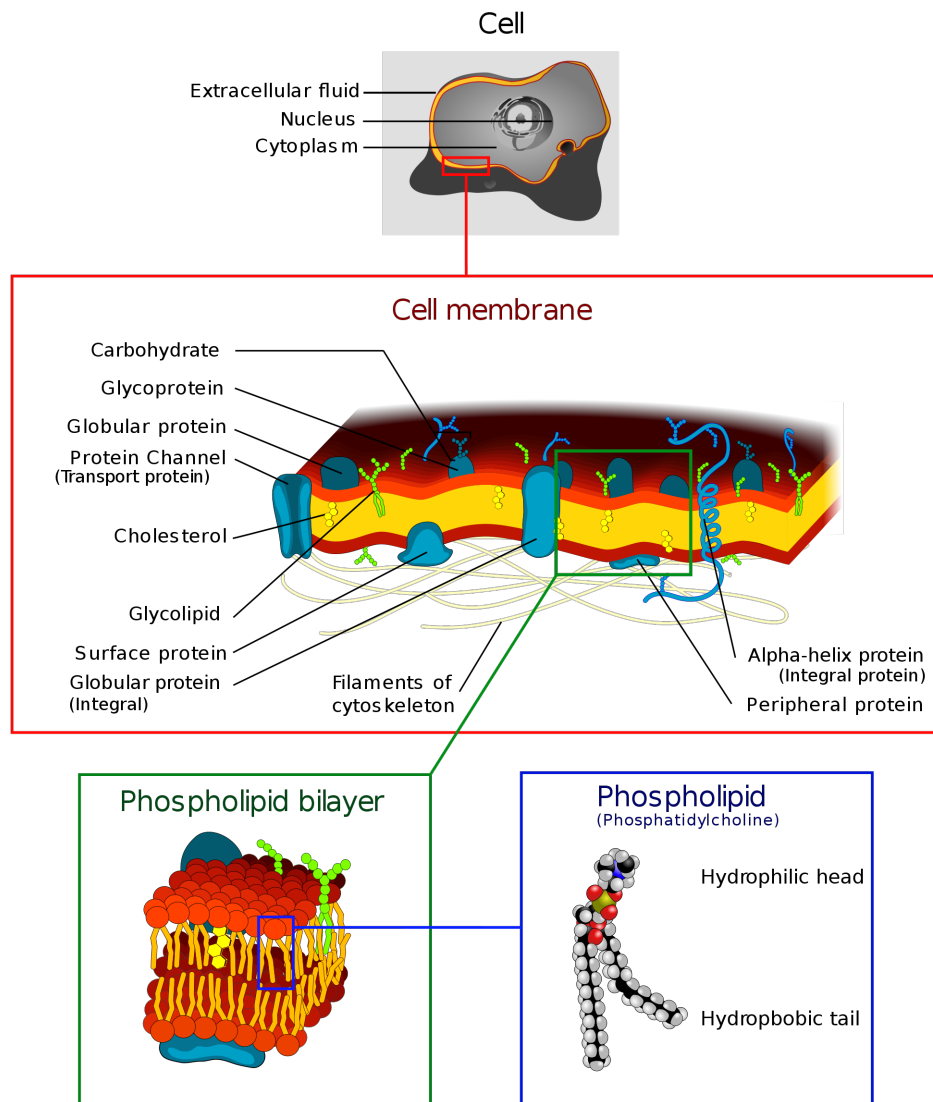


FIGURE 3.7: Detailed description of a biological cell membrane (*Wikipedia*).

Biological cell-membranes are considered to be *fluid* since the molecules are free to diffuse within the membrane like molecules diffuse in an ordinary fluid. The diffusion coefficient D is of the order $10^{-6} \text{ cm} \cdot \text{s}^{-1}$. Therefore there may be no elastic energy. A completely different type of membranes can be found in biological membranes. For instance, the plasma membrane

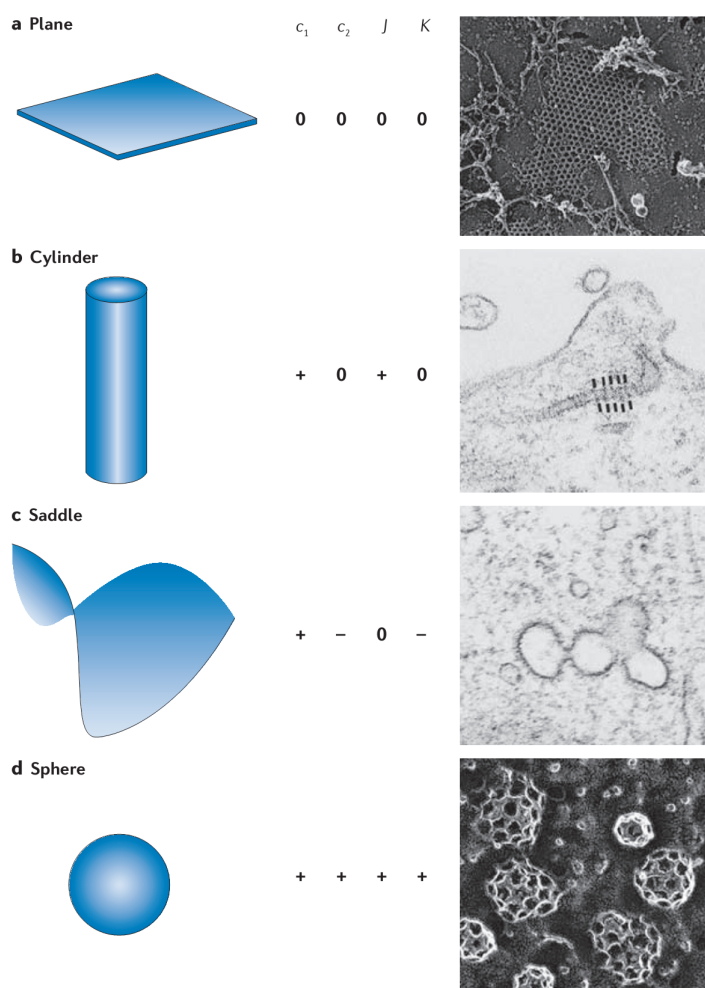


FIGURE 3.8: Membrane basic shapes [75].

of red blood cells has an additional membrane to the fluid lipid bilayer. The second membrane, which is coupled to the first one, is a spectrin network with fixed-connectivity analogous to a fishnet (see Fig. 3.9). This spectrin network constitutes the skeleton of the red blood cell and is therefore called the cytoskeleton.

The connectivity is considered to be fixed since the time-scales for breaking and reassembling the molecular connections of the spectrin network is very large compared with the time-scales involved in the shape fluctuations [76]. Therefore membrane with fixed-connectivity are referred to as *polymerized* membranes since they are a natural extension of one-dimensional

polymers to higher dimensions. As a consequence, polymerized membranes are regarded as thin elastic sheets and the thermodynamical fluctuations of these sheets are governed by bending and elastic energies.

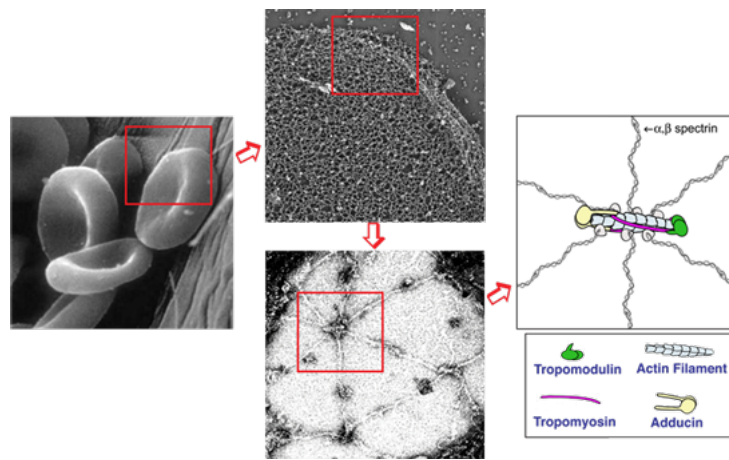


FIGURE 3.9: Red blood cell [77].

Albeit fluid and polymerized membranes are three-dimensional, they are both considered as two-dimensional surfaces because the aspect ratio, *i.e.* the ratio of its width to its height, is very large.

Another important membrane-like system of great importance in condensed matter physics is graphene. Graphene is a one atom thick layer of carbon atoms in a non-compact honeycomb lattice (see Fig. 3.10) making it the first truly two-dimensional system. Graphene was described for the first time by the German chemist Hans-Peter Boehm in 1962 [78] where he observed free-floating graphene sheets in a dilute alkaline solution. But in his work, the graphene sheets were not free-standing and were made of several layers. These free-standing sheets were thought of as a theoretical curiosity impossible to realise in nature because of the Mermin-Wagner theorem ([79], [80], [81]). This theorem states that one cannot have long range order or even a crystalline structure for two-dimensional systems with short-range interactions¹. For decades, graphene was studied theoretically but not much experimental interest was given to it. Not until the early twenty first century. In 2004, Andre Geim and Kostya

¹More precisely, the Mermin-Wagner theorem states that there is no spontaneous symmetry breaking for systems with short-range interactions and dimension $d \leq 2$. If the symmetry is discrete like in the two-dimensional Ising-model, this theorem does not hold.

Novosolev [82] made the first discovery of free-standing graphene. Their production technique of the graphene sheets is quite amusing. They used adhesive tape on graphite to isolate graphene layers. This discovery is very important from various aspects. First of all, it is the first genuinely two-dimensional material. Second, as a consequence of the symmetry of the honeycomb crystalline structure, the electrons obey the Dirac equation instead of Schrodinger's and have a linear dispersion relations as if they were massless relativistic particles. Finally, graphene has some extraordinary properties that seem to be contradictory. For instance, it is stronger than diamond but displays ripples (see fig. 3.10) which give an effective thickness ranging between 0.23 \AA [83] and 3.5 \AA [84]. It is a perfect conductor but at the same time optically transparent. Graphene also display an anomalous quantum Hall effect (QHE) because of the existence of a zero-energy Landau level.

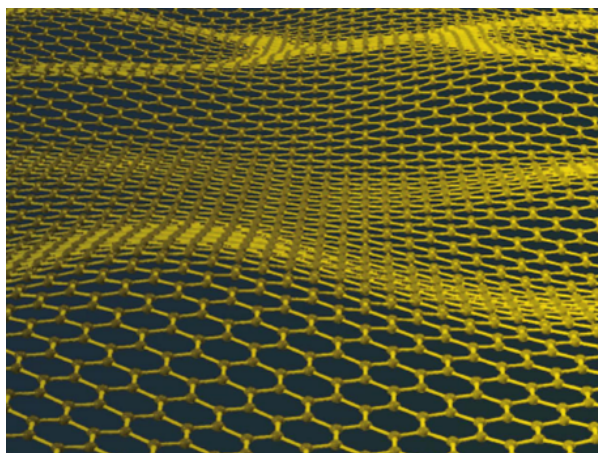


FIGURE 3.10: Graphene [85].

From a formal point of view, in high-energy physics, membranes appear as an extension of the original strings in string theory as shown by Joseph Polchinski in 1995. These membranes are called p -branes for p -dimensional membranes. For example a 1-brane is a string, a 2-brane is an ordinary membrane sheet etc. The most important p -branes are the Dirichlet branes or D-branes for short. They were discovered in 1989 by Dai, Leigh & Polchinski [87] and independently by Horava [88]. In superstring theory, the Calabi-Yau space (see 3.12) is a six-dimensional membrane that appear as the extra-dimensions of the four-dimensional space-time ([89], [90]).

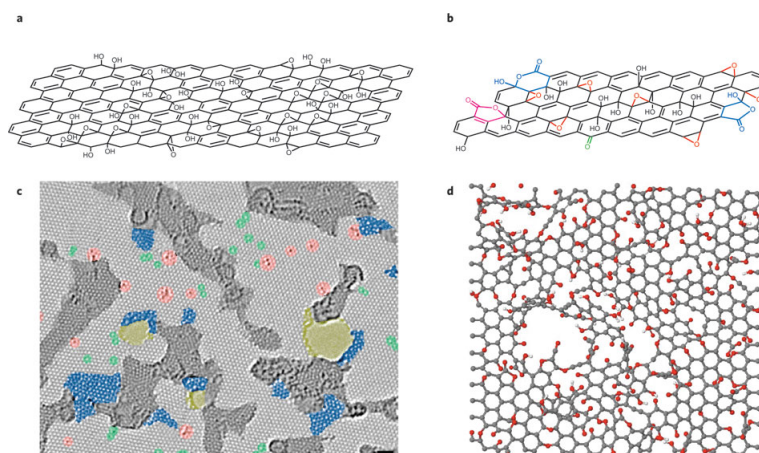


FIGURE 3.11: Graphene oxide [86].

The interest in membranes has been increasing these last years since the discovery of graphene ([91], [92]) and graphene-based sheets like graphene oxides (see Fig. 3.11). Membranes come in various shapes (see Fig. 3.8), sizes and composition fitting to any particular need and they display several extraordinary mechanical, optical, thermal and electronic properties that make them of great interest in bio- and nanotechnology: drug delivery systems, bio-electronic devices, electrochemical sensors, energy storage, etc. They can act as separators between two liquids or they can act as filters being permeable for some kind of molecules and not others. Since 1970, the reverse osmosis membrane technology has been used for water desalination. Reverse osmosis is a physical separation process in which properly pretreated water is delivered at moderate pressures against a semi-permeable membrane. The membrane rejects most solute ions and molecules, while allowing water of very low mineral content to pass through. This process also works as an absolute barrier for cysts and most viruses. This technology is also used for the removal of inorganic contaminants such as nitrates, arsenic and pesticides. Recent experiments have shown that graphene oxide is a perfect water filter [93]. Membranes can also be used when controlled release is needed such as in drugs and drug delivery systems, chemicals in agriculture, fertilisers, pheromones, oxygenation etc (see Fig. 3.13). Polymerized membranes can be fabricated by polymerization of fluid membranes. Several polymerization methods exist such as a chemical polymerisation, irradiation of the lipid bilayer with ultraviolet light.

To summarise we have seen in this introduction that membranes play an important role

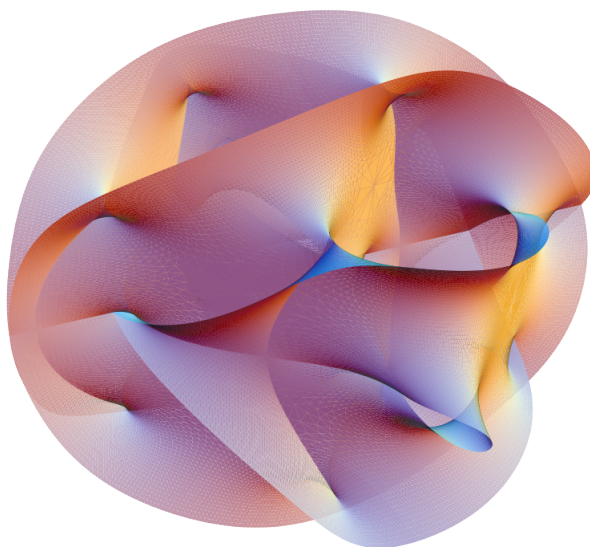


FIGURE 3.12: Three-dimensional projection of the Calabi-Yau manifold. Image from the cover of the November 2007 issue of Scientific American.

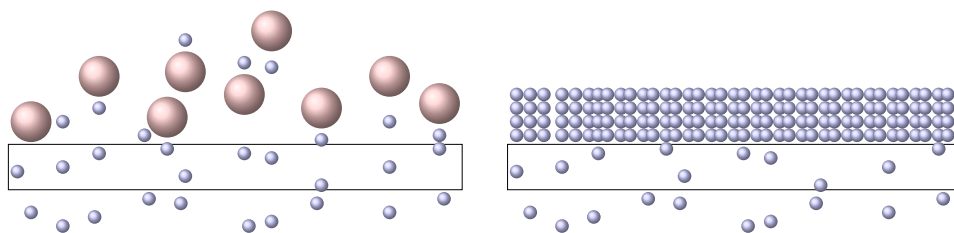


FIGURE 3.13: Applications: Separation (filters) on the right and controlled release (drugs, drug delivery systems, chemicals in agriculture, fertilisers, oxygenation, pheromones) on the left.

in many areas in biology and physics, such as cells, material science and even quantum gravity ([94], [95]). Therefore, understanding their structure as well as their long distance behaviour is crucial. Membranes can be divided in two groups: fluid and polymerized. The first ones are common objects in biology (lipid bilayers) and the second can be obtained, *e.g.*, by polymerization of these cells. Polymerized membranes are a natural extension of one dimensional

polymers to higher dimensions. In fluid membranes since the atoms or molecules are free to move, they have no shear modulus. On the contrary, polymerized membranes have a fixed connectivity. A fundamental problem is to understand the thermodynamical evolution of the shape of membranes due to fluctuations. As we have seen, membranes are rather complex systems. Therefore, in the following sections we will introduce the different models that have been proposed to explain the behaviour of membranes. These models are a simplification of real membranes but they still give great insight to the behaviour of membranes.

Mathematically, a membrane is a surface, also called a two-dimensional manifold. In mathematics, D -dimensional manifolds are generalisations of surfaces to higher dimensions and the natural language for manifolds is that of differential geometry. In the next section, we will introduce differential geometry and the properties of manifolds.

3.2 Differential Geometry of Membranes

3.2.1 Basic Definitions and Some Fundamental Properties

In this section, we discuss the mathematical description of membranes using differential geometry. Differential geometry is the branch of mathematics that studies geometrical objects in an analytical way, using differential and integral calculus (see lectures [96], [97], [98, Ch. 7]). The development of differential geometry started in the eighteenth and nineteenth centuries with the study of curves and surfaces mainly by Gauss, Riemann, Lobachevsky and Bolyai. The generalisation of the concept of curves and surfaces to higher dimensions is what we call manifolds. The name manifold comes from the German *Mannigfaltigkeit* which is the name given by Bernhard Riemann and later translated to manifold by William Clifford.

The concept of manifold is central in physics. Polymer chains on one hand and biological membranes and graphene-based sheets on another, which are of great importance in biophysics, chemistry, condensed matter physics and material science, are respectively one-dimensional and two-dimensional manifolds. Even the space-time continuum in general relativity is a Lorentzian²

²The space-time is also called a pseudo-Riemannian manifold, and often incorrectly called a Riemannian manifold.

four-dimensional manifold. Higher dimensional manifolds can also be found in string and superstring theory. In statistical physics where the phase space is a symplectic manifold³.

Mathematically, a D -dimensional manifold is an object that is locally flat (but not globally). Locally, a D -dimensional manifold is homeomorphic to the Euclidean space \mathbb{R}^D . Therefore, the manifold can be covered by patches parametrised in a local coordinate system $\{x_\mu\}$ with $\mu = 1, \dots, D$. The choice of the coordinate system is arbitrary and depends on the needs. If two neighbouring points on the manifold are parametrised by two different coordinate systems $\{x_\mu\}$ and $\{y_\mu\}$, then there is a continuous bijection between the two systems in the region where they overlap.

In this section we are only interested in smooth differentiable manifolds \mathcal{M} with an inner product g on each tangent space $\mathcal{T}_P\mathcal{M}$. These manifolds are called Riemannian manifolds. Manifolds do not need an embedding space. For instance, the space-time continuum is not a priori considered as embedded in a space of higher dimensions. But fluid and polymerized membranes, that interest us, do live in \mathbb{R}^3 . From now on, we will only focus on manifolds embedded in a d -dimensional Euclidean space \mathbb{R}^d , where $d > D$.

A D -dimensional manifold \mathcal{M} embedded in a d -dimensional Euclidean space can be parametrised by a mapping $\mathbb{R}^D \rightarrow \mathbb{R}^d$:

$$\vec{r}(x^\mu) = \{r^i(x^\mu)\} \quad (3.1)$$

where x^μ are the *internal* coordinates and r_i the *external* ones with the Greek and Latin indices running respectively from 1 to D and from 1 to d (see Fig. 3.14).

As an example, take a two-dimensional manifold embedded in a three-dimensional Euclidean space with local coordinates:

$$\vec{r}(\theta, \phi) = (\sin \theta \cos \phi, \sin \theta \sin \phi, \cos \theta) \quad (3.2)$$

$$\begin{cases} r^1 &= \sin \theta \cos \phi \\ r^2 &= \sin \theta \sin \phi \\ r^3 &= \cos \theta \end{cases} \quad (3.3)$$

³A symplectic manifold is a smooth manifold \mathcal{M} , equipped with a closed non-degenerate differential 2-form ω , called the symplectic form.

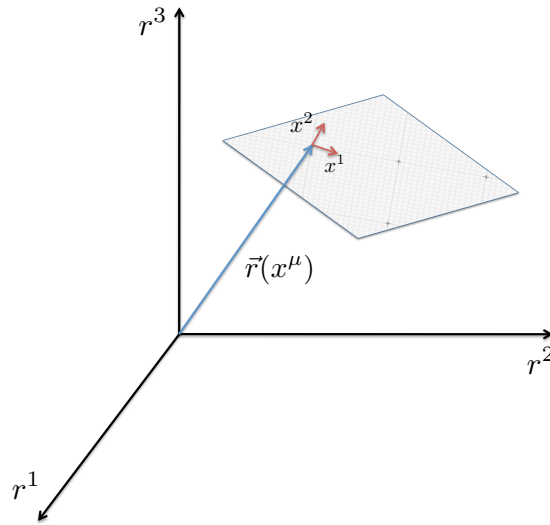


FIGURE 3.14: The vector \vec{r} represents the position of a point P of the manifold in the Euclidean space.

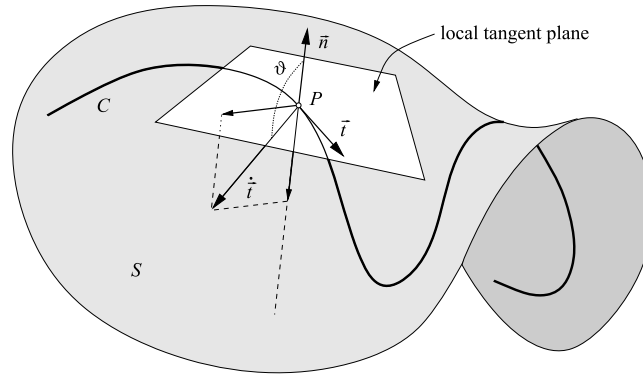
The manifold represented by these local coordinates is part of a unit sphere since $\vec{r}^2 = 1$. But these coordinates cannot represent the sphere correctly. There are two singularities, the North ($\theta = 0$) and the South poles ($\theta = \pi$). Although a sphere is locally Euclidean, it is still topologically different. This is the problem one encounters when representing the Earth on a flat map. Two maps are needed to represent a surface embedded in \mathbb{R}^3 .

The tangent vectors at each point P of the manifold reads:

$$\mathbf{e}_\mu = \frac{\partial \vec{r}}{\partial x^\mu}. \quad (3.4)$$

This vector belongs to the tangent plane $\mathcal{T}_p\mathcal{M}$ (Fig. 3.15) and they are noted in bold to make the difference with the vector that live outside of the tangent plane. The union of all the tangents planes at each point of the manifold is called the tangent bundle \mathcal{TM} .

Since the choice of the coordinates system is not unique, we need to know how to change the coordinates system. Given a new coordinate system $\{y_\mu\}_{\mu=1,\dots,D}$, the tangent vectors

FIGURE 3.15: Tangent plane at the point P [99].

read:

$$\mathbf{f}_\mu = \frac{\partial \vec{r}}{\partial y^\mu} = \frac{\partial \vec{r}}{\partial x^\nu} \frac{\partial x^\nu}{\partial y^\mu} = \mathbf{e}_\nu \frac{\partial x^\nu}{\partial y^\mu}. \quad (3.5)$$

With this we can express any given vector \vec{v} in any coordinate system:

$$\vec{v} = v^\mu \mathbf{e}_\mu = v'^\mu \mathbf{f}_\mu = v'^\mu \frac{\partial x^\nu}{\partial y^\mu} \mathbf{e}_\nu \quad (3.6)$$

where we have used the Einstein summation rule for repeated indices. We now have the expression of the new coordinates of the vector \vec{v} in terms of the old ones:

$$v'^\mu = v^\nu \frac{\partial y^\mu}{\partial x^\nu}. \quad (3.7)$$

This change of coordinates makes possible to connect different neighbouring maps.

From now on, I will concentrate on a two-dimensional manifold in three-dimensional Euclidean space:

$$\vec{r}(x, y) = (X(x, y), Y(x, y), Z(x, y)) \quad (3.8)$$

where the x and y are the internal coordinates and X , Y and Z the external ones.

The tangent vectors at each point of the manifold reads:

$$\mathbf{e}_x = \frac{\partial \vec{r}}{\partial x} = \partial_x \vec{r} \quad (3.9)$$

$$\mathbf{e}_y = \frac{\partial \vec{r}}{\partial y} = \partial_y \vec{r}. \quad (3.10)$$

Since the manifold is two-dimensional and \mathbf{e}_x and \mathbf{e}_y tangential to the surface, the normal unit vector at each point P of the manifold can be defined by:

$$\vec{n} = \frac{\mathbf{e}_x \wedge \mathbf{e}_y}{|\mathbf{e}_x \wedge \mathbf{e}_y|}. \quad (3.11)$$

The distance between two infinitesimally close points with coordinates x and $x + dx$, the arc-length ds^2 :

$$\begin{aligned} ds^2 &= (\vec{r}(x^\mu) - \vec{r}(x^\mu + dx^\mu))^2 = dx^\mu dx^\nu \frac{\partial \vec{r}}{\partial x^\mu}(x^\mu) \frac{\partial \vec{r}}{\partial x^\nu}(x^\mu) \\ &= \mathbf{e}_\mu \cdot \mathbf{e}_\nu dx^\mu dx^\nu = g_{\mu\nu} dx^\mu dx^\nu \end{aligned} \quad (3.12)$$

where $g_{\mu\nu}$ is called the *first fundamental form* or the *metric tensor*⁴.

The dual (inverse) tensor $g^{\mu\nu}$ is defined such that:

$$g_{\mu\rho} g^{\rho\nu} = \delta_\mu^\nu = \begin{cases} 1 & \text{if } \mu = \nu \\ 0 & \text{if } \mu \neq \nu \end{cases} \quad (3.14)$$

where δ_μ^ν is the Kronecker symbol. The position of the indices, up or down, shows on which space the components live, the tangent space or the cotangent space respectively. The metric tensor defines an isomorphism between the two different spaces and can be used to lower indices.

⁴In a more modern way, the first fundamental form is defined as the symmetric bilinear tensor:

$$g(X, Y) = \langle X, Y \rangle \quad (3.13)$$

where X and Y are two vector fields in the tangent bundle \mathcal{TM} . The coordinates are said to be locally orthogonal if the first fundamental form is diagonal.

The determinant of the first fundamental form reads:

$$\det(g_{\mu\nu}) = \frac{1}{2} \epsilon^{\mu\sigma} \epsilon^{\nu\rho} g_{\mu\nu} g_{\sigma\rho} \equiv g. \quad (3.15)$$

The determinant g is directly related to the arc-length ds by:

$$\begin{aligned} ds &= |\mathbf{e}_1 \wedge \mathbf{e}_2| = |\mathbf{e}_1^2 \mathbf{e}_2^2 - \mathbf{e}_1 \cdot \mathbf{e}_2|^{1/2} \\ &= (g_{11}g_{22} - g_{12}g_{21})^{1/2} = (\det g_{\mu\nu})^{1/2} = \sqrt{g}. \end{aligned} \quad (3.16)$$

There is a *second fundamental form* $C_{\mu\nu}$ which characterize the curvature of the manifold. Given a curve \mathcal{C} on the manifold parametrised by $x(t)$, the tangent vector $\vec{v}(t)$ at each point of the curve is given by:

$$\vec{v}(t) = \frac{\partial \vec{r}}{\partial t} \equiv \dot{\vec{r}}(t) \quad (3.17)$$

$$\dot{\vec{v}}(t) = \frac{\partial}{\partial t} \left(\frac{\partial \vec{r}}{\partial x^\mu} \frac{\partial x^\mu}{\partial t} \right) = \frac{\partial}{\partial t} (\mathbf{e}_\mu \dot{x}^\mu) \quad (3.18)$$

$$= \frac{\mathbf{e}_\mu}{\partial x^\nu} \frac{\partial x^\nu}{\partial t} \dot{x}^\mu + \mathbf{e}_\mu \frac{\partial \dot{x}^\mu}{\partial t} = \mathbf{e}_{\mu,\nu} \dot{x}^\mu \dot{x}^\nu + \mathbf{e}_\mu \ddot{x}^\mu. \quad (3.19)$$

Taking the scalar product with the normal unit vector \vec{n} :

$$\dot{\vec{v}}(t) \cdot \vec{n} = \mathbf{e}_{\mu,\nu} \cdot \vec{n} \dot{x}^\mu \dot{x}^\nu + \mathbf{e}_\mu \cdot \vec{n} \ddot{x}^\mu \quad (3.20)$$

where the last term in the r.h.s. vanishes by definition of the tangent vector and the normal unit vector and the term $\mathbf{e}_{\mu,\nu} \cdot \vec{n}$ is the second fundamental form $C_{\mu\nu}$. Just as the first fundamental form, the second fundamental form is a symmetric tensor since $\mathbf{e}_{\mu,\nu} = \frac{\partial^2 \vec{r}}{\partial x^\mu \partial x^\nu} = \mathbf{e}_{\nu,\mu}$. If $C_{\mu\nu}$ is diagonal, the coordinate lines are said to be conjugate. Moreover if both the first and second fundamental forms are diagonal, the coordinate lines coincide locally with the principal directions of curvature.

The first and second fundamental form serve to define the curvature of the manifold. The eigenvalues C_1 and C_2 of $C_\mu^\nu = C_{\mu\rho}g^{\rho\nu}$ are called the principal curvatures:

$$\det [C_\mu^\nu] = \det (C_{\mu\rho}g^{\rho\nu}) = \det (C_{\mu\rho}) \det (g^{\rho\nu}) \quad (3.21)$$

$$= \frac{\det (C_{\mu\rho})}{\det (g_{\rho\nu})} = \frac{C}{g} \quad (3.22)$$

where g and C are the determinants of the first and second fundamental forms respectively and the eigenvectors correspond to the principal directions of curvature.

Another expression for the second fundamental form can be derived by differentiating the scalar product $e_\mu \cdot \vec{n} = 0$:

$$\frac{\partial}{\partial x^\nu} (e_\mu \cdot \vec{n}) = e_{\mu,\nu} \cdot \vec{n} + e_\mu \cdot \vec{n}_{,\nu} = 0 \quad (3.23)$$

which leads to:

$$-e_\mu \cdot \vec{n}_{,\nu} = e_{\mu,\nu} \cdot \vec{n} = C_{\mu\nu}. \quad (3.24)$$

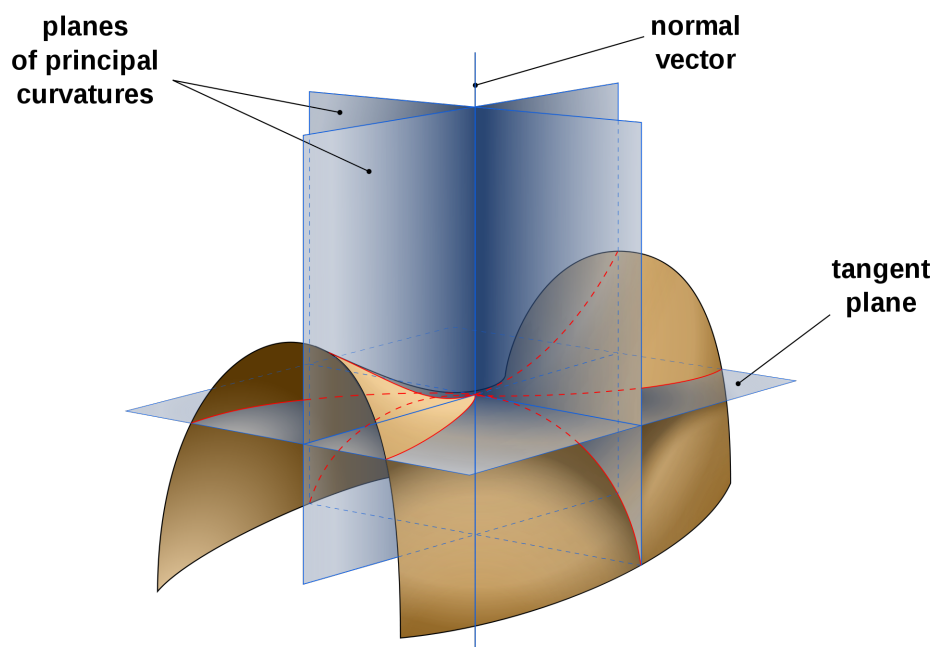
Given a point P on the manifold, the tangent vectors at that point constitutes a unique tangent plane. And there exists an infinite number of planes that are normal to the tangent plane. These normal planes' intersection with the manifold is a curve with radius of curvature $R(\alpha)$. The minimum and maximum of the radius of curvature $R(\alpha)$ are called the principal radius of curvature R_1 and R_2 respectively. And the principal curvatures are defined as the inverse of the principal radius of curvature:

$$C_i = \frac{1}{R_i}. \quad (3.25)$$

With combinations of the principal curvatures, we can construct two quantities that have a fundamental geometrical meaning, the mean curvature H and the Gaussian curvature K :

$$H = \frac{1}{2} \text{Tr} (C_\mu^\nu) = \frac{1}{2} (C_1 + C_2) \quad (3.26)$$

$$K = \det (C_\mu^\nu) = C_1 C_2 \quad (3.27)$$

FIGURE 3.16: Image by Eric Gaba (*Wikipedia*).

From these definitions, we can see that the mean and Gaussian curvatures are invariant under reparametrisation since they are a trace and a determinant respectively. Note that the convention regarding the sign of the curvature is arbitrary.

Using the second expression of the second fundamental forms, we get the equations of the mean and Gaussian curvatures in terms of the normal unit vector:

$$H = -\frac{1}{2} \nabla \vec{n} \quad (3.28)$$

$$K = -\frac{1}{2} \nabla (\vec{n} \cdot (\nabla \vec{n}) - (\vec{n} \cdot \nabla) \vec{n}) \quad (3.29)$$

where $\nabla \vec{n} = e_\mu \partial^\mu \vec{n}$.

Carl Friedrich Gauss proved that the Gaussian curvature does not depend on the way the manifold is embedded in the Euclidean space. He called this theorem *Theorema Egregium* for remarkable theorem in Latin. The Gaussian curvature K is an intrinsic property of the surface.

Gauss presented the theorem in this way (translated from Latin):

Theorem 3.1 (Gauss's Theorema Egregium (translated from Latin)). *Thus the formula of the preceding article leads itself to the remarkable Theorem. If a curved surface is developed upon any other surface whatever, the measure of curvature in each point remains unchanged.*

Theorem 3.2 (Gauss's Theorema Egregium (in modern language)⁵). *The Gaussian curvature of a surface is an intrinsic property of the manifold and hence does only depend on the first fundamental form (and its derivatives).*

An explicit expression for the Gaussian curvature in terms of the first fundamental form is provided by the Brioschi's formula:

$$K = \frac{C}{g} = \frac{R_{1212}}{g} \quad (3.30)$$

where the fourth rank tensor $R_{\mu\nu\rho\sigma}$ is the Riemann curvature tensor:

$$R_{\mu\nu\rho\sigma} = g_{\mu\lambda} R_{\nu\rho\sigma}^{\lambda} \quad (3.31)$$

$$R_{\nu\rho\sigma}^{\lambda} = \frac{\partial}{\partial x^{\rho}} \Gamma_{\nu\sigma}^{\lambda} - \frac{\partial}{\partial x^{\sigma}} \Gamma_{\nu\rho}^{\lambda} + \left(\Gamma_{\rho\omega}^{\lambda} \Gamma_{\nu\sigma}^{\omega} - \Gamma_{\sigma\omega}^{\lambda} \Gamma_{\nu\rho}^{\omega} \right) \quad (3.32)$$

where $\Gamma_{\nu\rho}^{\mu}$ are the Christoffel symbols:

$$\Gamma_{\nu\rho}^{\mu} = g^{\mu\lambda} \Gamma_{\lambda\nu\rho} = \frac{1}{2} g^{\mu\lambda} \left(\frac{\partial}{\partial x^{\rho}} g_{\lambda\nu} + \frac{\partial}{\partial x^{\nu}} g_{\lambda\rho} - \frac{\partial}{\partial x^{\lambda}} g_{\nu\rho} \right). \quad (3.33)$$

An important theorem in differential geometry is the Gauss-Bonnet theorem that relates the geometry of a two-dimensional manifold \mathcal{M} to its topology (the total curvature of a compact surface is 2π times its Euler characteristic χ)⁶:

$$\int_{\mathcal{M}} ds K = 2\pi\chi(\mathcal{M}) = 4\pi(1 - g(\mathcal{M})) \quad (3.34)$$

⁵ In mathematical language, the theorem may be stated as follows: The Gaussian curvature of a surface is invariant under local isometry.

⁶ The Gauss-Bonnet theorem is only valid for a two-dimensional compact manifold without any border.

where χ is the Euler characteristic and g the genus of the surface which characterizes the topology of the surface, i.g.:

$$\begin{cases} g = 0, \text{ sphere} \\ g = 1, \text{ torus} \\ g = 2, \text{ double torus} . \end{cases}$$

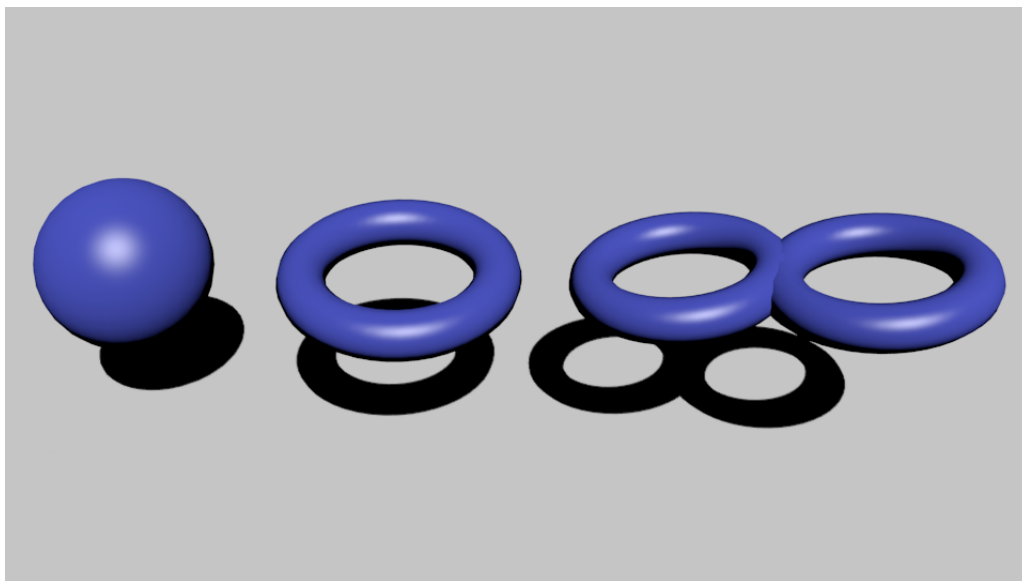


FIGURE 3.17: Sphere ($g=0$), torus ($g=1$) and double-torus ($g=2$).

3.2.2 Monge Parametrization

As we have already said different parametrisations can be used to describe a manifold. A very useful parametrisation when dealing with an almost flat surface is the Monge parametrization. We take an orthogonal coordinate system $\{x, y\}$ and the deviation of the manifold from a flat surface is described by a height function h :

$$\mathbb{R}^2 \rightarrow \mathbb{R}^3 \tag{3.35}$$

$$(x, y) \mapsto \vec{r} = (x, y, h(x, y)) . \tag{3.36}$$

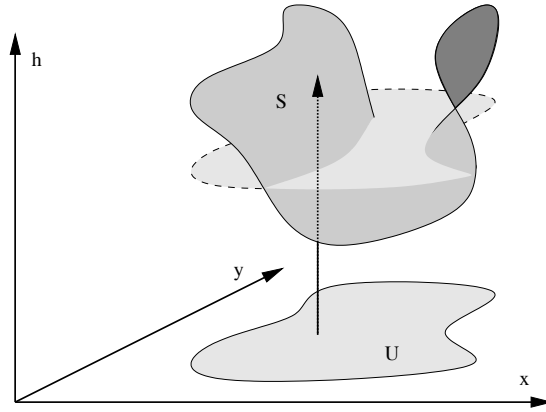


FIGURE 3.18: Illustration of the Monge parametrisation [99].

With this parametrisation, the tangent vectors reads:

$$\begin{aligned} \mathbf{e}_x &= (1, 0, \partial_x h) \\ \mathbf{e}_y &= (0, 1, \partial_y h). \end{aligned} \quad (3.37)$$

This leads to the following expression for the metric tensor $g_{\mu\nu}$:

$$g_{\mu\nu} = \begin{pmatrix} 1 + (\partial_x h)^2 & \partial_x h \partial_y h \\ \partial_x h \partial_y h & 1 + (\partial_y h)^2 \end{pmatrix} \quad (3.38)$$

and its determinant now reads:

$$\det(g_{\mu\nu}) = g = 1 + |\nabla h|^2 \quad (3.39)$$

where $|\nabla h|^2 = (\partial_x h)^2 + (\partial_y h)^2$.

From the expressions (3.37) and (3.39) of respectively the tangent vectors and the metric tensor, we derive the expression of the normal unit vector in the Monge parametrization:

$$\vec{n} = \frac{(-\partial_x h, -\partial_y h, 1)}{\sqrt{g}} = \frac{(-\partial_x h, -\partial_y h, 1)}{\sqrt{1 + |\nabla h|^2}}. \quad (3.40)$$

Now we can derive the expressions of the Mean and Gaussian curvatures by replacing (3.40) into (3.28) and (3.29):

$$H = \frac{\left(1 + (\partial_x h)^2\right) \partial_y \partial_y h - 2 \partial_x h \partial_y h \partial_x \partial_y h + \left(1 + (\partial_y h)^2\right) \partial_x \partial_x h}{\left(1 + |\nabla h|^2\right)^{3/2}} \quad (3.41)$$

$$K = \frac{\partial_x \partial_x h \partial_y \partial_y h - (\partial_x \partial_y h)^2}{\left(1 + |\nabla h|^2\right)^2}. \quad (3.42)$$

3.3 Deformations

In addition to the curvature we know from elastic theory that there are two elastic deformations that may contribute to the energy of a solid: *stretching* and *shearing* (see fig. 3.19).

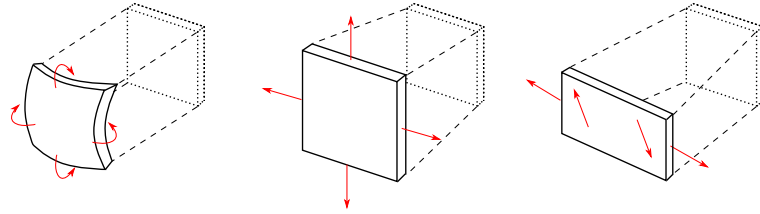


FIGURE 3.19: Deformations from left to right: bending, stretching, shearing (Image from the Thesis of Camilla Barbetta).

Now that we know which contributions may enter the energy of a membrane let us see how they are implemented depending on which type of membrane we are considering.

3.4 Long-Range Behaviour of Fluid Membranes

3.4.1 The Model

In 1970, Canham proposed a model for fluid membranes in the special case of red blood cells [100]. This model was generalised three years later by Helfrich [101]. The Canham-Helfrich model describes the contribution of the membrane bending to its free energy:

$$F_b = \int_{\mathcal{M}} ds \left\{ 2\kappa (H - C_0)^2 + \bar{\kappa} K \right\} \quad (3.43)$$

where H and K are respectively the mean and Gaussian curvatures. C_0 is the spontaneous curvature and κ and $\bar{\kappa}$ are the bending coupling constants or bending rigidities. Note that the bending coupling constants have the dimension of an energy since the Gaussian curvature and the square of the mean curvature have the inverse dimension of a surface and with integrate over a surface.

The spontaneous curvature C_0 translates *e.g.* the asymmetry between the two leaflets of the membrane. The spontaneous curvature plays an important role when the membrane has proteins with a non-symmetric shape which deforms the two leaflets differently. Therefore, the spontaneous curvature must be included. However, in most cases, the results one obtains with $C_0 = 0$ are accurate in comparison with the experimental data. This justifies the assumption of a vanishing spontaneous curvature we make in what follows.

The Helfrich-Canham free energy without spontaneous curvature is simply:

$$F_b = \int_{\mathcal{M}} ds \left\{ 2\kappa H^2 + \bar{\kappa} K \right\} . \quad (3.44)$$

The bending rigidity κ must be positive for the stability of the membrane. The Canham-Helfrich free energies (3.44) is invariant under local reparametrisation, *i.e.* under change of internal coordinate system, since it contains terms constructed with only geometrical quantities. This means that the energy of the membrane does only depend on the shape of the membrane and not on the position of its constituents. The invariance under reparametrisation is directly connected to the fluid nature of the membrane.

From the Gauss-Bonnet theorem (3.34), we see that the Gaussian bending energy is a constant except if the topology of the membrane changes. The topology may change by fission or fusion but this is a quite rare event for a phospholipid membrane. The fusion or fission are controlled by a machinery in biological systems. Therefore the Gaussian bending energy may be dropped. We are only left with the contribution of the mean curvature to the bending energy.

The Helrich-Canham free energy without spontaneous curvature simply reads:

$$F_b = 2\kappa \int_{\mathcal{M}} ds H^2 . \quad (3.45)$$

The contribution to the total energy comes from the bending deformation, a surface term and self-avoidance:

$$\begin{aligned} F &= F_b + F_{\text{tension}} + F_{\text{self-avoidance}} \\ &= 2\kappa \int_{\mathcal{M}} ds H^2 + \tau \int_{\mathcal{M}} ds + \frac{b}{2} \int ds ds' \delta(\vec{r}(s) - \vec{r}(s')) . \end{aligned} \quad (3.46)$$

The number of molecules of the membrane being fixed there is no fluctuations in area. Therefore the tension term vanishes. This is different from the problem of interfaces where the energy is dominated by surface tension. Self-avoidance term is neglected in what follows.

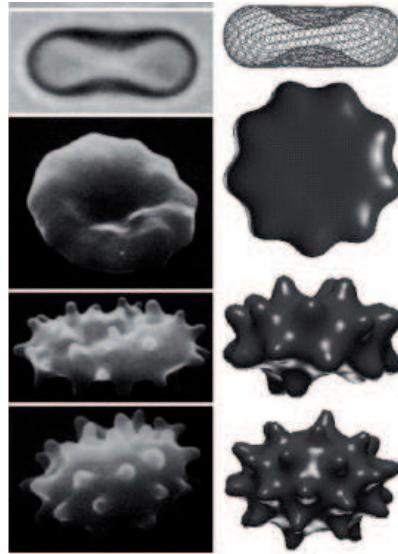


FIGURE 3.20: Red blood cell's shapes [102].

3.4.2 Fluid Membranes in Monge Parametrization

To lowest order in the height h , the mean curvature in the Monge Parametrization (3.41) reads:

$$H = \frac{1}{2} (\partial_x^2 h + \partial_y^2 h) . \quad (3.47)$$

With this approximation the free energy reads:

$$\begin{aligned} F &= 2\kappa \int dx dy \sqrt{g} \frac{(\partial_x^2 h + \partial_y^2 h)^2}{4} \\ &= \frac{\kappa}{2} \int dx dy \sqrt{1 + (\partial_x h)^2 + (\partial_y h)^2} (\partial_x^2 h + \partial_y^2 h)^2 \end{aligned} \quad (3.48)$$

$$\approx \frac{\kappa}{2} \int dx dy (\partial_x^2 h + \partial_y^2 h)^2 = \frac{\kappa}{2} \int dx dy (\nabla^2 h)^2 . \quad (3.49)$$

In Fourier space:

$$F = \int_{\mathbf{q}} \mathbf{q}^4 h(\mathbf{q}) h(-\mathbf{q}) = \int_{\mathbf{q}} \mathbf{q}^4 |h(\mathbf{q})|^2 \quad (3.50)$$

where we have used $h(-\mathbf{q}) = h^*(\mathbf{q})$:

$$h(\mathbf{q}) = \int_{\mathbf{x}} h(\mathbf{x}) e^{i\mathbf{q} \cdot \mathbf{x}} . \quad (3.51)$$

Now, we need to calculate the thermal average of the height-height correlation function (in the following, we will drop the subscript thermal for the average). By definition, this average reads:

$$\langle h(\mathbf{q}) h^*(\mathbf{q}) \rangle = \frac{\int \mathcal{D}h |h(\mathbf{q})|^2 e^{-F/k_B T}}{\int \mathcal{D}h e^{-F/k_B T}} . \quad (3.52)$$

In the harmonic approximation, this correlation function is easily evaluated because the free energy is Gaussian:

$$\langle x^2 \rangle = \frac{\int dx x^2 e^{-\alpha x^2}}{\int dx e^{-\alpha x^2}} = -\frac{\partial}{\partial \alpha} \ln \left(\int dx e^{-\alpha x^2} \right) = \frac{1}{2\alpha} . \quad (3.53)$$

The height correlation function reads:

$$\langle |h(\mathbf{q})|^2 \rangle = \frac{k_B T}{\kappa \mathbf{q}^4}. \quad (3.54)$$

Each harmonic mode contributes with a term $\frac{k_B T}{2}$ (equipartition theorem). In real space we find:

$$\langle h(0)h(\mathbf{x}) \rangle = k_B T \int_q \frac{1}{\kappa \mathbf{q}^4} \propto L^2. \quad (3.55)$$

Remark: with a tension term in the free energy $F_\tau = \int_q \tau \mathbf{q}^2 |h(\mathbf{q})|^2$, the height correlation functions reads:

$$\langle |h(\mathbf{q})|^2 \rangle = \frac{k_B T}{\kappa \mathbf{q}^4 + \tau \mathbf{q}^2} \quad (3.56)$$

The height fluctuations grow linearly with the size of the membrane. This means that two-dimensional fluid membranes are crumpled at all temperatures $T \neq 0$. Including higher order terms in the field h induces a scale dependence in the bending rigidity which is computed using the renormalization group [103]:

$$\kappa(L) = \kappa - \frac{3k_B T}{4\pi} \ln \left(\frac{L}{a} \right) \quad (3.57)$$

where L is the membrane size and a correspond to a microscopic lattice size. This equation shows that the bending rigidity decreases with the size of the membrane. Thus the height fluctuations eq. (3.55) grow even faster and the membrane remains crumpled. However, from RG calculation for any dimension $D > 2$ a fluid membranes exhibit a phase transition between a crumpled and a flat phase at finite temperature.

3.5 Polymerized Membranes

3.5.1 The Model

Lets us now consider polymerized membranes. Since the connectivity between the molecules is fixed a network is formed and shearing and stretching appear which affect the energy of the

membrane. In this section we show how this in-plane elasticity changes the thermodynamical behaviour and thus the shape of the membrane.

The bending energy is given by:

$$F_b = \frac{\kappa}{2} \int d^2x C_\mu^\nu C_\nu^\mu. \quad (3.58)$$

This energy is not coordinate independent because of the fixed connectivity. At rest the position of a point on the membrane is described by:

$$\vec{r}_0(x) = \zeta(x, y, 0) = \zeta \mathbf{x} \quad (3.59)$$

where $\mathbf{x} \equiv (x, y)$. If $\zeta = 0$ the membrane is crumpled and if $\zeta \neq 0$ it is flat up to small fluctuations. The metric tensor reads:

$$g_{\mu\nu}^0 = \partial_\mu \vec{r}_0 \cdot \partial_\nu \vec{r}_0 = \zeta^2 \delta_{\mu\nu}. \quad (3.60)$$

Due to fluctuations we have a deviation from the ground state \vec{r}_0 and the position now reads:

$$\vec{r}(\mathbf{x}) = (\mathbf{u}(\mathbf{x}) + \zeta \mathbf{x}, h(\mathbf{x})) \quad (3.61)$$

where \mathbf{u} is an *in-plane phonon* field and h corresponds to *out-of-plane height fluctuations*. From elasticity theory we know that the shearing and stretching contributions are given by:

$$F_{\text{elastic}} = \int d^2x \left\{ \mu \sigma_{\alpha\beta}^2 + \frac{\lambda}{2} \sigma_{\alpha\alpha}^2 \right\} \quad (3.62)$$

where μ and λ are the Lamé coefficients corresponding respectively to stretching and shearing deformations and $\sigma_{\alpha\beta}$ is the strain tensor given by:

$$\sigma_{\alpha\beta} = \partial_\alpha \vec{r} \cdot \partial_\beta \vec{r} - \zeta \delta_{\alpha\beta}. \quad (3.63)$$

With this contribution in addition to the bending energy and self-avoidance the total free energy reads:

$$F[\vec{r}] = \int d^2x \left\{ \frac{\kappa}{2} C_\alpha^\beta C_\beta^\alpha + \mu \sigma_{\alpha\beta}^2 + \frac{\lambda}{2} \sigma_{\alpha\alpha}^2 \right\} + \frac{b}{2} \int d^2x d^2y \delta^{(3)}(\vec{r}(\mathbf{x}) - \vec{r}(\mathbf{y})) \quad (3.64)$$

3.5.2 Mean Field Theory

Since the free energy is not purely geometric we re-write it in a more convenient way using explicitly the field \vec{r} and generalize it to a D -dimensional membrane embedded in a d -dimensional space. The free energy is given by:

$$F[r] = \int d^D x \left\{ \frac{\kappa}{2} (\partial_\mu \partial_\mu \vec{r})^2 + u (\partial_\mu \vec{r} \cdot \partial_\nu \vec{r})^2 + v (\partial_\mu \vec{r} \cdot \partial_\mu \vec{r})^2 + \frac{\tau}{2} (\partial_\mu \vec{r} \cdot \partial_\mu \vec{r}) \right\} \quad (3.65)$$

where τ is a tension term equivalent of the mass term of the $O(n)$ -model. From this form of the free energy we see that the equivalent of the order parameter $\vec{\phi}$ of the $O(n)$ -model is $\partial_\mu \vec{r}$ and there is no term depending directly on \vec{r} without a derivative. This comes from the translational invariance coupled with the fact that the field \vec{r} lives in the physical Euclidean space contrary to the field $\vec{\phi}$. Therefore membrane theory is said to be a derivative theory. As a consequence two terms of order \vec{r}^4 appear in the free energy and we have the constraint $\partial_\mu \partial_\nu \vec{r} = \partial_\nu \partial_\mu \vec{r}$. In the ground state \vec{r}_0 we find a mean field effective potential:

$$U(\zeta) = D \zeta^2 \left(\frac{\tau}{2} + \zeta^2 (u + Dv) \right) \quad (3.66)$$

and minimizing the potential we find two solutions depending on the sign of τ :

$$\zeta^2 = \begin{cases} 0 & : \tau \geq 0 \\ \frac{-\tau}{4(u+Dv)} & : \tau < 0. \end{cases} \quad (3.67)$$

When τ is positive, the membrane is in its high-temperature crumpled phase $\zeta = 0$. And when τ is negative below $T = T_c$, the membrane undergoes a phase transition from the crumpled phase to a low-temperature ordered flat phase $\zeta \neq 0$ (see fig. 3.21) and we have:

$$\frac{\tau}{2} = -2\zeta (u + Dv) \quad (3.68)$$

and we retrieve Eq. (3.64).

The mean field Landau theory is only valid if we are above the upper critical dimension. As for the $O(n)$ -model, the upper critical dimension for polymerized membranes is $D_{uc} = 4$ which is far from the physical case $D = 2$. Since the canonical dimension of the couplings u

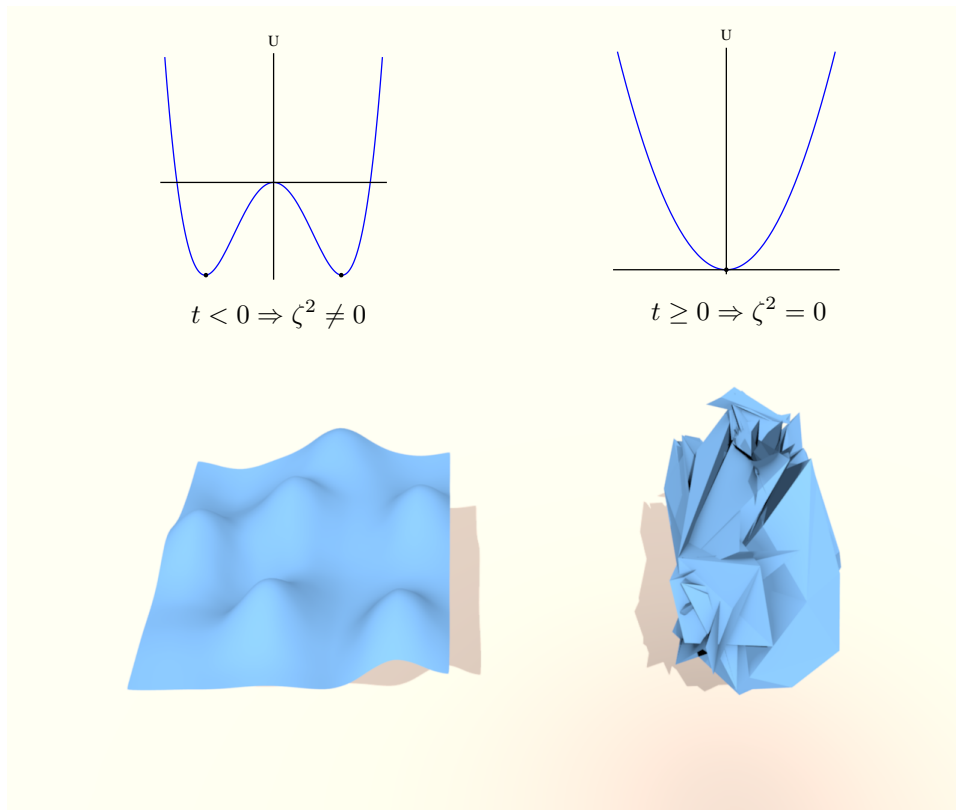


FIGURE 3.21: The mean field potential of polymerized membranes as a function of the order parameter. On the left, the membrane is in its low-temperature flat phase and on the right the membrane is in a high-temperature crumpled phase.

and v is:

$$[u] = [v] = D - 4 \quad (3.69)$$

they are of order $\epsilon = 4 - D$ in the vicinity of the upper critical dimension. This means that one can use a weak-coupling perturbative expansion in u and v in the vicinity of D_{uc} .

3.5.3 Perturbative RG for the Crumpled-to-Flat Transition

From the free energy eq. (3.65) Paczuski *et al.* [104] derived the flow equations of the couplings u and v within a weak-coupling ϵ -expansion:

$$\beta_u = -\epsilon u + \frac{1}{48\pi^2} \{ (d+21)u^2 + 20uv + 4v^2 \} \quad (3.70)$$

$$\beta_v = -\epsilon v + \frac{1}{48\pi^2} \left\{ \frac{d+15}{2}u^2 + (6d+34)uv + (12d+14)v^2 \right\}. \quad (3.71)$$

The stability of the fixed points of these equations depend on the dimension d :

- for $d > d_c(D=4) = 219$: there is one and only one non-trivial infrared stable fixed point corresponding to the crumpled-flat transition. The transition is of second order and we can get the critical exponents at order ϵ . Note that the anomalous dimension η is vanishing because it is of order ϵ^2 .
- for $d < d_c$: the stable fixed point disappears and the transition becomes of first order induced by fluctuations.

The important question here is whether the crumpled-flat transition of a two-dimensional membrane in three-dimensional space is a first or a second order transition. This information cannot be extracted from this computation since taking $D = 2$ gives an $\epsilon = 2$ which means that one needs much higher, probably five or six, loop orders to get accurate results.

3.5.4 The normal-normal Correlation Function in the Harmonic Approximation

Below the critical temperature, the membrane is flat. But unless the membrane is at zero temperature, it is not completely flat because of thermal fluctuations. At finite temperatures, there is a competition between the energy that flattens the membrane and the entropy that bends it. This induces ripples. The normal-normal correlation function $G_n(\vec{r}) = \langle \vec{n}(\vec{r}) \cdot \vec{n}(0) \rangle$ characterizes the flatness of the membrane. For a completely flat membrane the correlation is equal to 1 and for almost flat one $0 < G_n < 1$.

We recall that the normal unit vector in the Monge parametrisation is given by:

$$\vec{n} = \frac{(-\partial_x h, -\partial_y h, 1)}{\sqrt{1 + |\nabla h|^2}} \quad (3.72)$$

and to the second order in h :

$$\vec{n} = \left(-\partial_x h, -\partial_y h, 1 - \frac{1}{2} |\nabla h|^2 \right) + o(h^3) \quad (3.73)$$

In this approximation, the scalar product $\vec{n}(r_1) \cdot \vec{n}(r_2)$ reads:

$$\begin{aligned} \vec{n}(\vec{r}_1) \cdot \vec{n}(\vec{r}_2) &= 1 + \partial_x h(\mathbf{x}_1) \cdot \partial_x h(\mathbf{x}_2) + \partial_y h(\mathbf{x}_1) \cdot \partial_y h(\mathbf{x}_2) \\ &\quad - \frac{1}{2} \left\{ (\partial_x h(\mathbf{x}_1))^2 + (\partial_y h(\mathbf{x}_1))^2 + (\partial_x h(\mathbf{x}_2))^2 + (\partial_y h(\mathbf{x}_2))^2 \right\} \\ &= 1 - \frac{1}{2} \left\{ |\partial_x(h(\mathbf{x}_1) - h(\mathbf{x}_2))|^2 + |\partial_y(h(\mathbf{x}_1) - h(\mathbf{x}_2))|^2 \right\} \end{aligned} \quad (3.74)$$

where $\partial_x = \frac{\partial}{\partial x}$.

In Fourier space, the height function h reads:

$$h(\mathbf{x}) = \int_q e^{i\mathbf{q} \cdot \mathbf{x}} h(q) \quad (3.75)$$

where $\int_q = \int \frac{d^D q}{(2\pi)^D}$ with D the membrane dimension (here $D = 2$). We start with the part with derivative over x of eq. (3.74):

$$\begin{aligned} \partial_x(h(\mathbf{x}_1) - h(\mathbf{x}_2)) &= \partial_x \int_q h(q) (e^{i\mathbf{q} \cdot \mathbf{x}_1} - e^{i\mathbf{q} \cdot \mathbf{x}_2}) \\ &= \int_q h(q) q_x (e^{i\mathbf{q} \cdot \mathbf{x}_1} - e^{i\mathbf{q} \cdot \mathbf{x}_2}) \end{aligned} \quad (3.76)$$

which leads to:

$$|\partial_x(h(\mathbf{x}_1) - h(\mathbf{x}_2))|^2 = \int_{q, q'} h(\mathbf{q}) h^*(\mathbf{q}') q_x q'_x (e^{i\mathbf{q} \cdot \mathbf{x}_1} - e^{i\mathbf{q} \cdot \mathbf{x}_2}) (e^{-i\mathbf{q}' \cdot \mathbf{x}_1} - e^{-i\mathbf{q}' \cdot \mathbf{x}_2}) \quad (3.77)$$

The average contains two different averages a spatial and a thermal average. Lets start with the spatial average:

$$\begin{aligned}
\langle |\partial_x(h(\mathbf{x}_1) - h(\mathbf{x}_2))|^2 \rangle_x &= \int_{\mathbf{x}_1, \mathbf{x}_2} \delta(\mathbf{x} - (\mathbf{x}_1 - \mathbf{x}_2)) \int_{q, q'} h(q) h^*(q') q_x q'_x \\
&\times (e^{i\mathbf{q} \cdot \mathbf{x}_1} - e^{i\mathbf{q} \cdot \mathbf{x}_2}) (e^{-i\mathbf{q}' \cdot \mathbf{x}_1} - e^{-i\mathbf{q}' \cdot \mathbf{x}_2}) \\
&= \int_{\mathbf{x}_1} \int_{q, q'} h(q) h^*(q') q_x q'_x (e^{i\mathbf{q} \cdot \mathbf{x}_1} - e^{i\mathbf{q} \cdot (\mathbf{x}_1 - \mathbf{x})}) (e^{-i\mathbf{q}' \cdot \mathbf{x}_1} - e^{-i\mathbf{q}' \cdot (\mathbf{x}_1 - \mathbf{x})}) \\
&= \int_{r_1} \int_{q, q'} h(q) h^*(q') q_x q'_x e^{i(\mathbf{q} - \mathbf{q}') \cdot \mathbf{x}_1} (1 - e^{-i\mathbf{q} \cdot \mathbf{x}}) (1 - e^{i\mathbf{q}' \cdot \mathbf{x}}) \\
&= \int_{q, q'} \delta(\mathbf{q} - \mathbf{q}') h(q) h^*(q') q_x q'_x (1 - e^{-i\mathbf{q} \cdot \mathbf{x}}) (1 - e^{i\mathbf{q}' \cdot \mathbf{x}}) \\
&= \int_q h(q) h^*(q) q_x^2 (1 - e^{-i\mathbf{q} \cdot \mathbf{x}}) (1 - e^{i\mathbf{q} \cdot \mathbf{x}}) \\
&= \int_q h(q) h^*(q) q_x^2 \{2 - 2 \cos(\mathbf{q} \cdot \mathbf{x})\} \tag{3.78}
\end{aligned}$$

Similarly $\langle |\partial_y(h(\mathbf{x}_1) - h(\mathbf{x}_2))|^2 \rangle_x$ reads:

$$\langle |\partial_y(h(\mathbf{x}_1) - h(\mathbf{x}_2))|^2 \rangle_x = 2 \int_q h(\mathbf{q}) h^*(\mathbf{q}) q_y^2 \{1 - \cos(\mathbf{q} \cdot \mathbf{x})\} . \tag{3.79}$$

Replacing these results in the normal-normal correlation function leads to:

$$\langle \vec{n}(\vec{r}) \cdot \vec{n}(0) \rangle = 1 - \int_q \langle |h(\mathbf{q})|^2 \rangle_{\text{thermal}} q^2 (1 - \cos(\mathbf{q} \cdot \mathbf{x})) \tag{3.80}$$

where $q = |\mathbf{q}|$.

In the harmonic approximation the height correlation function reads:

$$\langle |h(\mathbf{q})|^2 \rangle_{\text{thermal}} = \frac{k_B T}{\kappa q^4} \tag{3.81}$$

which results from the equipartition theorem. The normal-normal correlation function in direct space is given by:

$$\langle \vec{n}(r) \cdot \vec{n}(0) \rangle = 1 - \int_q \frac{k_B T}{\kappa q^2} (1 - \cos(\mathbf{q} \cdot \mathbf{x})) . \tag{3.82}$$

Polymerized membranes in the harmonic approximation have divergent height fluctuations $\langle |h|^2 \rangle$ which means, that the out-of-plane fluctuations grow linearly with the size, leading to the destruction of any finite size membrane. Similarly, the normal correlation function behaves as $\langle \vec{n}(r) \cdot \vec{n}(0) \rangle \propto \ln(r)$. This means that the fluctuations destroy the flat phase which is in contradiction with the result from the ϵ -expansion. To avoid this divergence, we need to take into account the coupling between bending and stretching, *i.e.* go beyond the harmonic approximation. This result of the harmonic approximation is just an extension of the result found by Rudolf Peierls for one-dimensional systems [105].

3.5.5 Self-Consistent Screening Approximation (SCSA)

In the previous section, we saw that in the harmonic approximation, the flat phase cannot exist because of fluctuations. In this section, we show how this situation changes when we take into account the coupling between the out-of-plane bending and the in-plane elasticity and we recover the existence of the phase transition as in the ϵ -expansion. Nelson and Peliti [106] found that the coupling between the out-of-plane bending and in-plane phonons renormalized the bending rigidity $\kappa \propto q^{-\eta}$ with an anomalous dimension $\eta = 1$. The free energy now reads:

$$F = \int_x \left\{ \frac{\kappa}{2} (\nabla^2 \vec{h})^2 + \mu \sigma_{\alpha\beta}^2 + \frac{\lambda}{2} \sigma_{\alpha\alpha}^2 \right\} \quad (3.83)$$

where we have kept only the dominant term in the bending part. Within the Monge parametrization the strain tensor reads:

$$\sigma_{\alpha\beta} = \partial_\alpha \mathbf{u}_\beta + \partial_\beta \mathbf{u}_\alpha + \partial_\alpha \vec{h} \cdot \partial_\beta \vec{h} + \partial_\alpha \mathbf{u} \cdot \partial_\beta \mathbf{u} \quad (3.84)$$

where \vec{h} is now a $d - D$ vector field. The last term is of higher order in \mathbf{u} and will be neglected in the following ⁷. The term $\partial_\alpha \vec{h} \cdot \partial_\beta \vec{h}$ couples the out-of-plane bending with the in-plane elasticity. When this term is neglected, we are in the harmonic approximation. Including this term makes the problem highly non-linear.

This free energy is quadratic in the phonon modes u_α . Hence, we can perform a Gaussian integration to eliminate these modes [106]. The Gaussian integration can be efficiently

⁷This term must be included for the second order ϵ^2 of the weak-coupling ϵ -expansion.

performed by observing that $\partial_\alpha \vec{h} \cdot \partial_\beta \vec{h}$ can be written, as can any symmetric second-rank two-dimensional tensor, in the form [107]:

$$\partial_\alpha \vec{h} \cdot \partial_\beta \vec{h} = \partial_\alpha v_\beta + \partial_\beta v_\alpha + \mathcal{P}_{\alpha\beta}^\perp f \quad (3.85)$$

where v_α is a suitable two-dimensional vector field, $\mathcal{P}_{\alpha\beta}^\perp = (\nabla^2)^{-1} \epsilon_{\alpha\gamma} \epsilon_{\beta\sigma} \partial_\gamma \partial_\sigma$ is the transverse projector and f a scalar function. In Fourier space after integration, the effective free energy reads:

$$F_{\text{eff}} = \frac{\kappa}{2} \int_{\mathbf{q}} \mathbf{q}^4 |h(\mathbf{q})|^2 + \frac{1}{4(d-D)} \int_{\mathbf{q}_1, \mathbf{q}_2, \mathbf{q}_3, \mathbf{q}_4} \delta(\mathbf{q}_1 + \mathbf{q}_2 + \mathbf{q}_3 + \mathbf{q}_4) \times \mathcal{R}_{\alpha\beta, \gamma\delta}(\mathbf{q}_1 + \mathbf{q}_2) q_{1\alpha} q_{2\beta} q_{3\gamma} q_{4\delta} \vec{h}(\mathbf{q}_1) \cdot \vec{h}(\mathbf{q}_2) \vec{h}(\mathbf{q}_3) \cdot \vec{h}(\mathbf{q}_4). \quad (3.86)$$

The four-rank tensor \mathcal{R} is transverse to \mathbf{q} and can be written as:

$$\mathcal{R}(p) = K_0 N(q) + \mu M(q) \quad (3.87)$$

$$N_{\alpha\beta, \gamma\delta} = \frac{1}{D-1} \mathcal{P}_{\alpha\beta}^\perp \mathcal{P}_{\gamma\delta}^\perp \quad (3.88)$$

$$M_{\alpha\beta, \gamma\delta} = \frac{1}{2} \left(\mathcal{P}_{\alpha\gamma}^\perp \mathcal{P}_{\beta\delta}^\perp + \mathcal{P}_{\alpha\delta}^\perp \mathcal{P}_{\beta\gamma}^\perp \right) - N_{\alpha\beta, \gamma\delta} \quad (3.89)$$

where the transverse projector is expressed in Fourier space $\mathcal{P}_{\alpha\beta}^\perp = \delta_{\alpha\beta} - \frac{q_\alpha q_\beta}{\mathbf{q}^2}$ and K_0 a combination of the Lamé coefficient $K_0 = \frac{\mu(2\mu+D\lambda)}{(2\mu+\lambda)}$.

We are interested in the height correlation function:

$$\langle h_\alpha(\mathbf{q}) h_\beta^*(\mathbf{q}) \rangle = \delta_{\alpha\beta} G_h(\mathbf{q}) \quad (3.90)$$

where $G_h^{-1} = \kappa_R(\mathbf{q}) \mathbf{q}^4 = G_0^{-1} + \Sigma^{-1}$, κ_R is the renormalized bending rigidity, G_0 the correlation function in the harmonic approximation $G_0^{-1} = \kappa \mathbf{q}^4$ and Σ the self-energy. The SCSA is determined through a set of coupled integral equations for the self-energy Σ :

$$\Sigma(\mathbf{p}) = \frac{2}{(d-D)} p_\alpha p_\beta p_\gamma p_\delta \int_{\mathbf{q}} \tilde{\mathcal{R}}_{\alpha\beta, \gamma\delta}(\mathbf{q}) G_h(\mathbf{p} - \mathbf{q}) \quad (3.91)$$

where $\tilde{\mathcal{R}}$ is the screened four-rank tensor:

$$\tilde{\mathcal{R}} = \mathcal{R}(\mathbf{q}) - \mathcal{R}(\mathbf{q}) \Pi(\mathbf{q}) \tilde{\mathcal{R}}(\mathbf{q}) \quad (3.92)$$

where Π is the vacuum polarization:

$$\Pi_{\alpha\beta,\gamma\delta}(\mathbf{q}) = \int_p p_\alpha p_\beta p_\gamma p_\delta G_h(\mathbf{p}) G_h(\mathbf{q} - \mathbf{p}) \quad (3.93)$$

The only contribution of the vacuum polarization comes from the component Π_{sym} that is proportional to the symmetric tensor $S = \delta_{\alpha\beta}\delta_{\gamma\delta} + \delta_{\alpha\gamma}\delta_{\beta\delta} + \delta_{\alpha\delta}\delta_{\beta\gamma}$:

$$\Pi_{\text{sym}} = I(q)S \quad (3.94)$$

$$I(q) = \frac{1}{8} \int_p \mathbf{p}^2 (\mathbf{q} - \mathbf{p})^2 G(\mathbf{q}) G(\mathbf{q} - \mathbf{p}) \quad (3.95)$$

and after a bit of calculus we find for the four-rank tensor that obeys:

$$\tilde{\mathcal{R}}(\mathbf{q}) = \mu_R(\mathbf{q})M + K_R(\mathbf{q})N \quad (3.96)$$

where:

$$\mu_R(\mathbf{q}) = \frac{\mu}{1 + 2\mu I(\mathbf{q})} \quad (3.97)$$

$$K_R(\mathbf{q}) = \frac{K_0}{1 + (D + 1)K_0 I(\mathbf{q})} \quad (3.98)$$

and the self-energy reads:

$$\Sigma(\mathbf{p}) = \frac{2}{d - D} \int_q \frac{K_R(\mathbf{q}) + (D - 2)\mu_R(\mathbf{q})}{D - 1} [\mathbf{p}\mathcal{P}^\perp(\mathbf{q})\mathbf{p}]^2 G_h(\mathbf{q} - \mathbf{p}) \quad (3.99)$$

To solve these equations, we start with the correlation function G_0 in the harmonic approximation (3.81) which we use to compute the integral $I(q)$ (3.95). Then we injected this result in the expression of the renormalized couplings μ_R (3.97) and K_R (3.98) which serve to calculate the self-energy (3.99). This in turn is used to compute the new expression of the correlation function (3.90) and we restart the iteration until convergence is reached.

Assuming that $G(\mathbf{q}) \approx \Sigma(\mathbf{q}) \approx A/q^{4-\eta}$ in the long-wavelength limit, with A a non-universal amplitude and η the anomalous dimension, these equations (3.97-3.99) admit an analytic solution and we find for the anomalous dimension [108]:

$$d - D = \frac{2}{\eta} D(D - 1) \frac{\Gamma(1 + \eta/2)\Gamma(2 - \eta)\Gamma(\eta + D)\Gamma(2 - \eta/2)}{\Gamma\left(\frac{D+\eta}{2}\right)\Gamma(2 - \eta + D/2)\Gamma(\eta + D/2)\Gamma\left(\frac{D+4-\eta}{2}\right)} \quad (3.100)$$

where Γ is the Euler Gamma function $\Gamma(z) = \int_0^\infty e^{-t} t^{z-1} dt$ and the anomalous dimension η_u of the phonon modes results from the rotational invariance:

$$\eta_u = 4 - D - 2\eta. \quad (3.101)$$

In the physically interesting case $D = 2$ and $d = 3$, Le Doussal & Radzihovsky found $\eta = 0.821$ and $\eta_u = 0.358$ [108]. This means that the bending rigidity has an upward renormalization $\kappa_R(q) \sim q^{-\eta}$ which stabilizes the flat phase.

3.5.6 Conclusion

In this chapter we have discussed the long-range behaviour of both fluid and polymerized membranes. More specifically we have shown why fluid membranes are always crumpled and how the fixed-connectivity enriches the phase diagram of polymerized membranes by the appearance of a phase transition between the crumpled and flat phases. The existence of this long-range ordered flat phase seemed to be in apparent violation of the Mermin-Wagner theorem [79]. We have shown that the coupling between the out-of-plane bending and in-plane phonon modes stabilizes the flat phase. This results in the existence of long-range interactions which is beyond the domain of applicability of the Mermin-Wagner theorem.

We have presented some of the approaches used to tackle the problem of the transition between the crumpled and flat phases. The weak-coupling ϵ -expansion predicts a second-order transition for $d > d_c = 219$ in the vicinity of the upper critical dimension $D_{uc} = 4$ and below d_c the transition becomes first-order. However this leaves open the question for physical membranes ($D = 2$ and $d = 3$) where one has $\epsilon = 2$ which is out-of-reach of a one-loop computation [104]. Moreover some Monte Carlo simulations predict a second-order transition (see [98, Ch. 5 and 12] for reviews) whereas more recent simulations predict a first-order behaviour [109, 110].

The self-consistent screening approximation has been able to compute the exponents both at the crumpled-tubule transition and in the flat phase [108]. However the approach relies on a large- d expansion makes doubtful the quantitative predictions for small d and impossible the determination of the $d_c(D)$ line.

3.6 NPRG Approach to Polymerized Membranes

To tackle the problem of the order of the phase transition as well as the behaviour in the flat phase of physical membranes ($D = 2$ and $d = 3$) we use a non-perturbative renormalization group approach. With this approach we are able to compute the critical exponents in the whole (d, D) plane and more importantly to determine the $d_c(D)$ line separating a second-order transition from a first-order one. In general the effective average action is a functional of all the invariants of the system. With $O(d)$ rotational and $T(D)$ translational invariance Γ_k for polymerized membranes reads in the lowest order of the derivative expansion:

$$\Gamma_k[\vec{r}] = \int d^D x \left\{ \frac{Z_k(u_{\mu\nu})}{2} (\partial_\mu \partial_\mu \vec{r})^2 + U(u_{\mu\nu}) + o(\partial^6) \right\} \quad (3.102)$$

where $u_{\mu\nu} = \partial_\mu \vec{r} \cdot \partial_\nu \vec{r}$ is the strain tensor, Z_k corresponds to the field renormalization, U the running potential and the self-avoidance is neglected again. The tensor structure of $u_{\mu\nu}$ imposes that the potential is a function of an infinite number of invariants which are polynomials of the traces of $(u_{\mu\nu})^n$. The tensor structure of $u_{\mu\nu}$ imposes that the effective potential depend on a infinite number of invariants which are a polynomial of the trace of $(u_{\mu\nu})^n$. Since the dimension D of the membrane is finite, one can show that the traces $\text{Tr}[(u_{\mu\nu})^{D+i}]$, with $i \geq 1$, can be written as a combination of the trace with smaller powers of the tensor $u_{\mu\nu}$, *e.g.* for $D = 2$ we have the relation $\text{Tr}[(u_{\mu\nu})^3] = 3\text{Tr}[(u_{\mu\nu})^2]\text{Tr}[u_{\mu\nu}] - (\text{Tr}[u_{\mu\nu}])^3$. With this simplification, the effective potential reads:

$$U(u_{\mu\nu}) = \sum_{n_1, \dots, n_D \geq 0} a_{n_1, \dots, n_D} (\text{Tr}[(u_{\mu\nu})])^{n_1} \dots (\text{Tr}[(u_{\mu\nu})^D])^{n_D} . \quad (3.103)$$

Deriving the flow equations for a potential with a large number of invariants can be very complicated, except in some systems like in frustrated magnets [32]. This is even more difficult in our case of polymerized membranes since we are dealing with a derivative theory. Therefore in addition to the derivative expansion, we have performed a field expansion of the potential.

To know which terms one has at each order of the expansion is a bit more complicated than in usual systems like the $O(n)$ -model where at each order there is only one new term which is just the field at some even power. To find which term to add at each order we can use the Cayley-Hamilton theorem that states that every square matrix satisfies its own characteristic polynomial:

$$p(\lambda) = \det(\lambda I_D - u_{\mu\nu}) \quad (3.104)$$

where I_D is the D -dimensional identity matrix. Replacing λ by the matrix $u_{\mu\nu}$ yields the zero matrix:

$$p(u_{\mu\nu}) = 0 \quad (3.105)$$

and taking the trace of this polynomial provides directly the invariants. Indeed each term of the polynomial corresponds to an invariant. To derive the expression of the characteristic polynomial for a 2×2 matrix is straightforward but the greater the size of the matrix the more complicated and longer it becomes to derive it. Fortunately there exists method, called the Faddeev-Leverrier algorithm⁸ that considerably simplifies this task (see Appendix B).

The invariants at the second and third order are respectively given by:

$$\left\{ \begin{array}{l} \text{Tr}[(u_{\mu\nu})^2], \text{Tr}[(u_{\mu\nu})]^2 \\ \text{Tr}[(u_{\mu\nu})^3], \text{Tr}[(u_{\mu\nu})^2]\text{Tr}[(u_{\mu\nu})], \text{Tr}[(u_{\mu\nu})]^3 \end{array} \right. \quad (3.106)$$

We start with an ansatz for the effective average action at the lowest order of the field expansion r^4 :

$$\Gamma_k[\vec{r}] = \int d^D x \left\{ \frac{Z_k}{2} (\partial_\mu \partial_\mu \vec{r})^2 + u \text{Tr} [(u_{\mu\nu})^2] + v \text{Tr} [u_{\mu\nu}]^2 \right\} \quad (3.107)$$

We are interested in the critical behaviour of the membrane and for convergence reasons it is better to expand the potential around the minimum configuration ζ instead of the origin.

⁸The Faddeev-Leverrier algorithm has first discovered by Leverrier in 1840 and has since be re-discovered many times: Horst (1935), Souriau (1948), Frame (1949), Faddeev and Sorminskii (1949)

With this change the effective average action reads:

$$\Gamma_k[\vec{r}] = \int d^D x \left\{ \frac{Z_k}{2} (\partial^2 \vec{r})^2 + u (\partial_\mu \vec{r} \cdot \partial_\nu \vec{r} - \delta_{\mu\nu} \zeta^2)^2 + v (\partial_\mu \vec{r} \cdot \partial_\mu \vec{r} - D \zeta^2)^2 \right\} \quad (3.108)$$

where $\partial^2 = \partial_\mu \partial^\mu$, u and v the elastic coupling constants corresponding respectively to stretching and shearing. For thermodynamical stability we must have $u > 0$ and $u + Dv > 0$.

We want to derive the flow equations of the coupling constants. Therefore we first need the expression of the propagator and thus of the two-point correlation function $\Gamma_k^{(2)}$. Next section is dedicated to this task.

3.6.1 The propagator in Fourier Space

For a reason that we will see later the expression of the propagator is derived in a uniform configuration λ different from the minimum configuration ζ :

$$\vec{r}_\lambda(x) = \lambda x^\mu \mathbf{e}_\mu \quad (3.109)$$

which reads in Fourier space:

$$\vec{r}_\lambda(q) = -i \lambda \mathbf{e}_\mu \left(\frac{d}{dq_\mu} \delta(\mathbf{q}) \right). \quad (3.110)$$

The second functional derivative $\Gamma_k^{(2)}$ taken in this configuration λ reads:

$$\begin{aligned} \Gamma_k^{(2)}(q, i, q', j) \Big|_\lambda &= \delta(q + q') \left\{ Z_k q^4 + 4q^2 \lambda^2 u \theta(D - i) + 4q^2 (u + vD) (\lambda^2 - \zeta^2) \right. \\ &\quad \left. + 4\lambda^2 (u + 2v) q_i q_j \theta(D - i) \theta(D - j) \right\} \end{aligned} \quad (3.111)$$

where θ is the Heaviside step function. The inverse propagator can be written in the form:

$$\left(\Gamma_k^{(2)} + R_k \right) (q, i, q', j) = A(P_q^\perp)_{ij} + B(P_q^\parallel)_{ij} \quad (3.112)$$

where A and B are constants independent on the momenta p and the projectors P_q^\perp and P_q^\parallel are given by:

$$(P_q^\perp)_{ij} = \delta_{ij} - \frac{p_i p_j}{p^2} \quad (3.113)$$

$$(P_q^\parallel)_{ij} = \frac{p_i p_j}{p^2} \quad (3.114)$$

with the following properties:

$$P_q^\parallel P_q^\perp = 0 \quad (3.115)$$

$$P_q^\parallel + P_q^\perp = I_D \quad (3.116)$$

where I_D is the D -dimensional identity matrix. A matrix M of the form (3.112) can easily be inverted and its inverse matrix M^{-1} is of the same form:

$$M^{-1} = A' P_q^\perp + B' P_q^\parallel \quad (3.117)$$

with:

$$\begin{cases} A' = \frac{1}{A} \\ B' = \frac{1}{B} \end{cases} \quad (3.118)$$

With this structure of the inverse propagator, the propagator \mathcal{P} in Fourier space reads:

$$\begin{aligned} \mathcal{P}_{ij}(q, q')|_\lambda = \delta(q + q') \left\{ G_0^{(\lambda)}(q) \delta_{ij} \theta(i - D - 1) \right. \\ \left. + \theta(D - i) \theta(D - j) \left(G_1^{(\lambda)}(q) \left(\delta_{ij} - \frac{q_i q_j}{q^2} \right) + G_2^{(\lambda)}(q) \frac{q_i q_j}{q^2} \right) \right\} \quad (3.119) \end{aligned}$$

where:

$$\begin{cases} G_0^{(\lambda)}(q) = (Z_k q^4 + R_k(q) + 4q^2(u + vD) (\lambda^2 - \zeta^2))^{-1} \\ G_1^{(\lambda)}(q) = (Z_k q^4 + R_k(q) + 4q^2 \lambda^2 u + 4q^2(u + vD) (\lambda^2 - \zeta^2))^{-1} \\ G_2^{(\lambda)}(q) = (Z_k q^4 + R_k(q) + 8q^2 \lambda^2 (u + v) + 4q^2(u + vD) (\lambda^2 - \zeta^2))^{-1} . \end{cases} \quad (3.120)$$

The functions G_i are associated to the different excitation modes of the membrane around the flat phase:

- G_0 : $(d - D)$ Goldstone or capillary modes propagating outside of the membrane with a vanishing mass at the minimum $\lambda = \zeta$
- G_1 : $(D - 1)$ phonon modes inside the membrane with mass m_1 : $m_1^2 = 4\zeta^2 u$
- G_2 : one phonon mode inside the membrane with mass m_2 : $m_2^2 = 8\zeta^2(u + v)$.

We can now derive the flow equations for the running coupling constants. We start with the coupling ζ in the next section.

3.6.2 The Minimum Configuration ζ

The configuration ζ that minimizes the effective action is given by:

$$\vec{r}_{\min}(x) = \zeta x^\mu \mathbf{e}_\mu \quad (3.121)$$

and in Fourier space it reads:

$$\vec{r}_{\min}(q) = -i\zeta \mathbf{e}_\mu \left(\frac{d}{dq_\mu} \delta(q) \right). \quad (3.122)$$

By definition the first functional derivative of the effective action is vanishing at the minimum:

$$\Gamma_k^{(1)}(p, i) \Big|_{\min} = \frac{\delta \Gamma_k[\vec{r}]}{\delta r_i(p)} \Big|_{\min} = 0 \quad (3.123)$$

whose flow equation reads:

$$\begin{aligned} \partial_t \left(\Gamma_k^{(1)}(p, i) \Big|_{\min} \right) &= \partial_t \Gamma_k^{(1)}(p, i) \Big|_{\min} + \sum_j \int_q \partial_t r_j(q) \Big|_{\min} \Gamma_k^{(2)}(p, i, q, j) \Big|_{\min} \\ 0 &= \partial_t \Gamma_k^{(1)}(p, i) \Big|_{\min} + i \sum_j \partial_t \zeta \theta(D - j) \int_q \frac{d}{dq_j} \Gamma_k^{(2)}(p, i, q, j) \Big|_{\min} \end{aligned} \quad (3.124)$$

where the two terms on the right hand side are both vanishing and we cannot define from this the flow of ζ . This is completely different from the $O(n)$ -model and is directly related to the

derivative character of the theory. To overcome this problem we take the effective action in the configuration λ :

$$\Gamma_k[\vec{r}_\lambda] = VD(u + Dv) (\lambda^2 - \zeta^2)^2 = VU_k(u_{\mu\nu})|_\lambda \quad (3.125)$$

where V is the volume. In what follow the potential in the configuration λ is written $U_k(\lambda)$ for simplicity. Deriving the potential U_k with respect to λ and taking $\lambda = \zeta$ we find:

$$\left. \frac{\partial U_k}{\partial \lambda} \right|_{\lambda=\zeta} = 0 \quad (3.126)$$

which leads to:

$$\partial_t \left(\left. \frac{\partial U_k}{\partial \lambda} \right|_{\lambda=\zeta} \right) = 0 = \partial_t \left(\left. \frac{\partial U_k}{\partial \lambda} \right|_{\lambda=\zeta} \right) + \partial_t \zeta \left. \frac{\partial^2 U_k}{\partial \lambda^2} \right|_{\lambda=\zeta}. \quad (3.127)$$

From this we find the formal expression of the flow of ζ which reads:

$$\partial_t \zeta = - \frac{(\partial_\lambda \partial_t U_k)_{\lambda=\zeta}}{(\partial_\lambda^2 U_k)_{\lambda=\zeta}} = - \frac{(\partial_\lambda \partial_t U_k)_{\lambda=\zeta}}{8D\zeta^2 (u + Dv)_{\lambda=\zeta}}. \quad (3.128)$$

Now we have to compute the flow of the potential which reads:

$$\partial_t U_k(\lambda) = \frac{1}{2} \tilde{\partial}_t \text{Tr} \left\{ \int_q \ln \left(\Gamma_k^{(2)} + R_k \right) (q, -q)|_\lambda \right\} \quad (3.129)$$

where $\tilde{\partial}_t = \partial_t R_k \frac{\partial}{\partial R_k}$.

Taking the derivative of $\partial_t U_k$ with respect to λ we find:

$$\partial_\lambda \partial_t U_k(\lambda) = \frac{1}{2} \tilde{\partial}_t \text{Tr} \left\{ \int_q \sum_l \left(\Gamma_k^{(2)} + R_k \right)^{-1} (q, i, -q, l)|_\lambda \partial_\lambda \Gamma_k^{(2)} (q, l, -q, j)|_\lambda \right\} \quad (3.130)$$

Replacing the expression of the propagator (3.119) in this equation and taking $\lambda = \zeta$ we find for the flow equation of ζ :

$$\begin{aligned} \partial_t \zeta = \frac{2A_D}{D(u + Dv)\zeta} \left\{ (3u + (D + 2)v)L_{001}^{D+2}[\{m_i\}] \right. \\ \left. + (D - 1)(2u + Dv)L_{010}^{D+2}[\{m_i\}] + (d - D)(u + Dv)L_{100}^{D+2}[\{m_i\}] \right\} \end{aligned} \quad (3.131)$$

where $L_{abc}^{D+\alpha}$ is a threshold function and its expression will be given in the next section and $\{m_i\} = m_1, m_2, m_3$. As in the $O(n)$ -model the non-perturbative content is encoded in the threshold functions.

3.6.3 The Flow Equations of u and v and the Anomalous Dimension η_k

The definitions of the coupling constants u and v are given by:

$$u = \frac{1}{\zeta^2} \lim_{p \rightarrow 0} \frac{\partial}{\partial p^2} \Gamma_k^{(2)}(p, D, -p, D)|_{\min} \quad (3.132)$$

$$v = \frac{1}{\zeta^2} \lim_{p \rightarrow 0} \frac{\partial}{\partial p_D^2} \Gamma_k^{(2)}(p, D, -p, D)|_{\min} - \frac{1}{2}u \quad (3.133)$$

We first derive the formal expression of the flow equation of u :

$$\begin{aligned} \partial_t u = \lim_{p \rightarrow 0} \frac{\partial}{\partial p^2} \left\{ \frac{1}{\zeta^2} \partial_t \Gamma_k^{(2)}(p, D, -p, D)|_{\min} - \frac{2}{\zeta^2} \partial_t \zeta \Gamma_k^{(2)}(p, D, -p, D)|_{\min} \right. \\ \left. + \frac{1}{\zeta^2} \sum_j \int_q \partial_t r_j(q)|_{\min} \Gamma_k^{(3)}(p, D, -p, D, q, j) \right\} \\ = \frac{1}{\zeta^2} \lim_{p \rightarrow 0} \frac{\partial}{\partial p^2} \partial_t \Gamma_k^{(2)}(p, D, -p, D)|_{\min} + \frac{2}{\zeta} \partial_t \zeta (u + Dv) \end{aligned} \quad (3.134)$$

and similarly for v we find:

$$\begin{aligned} \partial_t v = -\frac{1}{\zeta} \partial_t \zeta (u + (D + 3)v) + \frac{1}{8\zeta^2} \left\{ \lim_{p \rightarrow 0} \frac{\partial}{\partial p_D^2} \partial_t \Gamma_k^{(2)}(p, D, -p, D)|_{\min} \right. \\ \left. - \lim_{p \rightarrow 0} \frac{\partial}{\partial p^2} \partial_t \Gamma_k^{(2)}(p, D, -p, D)|_{\min} \right\}. \end{aligned} \quad (3.135)$$

We are left with the computation of the flow of $\Gamma_k^{(2)}$ that reads in a graphical form:

$$\partial_t \Gamma_k^{(2)}(p, -p) = -\frac{1}{2} \begin{array}{c} \bullet \\ \circlearrowleft \\ \xrightarrow{p} \quad \xleftarrow{-p} \end{array} - \begin{array}{c} \bullet \\ \circlearrowright \\ \xrightarrow{p} \quad \xleftarrow{-p} \end{array} \quad (3.136)$$

and after some computation we finally get:

$$\partial_t u = \frac{16A_D}{D(D+2)} \left\{ 2(3u+2v)^2 L_{002}^{D+4}[\{m_i\}] + 4Du(u+v) L_{011}^{D+4}[\{m_i\}] + u^2(D^2+2D-8) L_{020}^{D+4}[\{m_i\}] + 2u^2 L_{200}^{D+4}[\{m_i\}] \right\} \quad (3.137)$$

$$\begin{aligned} \partial_t v = \frac{16A_D}{D(D+2)} & \left\{ -4u(u+v) L_{011}^{D+4}[\{m_i\}] \right. \\ & + (d-D)(u^2 + 2(D+2)uv + D(D+2)v^2) L_{200}^{D+4}[\{m_i\}] \\ & + ((3D+2)u^2 + (D^2+D-2)(4uv + Dv^2)) L_{020}^{D+4}[\{m_i\}] \\ & \left. + (9u^2 + 6(D+4)uv + (D^2+6D+12)v^2) L_{002}^{D+4}[\{m_i\}] \right\}. \end{aligned} \quad (3.138)$$

To find a fixed-point we need to work with dimensionless couplings. Therefore we will rescale the dimensionful couplings:

$$\left\{ \begin{array}{l} Z_k \sim k^{-\eta_k} \\ \zeta^2 = k^{D-2+\eta_k} \bar{\zeta}^2 \\ u = k^{D-4+2\eta_k} \bar{u} \\ v = k^{D-4+2\eta_k} \bar{v} \\ R_k(q^2) = Z_k q^4 r \left(y = \frac{q^2}{k^2} \right). \end{array} \right. \quad (3.139)$$

We only give the expression of the flow equations at the lowest order of the field expansions. Otherwise, they would be too long to be displayed. The flow equations of ζ^2 , u and v

at the order r^4 read (we have dropped the bar over the dimensionless couplings):

$$\begin{aligned} \partial_t \zeta^2 = & -(D-2 + \eta_k) \zeta^2 + \frac{4A_D}{D(u+Dv)} \left\{ (3u + (D+2)v) L_{001}^{D+2} \right. \\ & \left. + (D-1)(2u+Dv) L_{010}^{D+2} + (d-D)(u+Dv) L_{100}^{D+2} \right\} \end{aligned} \quad (3.140)$$

$$\begin{aligned} \partial_t u = & (D-4 + 2\eta_k)u + \frac{16A_D}{D(D+2)} \left\{ 2(3u+2v)^2 L_{002}^{D+4} \right. \\ & \left. + 4Du(u+v) L_{011}^{D+4} + u^2(D^2+2D-8) L_{020}^{D+4} + 2u^2 L_{200}^{D+4} \right\} \end{aligned} \quad (3.141)$$

$$\begin{aligned} \partial_t v = & (D-4 + 2\eta_k)v + \frac{16A_D}{D(D+2)} \left\{ -4u(u+v) L_{011}^{D+4} \right. \\ & + (d-D)(u^2 + 2(D+2)uv + D(D+2)v^2) L_{200}^{D+4} \\ & + ((3D+2)u^2 + (D^2+D-2)(4uv+Dv^2)) L_{020}^{D+4} \\ & \left. + (9u^2 + 6(D+4)uv + (D^2+6D+12)v^2) L_{002}^{D+4} \right\} \end{aligned} \quad (3.142)$$

and the anomalous dimension $\eta_k = -d \ln Z_k / dt$ is given by:

$$\begin{aligned} \eta_k = & \frac{2^5 \zeta^2 A_D}{D(D+2)} \left\{ 2(D-1)u^2 \left(K_{120}^{D+4} + K_{210}^{D+4} \right) + 24(u+v)^2 \left(K_{102}^{D+4} + K_{201}^{D+4} \right) \right. \\ & - 4 \left((D^2+D+4)u^2 + (D^2+3D+2)v^2 + 4(D+2)uv \right) L_{101}^{D+2} \\ & + (3D^2-5D+2)u^2 L_{110}^{D+2} + 16(D^2-3D+2)\zeta^4 u^4 L_{120}^{D+4} \\ & + (D^2-3D+2)u^2 N_{120}^{D+2} + (D^2+9D-10)u^2 N_{210}^{D+2} - 2^{10}(D-1)\zeta^8 u^6 L_{130}^{D+6} \\ & - 3 \times 2^{16} \zeta^8 (u+v)^6 L_{103}^{D+6} + 2^8 \zeta^4 (u+v)^3 (5(D+2)u + (D+14)v) L_{102}^{D+4} \\ & - 4(D-1)u^2 \left(M_{130}^{D+4} + M_{310}^{D+4} \right) - 3 \times 2^4 (u+v)^2 \left(M_{103}^{D+4} + M_{301}^{D+4} \right) \\ & - 2^7 (D-1)\zeta^4 u^4 N_{130}^{D+4} + 4(u+v)(5(D+2)u + (D+14)v) N_{102}^{D+2} \\ & \left. - 3 \times 2^{11} \zeta^4 (u+v)^4 N_{103}^{D+4} + 4(u+v)((D+14)u + 5(D+2)v) N_{201}^{D+2} \right\} \end{aligned} \quad (3.143)$$

where $A_D = \frac{2^{-D-1}\pi^{-D/2}}{\Gamma[D/2]}$ and the threshold functions L , M and N read:

$$L_{abc}^{D+\alpha}[m_{i=0,1,2}] = -\frac{1}{4A_D} \tilde{\partial}_t \int_q q^\alpha (P + m_0^2)^{-a} \times (P + q^2 m_1^2)^{-b} (P + q^2 m_2^2)^{-c} \quad (3.144)$$

$$M_{abc}^{D+\alpha}[m_{i=0,1,2}] = -\frac{1}{4A_D} \tilde{\partial}_t \int_q q^{\alpha+2} \left(\frac{\partial P}{\partial q^2} \right) (P + q^2 m_0^2)^{-a} \times (P + q^2 m_1^2)^{-b} (P + q^2 m_2^2)^{-c} \quad (3.145)$$

$$N_{abc}^{D+\alpha}[m_{i=0,1,2}] = -\frac{1}{4A_D} \tilde{\partial}_t \int_q q^{\alpha+2} \left(\frac{\partial P}{\partial q^2} \right)^2 (P + q^2 m_0^2)^{-a} \times (P + q^2 m_1^2)^{-b} (P + q^2 m_2^2)^{-c} \quad (3.146)$$

where $P = Z_k q^4 + R_k$ and m_i^2 masses that are given respectively by 0 , $4u\zeta^2$ and $8(u+v)\zeta^2$. The threshold functions control the relative role of the different modes, phonons and capillary waves, within the RG flow. The vanishing mass mode is associated with the $(d-D)$ transversal Goldstone capillary modes and the D massive modes split into $(D-1)$ modes with mass m_1 and one mode with mass m_2 . The set of equations (3.140 - 3.143) have been derived by Kownacki and Mouhanna [53]. The results, which we will discuss later, obtained with the lowest order field expansion still had some unanswered questions. Therefore we decided to go beyond and do an expansion up to the eight power of the field r^8 . The method presented above becomes heavy when adding higher orders and we used a different one to derive the flow equations. This method is presented in the next section.

3.6.4 Derivation of the Flow Equations

3.6.4.1 The Effective Action

To derive the flow equations of the coupling constant at the sixth and eighth order we use a general configuration Λ which is given below and we keep the formal expression of the potential as long as possible. The general effective action in a formal way is given by:

$$\Gamma_k[\vec{r}] = \Gamma_k^{(Z)}[r] + \Gamma^{(U)}[r]$$

where the first term corresponds to the kinetic part and the second term to the potential part.

As usual we need the propagator and thus the second functional derivative of the effective average action. Let us start with the kinetic part $\Gamma^{(Z)}$ whose second functional derivative in Fourier space reads:

$$\frac{\delta^2 \Gamma_k^{(Z)}}{\delta r^i(q) \delta r^j(q')} = \delta(q + q') \delta_{ij} Z_k q^4. \quad (3.147)$$

Now let us look at the second part. We first calculate it in real space and then in Fourier space. The first functional derivative reads:

$$\begin{aligned} \frac{\delta \Gamma_k^{(U)}}{\delta r^i(x)} &= \frac{\delta}{\delta r^i(x)} \int d^D y U_k(\partial r) \\ \frac{\delta \Gamma_k^{(U)}}{\delta r^i(x)} &= -\partial_\alpha \left(\frac{\delta U_k}{\delta (\partial_\alpha r^i(x))} \right) \end{aligned} \quad (3.148)$$

then we derive it again and find:

$$\begin{aligned} \frac{\delta^2 \Gamma_k^{(U)}}{\delta r^i(x) \delta r^j(y)} &= -\partial_\alpha \left(\frac{\delta^2 U_k}{\delta (\partial_\alpha r^i(x)) \delta (\partial_\beta r^j(y))} \right) \partial_\beta (\delta(x - y)) \\ &\quad - \frac{\delta^2 U_k}{\delta (\partial_\alpha r^i(x)) \delta (\partial_\beta r^j(y))} \partial_\alpha \partial_\beta (\delta(x - y)). \end{aligned} \quad (3.149)$$

In fact U_k is a function of $u_{\alpha\beta} = g_{\alpha\beta} - \zeta^2 \delta_{\alpha\beta}$ where the metric is equal to $g_{\alpha\beta} = \partial_\alpha \vec{r} \cdot \partial_\beta \vec{r}$. Therefore the first derivative of U_k with respect to $\partial_\mu r^i$ is given by:

$$\begin{aligned} \frac{\delta U_k}{\delta (\partial_\mu r^i)} &= \frac{\delta U_k}{\delta (u_{\alpha\beta})} \frac{\delta u_{\alpha\beta}}{\delta (\partial_\mu r^i)} \\ &= \frac{\delta U_k}{\delta (u_{\alpha\beta})} (\delta_{\alpha\mu} \partial_\beta r^i + \delta_{\mu\beta} \partial_\alpha r^i) \\ &= \frac{\delta U_k}{\delta (u_{\mu\alpha})} \partial_\alpha r^i + \frac{\delta U_k}{\delta (u_{\alpha\mu})} \partial_\alpha r^i \end{aligned} \quad (3.150)$$

and the second derivative reads:

$$\begin{aligned} \frac{\delta^2 U_k}{\delta(\partial_\mu r^i) \delta(\partial_\beta r^j)} &= \frac{\delta^2 U_k}{\delta(u_{\beta\mu}) \delta(u_{\alpha\sigma})} \partial_\mu r^j \partial_\sigma r^i + \frac{\delta^2 U_k}{\delta(u_{\mu\beta}) \delta(u_{\alpha\sigma})} \partial_\mu r^j \partial_\sigma r^i \\ &+ \frac{\delta^2 U_k}{\delta(u_{\beta\mu}) \delta(u_{\sigma\alpha})} \partial_\mu r^j \partial_\sigma r^i + \frac{\delta^2 U_k}{\delta(u_{\mu\beta}) \delta(u_{\sigma\alpha})} \partial_\mu r^j \partial_\sigma r^i \\ &+ \frac{\delta U_k}{\delta(u_{\alpha\beta})} \delta_{ij} + \frac{\delta U_k}{\delta(u_{\beta\alpha})} \delta_{ij}. \end{aligned} \quad (3.151)$$

Now we must take these derivatives eqs. (3.150) and (3.151) in the configuration Λ defined below.

3.6.4.2 The Configuration Λ

We consider a more general flat phase configuration Λ given by:

$$\vec{r}_\Lambda = \Lambda_{\alpha\beta} x_\alpha \mathbf{e}_\beta \quad (3.152)$$

where $\Lambda_{\alpha\beta}$ is a $D \times D$ matrix. This configuration is chosen so that:

$$\begin{cases} \partial_\alpha \vec{r} &= \Lambda_{\alpha\beta} \vec{e}_\beta \\ \partial_\alpha r_\Lambda^i &= \Lambda_{\alpha i} \theta(D-i) \\ u_{\alpha\beta}^\Lambda &= (\Lambda^2)_{\alpha\beta} - \zeta^2 \delta_{\alpha\beta} \\ \partial_\alpha \partial_\beta \vec{r}_\Lambda &= 0. \end{cases} \quad (3.153)$$

In this configuration the second derivative of U_k (3.151) reads:

$$\begin{aligned} \left(\frac{\delta^2 U_k}{\delta(\partial_\alpha r^i) \delta(\partial_\beta r^j)} \right) \Big|_\Lambda &= \Lambda_{\mu j} \Lambda_{\sigma i} \theta(D-i) \theta(D-j) \left\{ \frac{\delta^2 U_k}{\delta(u_{\beta\mu}) \delta(u_{\alpha\sigma})} \right. \\ &+ \frac{\delta^2 U_k}{\delta(u_{\mu\beta}) \delta(u_{\alpha\sigma})} + \frac{\delta^2 U_k}{\delta(u_{\beta\mu}) \delta(u_{\sigma\alpha})} + \left. \frac{\delta^2 U_k}{\delta(u_{\mu\beta}) \delta(u_{\sigma\alpha})} \right\} \Big|_\Lambda \\ &+ \delta_{ij} \left\{ \frac{\delta U_k}{\delta(u_{\alpha\beta})} + \frac{\delta U_k}{\delta(u_{\beta\alpha})} \right\} \Big|_\Lambda \end{aligned} \quad (3.154)$$

which for the potential part $\Gamma_k^{(U)}$ leads to:

$$\begin{aligned} & \left(\frac{\delta^2 \Gamma_k^{(U)}}{\delta (\partial_\alpha r^i(x)) \delta (\partial_\beta r^j(y))} \right) \Big|_\Lambda = -\Lambda_{\mu j} \Lambda_{\sigma i} \theta(D-i) \theta(D-j) \partial_\alpha \partial_\beta (\delta(x-y)) \times \\ & \left\{ \frac{\delta^2 U_k}{\delta (u_{\beta\mu}) \delta (u_{\alpha\sigma})} + \frac{\delta^2 U_k}{\delta (u_{\mu\beta}) \delta (u_{\alpha\sigma})} + \frac{\delta^2 U_k}{\delta (u_{\beta\mu}) \delta (u_{\sigma\alpha})} + \frac{\delta^2 U_k}{\delta (u_{\mu\beta}) \delta (u_{\sigma\alpha})} \right\} \Big|_\Lambda \\ & - \delta_{ij} \partial_\alpha \partial_\beta (\delta(x-y)) \left\{ \frac{\delta U_k}{\delta (u_{\alpha\beta})} + \frac{\delta U_k}{\delta (u_{\beta\alpha})} \right\} \Big|_\Lambda \end{aligned} \quad (3.155)$$

and in Fourier space this becomes:

$$\begin{aligned} & \left(\frac{\delta^2 \Gamma_k^{(U)}}{\delta r^i(q) \delta r^j(q')} \right) \Big|_\Lambda = \Lambda_{\mu j} \Lambda_{\sigma i} \theta(D-i) \theta(D-j) q_\alpha q_\beta \delta(q+q') \times \\ & \left\{ \frac{\delta^2 U_k}{\delta (u_{\beta\mu}) \delta (u_{\alpha\sigma})} + \frac{\delta^2 U_k}{\delta (u_{\mu\beta}) \delta (u_{\alpha\sigma})} + \frac{\delta^2 U_k}{\delta (u_{\beta\mu}) \delta (u_{\sigma\alpha})} + \frac{\delta^2 U_k}{\delta (u_{\mu\beta}) \delta (u_{\sigma\alpha})} \right\} \Big|_\Lambda \\ & + 2\delta_{ij} q_\alpha q_\beta \delta(q+q') \left(\frac{\delta U_k}{\delta (u_{\alpha\beta})} \right) \Big|_\Lambda . \end{aligned} \quad (3.156)$$

To simplify the notations in what follow we define:

$$U_{\text{eff}} = U_k (u_{\alpha\beta}^\Lambda = (\Lambda^2)_{\alpha\beta} - \zeta^2 \delta_{\alpha\beta}) . \quad (3.157)$$

The potential $U_k(u_{\alpha\beta})$ is a function of $\text{Tr}[u], \text{Tr}[u^2], \dots$. We can show that, for a $(D \times D)$ matrix u and $\forall i \geq 1$ the trace $\text{Tr}[u^{D+i}]$ is a polynomial function of $\text{Tr}[u], \dots, \text{Tr}[u^D]$. The potential U_k is then given by:

$$\begin{aligned} U_k(u_{\alpha\beta}) &= \sum_{n_1, \dots, n_D \geq 0} a[n_1, \dots, n_D] (\text{Tr}[u])^{n_1} \dots (\text{Tr}[u^D])^{n_D} \\ &= \sum_{n_\alpha} a[n_\alpha] T_1^{n_1} \dots T_D^{n_D} \end{aligned} \quad (3.158)$$

where $a[n_\alpha] = a[n_1, \dots, n_D]$ and $\text{Tr}[u^n] = T_n$ and the effective potential U_{eff} reads:

$$U_{\text{eff}} = \sum_{n_\alpha} a[n_\alpha] t_1^{n_1}(\Lambda) \dots t_D^{n_D}(\Lambda) \quad (3.159)$$

where $t_n(\Lambda) = \text{Tr}[(u^\Lambda)^n] = \text{Tr}[(\Lambda^2 - \zeta^2)^n]$ and where u^Λ is given in eq.(3.153).

For the potential U_k we need the derivatives of T_n with respect to the tensor $u_{\alpha\beta}$:

$$\begin{aligned} \frac{\delta T_n}{\delta u_{\alpha\beta}} &= \frac{\delta}{\delta u_{\alpha\beta}} (u_{a_1 a_2} u_{a_2 a_3} \dots u_{a_n a_1}) \\ &= \delta_{\alpha a_1} \delta_{\beta a_2} u_{a_2 a_3} \dots u_{a_n a_1} + \dots + \delta_{\alpha a_n} \delta_{\beta a_1} u_{a_1 a_2} \dots u_{a_{n-1} a_n} \\ &= n [u^{n-1}]_{\beta\alpha} \end{aligned} \quad (3.160)$$

which leads to:

$$\begin{aligned} \frac{\delta U_k}{\delta u_{\alpha\beta}} &= \sum_{n=1}^D \frac{\delta U_k}{\delta T_n} \frac{\delta T_n}{\delta u_{\alpha\beta}} \\ \frac{\delta U_k}{\delta u_{\alpha\beta}} &= \sum_{n=1}^D \frac{\delta U_k}{\delta T_n} n [u^{n-1}]_{\beta\alpha} \end{aligned} \quad (3.161)$$

and to:

$$\begin{aligned} \frac{\delta^2 U_k}{\delta u_{\alpha\sigma} \delta u_{\beta\mu}} &= \frac{\delta}{\delta u_{\alpha\sigma}} \left(\sum_{n=1}^D \frac{\delta U_k}{\delta T_n} n [u^{n-1}]_{\mu\beta} \right) \\ &= \sum_{n,m=1}^D n m \frac{\delta^2 U_k}{\delta T_m \delta T_n} [u^{n-1}]_{\mu\beta} [u^{m-1}]_{\sigma\alpha} \\ &\quad + \sum_{n=1}^D n \frac{\delta U_k}{\delta T_n} \frac{\delta}{\delta u_{\alpha\sigma}} [u^{n-1}]_{\mu\beta} \\ &= \sum_{n,m=1}^D n m \frac{\delta^2 U_k}{\delta T_m \delta T_n} [u^{n-1}]_{\mu\beta} [u^{m-1}]_{\sigma\alpha} \\ &\quad + \sum_{n=1}^D n \frac{\delta U_k}{\delta T_n} \left(\sum_{k=0}^{n-2} [u^k]_{\mu\alpha} [u^{n-2-k}]_{\sigma\beta} \right) \end{aligned} \quad (3.162)$$

Now that we have the expressions of the derivatives of U_k we take them in the configuration Λ which we take as a diagonal matrix:

$$\Lambda_{\alpha\beta} = \text{diag}(\lambda_1, \lambda_2, \dots, \lambda_D) \quad (3.163)$$

which implies:

$$\begin{cases} u_{\alpha\beta}^\Lambda &= \text{diag}(\lambda_1^2 - \zeta^2, \dots, \lambda_D^2 - \zeta^2) \\ t_n(\Lambda) &= \sum_{\alpha=1}^D (\lambda_\alpha^2 - \zeta^2)^n \\ \frac{\partial t_n(\Lambda)}{\partial \lambda_\alpha^2} &= n (\lambda_\alpha^2 - \zeta^2)^{n-1}. \end{cases} \quad (3.164)$$

With this, the first derivative of U_k in the configuration Λ is given by:

$$\begin{aligned} \left(\frac{\delta U_k}{\delta u_{\alpha\beta}} \right)_{|\Lambda} &= \sum_{n=1}^D n \left(\frac{\delta U_k}{\delta T_n} \right)_{|\Lambda} \delta_{\alpha\beta} (\lambda_\alpha^2 - \zeta^2)^{n-1} \\ &= \delta_{\alpha\beta} \sum_{n=1}^D \frac{\delta U_{\text{eff}}}{\delta t_n(\Lambda)} \frac{\partial t_n(\Lambda)}{\partial \lambda_\alpha^2} \\ &= \delta_{\alpha\beta} \frac{\partial U_{\text{eff}}}{\partial \lambda_\alpha^2} \end{aligned} \quad (3.165)$$

and the second derivative reads:

$$\begin{aligned} \left(\frac{\delta^2 U_k}{\delta u_{\alpha\sigma} \delta u_{\beta\mu}} \right)_{|\Lambda} &= \sum_{n,m=1}^D nm \frac{\delta^2 U_{\text{eff}}}{\delta t_m(\Lambda) \delta t_n(\Lambda)} \delta_{\mu\beta} (\lambda_\beta^2 - \zeta^2)^{n-1} \delta_{\alpha\sigma} (\lambda_\alpha^2 - \zeta^2)^{m-1} \\ &\quad + \sum_{n=1}^D n \frac{\delta U_{\text{eff}}}{\delta t_n(\Lambda)} \left(\sum_{k=0}^{n-2} \delta_{\alpha\mu} (\lambda_\alpha^2 - \zeta^2)^k \delta_{\beta\sigma} (\lambda_\beta^2 - \zeta^2)^{n-2-k} \right) \\ &= \delta_{\alpha\sigma} \delta_{\beta\mu} \frac{\partial^2 U_{\text{eff}}}{\partial \lambda_\alpha^2 \partial \lambda_\beta^2} + \delta_{\alpha\mu} \delta_{\beta\sigma} \sum_{n=1}^D n \frac{\delta U_{\text{eff}}}{\delta t_n(\Lambda)} \\ &\quad \times \left(\sum_{k=0}^{n-2} \delta_{\alpha\mu} (\lambda_\alpha^2 - \zeta^2)^k \delta_{\beta\sigma} (\lambda_\beta^2 - \zeta^2)^{n-2-k} \right) \end{aligned} \quad (3.166)$$

Now that we have the expressions of the derivative of U_k in the configuration Λ we compute the expression of the propagator in the minimum configuration ζ .

3.6.4.3 Propagator at the minimum

The minimum $\lambda_\alpha = \zeta$, $\alpha = 1, \dots, D$ is implicitly defined by:

$$\left(\frac{\partial U_{\text{eff}}}{\partial \lambda_\alpha^2} \right) \Big|_{\min} = 0, \forall \alpha \quad (3.167)$$

or equivalently by:

$$\left(\frac{\delta U_k}{\delta u_{\alpha\beta}} \right) \Big|_{\min} = 0. \quad (3.168)$$

For all $n \geq 0$ we have:

$$(\lambda_\alpha^2 - \zeta^2) \Big|_{\min}^n = \delta_{n,0}. \quad (3.169)$$

With this, the second derivative of U_k at the minimum is given by:

$$\begin{aligned} \left(\frac{\delta^2 U_k}{\delta u_{\alpha\sigma} \delta u_{\beta\mu}} \right) \Big|_{\min} &= \sum_{n,m=1}^D nm \left(\frac{\delta^2 U_{\text{eff}}}{\delta t_m(\Lambda) \delta t_n(\Lambda)} \right) \Big|_{\min} \delta_{\mu\beta} \delta_{\alpha\sigma} \delta_{n,1} \delta_{m,1} \\ &+ \sum_{n=1}^D n \left(\frac{\delta U_{\text{eff}}}{\delta t_n(\Lambda)} \right) \Big|_{\min} \delta_{\alpha\mu} \delta_{\beta\sigma} \sum_{k=0}^{n-2} \delta_{k,0} \delta_{n,k+2} \\ &= \delta_{\alpha\sigma} \delta_{\mu\beta} \left(\frac{\delta^2 U_{\text{eff}}}{\delta t_1(\Lambda) \delta t_1(\Lambda)} \right) \Big|_{\min} + 2 \delta_{\alpha\mu} \delta_{\beta\sigma} \left(\frac{\delta U_{\text{eff}}}{\delta t_2(\Lambda)} \right) \Big|_{\min}. \end{aligned} \quad (3.170)$$

Injecting this result into eq. (3.156) leads to:

$$\begin{aligned}
& \left(\frac{\delta^2 \Gamma_k^{(U)}}{\delta r^i(q) \delta r^j(q')} \right) \Big|_{min} = \delta_{\mu j} \delta_{\sigma i} \zeta^2 \theta(D-i) \theta(D-j) q_\alpha q_\beta \delta(q+q') \\
& \left\{ 4 \delta_{\beta \mu} \delta_{\alpha \sigma} \left(\frac{\delta^2 U_{\text{eff}}}{\delta t_1(\Lambda) \delta t_1(\Lambda)} \right) \Big|_{min} + 4 \left(\frac{\delta U_{\text{eff}}}{\delta t_2(\Lambda)} \right) \Big|_{min} (\delta_{\alpha \beta} \delta_{\sigma \mu} + \delta_{\alpha \mu} \delta_{\beta \sigma}) \right\} \\
& + \underbrace{2 \delta_{ij} q_i q_j \delta(q+q') \left(\frac{\delta U_k}{\delta u_{\alpha \beta}} \right) \Big|_{min}}_{=0} \tag{3.171} \\
& = 4 \zeta^2 \theta(D-i) \theta(D-j) \delta(q+q') \left\{ q_i q_j \left(\frac{\delta^2 U_{\text{eff}}}{\delta t_1(\Lambda) \delta t_1(\Lambda)} \right) \Big|_{min} \right. \\
& \left. + \left(\frac{\delta U_{\text{eff}}}{\delta t_2(\Lambda)} \right) \Big|_{min} (q^2 \delta_{ij} + q_i q_j) \right\}
\end{aligned}$$

Since we have: $(t_n(\Lambda))^k = \delta_{k,0}$, $\forall n \geq 1$, the derivatives of the effective potential U_{eff} are given by:

$$\frac{\delta U_{\text{eff}}}{\delta t_k(\Lambda)} = \sum_{\{n_\alpha\}} a[n_\alpha] n_k t_1^{n_1}(\Lambda) \dots t_k^{n_k-1}(\Lambda) \dots t_D^{n_D}(\Lambda) \tag{3.172}$$

and by:

$$\begin{aligned}
& \frac{\delta^2 U_{\text{eff}}}{\delta t_k(\Lambda) \delta t_{k'}(\Lambda)} \\
& = \begin{cases} \sum_{\{n_\alpha\}} a[n_\alpha] n_k n_{k'} t_1^{n_1}(\Lambda) \dots t_k^{n_k-1}(\Lambda) \dots t_{k'}^{n_{k'}-1}(\Lambda) \dots t_D^{n_D}(\Lambda), & \text{if } k \neq k' \\ \sum_{\{n_\alpha\}} a[n_\alpha] n_k (n_k - 1) t_1^{n_1}(\Lambda) \dots t_k^{n_k-2}(\Lambda) \dots t_D^{n_D}(\Lambda), & \text{if } k = k' \end{cases} \tag{3.173}
\end{aligned}$$

which become at the minimum:

$$\frac{\delta U_{\text{eff}}}{\delta t_k(\Lambda)} \Big|_{min} = a[0, \dots, \underbrace{1}_{k^{\text{th}}}, \dots, 0] \tag{3.174}$$

and:

$$\frac{\delta^2 U_{\text{eff}}}{\delta t_k(\Lambda) \delta t_{k'}(\Lambda)} \Big|_{\min} = \begin{cases} a[0, \dots, \underbrace{1}_{k^{\text{th}}}, \dots, \underbrace{1}_{k'^{\text{th}}}, \dots, 0], & \text{if } k \neq k' \\ 2 a[0, \dots, \underbrace{2}_{k^{\text{th}}}, \dots, 0], & \text{if } k = k'. \end{cases} \quad (3.175)$$

For the propagator we need:

$$\begin{cases} \frac{\delta U_{\text{eff}}}{\delta t_2(\Lambda)} \Big|_{\min} & = a[0, 1, 0, \dots, 0] \\ \frac{\delta^2 U_{\text{eff}}}{\delta t_1(\Lambda) \delta t_1(\Lambda)} \Big|_{\min} & = 2 a[2, 0, \dots, 0] \end{cases} \quad (3.176)$$

and to simplify the expressions we define u and v as:

$$\begin{cases} u & = a[0, 1, 0, \dots, 0] \\ v & = a[2, 0, \dots, 0]. \end{cases} \quad (3.177)$$

Injecting this in the second derivative of the potential part $\Gamma_k^{(U)}$ we find:

$$\left(\frac{\delta^2 \Gamma_k^{(U)}}{\delta r^i(q) \delta r^j(q')} \right) \Big|_{\min} = 4\zeta^2 \theta(D-i) \theta(D-j) \delta(q+q') (q_i q_j (u+2v) + u q^2 \delta_{ij}) \quad (3.178)$$

and finally we find for $(\Gamma_{\min}^{(2)} + R_k)$:

$$\begin{aligned} \left(\Gamma_{\min}^{(2)} + R_k \right)_{(q,i,q',j)} &= \delta(q+q') \left\{ \delta_{ij} G_0^{-1} \theta(i-D-1) \right. \\ &\quad \left. + \theta(D-i) \theta(D-j) \left(G_1^{-1} \left(\delta_{ij} - \frac{q_i q_j}{q^2} \right) + G_2^{-1} \frac{q_i q_j}{q^2} \right) \right\} \end{aligned} \quad (3.179)$$

where:

$$\begin{cases} G_0^{-1}(q) & = Z_k q^4 + R_k(q^2) \\ G_1^{-1}(q) & = Z_k q^4 + R_k(q^2) + 4\zeta^2 u q^2 \\ G_2^{-1}(q) & = Z_k q^4 + R_k(q^2) + 8\zeta^2 (u+v) q^2 \end{cases} \quad (3.180)$$

and the propagator is straightforward:

$$\begin{aligned} \mathcal{P}_{ij}(q, q') \Big|_{min} &= \delta(q + q') \{ \delta_{ij} G_0(q) \theta(i - D - 1) \\ &+ \theta(D - i) \theta(D - j) \left(G_1(q) \left(\delta_{ij} - \frac{q_i q_j}{q^2} \right) + G_2(q) \frac{q_i q_j}{q^2} \right) \}. \end{aligned} \quad (3.181)$$

This form of the propagator is always the same to all orders of the field expansion. Now we have all we need to derive the flow equations of the coupling constants.

3.6.4.4 Flow Equations of u and v

The effective potential can be written as:

$$U_{\text{eff}} = \sum_{\{n_\alpha\}} \frac{1}{(n_1!) \dots (n_D!)} \left(\frac{\delta^{n_1 + \dots + n_D} U_{\text{eff}}}{\delta t_1^{n_1} \dots \delta t_D^{n_D}} \right) \Big|_{min} t_1^{n_1} \dots t_D^{n_D} \quad (3.182)$$

with $a_{n_1, \dots, n_D} = \frac{1}{(n_1!) \dots (n_D!)} \left(\frac{\delta^{n_1 + \dots + n_D} U_{\text{eff}}}{\delta t_1^{n_1} \dots \delta t_D^{n_D}} \right) \Big|_{min}$ are the coupling constants. Since $\Gamma_k^{(2)}$ in the configuration Λ is not a function of the trace t_n but of the eigenvalues λ_α it is better to define the couplings as derivatives in respect to the eigenvalues or more precisely of the square $\rho_\alpha = \lambda_\alpha$.

The first and second derivatives of U_{eff} with respect to ρ are respectively given by:

$$\begin{aligned} \frac{\partial U_{\text{eff}}}{\partial \rho_\alpha} &= \sum_{n=1}^D \frac{\delta U_{\text{eff}}}{\delta t_n} \frac{\partial t_n}{\partial \rho_\alpha} \\ &= \sum_{n=1}^D n \frac{\delta U_{\text{eff}}}{\delta t_n} (\rho_\alpha - \zeta^2)^{n-1} \end{aligned} \quad (3.183)$$

and by:

$$\begin{aligned} \frac{\partial^2 U_{\text{eff}}}{\partial \rho_\alpha \partial \rho_\beta} &= \sum_{n,m=1}^D nm \frac{\delta^2 U_{\text{eff}}}{\delta t_n \delta t_m} (\rho_\alpha - \zeta^2)^{n-1} (\rho_\beta - \zeta^2)^{m-1} \\ &+ \delta_{\alpha\beta} \sum_{n=1}^D n(n-1) \frac{\delta U_{\text{eff}}}{\delta t_n} (\rho_\alpha - \zeta^2)^{n-2}. \end{aligned} \quad (3.184)$$

At the minimum the second derivative becomes:

$$\begin{aligned} \frac{\partial^2 U_{\text{eff}}}{\partial \rho_\alpha \partial \rho_\beta} \Big|_{\min} &= \frac{\delta^2 U_{\text{eff}}}{\delta t_1(\Lambda) \delta t_1(\Lambda)} \Big|_{\min} + 2\delta_{\alpha\beta} \frac{\delta U_{\text{eff}}}{\delta t_2(\Lambda)} \Big|_{\min} \\ &= 2(v + \delta_{\alpha\beta} u) \end{aligned} \quad (3.185)$$

from which we see that we need the flow of $\left(\frac{\partial^2 U_{\text{eff}}}{\partial \rho_\alpha \partial \rho_\beta}\right) \Big|_{\min}$:

$$\partial_t \left(\frac{\partial^2 U_{\text{eff}}}{\partial \rho_\alpha \partial \rho_\beta} \Big|_{\min} \right) = \left(\partial_t \frac{\partial^2 U_{\text{eff}}}{\partial \rho_\alpha \partial \rho_\beta} \Big|_{\min} \right) + \sum_{\gamma=1}^D \frac{\partial^3 U_{\text{eff}}}{\partial \rho_\alpha \partial \rho_\beta \partial \rho_\gamma} \Big|_{\min} \partial_t \zeta^2 \quad (3.186)$$

where:

$$\begin{aligned} \left(\partial_t \frac{\partial^2 U_{\text{eff}}}{\partial \rho_\alpha \partial \rho_\beta} \Big|_{\min} \right) &= \frac{1}{2} \tilde{\partial}_t \int_q \left(\frac{\partial^2}{\partial \rho_\alpha \partial \rho_\beta} \text{Tr} \left[\ln \left(\Gamma_\Lambda^{(2)} + R_k \right) \right] \right) \Big|_{\min} \\ &= \frac{1}{2} \tilde{\partial}_t \int_q \text{Tr} \left\{ \frac{\partial^2 \Gamma^{(2)}}{\partial \rho_\beta \partial \rho_\alpha} \mathcal{P}_\Lambda(q) + \frac{\partial \Gamma^{(2)}}{\partial \rho_\alpha} \frac{\partial \mathcal{P}_\Lambda(q)}{\partial \rho_\beta} \right\} \Big|_{\min} \end{aligned} \quad (3.187)$$

where $\mathcal{P}_\Lambda(q)$ is the propagator in the configuration Λ and since $\mathcal{P}_\Lambda(q) \mathcal{P}_\Lambda^{-1}(q) = I_D$ we have:

$$\frac{\partial \mathcal{P}_\Lambda}{\partial \rho_\beta} \mathcal{P}_\Lambda^{-1} + \mathcal{P}_\Lambda \frac{\partial \mathcal{P}_\Lambda^{-1}}{\partial \rho_\beta} = 0 \quad (3.188)$$

which leads to:

$$\frac{\partial \mathcal{P}_\Lambda}{\partial \rho_\beta} = -\mathcal{P}_\Lambda \frac{\partial \Gamma_\Lambda^{(2)}}{\partial \rho_\beta} \mathcal{P}_\Lambda \quad (3.189)$$

and at the minimum we have:

$$\left(\frac{\partial \mathcal{P}_\Lambda}{\partial \rho_\beta} \right) \Big|_{\min} = -\mathcal{P}_{\min} \left(\frac{\partial \Gamma_\Lambda^{(2)}}{\partial \rho_\beta} \right) \Big|_{\min} \mathcal{P}_{\min} \quad (3.190)$$

This finally leads to:

$$\left(\partial_t \frac{\partial^2 U_{\text{eff}}}{\partial \rho_\alpha \partial \rho_\beta} \right) \Big|_{\min} = \frac{1}{2} \tilde{\partial}_t \int_q \text{Tr} \left\{ \left(\frac{\partial^2 \Gamma_\Lambda^{(2)}}{\partial \rho_\alpha \partial \rho_\beta} \right) \Big|_{\min} \mathcal{P}_{\min} - \left(\frac{\partial \Gamma_\Lambda^{(2)}}{\partial \rho_\alpha} \right) \Big|_{\min} \mathcal{P}_{\min} \left(\frac{\partial \Gamma_\Lambda^{(2)}}{\partial \rho_\beta} \right) \Big|_{\min} \mathcal{P}_{\min} \right\}. \quad (3.191)$$

Now we have all the ingredients to derive the flow equations of u and v we simply need to compute the matrix products in this last equation and take the indices corresponding to each coupling. This last task is done by computer but the expression are not given here because they are too long. In the next sections we derive the flow of ζ with this method and then give the definition of all the couplings in terms of derivatives of U_{eff} with respect to ρ .

3.6.4.5 Flow of ζ^2

The flow of ζ^2 is obtained from the minimum condition:

$$\frac{\partial U_{\text{eff}}}{\partial \rho_\alpha} \Big|_{\min} = 0. \quad (3.192)$$

We take the derivative with respect to t of this condition:

$$\sum_{\alpha=1}^D \left(\partial_t \frac{\partial U_{\text{eff}}}{\partial \rho_\alpha} \right) \Big|_{\min} + \sum_{\alpha, \beta=1}^D \left(\frac{\partial^2 U_{\text{eff}}}{\partial \rho_\alpha \partial \rho_\beta} \right) \Big|_{\min} \partial \zeta^2 = 0 \quad (3.193)$$

which leads to:

$$\partial_t \zeta^2 = - \frac{\sum_{\alpha=1}^D \left(\partial_t \frac{\partial U_{\text{eff}}}{\partial \rho_\alpha} \right) \Big|_{\min}}{\sum_{\alpha, \beta=1}^D \left(\frac{\partial^2 U_{\text{eff}}}{\partial \rho_\alpha \partial \rho_\beta} \right) \Big|_{\min}}. \quad (3.194)$$

From eq. (3.185) we find for the denominator:

$$\sum_{\alpha, \beta=1}^D \left(\frac{\partial^2 U_{\text{eff}}}{\partial \rho_\alpha \partial \rho_\beta} \right) \Big|_{\min} = 2D(u + Dv) \quad (3.195)$$

and the numerator is given by:

$$\sum_{\alpha=1}^D \left(\partial_t \frac{\partial U_{\text{eff}}}{\partial \rho_\alpha} \right) \Big|_{\min} = \frac{1}{2} \tilde{\partial}_t \int_q \text{Tr} \left[\sum_{\alpha=1}^D \left(\frac{\partial \Gamma_\Lambda^{(2)}}{\partial \rho_\alpha} \right) \Big|_{\min} P_{\min} \right] \quad (3.196)$$

where this last step is again done by computer. In the next section we give the definitions of the coupling constants.

3.6.4.6 Definitions of the Coupling Constants

The effective average action at the order r^8 reads:

$$\begin{aligned} \Gamma_k[\vec{r}] = & \int d^D x \left\{ \frac{Z_k}{2} (\partial^2 \vec{r})^2 + u (\partial_\mu \vec{r} \cdot \partial_\nu \vec{r} - \zeta^2 \delta_{\mu\nu})^2 + v (\partial_\mu \vec{r} \cdot \partial_\mu \vec{r} - D\zeta^2)^2 \right. \\ & + w_1 (\partial_\mu \vec{r} \cdot \partial_\mu \vec{r} - D\zeta^2)^3 + w_2 (\partial_\mu \vec{r} \cdot \partial_\nu \vec{r} - \zeta^2 \delta_{\mu\nu})^2 (\partial_\alpha \vec{r} \cdot \partial_\alpha \vec{r} - D\zeta^2) \\ & + w_3 (\partial_\mu \vec{r} \cdot \partial_\nu \vec{r} - \zeta^2 \delta_{\mu\nu}) (\partial_\nu \vec{r} \cdot \partial_\alpha \vec{r} - \zeta^2 \delta_{\nu\alpha}) (\partial_\alpha \vec{r} \cdot \partial_\mu \vec{r} - \zeta^2 \delta_{\alpha\mu}) \\ & + C_1 (\partial_\mu \vec{r} \cdot \partial_\mu \vec{r} - D\zeta^2)^4 + C_2 (\partial_\mu \vec{r} \cdot \partial_\nu \vec{r} - \delta_{\mu\nu} \zeta^2)^2 (\partial_\alpha \vec{r} \cdot \partial_\alpha \vec{r} - D\zeta^2)^2 \\ & + C_3 (\partial_\mu \vec{r} \cdot \partial_\nu \vec{r} - \delta_{\mu\nu} \zeta^2)^2 (\partial_\alpha \vec{r} \cdot \partial_\beta \vec{r} - \delta_{\alpha\beta} \zeta^2)^2 \\ & + C_4 (\partial_\mu \vec{r} \cdot \partial_\nu \vec{r} - \zeta^2 \delta_{\mu\nu}) (\partial_\nu \vec{r} \cdot \partial_\alpha \vec{r} - \zeta^2 \delta_{\nu\alpha}) (\partial_\alpha \vec{r} \cdot \partial_\mu \vec{r} - \zeta^2 \delta_{\alpha\mu}) (\partial_\beta \vec{r} \cdot \partial_\beta \vec{r} - D\zeta^2) \\ & \left. + C_5 (\partial_\mu \vec{r} \cdot \partial_\nu \vec{r} - \zeta^2 \delta_{\mu\nu}) (\partial_\nu \vec{r} \cdot \partial_\alpha \vec{r} - \zeta^2 \delta_{\nu\alpha}) (\partial_\alpha \vec{r} \cdot \partial_\beta \vec{r} - \zeta^2 \delta_{\alpha\beta}) (\partial_\beta \vec{r} \cdot \partial_\mu \vec{r} - \zeta^2 \delta_{\beta\mu}) \right\} \end{aligned} \quad (3.197)$$

from which we see that adding two more orders of the field expansions adds eight new coupling constants labelled $w_{i=1,2,3}$ and $C_{i=1,2,3,4,5}$.

$$v = \frac{1}{2} \left(\frac{\partial^2 U_{\text{eff}}}{\partial \rho_1 \partial \rho_2} \right)_{\min} \quad (3.198)$$

$$u = \frac{1}{2} \left\{ \left(\frac{\partial^2 U_{\text{eff}}}{\partial \rho_1 \partial \rho_1} \right)_{\min} - \left(\frac{\partial^2 U_{\text{eff}}}{\partial \rho_1 \partial \rho_2} \right)_{\min} \right\} \quad (3.199)$$

$$w_1 = \frac{1}{3!} \left(\frac{\partial^3 U_{\text{eff}}}{\partial \rho_1 \partial \rho_2 \partial \rho_3} \right)_{\min} \quad (3.200)$$

$$w_2 = \frac{1}{2} \left\{ \left(\frac{\partial^3 U_{\text{eff}}}{\partial \rho_1 \partial \rho_1 \partial \rho_2} \right)_{\min} - \left(\frac{\partial^3 U_{\text{eff}}}{\partial \rho_1 \partial \rho_2 \partial \rho_3} \right)_{\min} \right\} \quad (3.201)$$

$$w_3 = \frac{1}{3!} \left\{ \left(\frac{\partial^3 U_{\text{eff}}}{\partial \rho_1 \partial \rho_1 \partial \rho_1} \right)_{\min} - 3 \left(\frac{\partial^3 U_{\text{eff}}}{\partial \rho_1 \partial \rho_1 \partial \rho_2} \right)_{\min} + 2 \left(\frac{\partial^3 U_{\text{eff}}}{\partial \rho_1 \partial \rho_2 \partial \rho_3} \right)_{\min} \right\} \quad (3.202)$$

$$C_1 = \frac{1}{4!} \left(\frac{\partial^4 U_{\text{eff}}}{\partial \rho_1 \partial \rho_2 \partial \rho_3 \partial \rho_4} \right)_{\min} \quad (3.203)$$

$$C_2 = \frac{1}{4} \left\{ \left(\frac{\partial^4 U_{\text{eff}}}{\partial \rho_1 \partial \rho_2 \partial \rho_2 \partial \rho_3} \right)_{\min} - \left(\frac{\partial^4 U_{\text{eff}}}{\partial \rho_1 \partial \rho_2 \partial \rho_3 \partial \rho_4} \right)_{\min} \right\} \quad (3.204)$$

$$C_3 = \frac{1}{8} \left\{ \left(\frac{\partial^4 U_{\text{eff}}}{\partial \rho_1 \partial \rho_1 \partial \rho_2 \partial \rho_2} \right)_{\min} - 2 \left(\frac{\partial^4 U_{\text{eff}}}{\partial \rho_1 \partial \rho_1 \partial \rho_2 \partial \rho_3} \right)_{\min} + \left(\frac{\partial^4 U_{\text{eff}}}{\partial \rho_1 \partial \rho_2 \partial \rho_3 \partial \rho_4} \right)_{\min} \right\} \quad (3.205)$$

$$C_4 = \frac{1}{3!} \left\{ \left(\frac{\partial^4 U_{\text{eff}}}{\partial \rho_1 \partial \rho_1 \partial \rho_1 \partial \rho_2} \right)_{\min} - 3 \left(\frac{\partial^4 U_{\text{eff}}}{\partial \rho_1 \partial \rho_1 \partial \rho_2 \partial \rho_3} \right)_{\min} + 2 \left(\frac{\partial^4 U_{\text{eff}}}{\partial \rho_1 \partial \rho_2 \partial \rho_3 \partial \rho_4} \right)_{\min} \right\} \quad (3.206)$$

$$C_5 = \frac{1}{4!} \left\{ \left(\frac{\partial^4 U_{\text{eff}}}{\partial \rho_1 \partial \rho_1 \partial \rho_1 \partial \rho_1} \right)_{\min} - 4 \left(\frac{\partial^4 U_{\text{eff}}}{\partial \rho_1 \partial \rho_1 \partial \rho_1 \partial \rho_2} \right)_{\min} - 3 \left(\frac{\partial^4 U_{\text{eff}}}{\partial \rho_1 \partial \rho_1 \partial \rho_2 \partial \rho_2} \right)_{\min} + 12 \left(\frac{\partial^4 U_{\text{eff}}}{\partial \rho_1 \partial \rho_1 \partial \rho_2 \partial \rho_3} \right)_{\min} - 6 \left(\frac{\partial^4 U_{\text{eff}}}{\partial \rho_1 \partial \rho_2 \partial \rho_3 \partial \rho_4} \right)_{\min} \right\} \quad (3.207)$$

With successive derivatives of the flow of effective potential U_{eff} (see Appendix) we obtain the flow equations of the running coupling constants. These equations are too long to be displayed here.

3.6.5 Crumpled to Flat Transition

We start with the crumpling transition. From the one loop structure of the Wetterich equation (2.39) we can recover the perturbative results at the order ϵ from the fourth order of the field expansion since the other couplings are irrelevant. We expand Eqs. (3.141) and (3.142) in powers of $\epsilon = D - 4$. The couplings u and v are of order ϵ at any non-trivial fixed-point. The threshold functions in these flow equations have a universal, cut-off independent, limit at vanishing masses in $D = 4$ given by $L_{abc}^8 = 1$. The flow equations in this limit read:

$$\partial_t u = -\epsilon u + \frac{(d+21)u^2 + 20uv + 4v^2}{24\pi^2} \quad (3.208)$$

$$\partial_t v = -\epsilon v + \frac{(d+15)u^2 + 4(3d+17)uv + 4(6d+7)v^2}{48\pi^2} \quad (3.209)$$

These are the equations derived in [104] (up to a change of variable $v \rightarrow v - u/4$).

The Crumpled to flat transition can be either first order or second depending on both the membrane dimension D and the embedding Euclidean space dimension d . What happens is that above $d_c(D)$ there are two fixed-points that are close to each other, one which is the *crumpling transition fixed-point* (CTFP) and the other is an unstable fixed point. Lowering the embedding dimension but staying above d_c the two fixed-points come closer and closer. At $d = d_c$, the fixed-points collapse on one another and annihilate each other just below d_c and the transition turns first order. Moreover there is an eigenvalue ω that represents how far the fixed-points are from each other (the sign of the eigenvalue depend on the fixed-point we are at). Tracking the evolution of the eigenvalue, one can construct the whole $d_c(D)$ line [53].

At the lowest order of the field expansion r^4 with a θ cut-off, $R_k(q) = (k^4 - q^4)\theta(k^2 - q^2)$, Kownacki and Mouhanna [53] found a smooth curve $d_c(D)$ which start at $d_c = 219$ for $D = 4$ and reaches $d_c = 2$ for $D = 2$ leading to predict a second order phase transition (see Fig. 3.22). For this transition they found a correlation exponent $\nu = 0.52$ and an anomalous dimension $\eta = 0.627$ which compares well with another recent NPRG computation by Braghin and Hasselmann [36], where the full momentum dependence of the elastic coupling was included and with a different cut-off function, $\eta = 0.64(5)$ as well as with the large- d result $\eta = 2/3$ ([111], [112]) and with the Monte Carlo simulations $\eta = 0.71(5)$ [113] but less with the Monte Carlo renormalization group result $\eta = 0.85(15)$ [114] and the self-consistent screening approximation result $\eta = 0.535$ [108]. However using another cut-off function $R_k = Z_k q^4 / (\exp(q^4/k^4) - 1)$, Kownacki and Mouhanna evaluated the error bar

on $d_c(D = 2)$ to be typically of order $\delta d_c(D = 2) \sim 1$. This means that at a weakly first-order transition cannot be excluded in agreement with recent Monte Carlo results ([109], [110]). Therefore we took an effective average action up to the eighth order (3.197).

Our results are plotted on Fig. 3.23. We find using the $d_c(D = 2) \approx 6.9$ and $d_c(D = 2) \approx 4.19$ for the sixth and eighth orders respectively. This discrepancy between the sixth and eighth orders in the value of the critical dimension d_c for a two-dimensional means that the field expansion is not converged yet. Using another cut-off, $R_k(q) = Z_k q^4 / (\exp(q^4/k^4) - 1)$, we find slight variation in the value of $d_c(D = 2)$ which are of order ~ 0.5 and ~ 0.1 for r^6 and r^8 respectively. Unfortunately going beyond the eighth order seems to be impossible because of the heavy computational resources that are needed. However these results seems to indicate that the transition is first order in agreement with recent Monte Carlo results ([109], [110]). We know that higher orders in the field expansion will change the value of $d_c(D = 2)$ but we believe that it will remain between 4 and 7 and hence we have a first order transition. Since we cannot go beyond the eighth order, we are currently concentrating on a full potential computation.

3.6.6 Symmetry Breaking, Goldstone Bosons and Flat Phase

Two-dimensional polymerized membranes have a stable low-temperature phase. This is related to the existence of long-range interactions mediated by phonons which makes it outside of the domain of applicability of the Mermin-Wagner theorem. In the high bending rigidity phase, *i.e.* the flat phase, the coupling between the out-of-plane bending and the in-plane elasticity modes strengthen the bending rigidity and stabilizes the flat phase. In the language of the renormalization group, we say that the fixed point of the flat phase is attractive.

In addition to avoiding the Mermin-Wagner theorem polymerized membranes are characterized by a quite original Goldstone spectrum. Indeed the Goldstone theorem on internal symmetry states that if a system is invariant under a global symmetry G and is broken down to a group H , the number of Goldstone bosons (massless modes) is equal to the number of broken generators ([115], [116]). However there are some exceptions to the validity of this theorem like when the global symmetry G is gauged into a local symmetry group ([117], [118]).

The crumpled phase is symmetric under the Euclidean group $E(d)$ which corresponds to translations and rotations. At the transition a symmetry breaking occurs and the membrane is

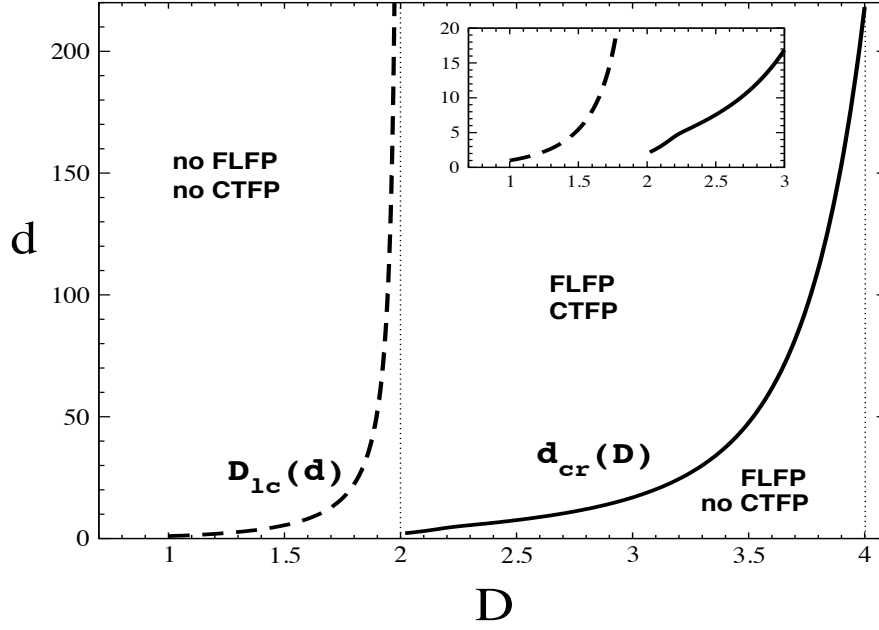


FIGURE 3.22: The critical dimension d_c as a function of the membrane dimension D . The transition is 2^{nd} order above the curve and 1^{st} order below it. This plot corresponds to the lowest order of the field expansion r^4 .

not $E(d)$ invariant any more. In the flat phase the membrane is $T(D)$ translational invariant and $O(D)$ and $O(d - D)$ rotational invariant. This corresponds to a symmetry breaking scheme given by:

$$\frac{O(d)}{O(D) \times O(d - D)} \quad (3.210)$$

The minimum configuration in the low-temperature phase is given by: $\vec{r}_{\min}(x) = \zeta x^\mu \mathbf{e}_\mu = \zeta x^i \mathbf{e}_i \theta(D - i)$. Let A be an element of $O(D) \times O(d - D)$ and it is of the form:

$$A_{ij} = \begin{cases} (B_D)_{ij} & \text{if } i, j \leq D \\ (C_{d-D})_{i-D, j-D} & \text{if } D < i, j \leq d \\ 0 & \text{else} \end{cases} \quad (3.211)$$

where B_D and C_{d-D} belong respectively to the $O(D)$ and $O(d - D)$ groups. Therefore there are $(d - D)$ translational broken generators and n_b the number of $O(d)$ broken generators. To

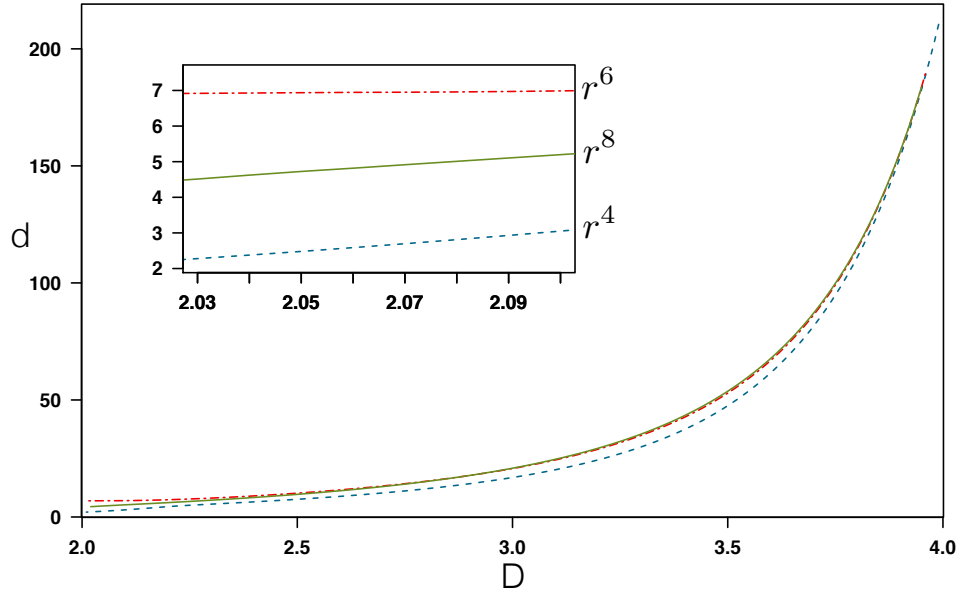


FIGURE 3.23: The critical dimension d_c as a function of the membrane dimension D . The transition is 2^{nd} order above the curve and 1^{st} order below it. plot at orders r^4 , r^6 and r^8

find the number of Goldstone modes we need the number of rotational broken generators. The $d(d-1)/2$ generators of $O(d)$ can be expressed as:

$$(M^{pq})_{ab} = i(\delta_{ap}\delta_{bq} - \delta_{aq}\delta_{bp}) \quad (3.212)$$

with $p, q = 1, \dots, d$ ($p < q$) are the indices of the name of the generator and $a, b = 1, \dots, d$ are the indices of line and column. The broken generators are the $M^{\alpha, (D+j)}$ with $\alpha = 1, \dots, D$ and $j = 1, \dots, d-D$. An excitation $\delta\vec{r}(\alpha, D+j)$ around the minimum generated by a broken generator $M^{\alpha, (D+j)}$ reads:

$$\begin{aligned} \delta r_a(\alpha, D+j) &= f(x) \sum_{b=1}^d (M^{\alpha, (D+j)})_{ab} r_{b|min} \\ &= \zeta f(x) \sum_{b=1}^d (M^{\alpha, (D+j)})_{ab} x_b \theta(D-b) \\ &= i\zeta f(x) \sum_{b=1}^D (\delta_{a\alpha}\delta_{b, D+j} - \delta_{a, D+j}\delta_{b\alpha}) x_b \end{aligned} \quad (3.213)$$

with $f(x)$ a function of x_μ . In this sum $\delta_{b,D+j}$ is vanishing since $b \leq D$ and the excitation now reads:

$$\delta r_a(\alpha, D+j) = i\zeta f(x)\delta_{a,D+j}x_\alpha \quad (3.214)$$

or:

$$\delta \vec{r}(\alpha, D+j) = -i\zeta f(x)x_\alpha \vec{h}_{D+j} \quad (3.215)$$

where \vec{h}_{D+j} are the $(d-D)$ out-of-plane vectors. We see that this excitation can be written as generated by the translational broken generators in the directions \vec{h}_{D+j} . Since each excitation generated by a rotational broken generator can be written as an excitation generated by a translational broken generator, the number of independent excitations is equal to the number of broken translational generators, *i.e.* $(d-D)$.

In the flat phase, the flow equations of the coupling constants can be obtained simply by considering the regime $\zeta \gg 1$, *i.e.* a regime where the phonon masses m_1 and m_2 are very large and dominated by the capillary waves⁹. In this limit we have for the threshold functions:

$$L_{abc}^{D+\alpha} = \begin{cases} 0 & \text{if } b, c \neq 0 \\ L_{a00}^{D+\alpha} & \text{else.} \end{cases} \quad (3.216)$$

With this the flows u and v read:

$$\partial_t u = (D-4+2\eta_k)u + \frac{32A_D}{D(D+2)}u^2 L_{200}^{D+4} \quad (3.217)$$

$$\partial_t v = (D-4+2\eta_k)v + \frac{16A_D}{D(D+2)}\{u^2 + 2(D+2)uv + D(D+2)v^2\} L_{200}^{D+4} \quad (3.218)$$

and for ζ^2 :

$$\partial_t \zeta^2 = -(D-2+\eta_k)\zeta^2 - \frac{4(d-D)A_D}{D\zeta^2}L_{100}^{D+2}. \quad (3.219)$$

⁹We recall that the coupling ζ is taken as dimensionless. The dimensionful coupling is always finite.

Using a θ cut-off, $R_k(q) = (k^4 - q^4)\theta(k^2 - q^2)$, these equations read:

$$\partial_t u = (D - 4 + 2\eta_k) u + \frac{256\tilde{d}\tilde{A}_D u^2}{D(D+2)(D+4)(D+8)} \quad (3.220)$$

$$\partial_t v = (D - 4 + 2\eta_k) v + \frac{128\tilde{d}\tilde{A}_D (u^2 + 2(D+2)uv + D(D+2)v^2)}{D(D+2)(D+4)(D+8)} \quad (3.221)$$

$$\partial_t \zeta^2 = -(D - 2 + \eta_k) \alpha - \frac{16\tilde{d}\tilde{A}_D (6 + D - \eta_k)}{\zeta^2 D(D^2 + 8D + 12)} \quad (3.222)$$

with $\tilde{d} = (d - D)$ and $\tilde{A}_D = A_D(8 + D - \eta_k)$. The anomalous dimension η_k now reads:

$$\eta_k = \frac{128A_D(D+4)(D^2-1)u(u+2v)}{(D^4+6D^3+8D^2)+128A_D(D^2-1)u(u+2v)}. \quad (3.223)$$

A remarkable fact is that in the flat phase the flow equations of u and v do not depend on coupling constants associated with higher orders than r^4 . In the flat phase the anomalous dimension η_k correspond to the exponent of the capillary waves and the exponent for the phonons η_u is obtain from the Ward identity (rotational invariance) $\eta_u = 4 - D - \eta_k$.

The equations (3.220 - 3.223) have three non-trivial fixed-points among which the *flat phase fixed-point* (FLFP). This fixed-point is stable in all the directions down to the lower critical dimension D_{lc} . In the large- d limit one finds that $\eta_k \sim O(1/d)$ in agreement with previous large- d result [112]. From eq. (3.223) we find that the FLFP is stable down to $D_{lc}(d \rightarrow \infty) = 2$ as predicted by [112] $D_{lc}(d \rightarrow \infty) = 2 - 2/d + O(1/d^2)$.

In the physically interesting case $d = 3$ and $D = 2$, one finds that $\eta^* = 0.849$ in very good agreement with another NPRG result $\eta = 0.85$ [36] as well as with the self-consistent screening result $\eta = 0.821$ [108] and with numerical simulations where $\eta = 0.750(5)$ [113] and $\eta = 0.81(3)$ [119] but not with large- d result $\eta = 2/3$ [112].

Note that within the NPRG approach by Braghin and Hasselmann [36] where a full momentum dependence of the couplings was included they were able to compute the height and normal correlation functions, G_{hh} and G_n . For small momentum q they retrieved the relation:

$$q^2 G_{hh}(q) \sim G_n(q). \quad (3.224)$$

Furthermore the behaviour of the correlation functions was in good agreement with Monte Carlo simulations [120, 121, 122, 123].

Last but not least from Eqs. (3.220 - 3.223) one can determine the line D_{lc} that separates the regions where the flat can or cannot exist. When we are at $D = D_{lc}$ the CTFP and the FLFP collapse on each other and become unstable. We have the relation $\eta_k(D_{lc}) = 2 - D_{lc}$ at the FLFP which give:

$$d = \frac{D_{lc}^4 + 6D_{lc}^3 - 3D_{lc}^2 + 4D_{lc}}{2(6 - D_{lc}^2 - D_{lc})} \quad (3.225)$$

and once inverted this equation gives the line $D_{lc}(d)$. With a NPRG approach Kownacki and Mouhanna obtained the whole D_{lc} line (see Fig. 3.22) and they find $D_{lc}(d = 3) = 1.33$. This value is quite stable with respect of cut-off change and compares well with previous results, large- d $D_{lc}(d = 3) = 4/3$ [112] and SCSA $D_{lc}(d = 3) = 1.5$ [108].

3.7 Conclusion

With a non-perturbative approach we are able to tackle the problem of polymerized membranes between the upper critical dimension D_{uc} , above the critical exponents take their mean field values, and the lower critical dimension $D_{lc}(d)$, below which there is no long-range or crystalline order, for any given Euclidean space dimension d . The results of Kownacki & Mouhanna are in good agreement with the results of Braghin & Hasselmann which shows that the momentum dependence is irrelevant for the transition. However our results show that the lowest order of the field expansion is not sufficient to determine the order of the transition. Moreover even with an expansion up to the eighth order we do not have convergence yet but the results seems to indicate that the crumpling transition for polymerized membranes between a high-temperature crumpled phase and the low-temperature flat phase is first order. However we need a full potential computation to completely settle this question. The study of the flat phase has shown that higher order terms are not needed for this phase and the results are in good agreement with several different approaches. This flat phase is also relevant for the study of the behaviour of graphene

In our work we have neglected the self-avoidance which must be included to correctly describe real physical membranes which are not phantom. There is an important controversy on

the effect of self-avoidance whether it breaks [124, 125, 126] or not the existence of the crumpled phase [127] as found in experimentally in graphite oxide [128]. Our aim is to perform a non-perturbative computation with self-avoidance although it is a complicated task from a technical point of view.

Appendix B

Cayley-Hamilton Theorem and Faddeev-Leverrier Algorithm

The Cayley-Hamilton theorem states that any square matrix satisfies its own characteristic polynomial. Given a $n \times n$ matrix M , the characteristic polynomial is given by:

$$p(\lambda) = \det(\lambda I_n - M) \quad (\text{B.1})$$

Replacing λ by M in this equation yields the zero matrix:

$$p(M) = 0 \quad (\text{B.2})$$

The Faddeev-Leverrier algorithm is a method to calculate a matrix's characteristic polynomial. Let M be a $n \times n$ matrix:

$$P_M(X) = \det(XI_n - M) = X^n - \sum_{k=1}^n \frac{1}{k} \text{Tr}(M_{k-1}) X^{n-k} \quad (\text{B.3})$$

with :

$$\begin{aligned} M_0 &= M \\ M_k &= M(M_{k-1} - \frac{1}{k}\text{Tr}(M_{k-1})I_n), \forall 1 \leq k \leq n-1 \end{aligned} \quad (\text{B.4})$$

For $n = 2$:

$$P_M(X) = X^2 - \text{Tr}(M_0)X - \frac{1}{2}\text{Tr}(M_1) \quad (\text{B.5})$$

For $n = 3$:

$$P_M(X) = X^3 - \text{Tr}(M_0)X^2 - \frac{1}{2}\text{Tr}(M_1)X - \frac{1}{3}\text{Tr}(M_2) \quad (\text{B.6})$$

If M is a 2×2 matrix, then :

$$\begin{aligned} \text{Tr}(M_2) &= \text{Tr}(M^3) - \frac{3}{2}\text{Tr}(M^2)\text{Tr}(M) + \frac{1}{2}(\text{Tr}(M))^3 \\ &= 0 \end{aligned} \quad (\text{B.7})$$

More generally, let M be a $n \times n$ matrix:

$$\text{Tr}(M_i) = 0 \forall i \geq n \quad (\text{B.8})$$

We said before that $k \leq n-1$ but there is no reason why we can't extend this to any given k .

$$M_1 = M^2 - M\text{Tr}(M) \quad (\text{B.9})$$

$$M_2 = M^3 - M^2\text{Tr}(M) - \frac{1}{2}M\text{Tr}(M^2) + \frac{1}{2}M(\text{Tr}(M))^2 \quad (\text{B.10})$$

$$M_3 = M^4 - M^3\text{Tr}(M) - \frac{1}{2}M^2\text{Tr}(M^2) + \frac{1}{2}M^2(\text{Tr}(M))^2 - \frac{1}{3} \left[M\text{Tr}(M^3) - \frac{3}{2}M\text{Tr}(M^2)\text{Tr}(M) + \frac{1}{2}M(\text{Tr}(M))^3 \right] \quad (\text{B.11})$$

$$M_4 = M^5 - M^4\text{Tr}(M) - \frac{1}{2}M^3\text{Tr}(M^2) + \frac{1}{2}M^3(\text{Tr}(M))^2 - \frac{1}{3}M^2\text{Tr}(M^3) + \frac{1}{2}M^2\text{Tr}(M^2)\text{Tr}(M) - \frac{1}{6}M^2(\text{Tr}(M))^3 - \frac{1}{4} \left[M\text{Tr}(M^4) - \frac{4}{3}M\text{Tr}(M)\text{Tr}(M^3) - \frac{1}{2}M(\text{Tr}(M^2))^2 + M(\text{Tr}(M))^2\text{Tr}(M^2) - \frac{1}{6}M(\text{Tr}(M))^4 \right] \quad (\text{B.12})$$

and the trace reads:

$$\text{Tr}(M_1) = \text{Tr}(M^2) - (\text{Tr}(M))^2 \quad (\text{B.13})$$

$$\text{Tr}(M_2) = \text{Tr}(M^3) - \frac{3}{2}\text{Tr}(M^2)\text{Tr}(M) + \frac{1}{2}(\text{Tr}(M))^3 \quad (\text{B.14})$$

$$\text{Tr}(M_3) = \text{Tr}(M^4) - \frac{4}{3}\text{Tr}(M^3)\text{Tr}(M) - \frac{1}{2}(\text{Tr}(M^2))^2 + \text{Tr}(M^2)(\text{Tr}(M))^2 - \frac{1}{6}(\text{Tr}(M))^4 \quad (\text{B.15})$$

$$\text{Tr}(M_4) = \text{Tr}(M^5) - \frac{5}{4}\text{Tr}(M^4)\text{Tr}(M) - \frac{5}{6}\text{Tr}(M^3)\text{Tr}(M^2) + \frac{5}{6}(\text{Tr}(M))^2\text{Tr}(M^3) + \frac{5}{8}(\text{Tr}(M^2))^2\text{Tr}(M) - \frac{5}{12}\text{Tr}(M^2)(\text{Tr}(M))^3 + \frac{1}{24}(\text{Tr}(M))^5 \quad (\text{B.16})$$

Appendix C

Derivatives of the Flow of U_{eff}

1st derivative reads:

$$\left(\partial_t \frac{\partial U_{\text{eff}}}{\partial \rho_{j_1}} \right)_{|_{\min}} = \frac{1}{2} \tilde{\partial}_t \int_q \text{Tr} \left\{ \frac{\partial \Gamma_{\Lambda}^{(2)}}{\partial \rho_{j_1}} P_{\Lambda} \right\} \quad (\text{C.1})$$

2nd derivative reads:

$$\left(\partial_t \frac{\partial U_{\text{eff}}}{\partial \rho_{j_1} \partial \rho_{j_2}} \right)_{|_{\min}} = \frac{1}{2} \tilde{\partial}_t \int_q \text{Tr} \left\{ \frac{\partial^2 \Gamma_{\Lambda}^{(2)}}{\partial \rho_{j_1} \partial \rho_{j_2}} P_{\Lambda} + \frac{\partial \Gamma_{\Lambda}^{(2)}}{\partial \rho_{j_1}} \frac{\partial P_{\Lambda}}{\partial \rho_{j_2}} \right\} \quad (\text{C.2})$$

3rd derivative reads:

$$\begin{aligned} \left(\partial_t \frac{\partial U_{\text{eff}}}{\partial \rho_{j_1} \partial \rho_{j_2} \partial \rho_{j_3}} \right)_{|_{\min}} &= \frac{1}{2} \tilde{\partial}_t \int_q \text{Tr} \left\{ \frac{\partial^3 \Gamma_{\Lambda}^{(2)}}{\partial \rho_{j_1} \partial \rho_{j_2} \partial \rho_{j_3}} P_{\Lambda} + \frac{\partial^2 \Gamma_{\Lambda}^{(2)}}{\partial \rho_{j_1} \partial \rho_{j_2}} \frac{\partial P_{\Lambda}}{\partial \rho_{j_3}} \right. \\ &\quad \left. + \frac{\partial^2 \Gamma_{\Lambda}^{(2)}}{\partial \rho_{j_1} \partial \rho_{j_3}} \frac{\partial P_{\Lambda}}{\partial \rho_{j_2}} + \frac{\partial \Gamma_{\Lambda}^{(2)}}{\partial \rho_{j_1}} \frac{\partial^2 P_{\Lambda}}{\partial \rho_{j_2} \partial \rho_{j_3}} \right\} \quad (\text{C.3}) \end{aligned}$$

4th derivative reads:

$$\begin{aligned}
& \left(\partial_t \frac{\partial U_{\text{eff}}}{\partial \rho_{j_1} \partial \rho_{j_2} \partial \rho_{j_3} \partial \rho_{j_4}} \right) \Big|_{\min} = \\
& \frac{1}{2} \tilde{\partial}_t \int_q \text{Tr} \left\{ \frac{\partial^4 \Gamma_{\Lambda}^{(2)}}{\partial \rho_{j_1} \partial \rho_{j_2} \partial \rho_{j_3} \partial \rho_{j_4}} P_{\Lambda} + \frac{\partial^3 \Gamma_{\Lambda}^{(2)}}{\partial \rho_{j_1} \partial \rho_{j_2} \partial \rho_{j_3}} \frac{\partial P_{\Lambda}}{\partial \rho_{j_4}} \right. \\
& + \frac{\partial^3 \Gamma_{\Lambda}^{(2)}}{\partial \rho_{j_1} \partial \rho_{j_2} \partial \rho_{j_4}} \frac{\partial P_{\Lambda}}{\partial \rho_{j_3}} + \frac{\partial^2 \Gamma_{\Lambda}^{(2)}}{\partial \rho_{j_1} \partial \rho_{j_2}} \frac{\partial^2 P_{\Lambda}}{\partial \rho_{j_3} \partial \rho_{j_4}} \\
& + \frac{\partial^3 \Gamma_{\Lambda}^{(2)}}{\partial \rho_{j_1} \partial \rho_{j_3} \partial \rho_{j_4}} \frac{\partial P_{\Lambda}}{\partial \rho_{j_2}} + \frac{\partial^2 \Gamma_{\Lambda}^{(2)}}{\partial \rho_{j_1} \partial \rho_{j_3}} \frac{\partial^2 P_{\Lambda}}{\partial \rho_{j_2} \partial \rho_{j_4}} \\
& \left. + \frac{\partial^2 \Gamma_{\Lambda}^{(2)}}{\partial \rho_{j_1} \partial \rho_{j_4}} \frac{\partial^2 P_{\Lambda}}{\partial \rho_{j_2} \partial \rho_{j_3}} + \frac{\partial \Gamma_{\Lambda}^{(2)}}{\partial \rho_{j_1}} \frac{\partial^3 P_{\Lambda}}{\partial \rho_{j_2} \partial \rho_{j_3} \partial \rho_{j_4}} \right\} \Big|_{\min} \quad (\text{C.4})
\end{aligned}$$

5th derivative reads:

$$\begin{aligned}
& \left(\partial_t \frac{\partial U_{\text{eff}}}{\partial \rho_{j_1} \partial \rho_{j_2} \partial \rho_{j_3} \partial \rho_{j_4} \partial \rho_{j_5}} \right) \Big|_{\min} = \\
& \frac{1}{2} \tilde{\partial}_t \int_q \text{Tr} \left\{ \frac{\partial^5 \Gamma_{\Lambda}^{(2)}}{\partial \rho_{j_1} \partial \rho_{j_2} \partial \rho_{j_3} \partial \rho_{j_4} \partial \rho_{j_5}} P_{\Lambda} + \frac{\partial^4 \Gamma_{\Lambda}^{(2)}}{\partial \rho_{j_1} \partial \rho_{j_2} \partial \rho_{j_3} \partial \rho_{j_4}} \frac{\partial P_{\Lambda}}{\partial \rho_{j_5}} \right. \\
& + \frac{\partial^4 \Gamma_{\Lambda}^{(2)}}{\partial \rho_{j_1} \partial \rho_{j_2} \partial \rho_{j_3} \partial \rho_{j_5}} \frac{\partial P_{\Lambda}}{\partial \rho_{j_4}} + \frac{\partial^3 \Gamma_{\Lambda}^{(2)}}{\partial \rho_{j_1} \partial \rho_{j_2} \partial \rho_{j_3}} \frac{\partial^2 P_{\Lambda}}{\partial \rho_{j_4} \partial \rho_{j_5}} \\
& + \frac{\partial^4 \Gamma_{\Lambda}^{(2)}}{\partial \rho_{j_1} \partial \rho_{j_2} \partial \rho_{j_4} \partial \rho_{j_5}} \frac{\partial P_{\Lambda}}{\partial \rho_{j_3}} + \frac{\partial^3 \Gamma_{\Lambda}^{(2)}}{\partial \rho_{j_1} \partial \rho_{j_2} \partial \rho_{j_4}} \frac{\partial^2 P_{\Lambda}}{\partial \rho_{j_3} \partial \rho_{j_5}} \\
& + \frac{\partial^3 \Gamma_{\Lambda}^{(2)}}{\partial \rho_{j_1} \partial \rho_{j_2} \partial \rho_{j_5}} \frac{\partial^2 P_{\Lambda}}{\partial \rho_{j_3} \partial \rho_{j_4}} + \frac{\partial^2 \Gamma_{\Lambda}^{(2)}}{\partial \rho_{j_1} \partial \rho_{j_2}} \frac{\partial^3 P_{\Lambda}}{\partial \rho_{j_3} \partial \rho_{j_4} \partial \rho_{j_5}} \\
& + \frac{\partial^4 \Gamma_{\Lambda}^{(2)}}{\partial \rho_{j_1} \partial \rho_{j_3} \partial \rho_{j_4} \partial \rho_{j_5}} \frac{\partial P_{\Lambda}}{\partial \rho_{j_2}} + \frac{\partial^3 \Gamma_{\Lambda}^{(2)}}{\partial \rho_{j_1} \partial \rho_{j_3} \partial \rho_{j_4}} \frac{\partial^2 P_{\Lambda}}{\partial \rho_{j_2} \partial \rho_{j_5}} \\
& + \frac{\partial^3 \Gamma_{\Lambda}^{(2)}}{\partial \rho_{j_1} \partial \rho_{j_3} \partial \rho_{j_5}} \frac{\partial^2 P_{\Lambda}}{\partial \rho_{j_2} \partial \rho_{j_4}} + \frac{\partial^2 \Gamma_{\Lambda}^{(2)}}{\partial \rho_{j_1} \partial \rho_{j_3}} \frac{\partial^2 P_{\Lambda}}{\partial \rho_{j_2} \partial \rho_{j_4} \partial \rho_{j_5}} \\
& + \frac{\partial^3 \Gamma_{\Lambda}^{(2)}}{\partial \rho_{j_1} \partial \rho_{j_4} \partial \rho_{j_5}} \frac{\partial^2 P_{\Lambda}}{\partial \rho_{j_2} \partial \rho_{j_3}} + \frac{\partial^2 \Gamma_{\Lambda}^{(2)}}{\partial \rho_{j_1} \partial \rho_{j_4}} \frac{\partial^3 P_{\Lambda}}{\partial \rho_{j_2} \partial \rho_{j_3} \partial \rho_{j_5}} \\
& \left. + \frac{\partial^2 \Gamma_{\Lambda}^{(2)}}{\partial \rho_{j_1} \partial \rho_{j_5}} \frac{\partial^3 P_{\Lambda}}{\partial \rho_{j_2} \partial \rho_{j_3} \partial \rho_{j_4}} + \frac{\partial \Gamma_{\Lambda}^{(2)}}{\partial \rho_{j_1}} \frac{\partial^4 P_{\Lambda}}{\partial \rho_{j_2} \partial \rho_{j_3} \partial \rho_{j_4} \partial \rho_{j_5}} \right\} \Big|_{\min} \quad (\text{C.5})
\end{aligned}$$

C.I Derivative of the Propagator

The product of the propagator with the inverse propagator gives the identity matrix:

$$P_{\Lambda} P_{\Lambda}^{-1} = I_D \quad (\text{C.6})$$

whose derivative is vanishing:

$$\frac{\partial P_{\Lambda}}{\partial \rho_{\alpha}} P_{\Lambda}^{-1} + P_{\Lambda} \frac{\partial P_{\Lambda}^{-1}}{\partial \rho_{\alpha}} = 0 \quad (\text{C.7})$$

$$\Rightarrow \frac{\partial P_{\Lambda}}{\partial \rho_{\alpha}} = -P_{\Lambda} \frac{\partial P_{\Lambda}^{-1}}{\partial \rho_{\alpha}} P_{\Lambda} \quad (\text{C.8})$$

Since the inverse propagator $P_{\Lambda}^{-1} = \Gamma_{\Lambda}^{(2)} + R_k$:

$$\frac{\partial P_{\Lambda}}{\partial \rho_{j_1}} = -P_{\Lambda} \frac{\partial \Gamma_{\Lambda}^{(2)}}{\partial \rho_{j_1}} P_{\Lambda} \quad (\text{C.9})$$

the second derivative reads:

$$\frac{\partial^2 P_{\Lambda}}{\partial \rho_{j_1} \partial \rho_{j_2}} = - \left\{ \frac{\partial P_{\Lambda}}{\partial \rho_{j_2}} \frac{\partial \Gamma_{\Lambda}^{(2)}}{\partial \rho_{j_1}} P_{\Lambda} + P_{\Lambda} \frac{\partial^2 \Gamma_{\Lambda}^{(2)}}{\partial \rho_{j_1} \partial \rho_{j_2}} P_{\Lambda} + P_{\Lambda} \frac{\partial \Gamma_{\Lambda}^{(2)}}{\partial \rho_{j_1}} \frac{\partial P_{\Lambda}}{\partial \rho_{j_2}} \right\} \quad (\text{C.10})$$

the third derivative reads:

$$\begin{aligned} \frac{\partial^3 P_{\Lambda}}{\partial \rho_{j_1} \partial \rho_{j_2} \partial \rho_{j_3}} = - & \left\{ \frac{\partial^2 P_{\Lambda}}{\partial \rho_{j_2} \partial \rho_{j_3}} \frac{\partial \Gamma_{\Lambda}^{(2)}}{\partial \rho_{j_1}} P_{\Lambda} + \frac{\partial P_{\Lambda}}{\partial \rho_{j_2}} \frac{\partial^2 \Gamma_{\Lambda}^{(2)}}{\partial \rho_{j_1} \partial \rho_{j_3}} P_{\Lambda} + \frac{\partial P_{\Lambda}}{\partial \rho_{j_2}} \frac{\partial \Gamma_{\Lambda}^{(2)}}{\partial \rho_{j_1}} \frac{\partial P_{\Lambda}}{\partial \rho_{j_3}} \right. \\ & + \frac{\partial P_{\Lambda}}{\partial \rho_{j_3}} \frac{\partial^2 \Gamma_{\Lambda}^{(2)}}{\partial \rho_{j_1} \partial \rho_{j_2}} P_{\Lambda} + P_{\Lambda} \frac{\partial^3 \Gamma_{\Lambda}^{(2)}}{\partial \rho_{j_1} \partial \rho_{j_2} \partial \rho_{j_3}} P_{\Lambda} + P_{\Lambda} \frac{\partial^2 \Gamma_{\Lambda}^{(2)}}{\partial \rho_{j_1} \partial \rho_{j_2}} \frac{\partial P_{\Lambda}}{\partial \rho_{j_3}} \\ & \left. + \frac{\partial P_{\Lambda}}{\partial \rho_{j_3}} \frac{\partial \Gamma_{\Lambda}^{(2)}}{\partial \rho_{j_1}} \frac{\partial P_{\Lambda}}{\partial \rho_{j_2}} + P_{\Lambda} \frac{\partial^2 \Gamma_{\Lambda}^{(2)}}{\partial \rho_{j_1} \partial \rho_{j_3}} \frac{\partial P_{\Lambda}}{\partial \rho_{j_2}} + P_{\Lambda} \frac{\partial \Gamma_{\Lambda}^{(2)}}{\partial \rho_{j_1}} \frac{\partial^2 P_{\Lambda}}{\partial \rho_{j_2} \partial \rho_{j_3}} \right\} \quad (\text{C.11}) \end{aligned}$$

Appendix D

New Definition of the Minimum Configuration ζ

In this appendix we show that we can define the minimum ζ by taking the derivative of the effective action (3.108) with respect to $\partial_\mu r_i$ instead of r_i . First let us define the derivation with respect to $\partial_\gamma r_j$:

$$\frac{\delta \partial_\mu r_i(x)}{\delta \partial_\gamma r_j(y)} = \delta_{ij} \delta_{\mu\gamma} \delta(x-y) \quad (\text{D.1})$$

$$\frac{\delta \partial_\nu \partial_\mu r_i(x)}{\delta \partial_\gamma r_j(y)} = \delta_{ij} \delta_{\mu\gamma} \partial_\mu(\delta(x-y)) + \delta_{ij} \delta_{\gamma\nu} \partial_\nu(\delta(x-y)) - \delta_{ij} \delta_{\mu\nu} \delta_{\gamma\mu} \partial_\mu(\delta(x-y)). \quad (\text{D.2})$$

In the last equation, there is no summation over the indices even if they are repeated. With this, the first derivative of the effective action is given by:

$$\frac{\delta \Gamma_k}{\delta(\partial_\gamma r_{j,y})} = -Z \partial_\gamma \partial_\nu \partial_\nu r_j + 4u (\partial_\gamma r_i \partial_\nu r_i \partial_\nu r_j - \zeta^2 \partial_\gamma r_j) + 4v \partial_\gamma r_j (\partial_\mu \vec{r} \partial_\mu \vec{r} - D\zeta^2) \quad (\text{D.3})$$

and by definition of the minimum we have:

$$\frac{\delta \Gamma_k}{\delta(\partial_\gamma r_{j,y})} \Big|_{\min} = 0. \quad (\text{D.4})$$

Note that we have changed the notation for simplicity: $r_j, y = r_j(y)$. The flow equation of (D.4), is given by:

$$\begin{aligned} \partial_t \left(\frac{\delta\Gamma_k}{\delta(\partial_\gamma r_{j,y})} \Big|_{\min} \right) &= \partial_t \left(\frac{\delta\Gamma_k}{\delta(\partial_\gamma r_{j,y})} \Big|_{\min} \right) \\ &+ \sum_{\alpha,l} \int_z \partial_t(\partial_\alpha r_{l,z}|_{\min}) \frac{\delta^2\Gamma_k}{\delta(\partial_\gamma r_{j,y})\delta(\partial_\alpha r_{l,z})|_{\min}} = 0. \end{aligned} \quad (\text{D.5})$$

The term $\partial_t(\partial_\alpha r_{l,z}|_{\min})$ gives the flow of ζ : $\partial_t(\partial_\alpha r_{l,z}|_{\min}) = \delta_{\alpha,l}\theta(D-l)\partial_t\zeta$. The previous equation becomes:

$$\partial_t \left(\frac{\delta\Gamma_k}{\delta(\partial_\gamma r_{j,y})} \Big|_{\min} \right) + \sum_{\alpha,l} \delta_{\alpha,l}\theta(D-l)\partial_t\zeta \int_z \left(\frac{\delta^2\Gamma_k}{\delta(\partial_\gamma r_{j,y})\delta(\partial_\alpha r_{l,z})} \Big|_{\min} \right) = 0 \quad (\text{D.6})$$

The first term of the r.h.s. of (D.5) is given by the derivative of the flow equation over $\partial_\gamma r_{j,y}$. And from the second term of the r.h.s., we see that the second derivative of the effective action is needed:

$$\begin{aligned} \frac{\delta^2\Gamma_k}{\delta(\partial_\gamma r_{j,y})\delta(\partial_\alpha r_{l,z})} &= -Z\delta_{lj}[\delta_{\alpha\gamma}\partial_\nu\partial_\nu(\delta(\vec{y}-\vec{z})) + \partial_\alpha\partial_\gamma(\delta(\vec{y}-\vec{z})) - \delta_{\alpha\gamma}\partial_\gamma\partial_\gamma(\delta(\vec{y}-\vec{z}))] \\ &+ 4u\delta(\vec{y}-\vec{z})[\delta_{\alpha\gamma}\partial_\mu r_l\partial_\mu r_j + \partial_\gamma r_l\partial_\alpha r_j + \partial_\gamma r_i\partial_\alpha r_i\delta_{jl} - \zeta^2\delta_{\alpha\gamma}\delta_{jl}] \\ &+ 4v\delta(\vec{y}-\vec{z})[\delta_{\alpha\gamma}\delta_{jl}\partial_\mu r_i\partial_\mu r_i + 2\partial_\gamma r_j\partial_\alpha r_l - D\zeta^2\delta_{\alpha\gamma}\delta_{jl}] \end{aligned} \quad (\text{D.7})$$

At the minimum:

$$\begin{aligned} \frac{\delta^2\Gamma_k}{\delta(\partial_\gamma r_{j,y})\delta(\partial_\alpha r_{l,z})} \Big|_{\min} &= -Z\delta_{lj}[\delta_{\alpha\gamma}\partial_\nu\partial_\nu(\delta(\vec{y}-\vec{z})) + \partial_\alpha\partial_\gamma(\delta(\vec{y}-\vec{z})) - \delta_{\alpha\gamma}\partial_\gamma\partial_\gamma(\delta(\vec{y}-\vec{z}))] \\ &+ 4u\zeta^2[\delta_{\alpha\gamma}\delta_{jl}\theta(D-l) + \delta_{\alpha j}\delta_{\gamma l}]\delta(\vec{y}-\vec{z}) + 8v\zeta^2\delta(\vec{y}-\vec{z})\delta_{\alpha l}\delta_{\gamma j} \end{aligned} \quad (\text{D.8})$$

The calculation is easier to do in Fourier space. Therefore we'll need the Fourier transform of (D.8):

$$\text{TF} \left[\frac{\delta^2 \Gamma_k}{\delta(\partial_\gamma r_{j,y}) \delta(\partial_\alpha r_{l,z})} \Big|_{\min} \right] (\vec{p}, \vec{q}) = \delta(\vec{p} + \vec{q}) \left\{ Z \delta_{lj} (\delta_{\alpha\gamma} \vec{p}^2 + p_\alpha p_\gamma - \delta_{\alpha\gamma} p_\gamma^2) \right. \\ \left. + 4u\zeta^2 (\delta_{\alpha\gamma} \delta_{lj} \theta(D-l) + \delta_{\gamma l} \delta_{\alpha j}) + 8v\zeta^2 \delta_{\alpha l} \delta_{\gamma j} \right\} \quad (\text{D.9})$$

Finally the r.h.s. of (D.5) becomes:

$$\sum_{\alpha,l} \int_z \partial_t (\partial_\alpha r_{l,z} |_{\min}) \frac{\delta^2 \Gamma_k}{\delta(\partial_\gamma r_{j,y}) \delta(\partial_\alpha r_{l,z})} \Big|_{\min} = \sum_{\alpha,l} \int_z \int_{q,p} e^{-ip \cdot y} e^{-iq \cdot z} \delta(p+q) \\ [Z \delta_{lj} (\delta_{\alpha\gamma} \vec{p}^2 + p_\alpha p_\gamma - \delta_{\alpha\gamma} p_\gamma^2) + 4u\zeta^2 (\delta_{\alpha\gamma} \delta_{lj} \theta(D-l) + \delta_{\gamma l} \delta_{\alpha j}) \\ + 8v\zeta^2 \delta_{\alpha l} \delta_{\gamma j}] \delta_{\alpha,l} \theta(D-l) \partial_t \zeta \quad (\text{D.10})$$

and after integration we find:

$$\sum_{\alpha,l} \int_z \partial_t (\partial_\alpha r_{l,z} |_{\min}) \frac{\delta^2 \Gamma_k}{\delta(\partial_\gamma r_{j,y}) \delta(\partial_\alpha r_{l,z})} \Big|_{\min} \\ = \sum_{\alpha,l} [4u\zeta^2 (\delta_{\alpha\gamma} \delta_{lj} \theta(D-l) + \delta_{\gamma l} \delta_{\alpha j}) + 8v\zeta^2 \delta_{\alpha l} \delta_{\gamma j}] \delta_{\alpha,l} \theta(D-l) \partial_t \zeta \quad (\text{D.11}) \\ = 8\zeta^2 \delta_{\gamma,j} (u + vD) \partial_t \zeta$$

From the Wetterich equation (2.39) we find for the first term of the r.h.s. of (D.5):

$$\left(\partial_t \frac{\delta \Gamma_k}{\delta(\partial_\gamma r_{j,y})} \right) \Big|_{\min} = \left(\frac{\delta(\partial_t \Gamma_k)}{\delta(\partial_\gamma r_{j,y})} \right) \Big|_{\min} \\ = \text{Tr} \int_{x,z,w} \partial_t R_k(x-z) \left(\Gamma_k^{(2)} + R_k \right)^{-1}(x,w) \frac{\delta \Gamma_k^{(2)}}{\delta(\partial_\gamma r_{j,y})}(w,z) \left(\Gamma_k^{(2)} + R_k \right)^{-1}(z,x) \\ = \text{Tr} \int_{q_i} \partial_t R_k(q_1) \left(\Gamma_k^{(2)} + R_k \right)^{-1}(q_1, -q_2) \text{TF} \left[\frac{\delta \Gamma_k^{(2)}}{\delta(\partial_\gamma r_{j,y})} \right] (q_2, -q_3, p) \\ \times \left(\Gamma_k^{(2)} + R_k \right)^{-1}(q_3, -q_1) \quad (\text{D.12})$$

The Fourier transform of $\frac{\delta\Gamma_k^{(2)}}{\delta(\partial_\gamma r_{j,y})}$:

$$\begin{aligned}
\text{TF} \left[\frac{\delta\Gamma_k^{(2)}}{\delta(\partial_\gamma r_{j,y})} \Big|_{\min} \right] ((n, q_2), (l, q_3), (\gamma, j, p)) &= \delta(p + q_2 + q_3) \{ 4u [2\delta_{n,l}(p_\gamma + q_{2,\gamma})(p_j + q_{2,j}) \\
&\times \theta(D - j) + (p_\mu + q_{2,\mu})^2 (\delta_{n,j}\delta_{\gamma,l} + \delta_{l,j}\delta_{\gamma,n}) + \delta_{n,j}(p_\gamma + q_{2,\gamma})(p_l + q_{2,l})\theta(D - l) \\
&+ \delta_{l,j}(p_\gamma + q_{2,\gamma})(p_n + q_{2,n})\theta(D - n) + p_\mu(q_{2,\mu} + p_\mu)(2\delta_{\gamma,l}\delta_{n,j} + \delta_{\gamma,j}\delta_{n,l} + \delta_{n,\gamma}\delta_{l,j}) \\
&- 2\delta_{n,j}\delta_{\gamma,l}p_\gamma(q_{2,\gamma} + p_\gamma) + \delta_{n,l}\theta(D - j)p_\gamma(q_{2,j} + p_j) + \delta_{l,j}\theta(D - n)p_\gamma(q_{2,n} + p_n) \\
&- \delta_{\gamma,n}\delta_{l,j}p_\gamma(p_\gamma + q_{2,\gamma}) + (p_\gamma + q_{2,\gamma})(2\delta_{n,j}p_l\theta(D - l) + \delta_{n,l}p_j\theta(D - j) + \delta_{l,j}p_n\theta(D - n))] \\
&+ 8v [\delta_{n,l}\delta_{\gamma,j}(p_\mu + q_{2,\mu})^2 + \delta_{n,j}\theta(D - l)(p_\gamma + q_{2,\gamma})(p_l + q_{2,l}) + \delta_{l,j}\theta(D - n) \\
&\times (p_\gamma + q_{2,\gamma})(p_n + q_{2,n}) + p_\gamma(\delta_{n,j}(p_l + q_{2,l})\theta(D - l) - \delta_{n,l}\delta_{\gamma,j}(p_\gamma + q_{2,\gamma}) \\
&- \delta_{l,j}\delta_{n,\gamma}(p_\gamma + q_{2,\gamma})) + p_\mu(p_\mu + q_{2,\mu}) + (p_\gamma + q_{2,\gamma})(\delta_{n,l}p_j\theta(D - j) + \delta_{l,j}p_n\theta(D - n))] \} \\
\end{aligned} \tag{D.13}$$

Using (D.13) in the flow equation (D.12), we find for $\partial_t \zeta$:

$$\partial_t \zeta = -\frac{1}{D(u + vD)\zeta^2} \int_q \left[\frac{16u(D - 1)q^2 + 8vD^2q^2}{(Zq^4 + R_k + u\zeta^2q^2)^2} + \frac{(3u + (D + 2)v)q^2}{(Zq^4 + R_k + 8\zeta^2(u + v)q^2)^2} \right] \tag{D.14}$$

which is the same result as the one found using the configuration λ .

Appendix E

Threshold Functions

The threshold functions L , M and N read:

$$L_{abc}^{D+\alpha} = -\frac{1}{4A_D} \tilde{\partial}_t \int_q q^\alpha \left\{ (P + q^2 m_0^2)^{-a} (P + q^2 m_1^2)^{-b} (P + q^2 m_2^2)^{-c} \right\} \quad (\text{E.1})$$

$$M_{abc}^{D+\alpha} = -\frac{1}{4A_D} \tilde{\partial}_t \int_q q^{\alpha+2} \left(\frac{\partial P}{\partial q^2} \right) \left\{ (P + q^2 m_0^2)^{-a} (P + q^2 m_1^2)^{-b} (P + q^2 m_2^2)^{-c} \right\} \quad (\text{E.2})$$

$$N_{abc}^{D+\alpha} = -\frac{1}{4A_D} \tilde{\partial}_t \int_q q^{\alpha+2} \left(\frac{\partial P}{\partial q^2} \right)^2 \left\{ (P + q^2 m_0^2)^{-a} (P + q^2 m_1^2)^{-b} (P + q^2 m_2^2)^{-c} \right\} \quad (\text{E.3})$$

where $A_D = \frac{2^{-D-1}\pi^{-D/2}}{\Gamma[D/2]}$, $P = Z_k q^4 + R_k$ and m_i^2 masses that are given respectively by 0 , $4u\zeta^2$ and $8(u+v)\zeta^2$. The threshold functions control the relative role of the different modes, phonons and capillary waves, within th RG flow.

$$\left\{ \begin{array}{l} Z_k \quad \sim k^{-\eta_k} \\ \zeta^2 \quad = k^{D-2+\eta_k} \bar{\zeta}^2 \\ u \quad = k^{D-4+2\eta_k} \bar{u} \\ v \quad = k^{D-4+2\eta_k} \bar{v} \\ R_k(q^2) = Z_k q^4 r \left(y = \frac{q^2}{k^2} \right) \end{array} \right. \quad (\text{E.4})$$

$$\partial_{t_{|q^2}} = k\partial_{k_{|q^2}} = k\partial_{k_{|y}} - 2y\partial_y \quad (\text{E.5})$$

$$\Rightarrow \partial_{t_{|q^2}} R_k = Z_k k^4 (-\eta_k y^2 r(y) - 2y^3 r'(y)) \quad (\text{E.6})$$

The dimensionless threshold functions read:

$$L_{abc}^{D+\alpha} = -\frac{1}{2} \int dy \frac{y^{(D+\alpha)/2-a-b-c} (\eta_k r(y) + 2yr'(y))}{(y + yr(y) + m_0^2)^a (y + yr(y) + m_1^2)^b (y + yr(y) + m_2^2)^c} \\ \times \left\{ \frac{a}{(y + yr(y) + m_0^2)} + \frac{b}{(y + yr(y) + m_1^2)} + \frac{c}{(y + yr(y) + m_2^2)} \right\} \quad (\text{E.7})$$

$$M_{abc}^{D+\alpha} = \frac{1}{2} \int dy y^{(D+\alpha)/2+2-a-b-c} \\ \times \frac{(2\eta_k r(y) + yr'(y)(6 + \eta_k) + 2y^2 r''(y)) (2 + 2r(y) + yr'(y))}{(y + yr(y) + m_0^2)^a (y + yr(y) + m_1^2)^b (y + yr(y) + m_2^2)^c} \\ - \frac{1}{2} \frac{y^{(D+\alpha)/2+3-a-b-c} (2 + 2r(y) + yr'(y))^2 (\eta_k r(y) + 2yr'(y))}{(y + yr(y) + m_0^2)^a (y + yr(y) + m_1^2)^b (y + yr(y) + m_2^2)^c} \\ \times \left\{ \frac{a}{(y + yr(y) + m_0^2)} + \frac{b}{(y + yr(y) + m_1^2)} + \frac{c}{(y + yr(y) + m_2^2)} \right\} \quad (\text{E.8})$$

$$N_{abc}^{D+\alpha} = \int dy \frac{y^{(D+\alpha)/2+1-a-b-c} (2\eta_k r(y) + yr'(y)(6 + \eta_k) + 2y^2 r''(y))}{(y + yr(y) + m_0^2)^a (y + yr(y) + m_1^2)^b (y + yr(y) + m_2^2)^c} \\ - \frac{y^{D/2+2-a-b-c} (2 + 2r(y) + yr'(y)) (\eta_k r(y) + 2yr'(y))}{(y + yr(y) + m_0^2)^a (y + yr(y) + m_1^2)^b (y + yr(y) + m_2^2)^c} \\ \times \left\{ \frac{a}{(y + yr(y) + m_0^2)} + \frac{b}{(y + yr(y) + m_1^2)} + \frac{c}{(y + yr(y) + m_2^2)} \right\} \quad (\text{E.9})$$

Chapter 4

Anisotropic Membranes

It seems that if one is working from the point of view of getting beauty in one's equations, and if one has really a sound insight, one is on a sure line of progress.

Paul A.M. Dirac

4.1 Introduction

A particularly interesting change in the behaviour of polymerized membranes occur when explicit in-plane anisotropy is included along one direction. Radzihovsky & Toner have shown that anisotropic membranes have a richer phase diagram than isotropic membranes. In anisotropic membranes a new phase appears between the previously known high-temperature crumpled and low-temperature flat phases [129, 130]. In this phase the membrane is flat in one direction and crumpled in the others and is therefore called *tubular phase* (see Fig. 4.1). The existence of this phase has been widely studied both experimentally [131] and numerically [132, 133] while the crumpled-tubule transition still lacks results from these points of view. The reason behind this is that although it has been largely studied from a theoretical point of view it still lacks accurate predictions for the critical exponents that we explain in this chapter.

Tubular structures are now well known to display several extraordinary mechanical, optical, thermal or electronic properties which make them of great interest in bio- and nanotechnology like drug delivery devices, sensors field emitters, filters, *etc.* Recent proposals consist,

for instance, to produce carbon nanotubes by folding graphene ribbons [134] or organic nanotubes by rolling up two-dimensional anisotropic sheets of amphiphilic rods [131]. In this context there is a clear need for understanding the mechanisms of formation, and more generally, the underlying physics of tubular structures.

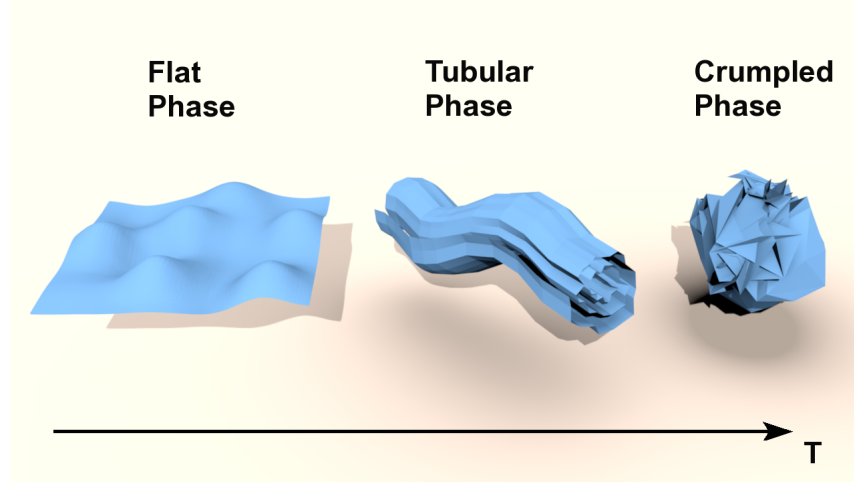


FIGURE 4.1: Phase transitions for anisotropic membranes.

In this chapter we are interested in the critical behaviour at the crumpled-tubule transition. We start by looking at the consequence of the anisotropy on the scaling behaviour. Then we discuss the problems encountered in perturbative approaches and we show that our non-perturbative approach is free from these difficulties.

4.2 Anisotropic Scaling Behaviour

We consider a membrane that is anisotropic in one particular direction y and isotropic in the $D - 1$ remaining, transverse, directions. We focus on the crumpled-tubule transition which is described at the lowest order of the field and derivative expansions by the following effective action:

$$\Gamma_k[\vec{r}] = \int d^{D-1}x dy \left\{ \frac{Z_y}{2} (\partial_y^2 \vec{r})^2 + t_\perp (\partial_\mu^\perp \vec{r})^2 + \frac{u_y}{2} (\partial_y \vec{r} \cdot \partial_y \vec{r} - \zeta_y^2)^2 \right\} \quad (4.1)$$

where Z_y, t_\perp, u_y and ζ_y are the running couplings: u_y is a positive elastic moduli, ζ_y or rather $t_y = u_y \zeta_y^2$, which corresponds to the temperature, parametrizes the approach to criticality. As a consequence of the anisotropy we see from a power-counting that $q_\perp \sim q_y^2$, an anisotropic scaling which characterizes a *Lifshitz-type* behaviour [135]. Moreover the upper critical dimension is lowered by the anisotropy from $D_{uc} = 4$, for isotropic membranes, to $D_{uc} = 5/2$. The couplings Z_y and t_\perp correspond to the field renormalizations in the y -direction and $D-1$ \perp -directions respectively and they scale as:

$$\begin{cases} Z_y & \sim k_y^{-\eta} \\ t_\perp & \sim k^{-\eta_\perp} \end{cases} \quad (4.2)$$

where k is the running momentum scale along the \perp -directions and k_y the one along the y -direction. The exponents η_\perp and η are the anomalous dimensions in these directions. The anisotropy yields, at the transition, the following scale transformations:

$$\begin{cases} x_\perp & = kx'_\perp \\ y & = k_y y' = k^z y' \end{cases} \quad (4.3)$$

where z is an *anisotropy scale exponent*.

At the fixed-point corresponding to the crumpled-tubule transition the two-point correlation function $\Gamma_k^{(2)}$ scale anisotropically as (see [136] for review):

$$\begin{cases} \Gamma_k^{(2)}(q_\perp \rightarrow 0, q_y = 0) & \sim q_\perp^{2-\eta_\perp} \\ \Gamma_k^{(2)}(q_\perp = 0, q_y \rightarrow 0) & \sim q_y^{4-\eta} \end{cases} \quad (4.4)$$

moreover an operator \mathcal{O} scales as :

$$\mathcal{O}(k^{-1}q_\perp, k^{-z}q_y) \sim k^\Delta \mathcal{O}(q_\perp, q_y) \quad (4.5)$$

where Δ is the scaling dimension of the operator \mathcal{O} . Combining Eqs. (4.4) and (4.5) one gets an identity between the anisotropy scale exponent z and the anomalous dimensions η and η_\perp :

$$z = \frac{2 - \eta_\perp}{4 - \eta}. \quad (4.6)$$

This scaling behaviour is characteristic of anisotropic systems that are encountered in statistical physics both in equilibrium and dynamical critical phenomena or in high-energy physics

where for example anisotropy between spatial and temporal dimensions in quantum field theory improves renormalizability properties and the ultra-violet behaviour (see [137] for review).

Since the different directions are not equivalent the crumpled-tubule transition is characterized by two correlation lengths ξ_{\perp} and ξ_y :

$$\begin{cases} \xi_{\perp} & \sim t_y^{-\nu_{\perp}} \\ \xi_y & \sim t_y^{-\nu_y} \end{cases} \quad (4.7)$$

where the correlation exponents are related through the anisotropy scale exponent z by:

$$\nu_y = z\nu_{\perp}. \quad (4.8)$$

The lower critical dimension D_{lc} is defined as the dimension below which the membrane remains crumpled. From a calculation of the normal fluctuations in the harmonic approximation one finds:

$$\begin{aligned} \langle |\partial_y \vec{h}(x)|^2 \rangle & \propto \int d^{D-1} q_{\perp} dq_y \frac{q_y^2}{Zq_y^4 + t_{\perp}q_{\perp}^2} \\ & \propto \int d^{D-1} q_{\perp} \frac{1}{q_{\perp}^{1/2}} \propto L^{3/2-D} \end{aligned} \quad (4.9)$$

which diverges only for $D \leq 3/2$ when $L \rightarrow \infty$ and hence defines the lower critical dimension $D_{lc} = 3/2$.

4.3 Perturbative RG

From this proximity of physical membranes $D = 2$ with $D_{uc} = 2.5$ one would expect that a weak-coupling perturbative approach to yield accurate results. However Radzihovsky and Toner have shown that the second-order ϵ -expansion [130] gives completely unreliable results. Among them one finds a *negative* value for the anomalous dimension η . But we know from physical grounds that η must be positive. Indeed a negative value for the exponent η corresponds to a downward renormalization, a decrease, of the bending rigidity rather than an increase do to fluctuations. Using a perturbative RG computation in the vicinity of $D = 2.5$

one finds at the fixed-point the equation for η :

$$\eta = \frac{(d+2)\epsilon^2}{8(d+8)^2} \times 2^{23/4} \Gamma\left[\frac{3}{4}\right] \int_0^\infty dx x^{5/4} Y(x)^3 \quad (4.10)$$

where the function Y comes from the computation of the correlation function G :

$$\begin{aligned} G(x_\perp, y) &= \int d^{3/2} q_\perp dq_y q_y^2 \frac{e^{i \mathbf{q}_\perp \cdot \mathbf{x}_\perp + i q_y y}}{q_\perp^2 + q_y^4} \\ &= 2^{-7/4} \pi^{-3/4} y^{-2} \left(\frac{x_\perp}{y^2}\right)^{1/4} Y\left(\frac{x_\perp}{y^2}\right) \end{aligned} \quad (4.11)$$

and is given by:

$$Y(x) = \int_0^\infty du u^{1/4} J_{-1/4}(xu) e^{-\sqrt{u/2}} \cos\left(\sqrt{\frac{u}{2}} + \frac{\pi}{4}\right) \quad (4.12)$$

where J is a Bessel function[†]. The integral of the function Y is negative and thus gives a negative value to the anomalous dimension which is a rather surprising result. This negativity is an artefact related to the computation in a fractional dimension $D_{uc} = 5/2$.

This unreliable result from perturbative RG and the absence of an alternative method such as the self-consistent screening approximation given the complexity of the field theoretical formulation, is an open door for a non-perturbative investigation.

4.4 Non-Perturbative Approach

We now attack the problem within the NPRG approach in order to clarify the issue of the value of the anomalous dimension η at the crumpled-tubule transition in the presence of a fractional upper critical dimension.

[†]The Bessel function J_α is given by:

$$J_\alpha(x) = \sum_{n=0}^{\infty} \frac{(-1)^n}{n! \Gamma[n + \alpha + 1]} \left(\frac{x}{2}\right)^{2n + \alpha}. \quad (4.13)$$

4.4.1 The propagator

As usual the starting point is the computation of the propagator \mathcal{P} . For the same reason as in isotropic membranes, *i.e.* translational invariance, we cannot obtain the flow of ζ_y from $\Gamma_k^{(1)}$ at the minimum and we therefore use a more general configuration λ given by:

$$\vec{r}_\lambda = \lambda_y \mathbf{e}_y. \quad (4.14)$$

From Eq. (4.1) it is easy to derive the second functional derivative $\Gamma_k^{(2)}$ in this configuration λ :

$$\Gamma_k^{(2)}(q, i, q', j)|_\lambda = \delta(q + q') \delta_{ij} \{ Z_y q_y^4 + 2t_\perp q_\perp^2 - 2u_y q_y^2 (\zeta_y^2 - \lambda_y^2 - 2\lambda_y^2 \delta_{iD}) \} \quad (4.15)$$

where we have taken the D^{th} direction to correspond to the y -direction. Since the two-point functions $\Gamma_k^{(2)}$ is diagonal the expression of the propagator \mathcal{P} is straightforward:

$$\mathcal{P}(q, i, q', j)|_\lambda = \delta(q + q') \left\{ \delta_{ij} (1 - \delta_{iD}) G_0^{(\lambda)}(q) + \delta_{ij} \delta_{iD} G_y^{(\lambda)}(q) \right\} \quad (4.16)$$

where:

$$\begin{cases} G_0^{(\lambda)} &= Z_y q_y^4 + R_k(q) + 2t_\perp q_\perp^2 - 2u_y \zeta_y^2 (\zeta_y^2 - \lambda_y^2) \\ G_y^{(\lambda)} &= Z_y q_y^4 + R_k(q) + 2t_\perp q_\perp^2 - 2u_y \zeta_y^2 (\zeta_y^2 - \lambda_y^2 - 2\lambda_y^2 \delta_{iD}) . \end{cases} \quad (4.17)$$

The transition from the crumpled to the tubule phase is accompanied with the breaking of the $O(d)$ symmetry into $O(d - 1)$ which identical to the symmetry breaking scheme of the $O(n)$ -model. Taking the trace over the propagator one sees that the functions G correspond to two different types of modes at criticality:

- $d - 1$ capillary Goldstone waves with vanishing mass
- one phonon mode with mass $m_y^2 = 4u_y \zeta_y^2$.

4.4.2 Flow equation of ζ_y

The effective potential in the configuration λ is given by:

$$\Gamma_k[\vec{r}_\lambda] = \int d^{D-1}x dy \frac{u_y}{2} (\lambda_y^2 - \zeta_y^2)^2 = U_{\text{eff}}(\lambda_y) \quad (4.18)$$

and we use the fact that the effective potential U_{eff} by definition is vanishing at the minimum $\lambda_y = \zeta_y$:

$$\left. \frac{\partial U_{\text{eff}}}{\partial \lambda_y} \right|_{\text{min}} = 0 \quad (4.19)$$

to derive the flow equation of ζ_y . Now we have the equality:

$$0 = \partial_t \left(\left. \frac{\partial U_{\text{eff}}}{\partial \lambda_y} \right|_{\text{min}} \right) = \left(\left. \frac{\partial}{\partial \lambda_y} \partial_t U_{\text{eff}} \right) \right|_{\text{min}} + \partial_t \zeta_y \left(\left. \frac{\partial^2 U_{\text{eff}}}{\partial \lambda_y^2} \right) \right|_{\text{min}} \quad (4.20)$$

where $t = \ln k_y/\Lambda$. From this equation we obtain:

$$\partial_t \zeta_y = - \frac{\left(\left. \frac{\partial}{\partial \lambda_y} \partial_t U_{\text{eff}} \right) \right|_{\text{min}}}{4\zeta_y^2 u_y}. \quad (4.21)$$

Now we need the flow of U_{eff} which reads:

$$\partial_t U_{\text{eff}} = \frac{1}{2} \text{Tr} \left\{ \tilde{\partial}_t \int_q \ln \left(\Gamma_k^{(2)} + R_k \right) (q, i, -q, j) \Big|_{\lambda_y} \right\}. \quad (4.22)$$

Finally we need to derive this equation with respect to λ_y to obtain the flow equation of ζ_y . This equation is given in the next section.

4.4.3 Flow equations

The other running coupling constants are defined as follow:

$$t_{\perp} = \frac{1}{2} \lim_{p_{\perp} \rightarrow 0} \left(\frac{\partial}{\partial p_{\perp}^2} \Gamma_k^{(2)}(p, D, -p, D) \Big|_{\min} \right) \quad (4.23)$$

$$u_y = \frac{1}{4\zeta_y^2} \lim_{p_y \rightarrow 0} \left(\frac{\partial}{\partial p_y^2} \Gamma_k^{(2)}(p, D, -p, D) \Big|_{\min} \right) \quad (4.24)$$

$$Z_y = \lim_{p_y \rightarrow 0} \left(\frac{\partial}{\partial p_y^4} \Gamma_k^{(2)}(p, D, -p, D) \Big|_{\min} \right). \quad (4.25)$$

The coupling t_{\perp} remains unrenormalized, $\partial_t t_{\perp} = 0$, because the interaction term u_y always carries a momentum q_y with every field \vec{r} in agreement with the perturbative result at all orders. The anomalous dimension η_{\perp} is vanishing implying that the anisotropy scale exponent $z = \frac{1}{2} + O(\epsilon^2)$ at order ϵ . From the flow equations of U_{eff} and of $\Gamma_k^{(2)}$ we derive the flow equations for ζ_y^2 and u_y which read:

$$\partial_t \zeta_y^2 = \frac{1}{(2\pi)^D} \int d^{D-1} q_{\perp} dq_y \partial_t R_k(q) q_y^2 \left\{ \frac{(d-1)}{(Z_y q_y^4 + m_{\perp}^2 q_{\perp}^2 + R_k(q))^2} + \frac{3}{(Z_y q_y^4 + m_{\perp}^2 q_{\perp}^2 + m_y^2 q_y^2 + R_k(q))^2} \right\} \quad (4.26)$$

$$\partial_t u_y = \frac{4u_y^2}{(2\pi)^D} \int d^{D-1} q_{\perp} dq_y \partial_t R_k(q) q_y^2 \left\{ \frac{(d-1)}{(Z_y q_y^4 + m_{\perp}^2 q_{\perp}^2 + R_k(q))^3} + \frac{9}{(Z_y q_y^4 + m_{\perp}^2 q_{\perp}^2 + m_y^2 q_y^2 + R_k(q))^3} \right\} \quad (4.27)$$

where $m_{\perp}^2 = 2t_{\perp}$ and $m_y^2 = 4u_y \zeta_y^2$. In general the cut-off function R_k must regularize both the y -direction and the \perp -directions. However since the membrane is not critical in the \perp -directions we can take a cut-off only regulates along the y -direction. With this simplification we can integrate analytically on q_{\perp} :

$$\int d^{D-1} q_{\perp} \frac{1}{(A + m_{\perp}^2 q_{\perp}^2)^p} = \left(\frac{\pi}{m_{\perp}^2} \right)^{\frac{D-1}{2}} \frac{\Gamma[p - \frac{D-1}{2}]}{\Gamma[p]} \frac{1}{A^{p - \frac{D-1}{2}}}. \quad (4.28)$$

Injecting this result in the flow equations (4.26) and (4.27) we obtain:

$$\partial_t \zeta_y^2 = \frac{1}{(2\pi)^D} \left(\frac{\pi}{m_\perp^2} \right)^{\frac{D-1}{2}} \Gamma[(5-D)/2] \int dq_y q_y^2 \partial_t R_k(q_y) \left\{ \frac{(d-1)}{(Z_y q_y^4 + R_k(q_y))^{\frac{5-D}{2}}} + \frac{3}{(Z_y q_y^4 + R_k(q_y) + m_y^2 q_y^2)^{\frac{5-D}{2}}} \right\} \quad (4.29)$$

$$\partial_t u_y = \frac{4u_y^2}{(2\pi)^D} \left(\frac{\pi}{m_\perp^2} \right)^{\frac{D-1}{2}} \frac{\Gamma[(7-D)/2]}{\Gamma[3]} \int dq_y q_y^2 \partial_t R_k(q_y) \left\{ \frac{(d-1)}{(Z_y q_y^4 + R_k(q_y))^{\frac{7-D}{2}}} + \frac{9}{(Z_y q_y^4 + R_k(q_y) + m_y^2 q_y^2)^{\frac{7-D}{2}}} \right\} \quad (4.30)$$

To find a fixed-point we must work with dimensionless coupling:

$$\bar{\zeta}_y^2 = k_y^{3-2D} Z_y^{(3-D)/2} t_\perp^{(D-1)/2} \zeta_y^2 \quad (4.31)$$

$$\bar{u}_y = k_y^{2D-5} Z_y^{(D-5)/2} t_\perp^{(1-D)/2} u_y \quad (4.32)$$

with $k_y = k^z$. In terms of these quantities the RG flow equations read (we suppress the bar over the dimensionless couplings):

$$\partial_t \zeta_y^2 = - \left(2D - 3 - \frac{D-3}{2} \eta \right) \zeta_y^2 - (d-1) l_{\frac{3-D}{2},0}^{2,D} - 3 l_{0,\frac{3-D}{2}}^{2,D} \quad (4.33)$$

$$\partial_t u_y = - \left(5 - 2D - \frac{5-D}{2} \eta \right) u_y + (D-3) u_y^2 \left\{ (d-1) l_{\frac{5-D}{2},0}^{4,D} + 9 l_{0,\frac{5-D}{2}}^{4,D} \right\}. \quad (4.34)$$

The anomalous dimension $\eta = -(1/Z_y) \partial_t Z_y$ can be derived along the same lines:

$$\eta = \frac{D-3}{3} u_y^2 \zeta_y^2 \left\{ -108 l_{0,\frac{5-D}{2}}^{2,D} - 12(d-1) l_{\frac{5-D}{2},0}^{2,D} - 540(D-5) u_y \zeta_y^2 l_{0,\frac{7-D}{2}}^{4,D} + (D-5)(D-7) \left(-288 u_y^2 \zeta_y^2 l_{0,\frac{9-D}{2}}^{6,D} + 9 M_{0,\frac{9-D}{2}}^{6,D} + (d-1) M_{\frac{9-D}{2},0}^{6,D} - 36 u_y \zeta_y^2 N_{0,\frac{9-D}{2}}^{6,D} \right) \right\} \quad (4.35)$$

where the threshold functions l , M and N are given by:

$$T_{a,b}^{\alpha,D} = K_D \tilde{\partial}_t \int dq_y q_y^\alpha \frac{F(q_y)}{[P(q_y)]^a [P(q_y) + m_y^2 q_y^2]^b} \quad (4.36)$$

where $K_D = (\pi/2)^{(D-1)/2} \Gamma[(3-D)/2]$, $P(q_y) = Z_y q_y^4 + R_{k_y}(q_y)$, $m_y^2 = 4u_y \zeta_y^2$ and $\tilde{\partial}_t = \partial_t R_{k_y} \partial / \partial R_{k_y}$. The function $F(q_y)$ is given by 1, (dP/dq_y^2) and $(dP/dq_y^2)^2$ for l , N and M respectively (for the dimensionless threshold functions see Appendix F).

Before proceeding the physical result, there are two important remarks we want to make. First we took a cut-off function independent on q_\perp since the \perp -directions are not critical but we can take a cut-off that does depend on q_\perp and not integrate exactly over q_\perp . We have checked that this does not change the physical results as expected. Second the flow equation have been derived with respect to k_y but again this derivation can also be done with respect to k . This changes the coordinates of the fixed-points but they are related to the previous ones through the anisotropy scale exponent z .

4.5 Physical Results

Thanks to the one-loop structure of the Wetterich equation (2.39) we recover the one-loop β function for u_y and $t_y = u_y \zeta_y^2$ found in [130] by expanding our flow equations around $D = 5/2 - \epsilon$. Moreover we recover the large- d results at leading order by assuming that $u_y \sim O(1/d)$ and $\zeta_y^2 \sim O(d)$. We find, using a cut-off function $R_{k_y}(q_y) = Z_y(k_y^4 - q_y^4)\theta(k_y^2 - q_y^2)$, a stable fixed-point with coordinates:

$$\begin{cases} \zeta_y^{2*} &= \frac{4 d K_D (3 - D)}{3 (2D - 3)} \\ u_y^* &= \frac{5 K_D (5 - 2D)}{4 d (3 - D)(5 - D)}. \end{cases} \quad (4.37)$$

This fixed-point exist for all values of D between the upper critical dimension $D_{uc} = 5/2$ and the lower critical dimension $D_{lc} = 3/2$. The corresponding critical exponents are given by:

$$\begin{cases} \nu_y &= \frac{1}{(2D - 3)} \\ \eta &= O(1/d). \end{cases} \quad (4.38)$$

Going to finite value of the embedding space dimension d we find a stable fixed-point at all d in contrast with the isotropic case where the order of the transition changes at some critical dimension $d_c(D)$ [53]. Now we concentrate on the case $d = 3$ where we find a non-trivial positive anomalous dimension between $D_{uc} = 5/2$ and $D_{lc} = 3/2$ as expected. Our results for the anomalous dimension η and the correlation exponent ν_{\perp} for a two-dimensional membrane in three-dimensional space are displayed in Figs. (4.2) and (4.3). They are plotted as functions of a parameter λ which parametrize a cut-off family. We have used three different cut-off families $R_{k_y}^{(i)}$:

$$\begin{cases} R_{k_y}^{(1)}(q_y) &= \lambda Z_y k_y^4 e^{-q_y^4/k_y^4} \\ R_{k_y}^{(2)}(q_y) &= \lambda \frac{Z_y}{e^{q_y^4/k_y^4} - 1} \\ R_{k_y}^{(3)} &= \lambda Z_y (k_y^4 - q_y^4) \theta(k_y^2 - q_y^2). \end{cases}$$

We have optimized the critical exponents by varying λ and looking for stationary values. For each cut-off family, we succeed to find a single PMS value for each exponent (see Figs. 4.2 - 4.3). For the correlation exponent along the \perp -direction we find from this optimization $\nu_{\perp} = 1.213(8)$ [54] in agreement with Radzihovskiy & Toner who found $\nu_{\perp} \approx 1.227$ in [130]. For the anomalous dimension η our approach yields a positive value $\eta = 0.358(4)$ which is largely different from the value found in [130]: $\eta \approx -0.0015$. Finally from these results we deduce the value of the anisotropy scale exponent and the correlation exponent in y -direction: $z = 0.5490(6)$ and $\nu_y = 0.665(5)$ which is slightly different from $\nu_y \approx 0.614$ found in [130]. The insensitivity of our results to both the variations of the parameter λ inside a cut-off family and of the family itself constitutes a strong indication of trustability of our results and validates *a posteriori* the use of the truncations (4.1). But obviously one has to use a richer ansatz to be sure that convergence is achieved.

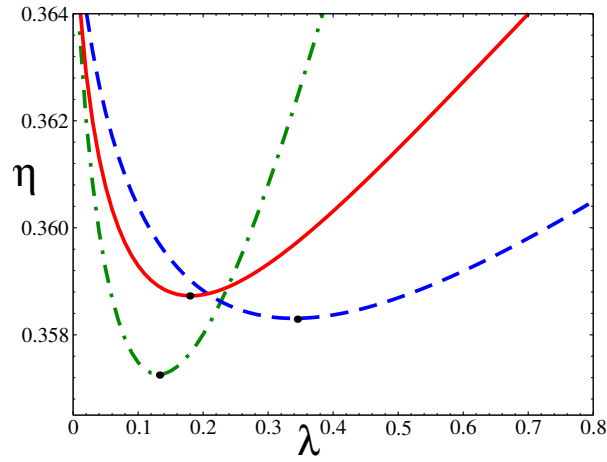


FIGURE 4.2: Anomalous dimension η as function of the cut-off parameter λ with different cut-off functions. Solid line, $R_{k_y}^{(1)}$; dashed line $R_{k_y}^{(2)}$ and dot-dashed line $R_{k_y}^{(3)}$ [54].

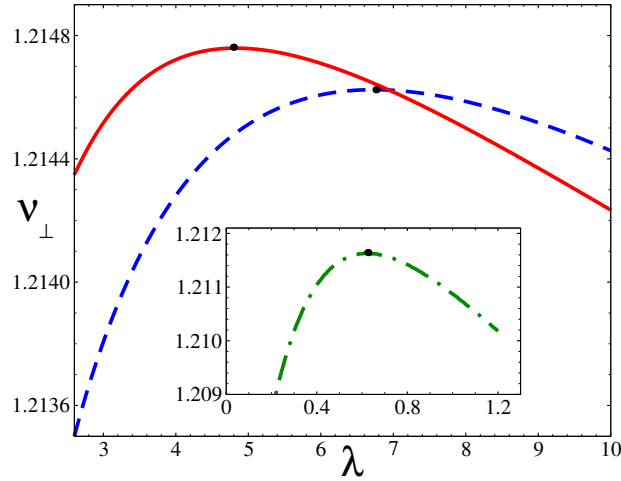


FIGURE 4.3: Correlation exponent ν_{\perp} as function of the cut-off parameter λ with different cut-off functions. Solid line, $R_{k_y}^{(1)}$; dashed line $R_{k_y}^{(2)}$ and dot-dashed line $R_{k_y}^{(3)}$ [54].

4.6 Conclusion

The NPRG approach overcomes the technical difficulties encountered within perturbative weak-coupling treatment for anisotropic membranes. In particular we do not have to work in real space and we can integrate exactly over the orthogonal momenta. As we said in the

introduction there is no numerical simulation for the crumpled-tubule transition and we hope that our result will be tested through numerical investigation in the near future. The next step for anisotropic membranes is to take into account of self-avoidance since its effects are believed to destroy the crumpled phase and one is only left with the transition between the tubular and flat phases.

Beyond the case of anisotropic membranes our approach is relevant for other systems involving anisotropy like Lifshitz critical behaviour which we discuss in the next chapter.

Appendix F

Threshold Functions

The dimensionless threshold functions read (once more we drop the bar over the dimensionless coupling):

$$l_{a,b}^{\alpha,D} = \left(\frac{\pi}{2}\right)^{\frac{D-1}{2}} \Gamma\left[\frac{3-D}{2}\right] \int_0^\infty dy y^{\frac{\alpha+1}{2}-a-b} \frac{(\eta r(y) + 2y r'(y))}{(y + y r(y))^a (y + y r(y) + m_y^2)^b} \left\{ \frac{a}{(y + y r(y))} + \frac{b}{(y + y r(y) + m_y^2)} \right\} \quad (\text{F.1})$$

$$N_{a,b}^{\alpha,D} = \left(\frac{\pi}{2}\right)^{\frac{D-1}{2}} \Gamma\left[\frac{3-D}{2}\right] \int_0^\infty dy y^{\frac{\alpha-1}{2}-a-b} \left\{ \frac{y^2 (\eta r(y) + 2y r'(y)) (2 + 2r(y) + y r'(y))}{(y + y r(y))^a (y + y r(y) + m_y^2)^b} \left(\frac{a}{(y + y r(y))} + \frac{b}{(y + y r(y) + m_y^2)} \right) - \frac{y (2\eta r(y) + \eta y r'(y) + 6y r'(y) + 2y^2 r''(y))}{(y + y r(y))^a (y + y r(y) + m_y^2)^b} \right\} \quad (\text{F.2})$$

$$\begin{aligned}
M_{a,b}^{\alpha,D} &= \left(\frac{\pi}{2}\right)^{\frac{D-1}{2}} \Gamma\left[\frac{3-D}{2}\right] \int_0^\infty dy y^{\frac{\alpha-1}{2}-a-b} \\
&\left\{ \frac{y^3 (\eta r(y) + 2y r'(y)) (2 + 2r(y) + yr'(y))^2}{(y + yr(y))^a (y + yr(y) + m_y^2)^b} \left(\frac{a}{(y + yr(y))} \right. \right. \\
&\left. \left. + \frac{b}{(y + yr(y) + m_y^2)} \right) - 2y^2 (2 + 2r(y) + yr'(y)) \right. \\
&\left. \times \frac{(2\eta r(y) + \eta yr'(y) + 6yr'(y) + 2y^2 r''(y))}{(y + yr(y))^a (y + yr(y) + m_y^2)^b} \right\} \tag{F.3}
\end{aligned}$$

Chapter 5

Lifshitz Critical Behaviour

Every word or concept, clear as it may seem to be, has only a limited range of applicability.

Werner Heisenberg

5.1 Introduction

In this chapter we leave the membrane systems and concentrate on another type of anisotropic systems. Similar problems, as those encountered in anisotropic membranes, are present in a more general case of anisotropic systems. Indeed various physical systems are characterized by an anisotropic scale invariance (ASI) such as equilibrium critical phenomena of anisotropic systems, like the Lifshitz critical behaviour or anisotropic membranes, as well as dynamical critical phenomena in- and out-of-equilibrium [138]. This ASI is also present in quantum field theory where theories with a broken Lorentz invariance at high-energy, *i.e.* anisotropy between the spatial and temporal dimensions, drastically improves the ultra-violet behaviour and renormalizability properties (see [137] for review). These ideas have been further extended towards anisotropic scale invariant gravity, like the Horava-Lifshitz gravity [94], and cosmology [139].

Lifshitz critical behaviour (LCB) [140, 141, 142] which occurs when a disordered phase encounters both a spatially homogeneous ordered phase and a spatially modulated ordered phase with a modulation momentum $\mathbf{q}_{\text{mod}} \neq 0$ (see Fig. 5.1). The spatially homogeneous phase can

be considered as a spatially modulated phase with vanishing momentum. This tricritical point, the *Lifshitz point* (LP), was introduced by Hornreich, Luban and Shtrikmann in 1975 [135] and has since dragged a lot of attention in condensed matter and statistical physics. This type of behaviour may be found in magnetic systems where a competition between ferromagnetic nearest-neighbour and anti-ferromagnetic next-to-nearest-neighbour interactions leads to the appearance of modulated phases like in the axial (or anisotropic) next-nearest-neighbour Ising- and XY-models (ANNNI and ANNNXY). It is also present in liquid crystals [143], high- T_c superconductors, polymer mixtures [144, 145], microemulsions, ferroelectrics [146], charge-transfer salts [147], domain-wall instabilities [148] (see [138, 149] for review). Experimentally LCB has been observed in manganese phosphide [150, 151, 152, 153, 154, 155] and one can hope for accurate determinations of the critical quantities in a near future.

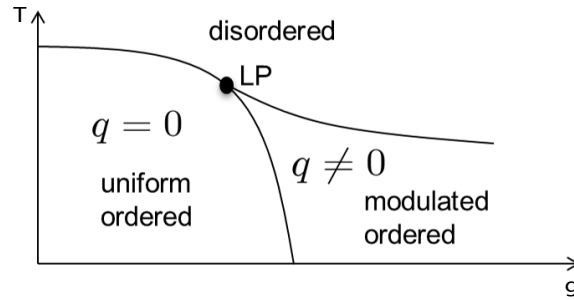


FIGURE 5.1: Schematic representation of a phase diagram with a Lifshitz point (LP) as a function of the temperature T and a parameter g which corresponds to the pressure or the magnetic field depending on the system.

5.2 The Model

In order to see how a LP arises we start with a mean field treatment of the simplest model in three dimensional space. First we start with the $O(n)$ -model with a small change in the kinetic part where the different space directions have different couplings. The effective action for this $O(n)$ -model reads:

$$\Gamma[\vec{\phi}] = \int d^3x \left\{ \sum_{i=x,y,z} \frac{\alpha_i}{2} (\partial_i \vec{\phi})^2 + \frac{\tau}{2} \vec{\phi}^2 + \frac{u}{4} \vec{\phi}^4 \right\} \quad (5.1)$$

where τ , α_i and u are the coupling constants. u and α_i are positive and τ may change sign which indicates a phase transition between a paramagnetic phase ($\tau > 0$) and a ferromagnetic phase ($\tau < 0$). But if one of the α_i , e.g. α_z , becomes negative, we need a higher order derivative term $(\partial_z^2 \vec{\phi})^2$ for thermodynamical stability and we have a tricritical point for $\tau = \alpha_z = 0$. The new effective action reads:

$$\Gamma[\vec{\phi}] = \int d^3x \left\{ \sum_{i=x,y,z} \frac{\alpha_i}{2} (\partial_i \vec{\phi})^2 + \frac{\beta_z}{4} (\partial_z^2 \vec{\phi})^2 + \frac{\tau}{2} \vec{\phi}^2 + \frac{u}{4} \vec{\phi}^4 \right\}. \quad (5.2)$$

In the following we take $\alpha_x = \alpha_y = \alpha$. We write the effective action in Fourier space:

$$\begin{aligned} \Gamma[\vec{\phi}] = \frac{1}{2} \int_q \left\{ \tau + \alpha_z q_z^2 + \alpha (q_x^2 + q_y^2) + \frac{\beta_z}{2} q_z^4 \right\} |\vec{\phi}_q|^2 \\ + \int_{q,q',q''} \frac{u}{4} \vec{\phi}_q \cdot \vec{\phi}_{q'} \cdot \vec{\phi}_{q''} \cdot \vec{\phi}_{-q-q'-q''} \end{aligned} \quad (5.3)$$

and the phase transition occurs when the minimum with respect to q_z of $\tau(q) = \tau + \alpha_z q_z^2 + \alpha(q_x^2 + q_y^2) + \frac{\beta_z}{2} q_z^4$ vanishes. We have two possibilities depending on the sign of α_z . If $\alpha_z > 0$ the minimum is given by:

$$\tau_{\min} = \tau \quad (5.4)$$

and the transition occurs at $\tau = 0$, with $q = 0$, which corresponds to the paramagnetic-ferromagnetic transition. Now if $\alpha_z < 0$ we have:

$$\alpha_z q_z + \beta_z q_z^3 = 0 \Rightarrow \begin{cases} q_z = 0 \\ q_z^2 = -\frac{\alpha_z}{\beta_z} \end{cases} \quad (5.5)$$

where the minimum τ_{\min} is given by:

$$\tau_{\min} = \tau - \frac{\alpha_z^2}{2\beta_z}. \quad (5.6)$$

In the ordered phase if $\alpha_z > 0$ the equilibrium expression of the order parameter ϕ_{eq} is given by:

$$\phi_{\text{eq}} = \left(\frac{-\tau}{u} \right)^{1/2} \quad (5.7)$$

which corresponds to a uniform magnetization and if $\alpha_z < 0$:

$$\phi_{\text{eq}}(q_0) = 2\phi_{q_0} \cos(q_0 z + \theta) \quad (5.8)$$

where $\phi_{q_0} = -\tau(q_0)/3u$ and $q_0 = -\alpha_z/\beta_z$. Now the magnetization is modulated with a modulation momentum q_0 . When $\tau = \alpha_z = 0$ the system is at the tricritical Lifshitz point.

A particularly interesting feature about the Lifshitz point is its scaling behaviour due to the spatial anisotropy which we discuss in the next section.

5.3 Anisotropic Scale Invariance

We generalize the study to the previous section to a system in a d -dimensional space with m anisotropic directions and hence $d - m$ transverse \perp -directions. The effective average action with an expansion around the minimum κ reads:

$$\Gamma_k[\vec{\phi}] = \int d^{d-m}x_{\perp} d^m x_{\parallel} \left\{ \frac{Z_{\parallel}}{2} (\partial_{\parallel}^2 \vec{\phi})^2 + \frac{Z_{\perp}}{2} (\partial_{\perp} \vec{\phi})^2 + \frac{\rho_0}{2} (\partial_{\parallel} \vec{\phi})^2 + u \left(\frac{\vec{\phi}^2}{2} - \kappa \right)^2 \right\} \quad (5.9)$$

where Z_{\parallel} , Z_{\perp} , ρ_0 , u and κ are the running coupling constants. Depending on the value of m we have three situations:

- $m \neq d$: anisotropic Lifshitz critical behaviour
- $m = d$: isotropic Lifshitz critical behaviour
- $m = 0$: isotropic $O(n)$ -model

The Lifshitz critical behaviour is characterized by an anisotropic scale invariance because the term $(\partial_{\perp}^2 \vec{\phi})^2$ is irrelevant at the Lifshitz critical point. Therefore, as for anisotropic membranes, at the LP the two-point correlation function scales as:

$$\begin{cases} \Gamma^{(2)}(q_{\perp} \rightarrow 0, q_{\parallel} = 0) \sim q_{\perp}^{2-\eta_{\ell 2}} \\ \Gamma^{(2)}(q_{\perp} = 0, q_{\parallel} \rightarrow 0) \sim q_{\parallel}^{4-\eta_{\ell 4}} \end{cases} \quad (5.10)$$

where $\eta_{\ell 2}$ and $\eta_{\ell 4}$ are the anomalous dimensions along the orthogonal and parallel directions respectively. Moreover an operator has the following asymptotic scaling behaviour:

$$\mathcal{O}(lq_{\perp}, l^{\theta}q_{\parallel}) \sim l^{-\Delta} \mathcal{O}(q_{\perp}, q_{\parallel}) \quad (5.11)$$

where Δ is the scaling dimension of the operator \mathcal{O} and θ an anisotropy scale exponent. From these scaling behaviours, we deduce the relation:

$$\theta = \frac{2 - \eta_{\ell 2}}{4 - \eta_{\ell 4}}. \quad (5.12)$$

Finally the behaviour near criticality is characterized by two correlation lengths: $\xi_{\perp} \sim \tau^{-\nu_{\ell 2}}$ and $\xi_{\parallel} \sim \tau^{-\nu_{\ell 4}}$ where the correlation exponents $\nu_{\ell 2}$ and $\nu_{\ell 4}$ are related by the anisotropy exponent θ : $\nu_{\ell 4} = \theta \nu_{\ell 2}$.

Pleimling & Henkel have introduced a theory of local scale invariance (LSI) [156, 136] for both equilibrium and out-of-equilibrium phenomena leading to conjecture exact expressions for the two-point correlation functions of anisotropic systems. From a Monte Carlo simulation of Lifshitz points [156] Pleimling and Henkel claim to be in agreement with this LSI. However in [157] Rutkevich et al. found that the ϵ -expansions of some scaling functions obtained from a two-loop expansion about the upper critical dimension seem to be inconsistent with the predictions of [136] and [156]. This question could be investigated within the NPRG in the near future using more sophisticated computation than those used here.

5.4 Critical Dimensions

Going from isotropic to anisotropic magnetic systems shifts the upper and lower critical dimension, d_{uc} and d_{lc} respectively:

$$\begin{cases} d_{uc} : 4 & \rightarrow 4 + \frac{m}{2} \\ d_{lc} : 2 & \rightarrow 2 + \frac{m}{2}. \end{cases} \quad (5.13)$$

Since the number of anisotropic directions m is lower or equal to the dimension d the region with non-trivial behaviour is the one sandwiched between the lines $d_{uc}(m)$, $d_{lc}(m)$ and $d = m$ (see 5.2).

In the minimal non-trivial case $m = 1$ we see that the ϵ -expansion around $d_{uc} = 9/2$ deals with an $\epsilon = 3/2$ in order to investigate the physical dimension $d = 3$. Thus to hope to get reliable results one needs the series to be Borel-summable which is not guaranteed and one needs to compute at least up to the fourth or fifth loop order. Interestingly in this minimal $m = 1$ case the physical dimension $d = 3$ is close to the lower critical dimension $d_{lc} = 2.5$ (for $n > 2$) and one would hope that an investigation by means of a low-temperature approach may give accurate results since $\epsilon = 0.5$. However, as for the isotropic $O(n)$ -model, in the low-temperature approach the series are suspected to be non-Borel summable and therefore of no practical use.

5.5 Perturbative RG

5.5.1 Weak-Coupling ϵ -Expansion

Using a momentum-shell RG in the vicinity of the upper critical dimension Hornreich, Luban & Shtrikman calculated the critical exponents for all m at order ϵ [135]. Several calculation to the order ϵ^2 have been performed. For instance Mukamel [158] calculated the anomalous dimension η_{ℓ_2} and η_{ℓ_4} for all m . Hornreich & Bruce [159] also calculated the anomalous dimension but only in the case $m = 1$ and their results agreed with the Mukamel's. However another calculation by Sak & Grest [160] for the cases $m = 2$ and $m = 6$ did not agree with the results obtained by Mukamel. This disagreement is linked to the different approximations

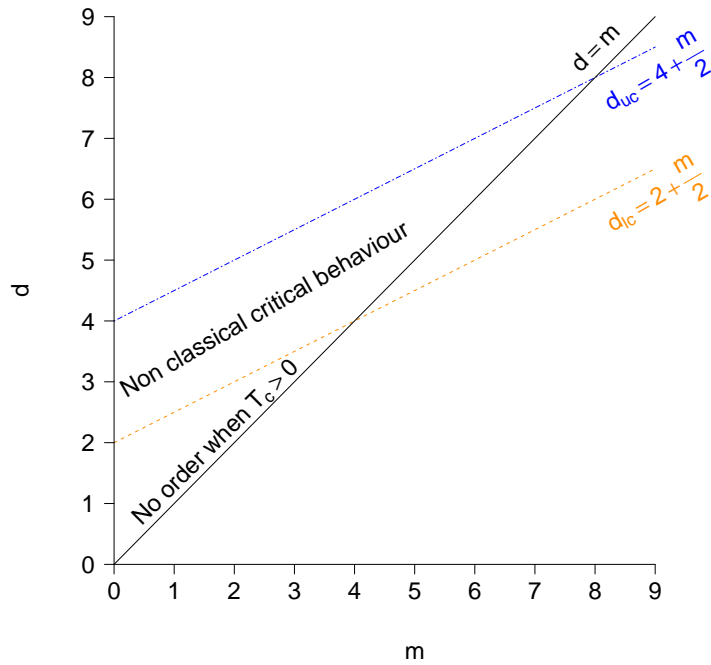


FIGURE 5.2: Upper and lower critical dimensions.

used in the momentum-shell integration. This controversy was been long-standing until the recent works of Shpot & Diehl [161] and Mergulhao & Carneiro [162].

To avoid the approximations of the momentum-shell integration Mergulhao & Carneiro [162, 163] used a different approach, a dimensional regularization, where the integrations are over the whole momentum space rather than just over momentum-shells. They used an expansion of the Green functions in the vicinity of the LP in terms of the massless Green functions calculated at the LP. With this approach Mergulhao & Carneiro recovered Sak & Grest's [160] results of the anomalous dimensions for $m = 2$ and $m = 6$.

The study of the general case was done by Shpot & Diehl [161] in a full two-loop calculation. To avoid 1) some of the technical difficulties which have their origin in the form of the propagator at the LP and 2) the renormalization prescriptions used by Mergulhao & Carneiro [162], Shpot & Diehl [164, 161] found it easier to work in direct space and they showed that the free propagator $G(x)$ at criticality is a generalized homogeneous function rather than homogeneous. This arises from the anisotropic scale invariance of the free theory and the scaling function is complicated for the general case (d, m, n) . The free propagator at the LP is given

by:

$$G(x) = \int_q \frac{e^{i(\mathbf{q}_{\parallel} \cdot \mathbf{x}_{\parallel} + \mathbf{q}_{\perp} \cdot \mathbf{x}_{\perp})}}{q_{\parallel}^4 + q_{\perp}^2} \quad (5.14)$$

which can be written in the form:

$$G(x) = r_{\perp}^{-2+\epsilon} \Phi \left(x_{\parallel} x_{\perp}^{-1/2} \right) \quad (5.15)$$

where $\Phi(v) = \Phi(v, m, d)$ is a complicated scaling function. After integration over q_{\perp} , the scaling function Φ can be expressed using generalized hypergeometrics, known as the Fox-Wright hypergeometric functions [165]. These functions are complicated but reduce to simple expressions for some special values of d and m such as $m = 2$ or $m = 6$ where the integrals can be performed analytically.

Indeed, these technical difficulties together with the choice of the renormalization prescription explain why it took almost twenty years to go from one-loop [135] to two-loop order [161, 162, 163] and it is believed that it will take even longer to go beyond.

5.5.2 Large- n Expansion

Similar difficulties as in the weak-coupling expansion appear in the large- n expansion [166, 167] and it is only recently that consistency between two-loop and large- n has been firmly established [165]. A very interesting point of the large- n results is the variation of the anomalous dimension $\eta_{\ell 4}$ with the dimension (see fig. 5.3). In the vicinity of the upper critical dimension d_{uc} the anomalous dimension $\eta_{\ell 4}$ is small and negative. Lowering the space dimension d further the anomalous dimension $\eta_{\ell 4}$ vanishes and becomes positive before it decreases again to zero at the lower critical dimension d_{lc} .

An important question for the physical case $d = 3$ is at which dimension d does the anomalous dimension $\eta_{\ell 4}$ change sign? The large- n result indicates that $\eta_{\ell 4}$ is positive for $d = 3$. However this is not conclusive for the physically interesting cases *i.e.* with finite values of n .

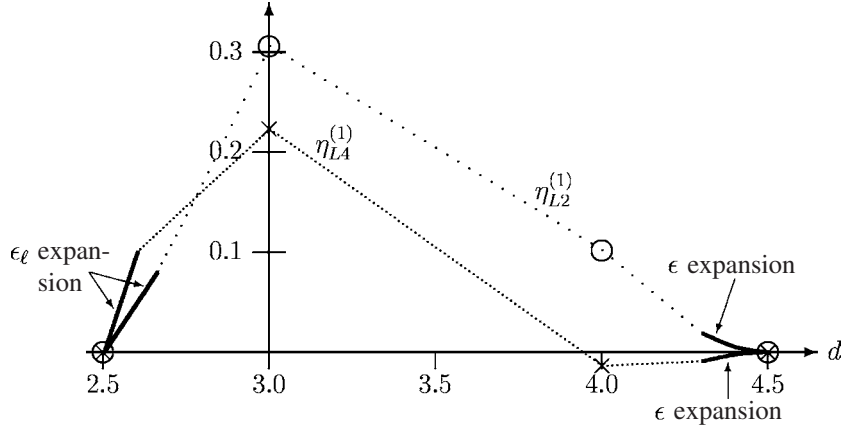


FIGURE 5.3: Behaviour of the anomalous dimensions η_{L2} (open circles) and η_{L4} (crosses) in a large- n expansion. The thick lines represent the limiting forms $\sim \epsilon$ and $\sim \epsilon^2$ [166].

5.6 NPRG Approach

From our work on anisotropic membranes where the NPRG approach was able to correctly tackle the problem of the crumpled-tubule transition and predict the value of the anomalous dimension we hoped that this approach will again prove to be reliable.

5.6.1 Lowest Order of the Derivative Expansion

We start with the lowest order of the field expansion given by Eq. (5.9). The problem with the definition of the minimum encountered in membranes is absent in LCB and therefore we derive the propagator directly in the ground state configuration $\phi_{i,\min} = \sqrt{2\kappa} \delta_{1i}$. After two functional derivatives of Γ_k Eq. (5.9), we get the two-point correlation function:

$$\Gamma_k^{(2)}(p, i, j, p')|_{\min} = \delta(p + p') \delta_{ij} \left\{ Z_{\parallel} p_{\parallel}^4 + Z_{\perp} p_{\perp}^2 + \rho_0 p_{\parallel}^2 + 4 u \kappa \delta_{1i} \right\} \quad (5.16)$$

where $p_{\parallel} = \sqrt{p_{\mu} p^{\mu}}$ and $p_{\perp} = \sqrt{p_{\nu} p^{\nu}}$ with $\mu = 1, \dots, m$ and $\nu = m + 1, \dots, d$. The two-point correlation function $\Gamma_k^{(2)}$ is diagonal and hence the propagator \mathcal{P} is given by:

$$\mathcal{P}(p, i, p', j)|_{\min} = \delta(p + p') \delta_{ij} \left\{ (1 - \delta_{1i}) G_0(p) + \delta_{1i} G_1(p) \right\} \quad (5.17)$$

where:

$$G_i(p) = \left(Z_{\parallel} p_{\parallel}^4 + Z_{\perp} p_{\perp}^2 + \rho_0 p_{\parallel}^2 + m_i^2 \right)^{-1} \quad (5.18)$$

with $m_0 = 0$ and $m_1^2 = 4u\kappa$. Taking the trace of the propagator we see that the vanishing mass m_0 corresponds to $n - 1$ Goldstone modes in the low-temperature phase and the mass m_1 to one radial mode.

5.6.2 Flow Equations

To derive the flow equations of the coupling constants we first determine their definitions from the functional derivatives of the effective action (5.9):

$$\begin{aligned} Z_{\parallel} &= \lim_{p \rightarrow 0} \frac{\partial}{\partial p_{\parallel}^4} \Gamma_k^{(2)}(p, 1, -p, 1) \Big|_{\min} \\ Z_{\perp} &= \lim_{p \rightarrow 0} \frac{\partial}{\partial p_{\perp}^2} \Gamma_k^{(2)}(p, 1, -p, 1) \Big|_{\min} \\ u &= \frac{1}{4\kappa} \lim_{p \rightarrow 0} \Gamma_k^{(2)}(p, 1, -p, 1) \Big|_{\min} \\ \rho_0 &= \lim_{p \rightarrow 0} \frac{\partial}{\partial p_{\parallel}^2} \Gamma_k^{(2)}(p, 1, -p, 1) \Big|_{\min} \end{aligned} \quad (5.19)$$

and the anomalous dimensions $\eta_{\ell 4}$ and $\eta_{\ell 2}$ are defined as:

$$\begin{cases} \eta_{\ell 4} &= -\frac{1}{\theta} \partial_t \ln Z_{\parallel} \\ \eta_{\ell 2} &= -\partial_t \ln Z_{\perp}. \end{cases} \quad (5.20)$$

The renormalized couplings flow to two different fixed-points depends on whether the RG transformation is over k_{\perp} or k_{\parallel} . However these fixed-points are equivalent and yield the same results for the critical exponents (this situation is identical to anisotropic membranes). We recall that we have taken the RG-time to be $t = \ln k_{\perp}/\Lambda$ and hence the flow equations

read:

$$\begin{aligned} \partial_t \kappa &= -(d - m + \theta(m + \eta_{\ell 4} - 4)) \kappa \\ &+ \frac{\Gamma \left[\frac{m+2-d}{2} \right]}{2^d \pi^{d/2} \Gamma \left[\frac{m}{2} \right]} \left\{ (n-1) L_{\frac{m+2-d}{2}, 0}^0(\rho_0, m_1) + 3 L_{0, \frac{m+2-d}{2}}^0(\rho_0, m_1) \right\} \end{aligned} \quad (5.21)$$

$$\begin{aligned} \partial_t u &= (d - m + \theta(m + 2\eta_{\ell 4} - 8)) u \\ &+ u^2 \frac{\Gamma \left[\frac{m+4-d}{2} \right]}{2^{d-1} \pi^{d/2} \Gamma \left[\frac{m}{2} \right]} \left\{ (n-1) L_{\frac{m+4-d}{2}, 0}^0(\rho_0, m_1) + 9 L_{0, \frac{m+4-d}{2}}^0(\rho_0, m_1) \right\} \end{aligned} \quad (5.22)$$

$$\begin{aligned} \partial_t \rho_0 &= \theta(\eta_{\ell 4} - 2) \rho_0 + \frac{1}{2^d \pi^{d/2} \Gamma \left[\frac{m}{2} \right] m u \kappa^2} \left\{ \Gamma \left[\frac{m+2-d}{2} \right] \left(M_{\frac{m+2-d}{2}, 0}^1(\rho_0, m_1) \right. \right. \\ &- M_{0, \frac{m+2-d}{2}}^1(\rho_0, m_1) \left. \right) - 2u \kappa \Gamma \left[\frac{m+4-d}{2} \right] \left(M_{\frac{m+4-d}{2}, 0}^1(\rho_0, m_1) \right. \\ &\left. \left. + M_{0, \frac{m+4-d}{2}}^1(\rho_0, m_1) \right) \right\}. \end{aligned} \quad (5.23)$$

Similarly the anomalous dimensions are given by:

$$\begin{aligned} \eta_{\ell 2} &= \frac{1}{2^d \pi^{d/2} \Gamma \left[\frac{m}{2} \right]} \left\{ -\frac{\Gamma \left[\frac{m-d}{2} \right]}{2u \kappa^2} \left(L_{\frac{m-d}{2}, 0}^0(m_1, \rho_0) - L_{0, \frac{m-d}{2}}^0(m_1, \rho_0) \right) \right. \\ &\left. + \frac{\Gamma \left[\frac{m+2-d}{2} \right]}{\kappa} \left(L_{\frac{m+2-d}{2}, 0}^0(m_1, \rho_0) + L_{0, \frac{m+2-d}{2}}^0(m_1, \rho_0) \right) \right\} \end{aligned} \quad (5.24)$$

$$\begin{aligned}
\eta_{\ell 4} = & \frac{2^{-d-1}\pi^{d/2}}{3mu\kappa^2\Gamma\left[\frac{m}{2}\right]} \left\{ \Gamma\left[\frac{m+4-d}{2}\right] \left(S_{\frac{m+4-d}{2},0}^1(m_1, \rho_0) - U_{0,\frac{m+4-d}{2}}^1(m_1, \rho_0) \right) \right. \\
& - 2u\kappa\Gamma\left[\frac{m+6-d}{2}\right] \left(S_{\frac{m+6-d}{2},0}^1(m_1, \rho_0) + S_{0,\frac{m+6-d}{2}}^1(m_1, \rho_0) \right) \left. \right\} \\
& + \frac{2^{-4-d}\pi^{-d/2}}{3u^3\kappa^4\Gamma\left[\frac{m+4}{2}\right]} \left\{ -9\Gamma\left[\frac{m+2-d}{2}\right] \left(T_{\frac{m+2-d}{2},0}^2(m_1, \rho_0) - T_{0,\frac{m+2-d}{2}}^2(m_1, \rho_0) \right) \right. \\
& + 18u\kappa\Gamma\left[\frac{m+4-d}{2}\right] \left(T_{\frac{m+4-d}{2},0}^2(m_1, \rho_0) + T_{0,\frac{m+4-d}{2}}^2(m_1, \rho_0) \right) \\
& - 16u^2\kappa^2\Gamma\left[\frac{m+6-d}{2}\right] \left(T_{\frac{m+6-d}{2},0}^2(m_1, \rho_0) - T_{0,\frac{m+6-d}{2}}^2(m_1, \rho_0) \right) \\
& \left. + 8u^3\kappa^3\Gamma\left[\frac{m+8-d}{2}\right] \left(T_{\frac{m+8-d}{2},0}^2(m_1, \rho_0) + T_{0,\frac{m+8-d}{2}}^2(m_1, \rho_0) \right) \right\} \\
& - \frac{2^{-d-2}\pi^{d/2}}{u\kappa^2\Gamma\left[\frac{m+4}{2}\right]} \left\{ -\Gamma\left[\frac{m+2-d}{2}\right] \left(U_{\frac{m+2-d}{2},0}^2(m_1, \rho_0) - U_{0,\frac{m+2-d}{2}}^2(m_1, \rho_0) \right) \right. \\
& \left. + 2u\kappa\Gamma\left[\frac{m+4-d}{2}\right] \left(U_{\frac{m+4-d}{2},0}^2(m_1, \rho_0) + U_{0,\frac{m+4-d}{2}}^2(m_1, \rho_0) \right) \right\}
\end{aligned} \tag{5.25}$$

and the threshold functions are given by:

$$T_{a,b}^\alpha(m_1, \rho_0) = -\frac{1}{A_m} \tilde{\partial}_t \int d^m q_{\parallel} \frac{q_{\parallel}^{2\alpha} F[q_{\parallel}]}{\left(P(q_{\parallel}^2) + m_0^2 \right)^a \left(P(q_{\parallel}^2) + m_1^2 \right)^b} \tag{5.26}$$

with $P(q_{\parallel}^2) = Z_{\parallel} q_{\parallel}^4 + \rho_0 q_{\parallel}^2 + R_k(q_{\parallel}^2)$ and $A_m = 2^{-m-1}\pi^{-m/2}/\Gamma[m/2]$. The function $F[q_{\parallel}]$ is given by 1, $(dP/dq_{\parallel}^2)^2$, $(dP/dq_{\parallel}^2)^3$, $(dP/dq_{\parallel}^2)^4$ and $(d^2P/d(q_{\parallel}^2)^2)^2$ for respectively L , M , S , T and U . Note that, as for anisotropic membranes we can integrate exactly over the momenta q_{\perp} since they enter quadratically in the effective action Γ_k (5.9) and therefore the threshold functions are integrals over q_{\parallel} only.

5.6.3 Upper Critical Dimension $d_{uc} = 4 + \frac{m}{2}$

From the one-loop structure of the Wetterich equation (2.39) we recover the ϵ -expansion results at leading order in the vicinity of the upper critical dimension d_{uc} . At d_{uc} the anomalous dimensions $\eta_{\ell 4}$ and $\eta_{\ell 2}$ vanish and the mass $m_1^2 = 4u\kappa$ is very small $m_1 \ll 1$. Taking

$d = 4 + m/2$ we have:

$$\begin{cases} m + 2 - d = \frac{m-4}{2} \\ m + 4 - d = \frac{m}{2} \\ m + 6 - d = \frac{m+4}{2} \end{cases}$$

and therefore the threshold functions involved in Eqs. (5.21-5.22) become:

$$\begin{aligned} L_{\frac{m+2-d}{2},0}^0(m_1, \rho_0) &\approx L_{\frac{m-4}{4},0}^0(0, 0) \\ L_{0,\frac{m+2-d}{2}}^0(m_1, \rho_0) &\approx L_{\frac{m-4}{4},0}^0(0, 0) - 3(m-4)u\kappa \\ L_{\frac{m+4-d}{2},0}^0(m_1, \rho_0) &\approx L_{0,\frac{m+4-d}{2}}^0(m_1, \rho_0) = L_{\frac{m}{4},0}^0(0, 0) = 1. \end{aligned} \quad (5.27)$$

Now the flow equations read:

$$\partial_t \kappa = -(2 - \epsilon)\kappa + \frac{\Gamma\left[\frac{m-4}{4}\right]}{2^{\frac{m+8}{2}} \pi^{\frac{m+8}{4}} \Gamma\left[\frac{m}{2}\right]} \left\{ (n+2)L_{\frac{m-4}{4},0}^0(0, 0) - 3(m-4)u\kappa \right\} \quad (5.28)$$

$$\partial_t u = -\epsilon u + u^2 \frac{(n+8)\Gamma\left[\frac{m}{4}\right]}{2^{\frac{m+6}{2}} \pi^{\frac{m+8}{4}} \Gamma\left[\frac{m}{2}\right]}. \quad (5.29)$$

At leading order, the coordinates of the non-trivial fixed-point are:

$$\begin{aligned} u^* &= \frac{\pi^{\frac{m+8}{4}} 2^{\frac{m+6}{2}} \Gamma[m/2] \epsilon}{(n+8)\Gamma[m/4]} \\ \kappa^* &= \frac{\Gamma[(m-4)/4](n+2)}{\pi^{\frac{m+8}{4}} 2^{\frac{m+12}{2}} \Gamma[m/2]} L_{\frac{m-4}{4},0}^0(0, 0) \end{aligned} \quad (5.30)$$

and the critical exponent ν_{\perp} is deduced from the flow equations by linearising around this non-trivial fixed point:

$$\begin{cases} \kappa = \kappa^* + \delta\kappa \rightarrow \partial_t \kappa = \partial_t \delta\kappa \\ u = u^* + \delta u \rightarrow \partial_t u = \partial_t \delta u. \end{cases}$$

With this the flow becomes:

$$\begin{aligned} \partial_t(\delta\kappa) = & -(2 - \epsilon)\delta\kappa - (4 - 2\epsilon)\kappa^* + \frac{\Gamma\left[\frac{m-4}{4}\right]}{\pi^{\frac{m+8}{4}} 2^{\frac{m+8}{2}} \Gamma\left[\frac{m}{2}\right]} \left[(n+2)L_{\frac{m-4}{4},0}^0(0,0) \right. \\ & \left. - 12\frac{m-4}{4}u^*\delta\kappa - 12\frac{m-4}{4}\kappa^*\delta u \right] \end{aligned} \quad (5.31)$$

and the exponent ν_{\perp} is given by the linear term $\delta\kappa$:

$$\begin{aligned} \frac{1}{\nu_{\perp}} &= 2 - \epsilon + \frac{\Gamma\left[\frac{m-4}{4}\right]}{\pi^{\frac{m+8}{4}} 2^{\frac{m+8}{2}} \Gamma\left[\frac{m}{2}\right]} 12\frac{m-4}{4}u^* \\ &= 2 - \epsilon + \frac{\Gamma\left[\frac{m-4}{4}\right]}{\pi^{\frac{m+8}{4}} 2^{\frac{m+8}{2}} \Gamma\left[\frac{m}{2}\right]} \frac{12(m-4)}{4} \frac{\pi^{\frac{m+8}{4}} 2^{\frac{m+6}{2}} \Gamma\left[\frac{m}{2}\right] \epsilon}{(n+8)\Gamma\left[\frac{m}{4}\right]} \\ &= 2 - \epsilon + \frac{6\epsilon}{(n+8)} = 2 - \frac{(n+2)\epsilon}{(n+8)} \end{aligned} \quad (5.32)$$

where we have used the equality $\Gamma[z+1] = z\Gamma[z]$. Finally, the exponent is given by:

$$\begin{aligned} \nu_{\perp} &= \frac{1}{2 - \frac{(n+2)\epsilon}{(n+8)}} \\ &= \frac{1}{2} + \frac{\epsilon n + 2}{4n + 8} + O(\epsilon^2). \end{aligned} \quad (5.33)$$

By a similar procedure ν_{\parallel} is given by:

$$\begin{aligned} \nu_{\parallel} &= \frac{1}{4 - \frac{2(n+2)\epsilon}{(n+8)}} \\ &= \frac{1}{4} + \frac{\epsilon n + 2}{8n + 8} + O(\epsilon^2) \end{aligned} \quad (5.34)$$

and the two correlation exponents are related by the anisotropic scale exponent $z = \nu_{\parallel}/\nu_{\perp}$:

$$\begin{aligned} z &= \left(\frac{1}{4} + \frac{\epsilon n + 2}{8n + 8} \right) \left(2 - \frac{(n+2)\epsilon}{(n+8)} \right) + O(\epsilon^2) \\ &= \frac{1}{2} + O(\epsilon^2) \end{aligned} \quad (5.35)$$

The other critical exponents are fixed using the generalized scaling relations:

$$\left\{ \begin{array}{l} \alpha = 2 - m\nu_{\parallel} - (d - m)\nu_{\perp} \\ \gamma = (4 - \eta_{\ell 4})\nu_{\parallel} = (2 - \eta_{\ell 2})\nu_{\perp} \\ \beta = \frac{1}{2}(2 - \alpha - \gamma) \\ \delta = \frac{\gamma}{\beta} + 1. \end{array} \right. \quad (5.36)$$

With the values of ν_{\parallel} , ν_{\perp} , $\eta_{\ell 4}$ and $\eta_{\ell 2}$ near the upper critical dimension, the critical exponents become:

$$\left\{ \begin{array}{l} \alpha = \frac{4 - n}{n + 8} \frac{\epsilon}{2} + O(\epsilon^2) \\ \gamma = 1 + \frac{\epsilon}{2} \frac{n + 2}{n + 8} + O(\epsilon^2) \\ \beta = \frac{1}{2} - \frac{\epsilon}{2} \frac{3}{n + 8} + O(\epsilon^2) \\ \delta = 1 + \epsilon \end{array} \right. \quad (5.37)$$

5.6.4 Lower Critical Dimension $d_{lc} = 2 + \frac{m}{2}$

As for the expansion near the upper critical dimension we recover the low-temperature results from the one-loop structure of the exact evolution equation (2.39).

The lower critical dimension d_{lc} is the dimension below which there is no phase transition. In Lifshitz systems, $d_{lc} = 2 + \frac{m}{2}$ for $n > 1$, where n is the number of field components.

The only physically interesting case is the one with $m = 1$ because when $m > 1$, $d_{lc} > 3$. Therefore at some point in the calculation, we take $m = 1$. In our approach since the temperature dependence is implicit a low-temperature expansion is equivalent to an expansion in power of $1/\kappa$. We start with the flow of the anomalous dimensions $\eta_{\ell 2}$ and $\eta_{\ell 4}$ which read

to the leading order in $1/\kappa$:

$$\eta_{\ell 2} \approx \frac{1}{2^d \pi^{d/2} \Gamma\left[\frac{m}{2}\right]} \frac{\Gamma\left[\frac{m+2-d}{2}\right]}{\kappa} L_{\frac{m+2-d}{2},0}^0(m_1, \rho_0) \quad (5.38)$$

$$\eta_{\ell 4} \approx \frac{1}{2^d \pi^{d/2} 6m(m+2) \Gamma\left[\frac{m}{2}\right] \kappa} \left\{ -2(m+2) \Gamma\left[\frac{m+6-d}{2}\right] S_{\frac{m+6-d}{2},0}^1 \right. \\ \left. + 4 \Gamma\left[\frac{m+8-d}{2}\right] T_{\frac{m+8-d}{2},0}^2 - 12 \Gamma\left[\frac{m+4-d}{2}\right] U_{\frac{m+4-d}{2},0}^2 \right\} \quad (5.39)$$

where we have taken the threshold functions $F_{a,b}^\alpha$ ($F = S, T$ or U) with non-vanishing parameter b to zero since we are in the large mass limit $m_1 \gg 1$. Since η is of order ϵ it is taken as vanishing in the threshold functions. Now we evaluate the threshold functions for $d = 2 + \frac{m}{2}$:

$$L_{\frac{m+2-d}{2},0}^0 = -\frac{1}{2} \int dy y^{\frac{m+2}{2}} \frac{2yr'(y)^{\frac{m+2-d}{2}}}{(y^2(1+r(y)) + \rho_0 y)^{\frac{m+2-d}{2}+1}}. \quad (5.40)$$

The coupling ρ_0 is of order $1/\kappa$ near d_{lc} and is therefore taken as vanishing $\rho_0 = 0$:

$$L_{\frac{m+2-d}{2},0}^0 = -\frac{m+2-d}{2} \int dy y^{\frac{m+4}{2}-(m+4-d)} \frac{r'(y)}{(1+r(y))^{\frac{m+4-d}{2}}}. \quad (5.41)$$

Taking $d = 2 + \frac{m}{2}$ we have:

$$\begin{cases} m+2-d & = \frac{m}{2} \\ m+4-d & = \frac{m+4}{2}. \end{cases}$$

Substituting this in the previous equation leads to:

$$L_{\frac{m+2-d}{2},0}^0 = -\frac{m}{4} \int dy \frac{r'(y)}{((1+r(y)))^{\frac{m+4}{4}}} = \left[(1+r(y))^{-\frac{m}{4}} \right]_0^\infty = 1 \quad (5.42)$$

since $r(\infty) = 0$ and $r(0) = \infty$.

Now we evaluate the threshold functions entering in $\eta_{\ell 4}$. First we start with the threshold S which reads:

$$\begin{aligned} S_{\frac{m+6-d}{2},0}^1(m_1, \rho_0) &= -\frac{m+6-d}{2} \int dy \frac{y^{\frac{m+6}{2}} r'(y) (2y + 2yr(y) + y^2 r'(y))^3}{(y^2(1+r(y)))^{\frac{m+8-d}{2}}} \\ &+ \frac{3}{2} \int dy \frac{y^{m/2} (2y + 2yr(y) + y^2 r'(y))^2 (6y^2 r'(y) + 2y^3 r''(y))}{(y^2(1+r(y)))^{\frac{m+6-d}{2}}} \end{aligned} \quad (5.43)$$

and with $m+6-d = \frac{m+8}{2}$ and $m+8-d = \frac{m+12}{2}$ becomes:

$$\begin{aligned} S_{\frac{m+6-d}{2},0}^1(m_1, \rho_0) &= -\frac{m+8}{4} \int dy \frac{r'(y) (2 + 2r(y) + yr'(y))^3}{(1+r(y))^{\frac{m+12}{4}}} \\ &+ 3 \int dy \frac{(2 + 2r(y)yr'(y))^2 (3r'(y) + yr''(y))}{(1+r(y))^{\frac{m+8}{4}}} \\ &= \int dy \frac{d}{dy} \left[\frac{(2 + 2r(y) + yr'(y))^3}{(1+r(y))^{\frac{m+8}{4}}} \right] \\ &= \frac{(2 + 2r(\infty) + yr'(\infty))^3}{(1+r(\infty))^{\frac{m+8}{4}}} - \frac{(2 + 2r(0) + yr'(0))^3}{(1+r(0))^{\frac{m+8}{4}}}. \end{aligned} \quad (5.44)$$

Similarly the thresholds T and U read:

$$T_{\frac{m+8-d}{2},0}^2(m_1, \rho_0) = \frac{(2 + 2r(\infty) + yr'(\infty))^4}{(1+r(\infty))^{\frac{m+12}{4}}} - \frac{(2 + 2r(0) + yr'(0))^4}{(1+r(0))^{\frac{m+12}{4}}} \quad (5.45)$$

$$\begin{aligned} U_{\frac{m+4-d}{2},0}^2(m_1, \rho_0) &= \frac{(2 + 2r(\infty) + 4yr'(\infty) + y^2 r''(\infty))^2}{(1+r(\infty))^{\frac{m+4}{4}}} \\ &- \frac{(2 + 2r(0) + 4yr'(0) + y^2 r''(0))^2}{(1+r(0))^{\frac{m+4}{4}}}. \end{aligned} \quad (5.46)$$

Although $r(0)$ diverges the numerator with $r(0)$ in the threshold functions are constant and therefore the parts with an $r(0)$ vanish (see Appendix). The threshold functions read:

$$\begin{aligned} S_{\frac{m+6-d}{2},0}^1 &= 8 \\ T_{\frac{m+8-d}{2},0}^2 &= 12 \\ U_{\frac{m+4-d}{2},0}^2 &= 4. \end{aligned} \tag{5.47}$$

Replacing the threshold functions by their value in the anomalous dimensions we find:

$$\begin{aligned} \eta_{\ell 2} &= \frac{\Gamma\left[\frac{m}{4}\right]}{2^{\frac{m+4}{2}} \pi^{\frac{m+4}{4}} \Gamma\left[\frac{m}{2}\right] \kappa} \\ \eta_{\ell 4} &= \frac{2\Gamma\left[\frac{m}{4}\right]}{2^{\frac{m+4}{2}} \pi^{\frac{m+4}{4}} \Gamma\left[\frac{m}{2}\right] \kappa} \end{aligned} \tag{5.48}$$

Now we have to find the fixed-point value κ^* . Replacing the threshold functions L by its value in the flow of κ we find:

$$\partial_t \kappa = -\epsilon \kappa + \frac{(n-2)\Gamma\left[\frac{m}{4}\right]}{2^{\frac{m+4}{2}} \pi^{\frac{m+4}{4}} \Gamma\left[\frac{m}{2}\right]} \tag{5.49}$$

which gives the fixed-point value:

$$\kappa^* = \frac{(n-2)\Gamma\left[\frac{m}{4}\right]}{2^{\frac{m+4}{2}} \pi^{\frac{m+4}{4}} \Gamma\left[\frac{m}{2}\right] \epsilon}. \tag{5.50}$$

Replacing κ^* in the anomalous dimensions:

$$\begin{aligned} \eta_{\ell 2}^* &= \frac{\epsilon}{n-2} \\ \eta_{\ell 4}^* &= \frac{2\epsilon}{n-2} \end{aligned} \tag{5.51}$$

which is in agreement with the results found in [168].

The correlation exponent ν_{\perp} is connected to the linear term $\delta\kappa$ in the flow $\partial_t\kappa$. Linearising the flow around $\kappa = \kappa^* + \delta\kappa$ we find:

$$\partial_t\kappa = -\epsilon(\kappa^* + \delta\kappa) + \frac{(n-2)\Gamma\left[\frac{m}{4}\right]}{2^d\pi^{d/2}\Gamma\left[\frac{m}{2}\right]} \quad (5.52)$$

which gives for ν_{\perp} :

$$\nu_{\perp} = \frac{1}{\epsilon} \xrightarrow{\epsilon \rightarrow \infty} \infty \quad (5.53)$$

as in the non-linear σ -model.

5.7 Higher Order Expansion and Physical Results

We have computed the critical exponents up to the twelfth order of the field expansion to see how the exponents evolve with the order of the expansion and to ensure that we have obtained converged results for the physical quantities. An important remark about the cut-off functions is that the θ cut-off cannot be used for the Lifshitz critical behaviour because of the non-analyticity of its derivatives that enter the threshold functions.

Now we concentrate on the uniaxial Heisenberg case $m = 1$ and $n = 3$. We find a non-trivial fixed-point with two directions of instability, corresponding the Lifshitz point, for any dimension between the upper and lower critical dimensions d_{uc} and d_{lc} . The anomalous dimensions $\eta_{\ell 2}$ and $\eta_{\ell 4}$ are displayed in figure 5.4. This figure calls for two important remarks. First, one sees that the NPRG approach allows for a smooth interpolation for the critical exponents between d_{lc} and d_{uc} . Second, from a direct investigation in $d = 3$ for $n = 3$ the LCB is characterized by a *negative* value for $\eta_{\ell 4}$. This result is in disagreement with the perturbative, large- n and low-temperature, methods which give a positive value for $\eta_{\ell 4}$.

For the physical dimension $d = 3$ we have used a cut-off family parametrize by λ :

$$R_{k_{\perp}}^{\lambda}(q_{\parallel}) = \frac{\lambda Z_{\parallel}}{e^{q_{\parallel}^4/k_{\perp}^{2\theta}} - 1} \quad (5.54)$$

and by varying the parameter λ we seek for stationary values of the critical exponents. Stationarity is a condition that must necessarily be fulfilled by any putative physical quantity to ensure

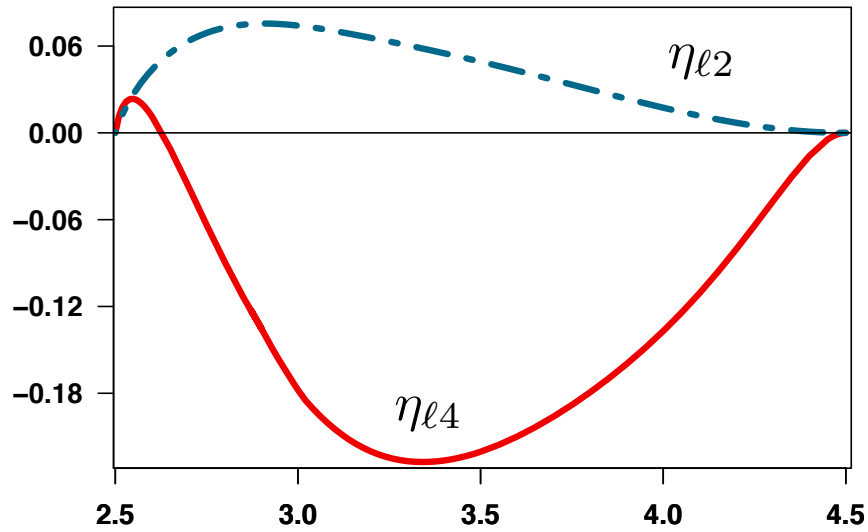


FIGURE 5.4: Anomalous dimensions $\eta_{\ell 2}$ and $\eta_{\ell 4}$ as functions of the dimension d between d_{uc} and d_{lc} using a field truncation up to $\vec{\phi}^8$ for $n = 3$ and $m = 1$.

its quasi-independence with respect to both the cut-off function and the truncation [39]. We have studied the convergence of the physical quantities by adding successively powers of the field up to the twelfth order. We find at almost any order[†] of the field expansion stationary values for the critical exponents. This is illustrated in figs. 5.5 and 5.6 which represent respectively the critical exponents $\eta_{\ell 2}$ and $\nu_{\ell 2}$ in the vicinity of their stationary value for different truncations of the effective action.

The critical exponents vary very smoothly with the cut-off parameter λ which indicates that the results have a weak dependence on the cut-off function. This fact has been confirmed by using other cut-off families that lead to the same result. More importantly from figs. 5.5 and 5.6 we can see that we have a rapid convergence when adding higher orders of the field expansion. Between the orders $\vec{\phi}^{10}$ and $\vec{\phi}^{12}$ only the third digit of $\eta_{\ell 2}$ and $\nu_{\ell 2}$ changes. This is a clear indication of the good convergence of our results, at least with respect to the field expansion. Indeed higher order derivative terms may change the values of the critical exponents.

[†]The $\vec{\phi}^6$ case seems to be special in the sense that it does not exhibit clear stationary values.

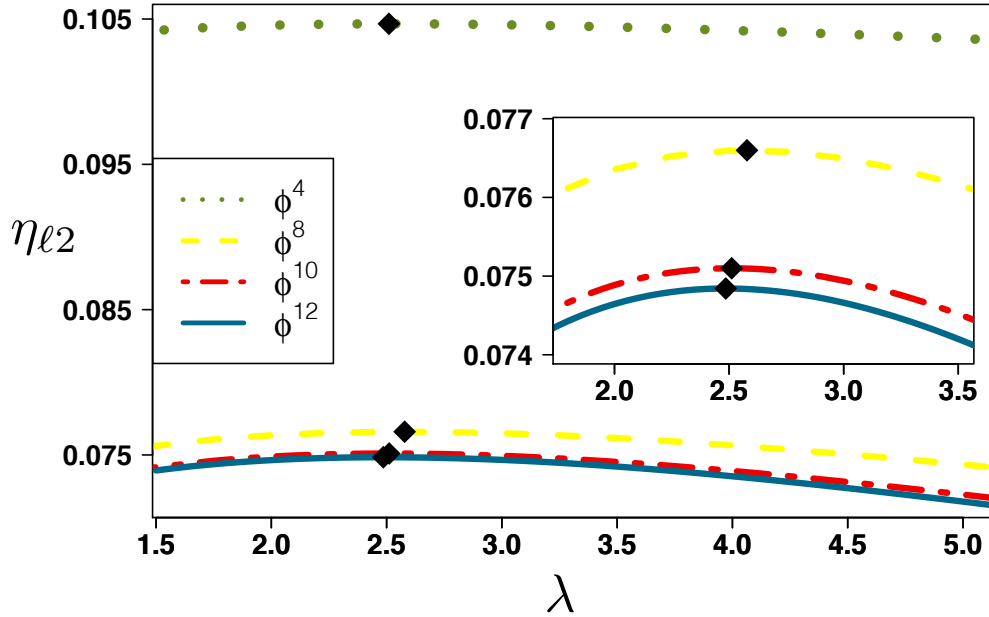


FIGURE 5.5: The anomalous dimension $\eta_{\ell 2}$ as function of λ for truncations from $\vec{\phi}^4$ (upper curve) to $\vec{\phi}^{12}$ (lower curve). Stationary points are indicated by black diamonds.

Our results are summarized in table 5.1 in the column NPRG together with the weak-coupling [161] and large- n [166, 167] results for comparison. Note that the error bars in our values are evaluated from the direct analysis of the convergence of the field expansion. From this table one can see that our results differ heavily from the ones obtained from a weak-coupling expansion. This discrepancy is not surprising since these perturbative results have been only obtained at low loop orders. From our convergence study, although based on a different approximation, one can see the necessity of taking into account several orders to obtain converged values for the critical exponents. Finally, we note, amazingly, that our correlation length exponents $\nu_{\ell 4}$ and $\nu_{\ell 4}$ are close to the values obtained within a very recent large- n expansion [167], contrary to the anomalous dimension $\eta_{\ell 4}$ and $\eta_{\ell 2}$ both quantitatively and qualitatively (different sign for $\eta_{\ell 4}$).

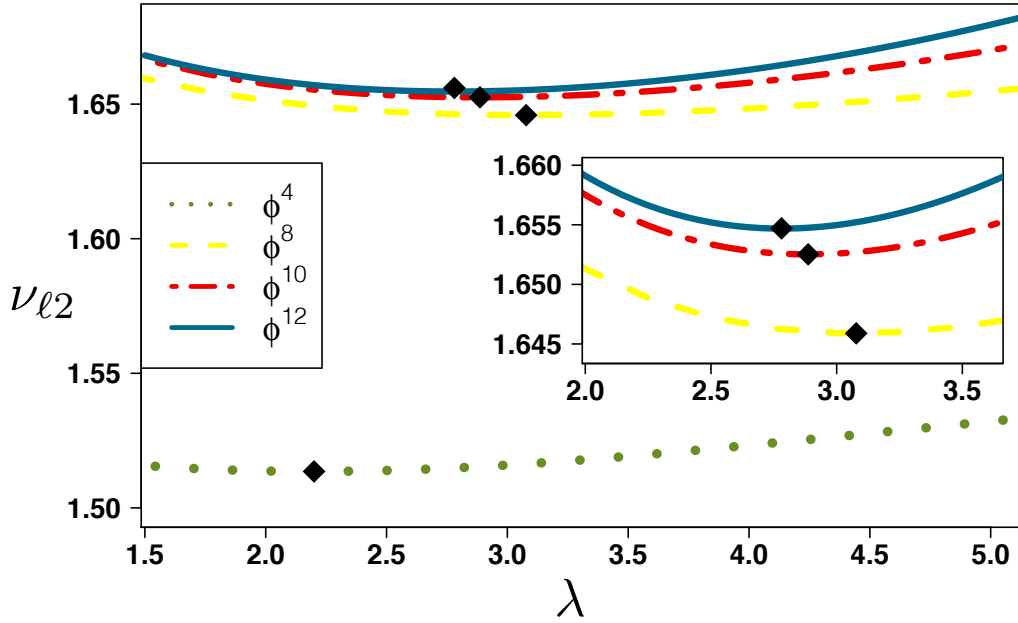


FIGURE 5.6: The correlation exponents $\nu_{\ell 2}$ as function of λ for truncations from $\vec{\phi}^4$ (upper curve) to $\vec{\phi}^{12}$ (lower curve). Stationary points are indicated by black diamonds.

	NPRG	$O(\epsilon^2)$ [161]	$O(1/n)$ [166, 167]
$\nu_{\ell 4}$	0.78(1)	0.392	0.755
$\nu_{\ell 2}$	1.655(5)	0.798	1.575
$\eta_{\ell 4}$	-0.18(2)	-0.021	0.074
$\eta_{\ell 2}$	0.075(1)	0.044	0.102

TABLE 5.1: This table shows some data

5.8 Conclusion

We have shown that the NPRG provides convergent values for the critical exponents while avoiding the technical difficulties of the perturbative approaches. Moreover our approach is systematically improvable without any difficulty through a field expansion. Although higher order derivative terms should play a small role they can and should be included to conclude on their importance in the convergence of the critical exponents. Currently we are performing a computation with higher derivative terms with a full potential. Finally we hope that our

work will stimulate new investigations of the Lifshitz critical behaviour by means of numerical simulations and experiments to confirm the adequacy of our quantitative predictions.

Appendix G

Threshold Functions

The dimensionless threshold functions are given by:

$$L_{a,b}^\alpha = -\frac{1}{2} \int dy \frac{y^{\frac{2\alpha+m-2}{2}} (\theta\eta_{\ell 4} r(y) + 2yr'(y))}{(y^2(1+r(y)) + \rho_0 y + m_0^2)^a (y^2(1+r(y)) + \rho_0 y + m_1^2)^b} \left\{ \frac{a}{(y^2(1+r(y)) + \rho_0 y + m_0^2)} + \frac{b}{(y^2(1+r(y)) + \rho_0 y + m_1^2)} \right\} \quad (\text{G.1})$$

$$M_{a,b}^\alpha = -\frac{1}{2} \int dy \frac{y^{\frac{m+2\alpha+2}{2}} (\theta\eta_{\ell 4} r(y) + 2yr'(y)) (y^2 r'(y) + 2y + 2yr(y) + \rho_0)^2}{(y^2(1+r(y)) + \rho_0 y + m_0^2)^a (y^2(1+r(y)) + \rho_0 y + m_1^2)^b} \left\{ \frac{a}{(y^2(1+r(y)) + \rho_0 y + m_0^2)} + \frac{b}{(y^2(1+r(y)) + \rho_0 y + m_1^2)} \right\} \\ + \int dy y^{\frac{m+2\alpha}{2}} (y^2 r'(y) + 2y + 2yr(y) + \rho_0) \\ \times \frac{(2y^2 r''(y) + yr'(y)(6 + \eta_{\ell 4}) + 2\theta\eta_{\ell 4} r(y))}{(y^2(1+r(y)) + \rho_0 y + m_0^2)^a (y^2(1+r(y)) + \rho_0 y + m_1^2)^b} \quad (\text{G.2})$$

$$\begin{aligned}
S_{a,b}^\alpha &= -\frac{1}{2} \int dy \frac{y^{\frac{m+2\alpha+2}{2}} (\theta\eta_{\ell 4} r(y) + 2yr'(y)) (y^2 r'(y) + 2y + 2yr(y) + \rho_0)^3}{(y^2(1+r(y)) + \rho_0 y + m_0^2)^a (y^2(1+r(y)) + \rho_0 y + m_1^2)^b} \\
&\quad \left\{ \frac{a}{(y^2(1+r(y)) + \rho_0 y + m_0^2)} + \frac{b}{(y^2(1+r(y)) + \rho_0 y + m_1^2)} \right\} \\
&\quad + \frac{3}{2} \int dy y^{\frac{m+2\alpha}{2}} (y^2 r'(y) + 2y + 2yr(y) + \rho_0)^2 \\
&\quad \times \frac{(2y^2 r''(y) + yr'(y)(6 + \theta\eta_{\ell 4}) + 2\theta\eta_{\ell 4} r(y))}{(y^2(1+r(y)) + \rho_0 y + m_0^2)^a (y^2(1+r(y)) + \rho_0 y + m_1^2)^b}
\end{aligned} \tag{G.3}$$

$$\begin{aligned}
T_{a,b}^\alpha &= -\frac{1}{2} \int dy \frac{y^{\frac{m+2\alpha+2}{2}} (\theta\eta_{\ell 4} r(y) + 2yr'(y)) (y^2 r'(y) + 2y + 2yr(y) + \rho_0)^4}{(y^2(1+r(y)) + \rho_0 y + m_0^2)^a (y^2(1+r(y)) + \rho_0 y + m_1^2)^b} \\
&\quad \left\{ \frac{a}{(y^2(1+r(y)) + \rho_0 y + m_0^2)} + \frac{b}{(y^2(1+r(y)) + \rho_0 y + m_1^2)} \right\} \\
&\quad + 2 \int dy y^{\frac{m+2\alpha}{2}} (y^2 r'(y) + 2y + 2yr(y) + \rho_0)^3 \\
&\quad \times \frac{(2y^2 r''(y) + yr'(y)(6 + \eta_{\ell 4}) + 2\theta\eta_{\ell 4} r(y))}{(y^2(1+r(y)) + \rho_0 y + m_0^2)^a (y^2(1+r(y)) + \rho_0 y + m_1^2)^b}
\end{aligned} \tag{G.4}$$

$$\begin{aligned}
U_{a,b}^\alpha &= -\frac{1}{2} \int dy \frac{y^{\frac{m+2\alpha+2}{2}} (\theta\eta_{\ell 4} r(y) + 2yr'(y)) (y^2 r''(y) + 4yr'(y) + 2r(y) + 2)^2}{(y^2(1+r(y)) + \rho_0 y + m_0^2)^a (y^2(1+r(y)) + \rho_0 y + m_1^2)^b} \\
&\quad \left\{ \frac{a}{(y^2(1+r(y)) + \rho_0 y + m_0^2)} + \frac{b}{(y^2(1+r(y)) + \rho_0 y + m_1^2)} \right\} \\
&\quad + \int dy y^{\frac{m+2\alpha-2}{2}} (y^2 r''(y) + 4yr'(y) + 2r(y) + 2) \\
&\quad \times \frac{(2y^3 r'''(y) + y^2 r''(y)(12 + \eta_{\ell 4}) + 4yr'(y)(\theta\eta_{\ell 4} + 3) + 2\theta\eta_{\ell 4} r(y))}{(y^2(1+r(y)) + \rho_0 y + m_0^2)^a (y^2(1+r(y)) + \rho_0 y + m_1^2)^b}
\end{aligned} \tag{G.5}$$

Chapter 6

Disordered Membranes

6.1 Introduction

In the introduction on membranes in Chapter 2 we have shown how complex these systems are. Membranes are far from being homogeneous except for specific case like graphene. The presence of proteins or cholesterol in biological membranes or impurities and defects (disclinations and dislocations) induce heterogeneities. Such defects may also appear during the fabrication process of polymerized membranes. After the works on homogeneous polymerized membranes our interest switched to the study of the effects of heterogeneities. In this chapter we discuss the different types of randomness that can be present in a membrane and we show how they modify the phase diagram.

Our work on disordered membranes is a work in progress and therefore no results are presented in this chapter.

6.2 Replica Formalism

There are two types of disorder *annealed* and *quenched*. In the first type the disorder and the degrees of freedom of the system fluctuate together which means that the time scale of variation of the disorder is equivalent the one of the degrees of freedom. In membranes, as in spin-glasses, we deal with quenched disorder where the random couplings, corresponding to

the disorder, are constant over the time scale over which the degrees of freedom fluctuate. Consider a Hamiltonian $\mathcal{H}[S, J]$ where S are the degrees of freedom and J the random coupling. For quenched disorder the partition function depend on J :

$$\mathcal{Z}[J] = \text{Tr}_{\{S\}} e^{-\mathcal{H}[S, J]} \quad (6.1)$$

which means that the free energy F also depend on J . This is not satisfying since it means that the free energy is different for each realization of the disorder. However in the thermodynamic limit the free energy does not depend on J and one must average over the disorder and this free energy is called the *quenched average* free energy. This makes the computation a little bit difficult since we must average over the disorder in the free energy and not in the partition function. To overcome this difficulty in quenched disordered systems, studying the effects of randomness implies to use the replica formalism (see [169, 170] for lectures). This formalism consists in replacing the partition function $\ln \mathcal{Z}$ by $(\mathcal{Z}^n - 1)/n$ where n corresponds to the number of replicas of the original system. Then one takes advantage of the relation:

$$\ln \mathcal{Z} = \lim_{n \rightarrow 0} \frac{\mathcal{Z}^n - 1}{n} \quad (6.2)$$

which transforms the task of averaging $\ln \mathcal{Z}$ by \mathcal{Z}^n . After taking the average over the disorder one obtains a replicated free energy which is of the form:

$$F_n[\vec{\phi}^\alpha] = \int d^d x \left\{ \sum_{\alpha=1}^n \left(\frac{1}{2} (\partial \vec{\phi}^\alpha)^2 + U(\vec{\phi}^\alpha) \right) - \frac{1}{2} \sum_{\alpha, \beta=1}^n V(\vec{\phi}^\alpha, \vec{\phi}^\beta) + \dots \right\} \quad (6.3)$$

which is an expansion in the number of replicas where α and β are replica indices. . The free energy is $O(n)$ invariant in the replica space as well as under the permutation between replicas. If the probability distribution is Gaussian the free energy only contains term with up to two replicas at the beginning of the flow.

In what follow we use the same notations as in ref. [171] where the average over disorder is noted with square brackets [] and the thermal average with angle brackets $\langle \rangle$.

6.3 The Model

There are two ways that randomness can appear in the free energy, either in the curvature part or in the strain part. From a geometric point of view an asymmetry between the two leaflets of a membrane leads to a spontaneous curvature \vec{c} which couples to the curvature $-\partial^2 \vec{r}(x) \cdot \vec{c}(x)$ and to a random stress which changes the preferred metric $g_{\alpha\beta}^0$.

Radzihovsky & Nelson [172] proposed a modification to the free energy to take into account of random impurities. One year later Morse & Lubensky showed [171] that starting with only random spontaneous curvature always generates random stress which means that both type of disorder must be taken into account. From the free energy of homogeneous membranes they added the two sources of randomness:

$$F[\vec{r}] = \int d^D x \left\{ \frac{\kappa}{2} \left(\partial^2 \vec{r}(x) - \frac{\vec{c}(x)}{2} \right)^2 + \frac{\mu}{4} (\partial_i \vec{r}(x) \cdot \partial_j \vec{r}(x))^2 + \frac{\lambda}{8} (\partial_i \vec{r}(x) \cdot \partial_i \vec{r}(x))^2 - \sigma_{ij}(x) \partial_i \vec{r}(x) \cdot \partial_j \vec{r}(x) \right\} \quad (6.4)$$

where κ is the usual bending rigidity and μ and λ the elastic moduli and where \vec{c} is the random curvature source and σ the random stress source. We consider the sources to have a Gaussian distribution. Therefore their variances are given by:

$$\begin{cases} [c_i(x)c_j(x')] & = \Delta_\kappa \delta_{ij} \delta(x - x') \\ [\sigma_{ab}(x)\sigma_{cd}(x')] & = (\Delta_\lambda \delta_{ab} \delta_{cd} + 2\Delta_\mu I_{abcd}) \delta(x - x') \end{cases} \quad (6.5)$$

where:

$$I_{abcd} = \frac{1}{2} (\delta_{ac} \delta_{bd} + \delta_{ad} \delta_{bc}) \quad (6.6)$$

is the identity in replica space. The variance of c_i must be positive. Moreover the stress tensor can be decomposed into a scalar and a symmetric part via $\sigma_{ab} = \sigma^L \delta_{ab} + \sigma_{ab}^T$ where $\sigma_{aa}^T = 0$.

And the variances of σ^L and σ_{ab}^T must be positive which leads to:

$$\begin{cases} \Delta_\kappa \geq 0 \\ \Delta_\mu \geq 0 \\ \Delta_\mu \geq -\frac{D}{2}\Delta_\lambda. \end{cases} \quad (6.7)$$

Surprisingly the upper critical dimension remains unchanged with respect to the pure case: $D_{uc} = 4$. This is different from the situation in the random field $O(n)$ model (RFO(n)M) where the upper critical dimension is shifted from 4 to 6. Before discussing the critical behaviour at this new fixed-point let us see what are the effects of disorder on the flat-phase. In the Monge parametrization and keeping only the non-linear terms relevant for the flat phase the free energy is given by:

$$F = \frac{1}{2} \int d^D x \left\{ \kappa \left(\partial^2 \vec{h}(x) \right)^2 - 2\vec{c}(x) \cdot \partial^2 \vec{h}(x) \right. \quad (6.8)$$

$$\left. + \lambda u_{aa}(x)^2 + 2\mu u_{ab}(x)^2 - 2\sigma_{ab}(x) u_{ab}(x) \right\} \quad (6.9)$$

where \vec{h} is the height field and u_{ab} the strain tensor. As for homogeneous membranes one can integrate exactly over the phonon modes and evaluate the effects of disorder [172] through the height correlation function which is given by:

$$[\langle |h(q)|^2 \rangle] = \frac{k_B T}{\kappa_R^D(q) q^4} \quad (6.10)$$

where $\kappa_R^D(q)$ is the renormalized disorder bending rigidity and the superscript D stands for disorder and not the membrane dimension and is given by:

$$\kappa_R^D(q) = \kappa + k_B T \int_p \frac{K_0}{\kappa |\mathbf{q} + \mathbf{p}|^4} \left(q_i P_{ij}^\perp(p) q_j \right)^2 - \Delta_\kappa \int_p \frac{K_0^2}{\kappa |\mathbf{q} + \mathbf{p}|^4} \left(q_i P_{ij}^\perp(p) q_j \right)^2 \quad (6.11)$$

where $K_0 = 4\mu(\mu + \lambda)/(2\mu + \lambda)$ and $P_{ij}^\perp = \delta_{ij} - p_i p_j / p^2$ the transverse projection operator. One sees that the first correction term is temperature dependent and increases the bending rigidity as in homogeneous membrane. Lowering the temperature the strength of this term

decreases and κ_R^D is dominated by the temperature-independent term which softens the bending rigidity. Nelson & Radzihovsky found that randomness does not affect the behaviour of the stable flat phase. However they found another fixed-point corresponding to a random flat phase at $T = 0$ where the bending rigidity is softened by the randomness. Adding the random spontaneous curvature changes the renormalized disorder bending rigidity which now reads [171]:

$$\begin{aligned} \kappa_R^D(q) = & \kappa + (k_B T \kappa + \Delta_\kappa) \int_p \frac{K_0}{\kappa^2 |\mathbf{q} + \mathbf{p}|^4} \left(q_i P_{ij}^\perp(p) q_j \right)^2 \\ & - \Delta_\kappa \int_p \frac{K_0^2}{\kappa |\mathbf{q} + \mathbf{p}|^4} \left(q_i P_{ij}^\perp(p) q_j \right)^2 \end{aligned} \quad (6.12)$$

from which we see that the random spontaneous curvature participates to the stiffening of the bending rigidity through *order from disorder*. Now at $T = 0$ there is a competition between random curvature and random stress.

The thermal fluctuations are characterized by linear response functions:

$$\begin{cases} \chi_{u_a u_b}(q) &= T^{-1} ([\langle u_a(q) u_b(-q) \rangle] - [\langle u_a(q) \rangle \langle u_b(-q) \rangle]) \\ \chi_{h_i h_j}(q) &= T^{-1} ([\langle h_i(q) h_j(-q) \rangle] - [\langle h_i(q) \rangle \langle h_j(-q) \rangle]) \end{cases} \quad (6.13)$$

and the disorder-induced fluctuations are given by:

$$\begin{cases} C_{u_a u_b}(q) &= [\langle u_a(q) \rangle \langle u_b(-q) \rangle] \\ C_{h_i h_j}(q) &= [\langle h_i(q) \rangle \langle h_j(-q) \rangle] . \end{cases} \quad (6.14)$$

These functions χ and C are related to the impurity-averaged Green functions through:

$$\begin{cases} G_{u_a u_b}(q) &= T \chi_{u_a u_b}(q) + C_{u_a u_b}(q) \\ G_{h_i h_j}(q) &= T \chi_{h_i h_j}(q) + C_{h_i h_j}(q) . \end{cases} \quad (6.15)$$

In the long-wave length limit these functions behave as:

$$\begin{cases} \chi_{u_a u_b}(q) &\sim q^{-(2+\eta_u)} \\ \chi_{h_i h_j}(q) &\sim q^{-(4-\eta_h)} \\ C_{u_a u_b}(q) &\sim q^{-(2+\eta'_u)} \\ C_{h_i h_j}(q) &\sim q^{-(4-\eta'_h)} . \end{cases} \quad (6.16)$$

The unprimed and primed critical exponents, which describe respectively the divergences of the replica diagonal and replica off-diagonal parts of the Green functions, obey the same Ward identity: $\eta_u + 2\eta_h = 4 - D$ at the non-zero temperature flat phase fixed-point and $\eta'_u + 2\eta'_h = 4 - D$ at the zero temperature disordered flat phase.

6.4 Perturbative RG

From a weak-coupling ϵ -expansion in the vicinity of $D = 4$ Nelson & Radzihovsky [172], and later Morse & Lubensky [171], have found two non-trivial fixed points. The first one corresponds to a homogeneous flat phase at non-zero temperature ($T \neq 0$) and the second non-trivial fixed-point corresponds to a random flat phase at zero temperature ($T = 0$).

Examining the flow equations Morse & Lubensky [173] noted that the study of the fixed-points can be restricted to an attractive subspace where $\lambda/\mu = \Delta_\lambda/\Delta_\mu = -1/3$. This space is shown of fig. 6.1.

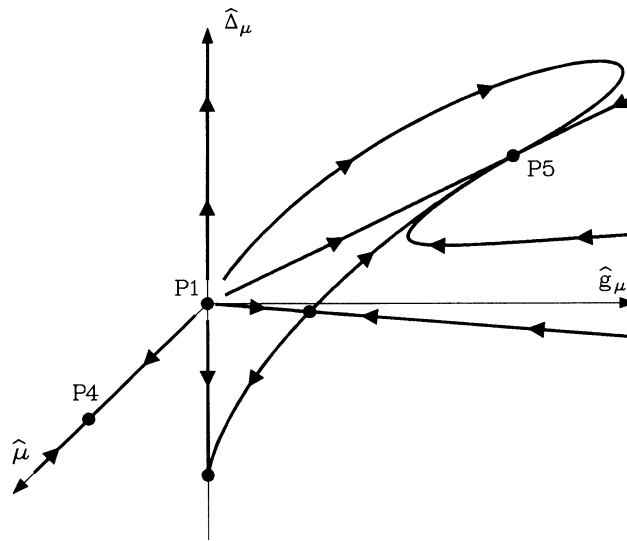


FIGURE 6.1: Flow diagram in the $\lambda/\mu = \Delta_\lambda/\Delta_\mu = -1/3$ subspace. All the fixed-points, except the $T \neq 0$ fixed-point $P4$, lie in the $\mu = 0$ ($T = 0$) plane. $P1$ is the unstable Gaussian fixed-point and $P5$ is the physical $T = 0$ fixed-point. The two unlabeled fixed-points are non-physical [171].

Below $D = 4$ at $T \neq 0$ the couplings are attracted to the fixed-point $P4$ which corresponds to the homogeneous flat phase where the randomness is irrelevant. When the temperature is lowered to $T = 0$ the couplings in the plane $\mu = 0$ flow to $P5$ which is the fixed-point associated with a rough flat phase where the random spontaneous curvature and the random stress are non-vanishing. The fixed-point $P5$ is weakly unstable with respect to the temperature.

At the fixed-points $P4$ and $P5$ the unprimed and primed anomalous dimensions η are related by scaling relations. These relations were derived by Morse & Lubensky in [171]. We start with the homogeneous flat phase fixed-point $P4$ where the scaling relations are given by:

$$\begin{cases} \eta + 2\eta_u &= 4 - D \\ \eta' &= 2\eta \\ \eta'_u &= 0. \end{cases} \quad (6.17)$$

The first relation is obtained from rotational invariance. The last relation is only valid when $d - D$ is lower than 24 which is true in the physical case $D = 2$ and $d = 3$.

At the fixed-point $P5$ the scaling relations are given by:

$$\begin{cases} \eta' + 2\eta'_u &= 4 - D \\ \eta &= \eta' - \phi_T \\ \eta_u &= \eta'_u + \phi_T \end{cases} \quad (6.18)$$

where again the first relation is obtained from rotational invariance. The exponent ϕ_T is an eigenvalue of the flow equations and corresponds to the scaling of the coupling μ near the fixed-point $P5$: $\mu \sim k^{\phi_T}$. The calculation of ϕ_T to order ϵ gives $\phi_T = 0$ for all $d > D$. This is in agreement with a large- d expansion to order $o(1/d)$ and with numerical simulations for $d = 3$ and $D = 2$ [174].

From these results Morse & Lubensky conjecture that the exponent ϕ_T remains vanishing at all orders of the expansions. This is an interesting project to verify under the NPRG approach. Moreover it is important to go beyond the ϵ -expansion to compute accurate values for the critical exponents.

6.5 NPRG

6.5.1 Effective Action

The formalism that we use for disordered membranes is based on the works of TISSIER, MOUHANNA, VIDAL & DELAMOTTE [175] and of TISSIER & TARJUS [55, 176]. The effective action is expanded in as a series of free replica:

$$\Gamma[\phi^\alpha] = \sum_{\alpha=1}^n \Gamma_1[\phi^\alpha] - \frac{1}{2} \sum_{\alpha, \beta=1}^n \Gamma_2[\phi^\alpha, \phi^\beta] + \dots \quad (6.19)$$

For disordered polymerized membranes we take a Gaussian distribution and the effective action at lowest order of the field and derivative expansions is given by:

$$\begin{aligned} \Gamma[\vec{r}] = & \sum_{\alpha=1}^n \int d^D x \left\{ \frac{Z}{2} (\partial_i \partial_i \vec{r}^\alpha(x))^2 + \frac{\lambda}{8} (\partial_i \vec{r}^\alpha(x) \cdot \partial_i \vec{r}^\alpha(x) - D\zeta^2)^2 \right. \\ & + \frac{\mu}{4} (\partial_i \vec{r}^\alpha(x) \cdot \partial_j \vec{r}^\alpha(x) - \zeta^2 \delta_{ij})^2 \left. \right\} - \sum_{\alpha, \beta=1}^n \int d^D x \left\{ \frac{\Delta_\kappa}{2} (\partial_i \partial_i \vec{r}^\alpha(x)) (\partial_j \partial_j \vec{r}^\beta(x)) \right. \\ & + \frac{\Delta_\lambda}{8} (\partial_i \vec{r}^\alpha(x) \cdot \partial_i \vec{r}^\alpha(x) - D\zeta^2) (\partial_j \vec{r}^\beta(x) \cdot \partial_j \vec{r}^\beta(x) - D\zeta^2) \\ & \left. + \frac{\Delta_\mu}{8} (\partial_i \vec{r}^\alpha(x) \cdot \partial_j \vec{r}^\alpha(x) - \zeta^2 \delta_{ij}) (\partial_i \vec{r}^\beta(x) \cdot \partial_j \vec{r}^\beta(x) - \zeta^2 \delta_{ij}) \right\} \end{aligned} \quad (6.20)$$

where $Z, \lambda, \mu, \Delta_\kappa, \Delta_\lambda, \Delta_\mu$ and ζ are the running coupling constants. The Latin indices correspond to the membrane internal coordinates and the Greek indices to the replica space. We must be careful when expanding the expression. The second sum over α and β will generate a n because some terms depend only on α or β .

The cut-off function \mathcal{R}_k is not diagonal in the replica space in general [55]:

$$(\mathcal{R}_k(q))_{ij}^{\alpha\beta} = \left(R_k(q) \delta_{\alpha\beta} + \tilde{R}_k(q) 1_{\alpha\beta} \right) \delta_{ij} \quad (6.21)$$

where $1_{\alpha\beta} = 1 \forall \alpha, \beta$. Taking only a diagonal cut-off may violate certain symmetries and induces wrong values for the critical exponents [55], [177], [178]. For example in [178] TISSIER &

Tarjus showed that taking \tilde{R}_k to zero violates superrotational invariance and the dimensional-reduction, that occurs in the RFO(n) model, could not be recovered. Moreover the cut-off \tilde{R}_k reduces the variance of the random sources, *i.e.* reduces the fluctuations of the bare disorder:

$$\mathbb{P}(h) = e^{-\int \frac{f(q)f(-q)}{\Delta - \tilde{R}_k}} \quad (6.22)$$

where f corresponds to a random source and Δ its variance. The probability eq. (6.22) means that \tilde{R}_k must stay finite in the limit $k \rightarrow \Lambda$ or else the probability will not make any sense. Indeed \tilde{R}_k reduces the variance of the random sources which gives an additional condition on the cut-off at the beginning of the flow:

$$\begin{cases} \tilde{R}_\Lambda \leq \Delta_\kappa \\ \tilde{R}_\Lambda \leq \Delta_\lambda. \end{cases} \quad (6.23)$$

6.5.2 Propagator

The configuration that minimizes the effective action (6.20) is given by:

$$r_a^\alpha(x) = \zeta x_a \theta(D - a) 1_\alpha \quad (6.24)$$

where 1_α is equal to 1 for all α . In this configuration the two-point correlation function reads:

$$\begin{aligned} & \left(\Gamma_k^{(2)} + \mathcal{R}_k \right) (p, i, \alpha, q, j, \beta) \Big|_{\min} = \delta_{\alpha\beta} \delta(p + q) \left\{ G_0^{-1}(p) \delta_{ij} \theta(i - D - 1) \right. \\ & \left. + \theta(D - i) \theta(D - j) \left[G_1^{-1}(p) \left(\delta_{ij} - \frac{p_i p_j}{p^2} \right) + G_2^{-1}(p) \frac{p_i p_j}{p^2} \right] \right\} \\ & + 1_{\alpha\beta} \delta(p + q) \left\{ \tilde{G}_0^{-1}(p) \delta_{ij} \theta(i - D - 1) \right. \\ & \left. + \theta(D - i) \theta(D - j) \left[\tilde{G}_1^{-1}(p) \left(\delta_{ij} - \frac{p_i p_j}{p^2} \right) + \tilde{G}_2^{-1}(p) \frac{p_i p_j}{p^2} \right] \right\} \end{aligned} \quad (6.25)$$

where:

$$\begin{cases} G_i(p) = (P(p) + m_i^2 p^2)^{-1} \\ \tilde{G}_i(p) = -(\tilde{P}(p) + \tilde{m}_i^2 p^2)^{-1} \end{cases} \quad (6.26)$$

with $P(p) = Z(p^2)^2 + R_k$ and $\tilde{P}(p) = \Delta_\kappa(p^2)^2 + \tilde{R}_k$. The masses m_i^2 and \tilde{m}_i^2 , with $i = 0, 1, 2$, are respectively given by $0, \zeta^2\mu, \zeta^2(2\mu + \lambda), 0, \frac{1}{2}\zeta^2\Delta_\mu$ and $\zeta^2(\Delta_\mu + \Delta_\lambda)$.

The propagator \mathcal{P} is the inverse of $(\Gamma_k^{(2)} + \mathcal{R}_k)$. Therefore, we have:

$$(\Gamma_k^{(2)} + \mathcal{R}_k) \mathcal{P} = \mathbb{1} \quad (6.27)$$

which can be written using indices as:

$$(\Gamma_k^{(2)} + \mathcal{R}_k)(i, \alpha, j, \beta) \mathcal{P}(j, \beta, k, \sigma) = \delta_{\alpha\sigma} \delta_{ik} \quad (6.28)$$

with Einstein summation rule over β and j .

To compute the expression of the propagator we must do the inversion of $(\Gamma_k^{(2)} + R_k)$ both in the replica and field spaces. We suppose that the propagator is of the form:

$$\begin{aligned} \mathcal{P}(i, \alpha, j, \beta) = & \delta_{\alpha\beta} \delta(p_1 + p_2) \left\{ a \delta_{ij} \theta(i - D - 1) \right. \\ & \left. + \theta(D - i) \theta(D - j) \left[b \left(\delta_{ij} - \frac{p_i p_j}{p^2} \right) + c \frac{p_i p_j}{p^2} \right] \right\} \\ & + 1_{\alpha\beta} \delta(p_1 + p_2) \left\{ \tilde{a} \delta_{ij} \theta(i - D - 1) \right. \\ & \left. + \theta(D - i) \theta(D - j) \left[\tilde{b} \left(\delta_{ij} - \frac{p_i p_j}{p^2} \right) + \tilde{c} \frac{p_i p_j}{p^2} \right] \right\}. \end{aligned} \quad (6.29)$$

Then, let M be a operator of the form:

$$M_{\alpha\beta, ij} = X_{ij} \delta_{\alpha\beta} + Y_{ij} 1_{\alpha\beta} \quad (6.30)$$

where the Latin and Greek indices correspond to different spaces and $1_{\alpha\beta} = 1 \forall \alpha, \beta$.

$$M_{\alpha\beta, ij}^{-1} M_{\beta\sigma, jk} = \delta_{\alpha\sigma} \delta_{ik} \quad (6.31)$$

We assume that the inverse matrix M^{-1} is of the form:

$$M_{\alpha\beta, ij}^{-1} = X'_{ij} \delta_{\alpha\beta} + Y'_{ij} 1_{\alpha\beta}. \quad (6.32)$$

In what follows, we drop the subscripts i and j but we must keep in mind that we are dealing with matrices. Therefore:

$$M_{\alpha\beta}^{-1}M_{\beta\sigma} = (X'\delta_{\alpha\beta} + Y'1_{\alpha\beta})(X\delta_{\beta\sigma} + Y1_{\beta\sigma}) \quad (6.33)$$

$$= X'X\delta_{\alpha\sigma} + X'Y1_{\alpha\sigma} + Y'X1_{\alpha\sigma} + nY'Y1_{\alpha\sigma} \quad (6.34)$$

which leads to:

$$\begin{cases} X'X & = \mathbb{1}, \\ X'Y + Y'X + nY'Y & = 0 \end{cases} \quad (6.35)$$

and the expressions of X' and Y' are given by:

$$\begin{cases} X' & = X^{-1} \\ Y' & = -X^{-1}Y(X + nY)^{-1}. \end{cases} \quad (6.36)$$

We do not need an expansion over replicas because we know how to compute the inverse $(X + nY)^{-1}$ exactly. Replacing X and Y by their expressions, we find (we drop the explicit momentum dependence of the functions G_i but this will be restored in the final expression):

$$\begin{aligned} X' &= G_0\delta_{ij}\theta(i - D - 1) + \theta(D - i)\theta(D - j) \left[G_1 \left(\delta_{ij} - \frac{p_i p_j}{p^2} \right) + G_2 \frac{p_i p_j}{p^2} \right] \\ Y' &= - \left\{ G_0\delta_{ia_1}\theta(i - D - 1) + \theta(D - i)\theta(D - a_1) \left[G_1 \left(\delta_{ia_1} - \frac{p_i p_{a_1}}{p^2} \right) \right. \right. \\ &\quad \left. \left. + G_2 \frac{p_i p_{a_1}}{p^2} \right] \right\} \times \left\{ \tilde{G}_0^{-1}\delta_{a_1 a_2}\theta(a_1 - D - 1) + \theta(D - a_1)\theta(D - a_2) \right. \\ &\quad \left. \left[\tilde{G}_1^{-1} \left(\delta_{a_1 a_2} - \frac{p_{a_1} p_{a_2}}{p^2} \right) + \tilde{G}_2^{-1} \frac{p_{a_1} p_{a_2}}{p^2} \right] \right\} \times \left\{ \frac{\delta_{a_1 a_2}\theta(a_1 - D - 1)}{(G_0^{-1} + n\tilde{G}_0^{-1})} \right. \\ &\quad \left. + \theta(D - a_1)\theta(D - a_2) \left[\frac{\left(\delta_{a_1 a_2} - \frac{p_{a_1} p_{a_2}}{p^2} \right)}{(G_1^{-1} + n\tilde{G}_1^{-1})} + \frac{\frac{p_{a_1} p_{a_2}}{p^2}}{(G_2^{-1} + n\tilde{G}_2^{-1})} \right] \right\} \end{aligned} \quad (6.37)$$

with summation over the indices a_i . Finally, the propagator at the minimum is given by (we restore the momenta p):

$$\begin{aligned}
\mathcal{P}(p, i, \alpha, q, j, \beta) \Big|_{\min} &= \delta_{\alpha\beta} \delta(p+q) \left\{ G_0(p) \delta_{ij} \theta(i-D-1) \right. \\
&+ \theta(D-i) \theta(D-j) \left[G_1(p) \left(\delta_{ij} - \frac{p_i p_j}{p^2} \right) + G_2(p) \frac{p_i p_j}{p^2} \right] \left. \right\} \\
&- 1_{\alpha\beta} \delta(p+q) \left\{ \frac{G_0(p)^2}{nG_0(p) + \tilde{G}_0(p)} \delta_{ij} \theta(i-D-1) \right. \\
&+ \theta(D-i) \theta(D-j) \left[\frac{G_1(p)^2}{nG_1(p) + \tilde{G}_1(p)} \left(\delta_{ij} - \frac{p_i p_j}{p^2} \right) + \frac{G_2(p)^2}{nG_2(p) + \tilde{G}_2(p)} \frac{p_i p_j}{p^2} \right] \left. \right\}
\end{aligned} \tag{6.38}$$

6.5.3 Flow Equations

From the two-point correlation function $\Gamma_k^{(2)}(p, i, \alpha, p', j, \beta)$ we find that the definitions of the coupling constants are given by:

$$\Delta_\kappa = - \lim_{p \rightarrow 0} \frac{d}{dp^4} \Gamma_k^{(2)}(p, D+1, 1, -p, D+1, 2) \Big|_{\min} \tag{6.39}$$

$$\Delta_\kappa = \lim_{p \rightarrow 0} \frac{d}{dp^4} \Gamma_k^{(2)}(p, D+1, 1, -p, D+1, 1) \Big|_{\min} + \Delta_\kappa \tag{6.40}$$

$$\Delta_\mu = - \lim_{p \rightarrow 0} \frac{d}{dp^2} \Gamma_k^{(2)}(p, D, 1, -p, D, 2) \Big|_{\min} \tag{6.41}$$

$$\mu = \lim_{p \rightarrow 0} \frac{d}{dp^2} \Gamma_k^{(2)}(p, D, 1, -p, D, 1) \Big|_{\min} + \frac{\Delta_\mu}{2} \tag{6.42}$$

$$\Delta_\lambda = - \lim_{p \rightarrow 0} \frac{d}{dp_D^2} \Gamma_k^{(2)}(p, D, 1, -p, D, 2) \Big|_{\min} - \frac{\Delta_\mu}{2} \tag{6.43}$$

$$\lambda = - \lim_{p \rightarrow 0} \frac{d}{dp_D^2} \Gamma_k^{(2)}(p, D, 1, -p, D, 1) \Big|_{\min} + \Delta_\lambda + \frac{\Delta_\mu}{2} - \mu \tag{6.44}$$

from which we derive the flow equations in similar manner as in the previous chapters. These flow equations read:

$$\begin{aligned}
\partial_t \zeta^2 = & \frac{2A_D}{D(D\lambda + 2\mu)} \left\{ 2(d - D)(D\lambda + 2\mu) \left(L_{1,0,0,0}^{D+2} + L_{2,0,0,1}^{D+2} \right) \right. \\
& + (D - 1) \left((D\lambda + 4\mu)(\Delta_\mu \zeta^2 L_{0,2,0,0}^{D+4} + 2L_{0,2,0,1}^{D+2}) + 2L_{0,1,0,0}^{D+2}(D\lambda - \Delta_\mu + 4\mu) \right) \\
& + 2 \left[((D + 2)\lambda + 6\mu) \left(\zeta^2(\Delta_\lambda + \Delta_\mu) L_{0,0,2,0}^{D+4} + L_{0,0,2,1}^{D+2} \right) \right. \\
& \left. \left. + L_{0,0,1,0}^{D+2}((D + 2)\lambda - 2\Delta_\lambda - 2\Delta_\mu + 6\mu) \right] \right\}
\end{aligned} \tag{6.45}$$

$$\begin{aligned}
\partial_t \mu = & \frac{4A_D}{D(D + 2)} \left\{ 2\mu^2(d - D)L_{2,0,0,0}^{D+4} + \frac{\mu}{\lambda + \mu} \right. \\
& \times (\Delta_\mu ((-D^2 + D + 4)\lambda + (4 - (D - 2)D)\mu) + (D - 2)(D + 4)\mu(\lambda + \mu)) L_{0,2,0,0}^{D+4} \\
& + \frac{D(2\mu(\Delta_\lambda \mu + (\lambda + \mu)(\lambda + 2\mu)) - \Delta_\mu(\lambda^2 + 4\lambda\mu + 2\mu^2))}{\zeta^2(\lambda + \mu)^2} \left(L_{0,1,0,0}^{D+2} - L_{0,0,1,0}^{D+2} \right) \\
& + 4\zeta^2(\Delta_\lambda + \Delta_\mu)(\lambda + 3\mu)^2 L_{0,0,3,0}^{D+6} + (D - 2)(D + 4)\Delta_\mu \zeta^2 \mu^2 L_{0,3,0,0}^{D+6} \\
& - \frac{2}{\lambda + \mu} L_{0,0,2,0}^{D+4} (\mu^2(2(D + 3)(\Delta_\lambda + \Delta_\mu) - 15\lambda) + \lambda\mu((D + 8)(\Delta_\lambda + \Delta_\mu) - 7\lambda) \\
& + \lambda^2(2(\Delta_\lambda + \Delta_\mu) - \lambda) - 9\mu^3) + \frac{2D\mu(\lambda + 2\mu)}{\zeta^2(\lambda + \mu)} \left(L_{0,2,0,1}^{D+2} - L_{0,0,2,1}^{D+2} \right) \\
& \left. + 4\mu^2(d - D)L_{3,0,0,1}^{D+4} + 4(\lambda + 3\mu)^2 L_{0,0,3,1}^{D+4} + 2(D - 2)(D + 4)\mu^2 L_{0,3,0,1}^{D+4} \right\}
\end{aligned} \tag{6.46}$$

$$\begin{aligned}
\partial_t \lambda = & \frac{2A_D}{D(D+2)} \left\{ (d-D)L_{2,0,0,0}^{D+4} (D(D+2)\lambda^2 + 4(D+2)\lambda\mu + 4\mu^2) \right. \\
& + 2(d-D)L_{3,0,0,1}^{D+4} (D(D+2)\lambda^2 + 4(D+2)\lambda\mu + 4\mu^2) \\
& + \Delta_\mu \zeta^2 L_{0,3,0,0}^{D+6} (D(D^2+D-2)\lambda^2 + 8(D^2+D-2)\lambda\mu + 4(3D+2)\mu^2) \\
& + \frac{1}{\lambda+\mu} L_{0,2,0,0}^{D+4} (-2(D^2+D-2)\Delta_\mu \lambda^2 + (\lambda+\mu)(D(D^2+D-2)\lambda^2 \\
& + 8(D^2+D-2)\lambda\mu + 4(3D+2)\mu^2) - 2(D(D+3)+4)\Delta_\mu \lambda\mu - 4(D+4)\Delta_\mu \mu^2) \\
& + 2L_{0,3,0,1}^{D+4} (D(D^2+D-2)\lambda^2 + 8(D^2+D-2)\lambda\mu + 4(3D+2)\mu^2) \\
& + 2\zeta^2(\Delta_\lambda + \Delta_\mu)L_{0,0,3,0}^{D+6} ((D(D+6)+12)\lambda^2 + 12(D+4)\lambda\mu + 36\mu^2) \\
& + \frac{4}{\zeta^2(\lambda+\mu)^2} L_{0,0,1,0}^{D+2} (2\mu(\Delta_\lambda \mu + (\lambda+\mu)(\lambda+2\mu)) - \Delta_\mu(\lambda^2 + 4\lambda\mu + 2\mu^2)) \\
& + \frac{4}{\zeta^2(\lambda+\mu)^2} L_{0,1,0,0}^{D+2} (\Delta_\mu(\lambda^2 + 4\lambda\mu + 2\mu^2) - 2\mu(\Delta_\lambda \mu + (\lambda+\mu)(\lambda+2\mu))) \\
& + \frac{1}{\lambda+\mu} L_{0,0,2,0}^{D+4} (\lambda^2((D(D+6)+12)\lambda - 4(D+4)(\Delta_\lambda + \Delta_\mu)) + 4\mu^2(3(D+7)\lambda \\
& - 2(\Delta_\lambda + \Delta_\mu)) + \lambda\mu((D(D+18)+60)\lambda - 4(D+8)(\Delta_\lambda + \Delta_\mu)) + 36\mu^3) \\
& + \frac{8\mu(\lambda+2\mu)}{\zeta^2(\lambda+\mu)} L_{0,0,2,1}^{D+2} - \frac{8\mu(\lambda+2\mu)}{\zeta^2(\lambda+\mu)} L_{0,2,0,1}^{D+2} \\
& \left. + 2L_{0,0,3,1}^{D+4} ((D(D+6)+12)\lambda^2 + 12(D+4)\lambda\mu + 36\mu^2) \right\}
\end{aligned} \tag{6.47}$$

$$\begin{aligned}
\partial_t \Delta_\mu = & \frac{2A_D}{D(D+2)} \left\{ -8(\Delta_\lambda + \Delta_\mu)^2 (\lambda + 3\mu)^2 L_{0,0,4,0}^{D+8} \zeta^4 \right. \\
& + 16(\Delta_\lambda + \Delta_\mu)(\lambda + 3\mu) \zeta^2 \left[(\Delta_\lambda + 2\Delta_\mu) L_{0,0,3,0}^{D+6} - (\lambda + 3\mu) L_{0,0,4,1}^{D+6} \right] \\
& + (D-2) \Delta_\mu \mu \zeta^2 \left[2(D+6) \Delta_\mu L_{0,3,0,0}^{D+6} - 4(D+4) \mu L_{0,4,0,1}^{D+6} - (D+4) \Delta_\mu \mu \zeta^2 L_{0,4,0,0}^{D+8} \right] \\
& - \frac{4}{(\lambda + \mu)^2} \left(-6\Delta_\mu \mu^3 + 2((\Delta_\lambda + \Delta_\mu)(\Delta_\lambda + 2(D+1)\Delta_\mu) - 7\Delta_\mu \lambda) \mu^2 \right. \\
& + 2\lambda(2(\Delta_\lambda + \Delta_\mu)(\Delta_\lambda + (D+2)\Delta_\mu) - 5\Delta_\mu \lambda) \mu + \lambda^2((\Delta_\lambda + \Delta_\mu)(2\Delta_\lambda + (D+4)\Delta_\mu) \\
& \left. - 2\Delta_\mu \lambda) \right) L_{0,0,2,0}^{D+4} + 8(d-D) \Delta_\mu \mu \left[L_{2,0,0,0}^{D+4} + 2L_{3,0,0,1}^{D+4} \right] \\
& + 16(\Delta_\lambda + 2\Delta_\mu)(\lambda + 3\mu) L_{0,0,3,1}^{D+4} - 8(\lambda + 3\mu)^2 L_{0,0,4,2}^{D+4} \\
& - \frac{\Delta_\mu}{(\lambda + \mu)^2} \left(-8(D-2) \mu^3 + (\Delta_\mu D^2 + 4(\Delta_\lambda + \Delta_\mu - 4\lambda)D - 6\Delta_\mu + 32\lambda) \mu^2 \right. \\
& + 2\lambda \left((D^2 - 6) \Delta_\mu - 4(D-2)\lambda \right) \mu + (D^2 - 6) \Delta_\mu \lambda^2 \right) L_{0,2,0,0}^{D+4} \\
& + 4(D-2)(D+6) \Delta_\mu \mu L_{0,3,0,1}^{D+4} - 4(D-2)(D+4) \mu^2 L_{0,4,0,2}^{D+4} \\
& + 8(D-d) \mu^2 L_{4,0,0,2}^{D+4} + \frac{8D \Delta_\mu (\Delta_\lambda + \Delta_\mu) \mu (\lambda + 2\mu) (L_{0,1,0,0}^{D+2} - L_{0,0,1,0}^{D+2})}{(\lambda + \mu)^3 \zeta^2} \\
& - \frac{4}{(\lambda + \mu)^2 \zeta^2} \left(((D+2)\Delta_\lambda + 2(D+1)\Delta_\mu) \lambda^2 + 4(D\Delta_\lambda + \Delta_\lambda + 2D\Delta_\mu + \Delta_\mu) \mu \lambda \right. \\
& \left. + ((5D+2)\Delta_\lambda + (9D+2)\Delta_\mu) \mu^2 \right) L_{0,0,2,1}^{D+2} \\
& - \frac{2}{(\lambda + \mu)^2 \zeta^2} \left((D^2 + D - 2) \Delta_\mu \lambda^2 + 2(D(D+2) - 2) \Delta_\mu \mu \lambda \right. \\
& \left. + (4D\Delta_\lambda + (D^2 + 9D - 2)\Delta_\mu) \mu^2 \right) L_{0,2,0,1}^{D+2} \\
& + \frac{4D(\lambda + 3\mu)(2\Delta_\lambda \mu + \Delta_\mu(\lambda + 4\mu))(L_{0,1,0,1}^D - L_{0,0,1,1}^D)}{(\lambda + \mu)^3 \zeta^4} \\
& - \frac{4 \left((D+1)\lambda^2 + 2(2D\mu + \mu)\lambda + (5D+1)\mu^2 \right) (L_{0,2,0,2}^D + L_{0,0,2,2}^D)}{(\lambda + \mu)^2 \zeta^4} \\
& \left. + \frac{8 \left((D+1)\lambda^2 + 2(2D\mu + \mu)\lambda + (5D+1)\mu^2 \right) (L_{0,1,0,2}^{D-2} - L_{0,0,1,2}^{D-2})}{(\lambda + \mu)^3 \zeta^6} \right\}
\end{aligned}$$

(6.48)

$$\begin{aligned}
\partial_t \Delta_\lambda = & \frac{A_D}{2D(D+2)} \left\{ \frac{32\Delta_\mu(\Delta_\lambda + \Delta_\mu)\mu(\lambda + 2\mu)}{(\lambda + \mu)^3 \zeta^2} \left(L_{0,0,1,0}^{D+2} - L_{0,1,0,0}^{D+2} \right) \right. \\
& - 4(\Delta_\lambda + \Delta_\mu)^2 \left((D(D+6) + 12)\lambda^2 + 12(D+4)\mu\lambda + 36\mu^2 \right) \zeta^4 L_{0,0,4,0}^{D+8} \\
& + \Delta_\mu^2 \left(-D(D^2 + D - 2)\lambda^2 - 8(D^2 + D - 2)\mu\lambda - 4(3D+2)\mu^2 \right) \zeta^4 L_{0,4,0,0}^{D+8} \\
& + 16(\Delta_\lambda + \Delta_\mu) \left((D(D+5) + 8)\Delta_\lambda\lambda + 6(D+3)\Delta_\lambda\mu + 2\Delta_\mu((D+4)\lambda + 6\mu) \right) \zeta^2 L_{0,0,3,0}^{D+6} \\
& - 8(\Delta_\lambda + \Delta_\mu) \left((D(D+6) + 12)\lambda^2 + 12(D+4)\mu\lambda + 36\mu^2 \right) \zeta^2 L_{0,0,4,1}^{D+6} \\
& + 4\Delta_\mu \left((D^2 + D - 2)(2D\Delta_\lambda + 3\Delta_\mu)\lambda + 2(4(D^2 + D - 2)\Delta_\lambda + (5D+2)\Delta_\mu)\mu \right) \zeta^2 L_{0,3,0,0}^{D+6} \\
& + 4\Delta_\mu \left(-D(D^2 + D - 2)\lambda^2 - 8(D^2 + D - 2)\mu\lambda - 4(3D+2)\mu^2 \right) \zeta^2 L_{0,4,0,1}^{D+6} \\
& + 8(\Delta_\lambda\lambda D^2 - 2\Delta_\lambda^2 D - 2\Delta_\lambda\Delta_\mu D + 4\Delta_\lambda\lambda D + \Delta_\mu\lambda D - 6\Delta_\lambda^2 + 4\Delta_\mu^2 - 2\Delta_\lambda\Delta_\mu \\
& + 4\Delta_\lambda\lambda + 4\Delta_\mu\lambda + 6((D+2)\Delta_\lambda + \Delta_\mu)\mu - \frac{8\Delta_\mu(\Delta_\lambda + \Delta_\mu)\lambda}{\lambda + \mu} + \frac{2\Delta_\mu(\Delta_\lambda + \Delta_\mu)\lambda^2}{(\lambda + \mu)^2} \left. \right) L_{0,0,2,0}^{D+4} \\
& + 16((D(D+5) + 8)\Delta_\lambda\lambda + 6(D+3)\Delta_\lambda\mu + 2\Delta_\mu((D+4)\lambda + 6\mu)) L_{0,0,3,1}^{D+4} \\
& - 4((D(D+6) + 12)\lambda^2 + 12(D+4)\mu\lambda + 36\mu^2) L_{0,0,4,2}^{D+4} \\
& + \frac{4}{(\lambda + \mu)^2} \left(\Delta_\mu(2(\lambda + \mu)^2((D^2 + D - 2)\lambda + 4D\mu) - \Delta_\mu((2D+3)\lambda^2 \right. \\
& + 2(2D+3)\mu\lambda + (2D-1)\mu^2)) - 2\Delta_\lambda((-D^2 - D + 2)(D\lambda + 4\mu)(\lambda + \mu)^2 \\
& + \Delta_\mu((D^2 + D - 2)\lambda^2 + 2(D^2 + D - 2)\mu\lambda + (D^2 + D - 4)\mu^2)) \left. \right) L_{0,2,0,0}^{D+4} \\
& + 8((D^2 + D - 2)(2D\Delta_\lambda + 3\Delta_\mu)\lambda + 2(4(D^2 + D - 2)\Delta_\lambda + (5D+2)\Delta_\mu)\mu) L_{0,3,0,1}^{D+4} \\
& + 4(-D(D^2 + D - 2)\lambda^2 - 8(D^2 + D - 2)\mu\lambda - 4(3D+2)\mu^2) L_{0,4,0,2}^{D+4} \\
& + 8(d-D)((D+2)(D\Delta_\lambda + \Delta_\mu)\lambda + 2((D+2)\Delta_\lambda + \Delta_\mu)\mu) \left(L_{2,0,0,0}^{D+4} + 2L_{3,0,0,1}^{D+4} \right) \\
& - 4(d-D)(D(D+2)\lambda^2 + 4(D+2)\mu\lambda + 4\mu^2) L_{4,0,0,2}^{D+4} \\
& + \frac{8}{(\lambda + \mu)^2 \zeta^2} \left(((D+2)\Delta_\lambda + (D+4)\Delta_\mu)\lambda^2 + 2((D+4)\Delta_\lambda + (D+8)\Delta_\mu)\mu\lambda \right. \\
& + ((D+10)\Delta_\lambda + (D+18)\Delta_\mu)\mu^2 \left. \right) L_{0,0,2,1}^{D+2} \\
& + \frac{4}{(\lambda + \mu)^2 \zeta^2} \left((D^2 + D - 2)\Delta_\mu\lambda^2 + 2D(D+1)\Delta_\mu\mu\lambda \right. \\
& + (8\Delta_\lambda + (D^2 + D + 14)\Delta_\mu)\mu^2 \left. \right) L_{0,2,0,1}^{D+2} \\
& + \frac{16(\lambda + 3\mu)(2\Delta_\lambda\mu + \Delta_\mu(\lambda + 4\mu))}{(\lambda + \mu)^3 \zeta^4} (L_{0,0,1,1}^D - L_{0,1,0,1}^D) \\
& + \frac{8((D+3)\lambda^2 + 2(D+5)\mu\lambda + (D+11)\mu^2)}{(\lambda + \mu)^2 \zeta^4} (L_{0,2,0,2}^D + L_{0,0,2,2}^D) \\
& + \frac{16((D+3)\lambda^2 + 2(D+5)\mu\lambda + (D+11)\mu^2)}{(\lambda + \mu)^3 \zeta^6} \left(L_{0,0,1,2}^{D-2} - L_{0,1,0,2}^{D-2} \right) \left. \right\}
\end{aligned}$$

(6.49)

where the threshold function is given by:

$$L_{a_0, a_1, a_2, b}^{D+\alpha} = -\frac{1}{4A_D} \tilde{\partial}_t \int d^D q q^\alpha G_0^{a_0}(q) G_1^{a_1}(q) G_2^{a_2}(q) \tilde{P}^b. \quad (6.50)$$

The anomalous dimension η and the flow $\partial_t \Delta_\kappa$ are not given here since their expressions are too long to be displayed.

6.5.4 Conclusion

As we have already said in the introduction, our work on disordered membranes is still in progress and therefore we do not present any result. As a consequence there is no conclusion in this chapter.

The equations have been checked in the limit of vanishing disorder and they are currently being compared with the weak-coupling perturbative results.

Conclusion

In this thesis we have studied different types of polymerized membranes: homogeneous, anisotropic and with impurities. In addition we have also studied Lifshitz critical behaviour which occurs in anisotropic systems.

Polymerized membranes are important systems in biology, chemistry and physics which make the understanding of their behaviour of great importance. While fluid membranes are always crumpled polymerized membranes exhibit some interesting properties such as the existence of a flat phase which seems to be in apparent violation of the Mermin-Wagner theorem. But as we have seen that the flat phase results from the existence of a coupling between the out-of-plane bending and in-plane elasticity which induces a long-range interaction and is therefore beyond the range of applicability of the Mermin-Wagner theorem.

Perturbative approaches have been able to predict qualitatively the behaviour of polymerized membranes. However since the upper critical dimension $D_{uc} = 4$ is far from the physical dimension $D = 2$ the calculations of the critical exponents are not reliable. We have computed the critical dimension line $d_c(D)$ separating a first-order transition from a second-order transition which is not possible using neither an ϵ nor a large- d expansion. Albeit we cannot bring a definite answer to the order of the transition in $d = 3$ and $D = 2$, our results seem to indicate that the transition is of first-order.

For tubular membranes, we managed to calculate the universal critical exponents and more importantly the anomalous dimension η for the transition between the crumpled phase and the tubular phase. This was not possible using a perturbative approach where the value of η was qualitatively and quantitatively wrong. This work lead to us to study another anisotropic system, an anisotropic $O(n)$ -model, where technical difficulties have plagued the perturbative approaches. An important result of our work is that the non-perturbative renormalization

group overcomes the technical difficulties present in perturbative approaches such as those in anisotropic membranes and Lifshitz critical behaviour.

Currently we are finishing our work on disordered membranes and we are studying 1) anisotropic membranes with higher orders of the derivative and field expansions and 2) Lifshitz critical behaviour with a full potential.

In a near future our aim is 1) to use a full potential to completely determine the order of the phase transition between the crumpled and flat phases in polymerized membranes 2) to investigate the question of local scale invariance in Lifshitz critical behaviour.

In the long term we hope to be able to study the effects of self-avoidance on the critical behaviour of polymerized membranes and most importantly to solve the question of the existence of the crumpled phase.

Bibliography

- [1] Thomas Andrews. No Title. *Philosophical Transactions of the Royal Society of London*, 159(575), 1869.
- [2] Charles Cagniard de la Tour. No Title. *Annales de chimie et de Physique*, 21:127, 1822.
- [3] Charles Cagniard de la Tour. No Title. *Annales de chimie et de Physique*, 21:178, 1822.
- [4] Bertrand Berche, Malte Henkel, and Ralph Kenna. Critical Phenomena: 150 Years Since Cagniard de la Tour. *Journal of Physics Studies*, 13(3):3201, 2009.
- [5] Tian Yu Cao. *Conceptual Foundations of Quantum Field Theory*. Cambridge University Press, 1999.
- [6] Ernst C.G. Stueckelberg and Andre Petermann. La Normalisation des Constantes dans la Theorie des Quanta. *Helvetica Physica Acta*, 26(5):499--520, 1953.
- [7] Murray Gell-Mann and Francis Low. Quantum Electrodynamics at Small Distances. *Physical Review*, 95(5):1300--1312, September 1954.
- [8] Freeman John Dyson. The Renormalization Method in Quantum Electrodynamics. *Proceedings of the Royal Society A: Mathematical, Physical and Engineering Sciences*, 207(1090):395--401, July 1951.
- [9] F. J. W. Hahne, editor. *Critical Phenomena - Lecture Notes in Physics 186*, volume 186 of *Lecture Notes in Physics*. Springer Berlin Heidelberg, Berlin, Heidelberg, 1983.
- [10] Nigel Goldenfeld. *Lectures on Phase Transitions and the Renormalization Group*. Perseus Books, 1992.
- [11] Shang-Keng Ma. *Modern Theory of Critical Phenomena*. 1976.

- [12] G. Toulouse and P. Pfeuty. *Groupe de Renormalisation*. Press Universitaires de Grenoble, 1975.
- [13] Christof Wetterich. Exact evolution equation for the effective potential. *Physics Letters B*, 301(1):90--94, February 1993.
- [14] Leo P. Kadanoff. Scaling Laws for Ising Models Near T_c. *Physics*, 2(6):263--272, 1966.
- [15] B. Widom. Equation of State in the Neighborhood of the Critical Point. *The Journal of Chemical Physics*, 43(11):3898, 1965.
- [16] Kenneth G. Wilson. Renormalization Group and Critical Phenomena. II. Phase Space Cell Analysis of Critical Behavior. *Physical Review B*, 4(9):3184--3205, 1971.
- [17] Th. Niemeijer and J.M.J. van Leeuwen. Renormalization group and critical exponents for a Gaussian spin model with long range interactions. *Physics Letters A*, 41(3):211--212, September 1972.
- [18] Th. Niemeijer and J.M.J. van Leeuwen. Wilson Theory for Spin Systems on a Triangular Lattice. *Physical Review Letters*, 31(23):1411--1414, December 1973.
- [19] Kenneth G. Wilson and John B. Kogut. The Renormalization Group and The Epsilon Expansion. *Physics Reports*, 12(2):75 -- 200, 1974.
- [20] Kenneth G. Wilson. The renormalization group: Critical phenomena and the Kondo problem. *Reviews of Modern Physics*, 47(4):773--840, 1975.
- [21] Thomas Bell and Kenneth G. Wilson. Nonlinear renormalization groups. *Physical Review B*, 10(9):3935--3944, November 1974.
- [22] Kenneth G. Wilson and Michael E. Fisher. Critical Exponents in 3.99 Dimensions. *Physical Review Letters*, 28(4):240--243, January 1972.
- [23] Franz J. Wegner and Anthony Houghton. Renormalization Group Equation for Critical Phenomena. *Physical Review A*, 8(1):401--412, July 1973.
- [24] Joseph Polchinski. Renormalization and Effective Lagrangians. *Nuclear Physics B*, 231:269--295, 1984.
- [25] Georg Keller and Christoph Kopper. Perturbative renormalization of QED via flow equations. *Physics Letters B*, 273(3):323--332, December 1991.

- [26] Georg Keller, Christoph Kopper, and Manfred Salmhofer. Perturbative Renormalization and Effective Lagrangians in ϕ^4 . *Helvetica Physica Acta*, 65(1):32--52, 1992.
- [27] Georg Keller and Christoph Kopper. Renormalizability proof for QED based on flow equations. *Communications in Mathematical Physics*, 176(1):193--226, February 1996.
- [28] S. Seide and Christof Wetterich. Equation of state near the endpoint of the critical line. *Nuclear Physics B*, 562:524--546, 1999.
- [29] Jurgen Berges, Nikolaos Tetradis, and Christof Wetterich. Non-perturbative renormalization flow in quantum field theory and statistical physics. *Physics Reports*, 363:223 -- 386, 2002.
- [30] L. Rosa, P. Vitale, and Christof Wetterich. Critical Exponents of the Gross-Neveu Model from the Effective Average Action. *Physical Review Letters*, 86(6):958--961, February 2001.
- [31] F. Höfling, C. Nowak, and Christof Wetterich. Phase transition and critical behavior of the $d=3$ Gross-Neveu model. *Physical Review B*, 66(20), November 2002.
- [32] Bertrand Delamotte, Dominique Mouhanna, and Matthieu Tissier. Nonperturbative renormalization-group approach to frustrated magnets. *Physical Review B*, 69(13):134413, April 2004.
- [33] Jan Pawłowski. Aspects of the functional renormalisation group. *Annals of Physics*, 322(12):2831--2915, December 2007.
- [34] Ken-Ichi Aoki, Keiichi Morikawa, Wataru Souma, Jun-Ichi Sumi, and Haruhiko Terao. Rapidly Converging Truncation Scheme of the Exact Renormalization Group. *Progress of Theoretical Physics*, 99(3):451--466, March 1998.
- [35] Tim R. Morris and John F. Tighe. Convergence of derivative expansions of the renormalization group. *Journal of High Energy Physics*, 1999(08):007--007, August 1999.
- [36] F. Braghin and Nils Hasselmann. Thermal fluctuations of free-standing graphene. *Physical Review B*, 82(3):5, July 2010.
- [37] Nils Hasselmann. Effective Average Action Based Approach to Correlation Functions at Finite Momenta. *arXiv*, 2012.

- [38] Jean-Paul Blaizot, Ramón Méndez-Galain, and Nicolás Wschebor. Nonperturbative renormalization group and momentum dependence of n-point functions. I. *Physical Review E*, 74(5):48, November 2006.
- [39] Léonie Canet, Bertrand Delamotte, Dominique Mouhanna, and Julien Vidal. Optimization of the derivative expansion in the nonperturbative renormalization group. *Physical Review D*, 67(6), March 2003.
- [40] Nikolaos Tetradis and Christof Wetterich. Critical exponents from the effective average action. *Nuclear Physics B*, 422(3):541--592, July 1994.
- [41] Daniel F. Litim. Optimisation of the exact renormalisation group. *Physics Letters B*, 486(1-2):92--99, July 2000.
- [42] V.L. Berezinskii. Destruction of Long-range Order in One-dimensional and Two-dimensional Systems having a Continuous Symmetry Group I. Classical Systems. *Soviet Physics Journal of Experimental and Theoretical Physics*, 32(3):493, 1970.
- [43] John Michael Kosterlitz and David James Thouless. Ordering, metastability and phase transitions in two-dimensional systems. *Journal of Physics C: Solid State Physics*, 6(7):1181--1203, April 1973.
- [44] M. Graßer and Christof Wetterich. Kosterlitz-Thouless Phase Transition in the Two Dimensional Linear σ Model. *Physical Review Letters*, 75(3):378--381, July 1995.
- [45] G. v. Gersdorff and Christof Wetterich. Nonperturbative renormalization flow and essential scaling for the Kosterlitz-Thouless transition. *Physical Review B*, 64(5):1--5, July 2001.
- [46] R. Guida and Jean Zinn-Justin. Critical Exponents of the N-Vector Model. *Journal of Physics A: Mathematical and General*, 31(40):8103--8121, October 1998.
- [47] Martin Hasenbusch. Monte Carlo Studies of the Three-Dimensional Ising Model in Equilibrium. *International Journal of Modern Physics C*, 12(07):911--1009, September 2001.
- [48] Federico Benitez, Jean-Paul Blaizot, Hugues Chaté, Bertrand Delamotte, R. Méndez-Galain, and Nicolás Wschebor. Solutions of renormalization-group flow equations with full momentum dependence. *Physical Review E*, 80(3), September 2009.

- [49] T. Machado and Nicolas Dupuis. From local to critical fluctuations in lattice models: A nonperturbative renormalization-group approach. *Physical Review E*, 82(4), October 2010.
- [50] Ulli Wolff. Comparison Between Cluster Monte Carlo Algorithms in the Ising Model. *Physics Letters B*, 228(3):379--382, September 1989.
- [51] Martin Hasenbusch and Steffen Meyer. Critical Exponents of the 3D XY Model from Cluster Update Monte Carlo. *Physics Letters B*, 241(2):238--242, May 1990.
- [52] Christian Holm and Wolfhard Janke. Critical Exponents of the Classical Three-Dimensional Heisenberg Model: A Single-Cluster Monte Carlo Study. *Physical Review B*, 48(2):936--950, July 1993.
- [53] Jean-Philippe Kownacki and Dominique Mouhanna. Crumpling transition and flat phase of polymerized phantom membranes. *Physical Review E*, 79(4):4, April 2009.
- [54] Karim Essafi, Jean-Philippe Kownacki, and Dominique Mouhanna. Crumpled-to-Tubule Transition in Anisotropic Polymerized Membranes: Beyond the ϵ -Expansion. *Physical Review Letters*, 106(12):128102, March 2011.
- [55] Gilles Tarjus and Matthieu Tissier. Nonperturbative functional renormalization group for random field models and related disordered systems. I. Effective average action formalism. *Physical Review B*, 78(2):024203, July 2008.
- [56] Léonie Canet, Hugues Chaté, Bertrand Delamotte, and Nicolás Wschebor. Nonperturbative renormalization group for the Kardar-Parisi-Zhang equation: General framework and first applications. *Physical Review E*, 84(6), December 2011.
- [57] Nicolas Dupuis and K. Sengupta. Non-perturbative renormalization group approach to zero-temperature Bose systems. *Europhysics Letters (EPL)*, 80(5):50007, December 2007.
- [58] L.N. Granda. Nonperturbative renormalization group for Einstein gravity with matter. *Europhysics Letters (EPL)*, 42(5):487--492, June 1998.
- [59] Oliver J. Rosten. Fundamentals of the Exact Renormalization Group. *arXiv*, page 172, March 2010.

- [60] Peter Kopietz, Lorenz Bartosch, and Florian Schütz. *Introduction to the Functional Renormalization Group*, volume 798 of *Lecture Notes in Physics*. Springer Berlin Heidelberg, Berlin, Heidelberg, 2010.
- [61] Robert Hooke. *Micrographia*. 1665.
- [62] William Bowman. On the Minute Structure and Movements of Voluntary Muscle. *Philosophical Transactions of the Royal Society of London*, 130:457--501, 1840.
- [63] Kleinzeller. Ernest Overton's Contribution to the Cell Membrane Concept: a Centennial Appreciation. *News in Physiological Sciences*, 12:49--53, 1997.
- [64] H. Fricke. The Electric Capacity of Cell Suspensions. *Physical Review Series II*, 21:708--709, 1923.
- [65] E. Gorter and F. Grendel. On Bimolecular Layers of Lipoids on the Chromocytes of the Blood. *Journal of Experimental Medicine*, 41:439--443, 1925.
- [66] William D. Harkins, F.E. Brown, and E.C.H. Davies. The Structure of the Surfaces of Liquids, and Solubility as Related to the Work Done by the Attraction of Two Liquid Surfaces as They Approach Each Other. *Journal of the American Chemical Society*, 39(3):354--364, 1917.
- [67] H. Fernandez-Moran and J.-B. Finean. Electron microscope and low-angle x-ray diffraction studies of the nerve myelin sheath. *Journal of Biophysical and Biochemical Cytology*, 25:725--748, 1957.
- [68] J.K. Blasie and C.R. Worthington. Planar liquid-like arrangement of photopigment molecules in frog retinal receptor disk membranes. *Journal of Molecular Biology*, 39(3):417--439, 1969.
- [69] James Frederic Danielli and Hugh Davson. A contribution to the theory of permeability of thin films. *Journal of Cellular and Comparative Physiology*, 5(4):495--508, February 1935.
- [70] Dennis Chapman. Phase transitions and fluidity characteristics of lipids and cell membranes. *Quarterly Reviews of Biophysics*, 8(02):185--235, March 1975.
- [71] S.J. Singer and G.L. Nicolson. The Fluid Mosaic Model of the Structure of Cell Membranes. *Science*, 175(4023):720--731, February 1972.

- [72] W. Bloom and D.W. Fawcett. *A Textbook of Histology*. 12th edition, 1994.
- [73] Joachim Pietzsch. Mind the Membrane. *Horizon Symposia, Nature*, October, 2004.
- [74] C. Tanford. The hydrophobic effect and the organization of living matter. *Science*, 200(4345):1012--1018, June 1978.
- [75] Joshua Zimmerberg and Michael M Kozlov. How proteins produce cellular membrane curvature. *Nature reviews. Molecular cell biology*, 7(1):9--19, January 2006.
- [76] R. Waugh and E.A. Evans. Thermoelasticity of red blood cell membrane. *Biophysical journal*, 26(1):115--31, April 1979.
- [77] Jeannette D. Moyer, Roberta B. Nowak, Nancy E. Kim, Sandra K. Larkin, Luanne L. Peters, John Hartwig, Frans A. Kuypers, and Velia M. Fowler. Tropomodulin 1-null mice have a mild spherocytic elliptocytosis with appearance of tropomodulin 3 in red blood cells and disruption of the membrane skeleton. *Blood*, 116(14):2590--9, October 2010.
- [78] Hans-Peter Boehm, A. Clauss, G.O. Fischer, and U. Hofmann. Das Adsorptionsverhalten sehr dünner Kohlenstoff-Folien. *Zeitschrift für anorganische und allgemeine Chemie*, 316(3-4):119--127, July 1962.
- [79] N.D. Mermin and H. Wagner. Absence of ferromagnetism or antiferromagnetism in one or two dimensional isotropic heisenberg models. *Physical Review Letters*, 17(22):1133--1136, 1966.
- [80] N.D. Mermin. Crystalline Order in Two Dimensions. *Physical Review*, 176(1):250--254, December 1968.
- [81] Sidney Coleman. There are no Goldstone bosons in two dimensions. *Communications in Mathematical Physics*, 31(4):259--264, December 1973.
- [82] Kostya S. Novoselov, Andre K. Geim, S.V. Morozov, D. Jiang, Y. Zhang, S.V. Dubonos, I.V. Grigorieva, and A.A. Firsov. Electric field effect in atomically thin carbon films. *Science*, 306(5696):666--9, October 2004.
- [83] Tim J. Booth, Peter Blake, Rahul R. Nair, Da Jiang, Ernie W. Hill, Ursel Bangert, Andrew Bleloch, Mhairi Gass, Kostya S. Novoselov, Mikhail I. Katsnelson, and Andre K.

- Geim. Macroscopic graphene membranes and their extraordinary stiffness. *Nano letters*, 8(8):2442--2446, August 2008.
- [84] L.J. Karssemeijer and Annalisa Fasolino. Phonons of graphene and graphitic materials derived from the empirical potential LCBOPII. *Surface Science*, 605(17-18):1611--1615, September 2011.
- [85] Robert F. Service. Materials Science. Carbon Sheets an Atom Thick Give Rise to Graphene Dreams. *Science*, 324(5929):875--877, May 2009.
- [86] Kian Ping Loh, Qiaoliang Bao, Goki Eda, and Manish Chhowalla. Graphene Oxide as a Chemically Tunable Platform for Optical Applications. *Nature chemistry*, 2(12):1015--24, December 2010.
- [87] J. Dai, R.G. Leigh, and Joseph Polchinski. New Connections between String Theories. *Modern Physics Letters A*, 4(21):2073--2083, 1989.
- [88] Petr Hořava. Strings on world-sheet orbifolds. *Nuclear Physics B*, 327(2):461--484, November 1989.
- [89] Eugenio Calabi. The Space of Kähler Metrics. In *Proceedings of the International Congress of Mathematicians*, pages 206--207, Amsterdam, 1954.
- [90] Shing-Tung Yau. On the Ricci Curvature of a Compact Kähler Manifold and the Complex Monge-Ampère Equation, I. *Communications on Pure and Applied Mathematics*, 31(3):339--411, May 1978.
- [91] Andre K. Geim and Kostya S. Novoselov. The rise of graphene. *Nature*, pages 183--191, 2007.
- [92] A. Castro Neto, F. Guinea, N. Peres, Kostya S. Novoselov, and Andre K. Geim. The electronic properties of graphene. *Reviews of Modern Physics*, 81(1):109--162, January 2009.
- [93] Rahul R. Nair, H A Wu, P N Jayaram, I V Grigorieva, and Andre K. Geim. Unimpeded Permeation of Water Through Helium-Leak-Tight Graphene-Based Membranes. *Science*, 335(6067):442--444, January 2012.
- [94] Petr Hořava. Quantum gravity at a Lifshitz point. *Physical Review D*, 79(8):084008, April 2009.

- [95] Alessandro Codello and Omar Zanusso. Fluid membranes and 2d quantum gravity. *Physical Review D*, 83(12):1-8, June 2011.
- [96] Jeffrey M. Lee. *Differential Geometry, Analysis and Physics*. 2000.
- [97] Gabriel Lugo. *Differential Geometry in Physics*. 2006.
- [98] David R. Nelson, T. Piran, and Steven Weinberg. *Statistical Mechanics of Membranes and Surfaces*. World Scientific, 2nd edition, 1988.
- [99] Markus Deserno. *Notes on Differential Geometry with special emphasis on surfaces in R^3* . 2004.
- [100] P.B. Canham. The minimum energy of bending as a possible explanation of the bi-concave shape of the human red blood cell. *Journal of Theoretical Biology*, 26(1):61-81, January 1970.
- [101] W. Helfrich. Elastic Properties of Lipid Bilayers - Theory and Possible Experiments. *Zeitschrift für Naturforschung C*, 28(11):693 -- 703, 1973.
- [102] Kenneth A. Brakke. The Surface Evolver. *Experimental Mathematics*, 1(2):141-165, January 1992.
- [103] L. Peliti and S. Leibler. Effects of Thermal Fluctuations on Systems with Small Surface Tension. *Physical Review Letters*, 54(15):1690-1693, April 1985.
- [104] Maya Paczuski, Mehran Kardar, and David R. Nelson. Landau Theory of the Crumpling Transition. *Physical Review Letters*, 60(25):2638-2640, 1988.
- [105] Rudolf Ernst Peierls. No Title. *Helvetica Physica Acta*, 7:81, 1923.
- [106] David R. Nelson and L. Peliti. Fluctuations in Membranes with Crystalline and Hexatic Order. *Journal de Physique France*, 48:1085-1092, 1987.
- [107] S. Sachdev and David R. Nelson. Crystalline and fluid order on a random topography. *Journal of Physics C: Solid State Physics*, 17(30):5473-5489, October 1984.
- [108] Pierre Le Doussal and Leo Radzihovsky. Self-consistent theory of polymerized membranes. *Physical Review Letters*, 69(8):1209-1212, August 1992.
- [109] Jean-Philippe Kownacki and H. Diep. First-order transition of tethered membranes in three-dimensional space. *Physical Review E*, 66(6), December 2002.

- [110] Hiroshi Koibuchi, Nobuyuki Kusano, Atsusi Nidaira, Komei Suzuki, and Mitsuru Yamada. First-order phase transition of fixed connectivity surfaces. *Physical Review E*, 69(6), June 2004.
- [111] François David and E. Guitter. Crumpling Transition in Elastic Membranes - Renormalization Group Treatment. *Europhysics Letters*, 5(8):709 -- 713, 1988.
- [112] J.A. Aronovitz and Tom C. Lubensky. Fluctuations of Solid Membranes. *Physical Review Letters*, 60(25):2634--2637, 1988.
- [113] Mark J. Bowick, Simon M. Catterall, Marco Falcioni, Gudmar Thorleifsson, and Konstantinos N. Anagnostopoulos. The Flat Phase of Crystalline Membranes. *Journal de Physique I*, 6(10):1321, 1996.
- [114] D. Espriu and Alex Travesset. MCRG study of fixed-connectivity surfaces. *Nuclear Physics B*, 468(3):514--540, June 1996.
- [115] Jeffrey Goldstone. Field Theories with Superconductor Solutions. *Il Nuovo Cimento*, 19:154, 1961.
- [116] Jeffrey Goldstone, Abdus Salam, and Steven Weinberg. Broken Symmetries. *Physical Review*, 127(3):965--970, August 1962.
- [117] H.B. Nielsen and S. Chadha. On How to Count Goldstone Bosons. *Nuclear Physics B*, 105:445--453, 1976.
- [118] Ian Low and Aneesh Manohar. Spontaneously Broken Spacetime Symmetries and Goldstone's Theorem. *Physical Review Letters*, 88(10):10--13, February 2002.
- [119] Z. Zhang, H. Davis, and D. Kroll. Scaling behavior of self-avoiding tethered vesicles. *Physical Review E*, 48(2):R651--R654, August 1993.
- [120] Annalisa Fasolino, J.H. Los, and Mikhail I. Katsnelson. Intrinsic ripples in graphene. *Nature materials*, 6(11):858--61, November 2007.
- [121] J.H. Los, Mikhail I. Katsnelson, O. Yazyev, K. Zakharchenko, and Annalisa Fasolino. Scaling Properties of Flexible Membranes from Atomistic Simulations: Application to Graphene. *Physical Review B*, 80(12), September 2009.

- [122] K. Zakharchenko, M. Katsnelson, and Annalisa Fasolino. Finite Temperature Lattice Properties of Graphene beyond the Quasiharmonic Approximation. *Physical Review Letters*, 102(4), January 2009.
- [123] K. Zakharchenko, J.H. Los, Mikhail I. Katsnelson, and Annalisa Fasolino. Atomistic Simulations of Structural and Thermodynamic Properties of Bilayer Graphene. *Physical Review B*, 81(23), June 2010.
- [124] Michael Plischke and David Boal. Absence of a Crumpling Transition in Strongly Self-Avoiding Tethered Membranes. *Physical Review A*, 38(9):4943--4945, November 1988.
- [125] Farid Abraham, W. Rudge, and M. Plischke. Molecular Dynamics of Tethered Membranes. *Physical Review Letters*, 62(15):1757--1759, April 1989.
- [126] David Boal, Edward Levinson, Damin Liu, and Michael Plischke. Anisotropic Scaling of Tethered Self-Avoiding Membranes. *Physical Review A*, 40(6):3292--3300, September 1989.
- [127] A. Baumgärtner and W. Renz. Crumpled Self-Avoiding Tethered Surfaces. *Europhysics Letters (EPL)*, 17(5):381--386, February 1992.
- [128] Terence Hwa, Etsuo Kokufuta, and Toyochi Tanaka. Conformation of Graphite Oxide Membranes in Solution. *Physical Review A*, 44(4):2235, 1991.
- [129] Leo Radzihovsky and John Toner. A New Phase of Tethered Membranes: Tubules. *Physical Review Letters*, 75(26):4752--4755, December 1995.
- [130] Leo Radzihovsky and John Toner. Elasticity, shape fluctuations, and phase transitions in the new tubule phase of anisotropic tethered membranes. *Physical Review E*, 57(2):1832--1863, February 1998.
- [131] Eunji Lee, Jung-Keun Kim, and Myongsoo Lee. Reversible Scrolling of Two-Dimensional Sheets from the Self-Assembly of Laterally Grafted Amphiphilic Rods. *Angewandte Chemie (International ed. in English)*, 48(20):3657--60, January 2009.
- [132] Mark J. Bowick and E. Gitter. Effects of self-avoidance on the tubular phase of anisotropic membranes. *Physical Review E*, 56(6):7023--7032, December 1997.

- [133] Hiroshi Koibuchi. Shape Transformations of a Model of Self-Avoiding Triangulated Surfaces of Sphere Topology. *International Journal of Modern Physics C*, 21(11):1341--1358, November 2010.
- [134] Decai Yu and Feng Liu. Synthesis of Carbon Nanotubes by Rolling Up Patterned Graphene Nanoribbons Using Selective Atomic Adsorption. *Nano letters*, 7(10):3046--50, October 2007.
- [135] R.M. Hornreich, Marshall Luban, and S. Shtrikman. Critical Behavior at the Onset of \vec{k} -Space Instability on the λ Line. *Physical Review Letters*, 35(25):1678--1681, December 1975.
- [136] Malte Henkel. Phenomenology of Local Scale Invariance: from Conformal Invariance to Dynamical Scaling. *Nuclear Physics B*, 641(3):405--486, October 2002.
- [137] Jean Alexandre. Lifshitz-Type Quantum Field Theories in Particle Physics. *International Journal of Modern Physics A*, 26(26):4523--4541, October 2011.
- [138] Hans Werner Diehl. Critical Behavior at M-Axial Lifshitz Points. *Acta Physica Slovaca*, 52(4):271--283, May 2002.
- [139] Yu Nakayama. Anisotropic scale invariant cosmology. *General Relativity and Gravitation*, 43(1):235--244, September 2010.
- [140] R.M. Hornreich. Renormalization Group Analysis of Critical Modes at the Ferromagnetic Lifshitz Point in Crystalline Systems. *Physical Review B*, 19(11):5914 -- 5920, 1979.
- [141] R.M. Hornreich. The Lifshitz Point : Phase Diagrams and Critical Behavior. *Journal of Magnetism and Magnetic Materials*, 15-18:387--392, 1980.
- [142] W. Selke. Spatially Modulated Structures in Systems with Competing Interactions. In Cyril Domb and J. L. Lebowitz, editors, *Phase Transitions and Critical Phenomena Vol. 15*. Academic Press, 1992.
- [143] M. Škarabot, R. Blinc, I. Musčević, A. Rastegar, and Th. Rasing. Lifshitz Point in the Phase Diagram of a Ferroelectric Liquid Crystal in an External Magnetic Field. *Physical Review E*, 61(4):3961--3968, April 2000.

- [144] Frank Bates, Wayne Maurer, Timothy Lodge, Mark Schulz, Mark Matsen, Kristoffer Almdal, and Kell Mortensen. Isotropic Lifshitz Behavior in Block Copolymer-Homopolymer Blends. *Physical Review Letters*, 75(24):4429--4432, December 1995.
- [145] Dietmar Schwahn, Kell Mortensen, Henrich Frielinghaus, and Kristoffer Almdal. Crossover from 3D Ising to Isotropic Lifshitz Critical Behavior in a Mixture of a Homopolymer Blend and Diblock Copolymer. *Physical Review Letters*, 82(25):5056--5059, June 1999.
- [146] R M Yevych, Yu M Vysochanskii, M M Khoma, and S I Perechinskii. Lattice Instability at Phase Transitions Near the Lifshitz Point in Proper Monoclinic Ferroelectrics. *Journal of physics. Condensed matter : an Institute of Physics journal*, 18(16):4047--64, April 2006.
- [147] Elihu Abrahams and I.E. Dzyaloshinskii. A Possible lifshitz Point for TTF-TCNQ. *Solid State Communications*, 23(12):883--885, September 1977.
- [148] J. Lajzerowicz and J.J. Niez. Phase Transition in a Domain Wall. *Journal de Physique Lettres France*, 40(7):165, 1979.
- [149] Malte Henkel and Michel Pleimling. *Non-Equilibrium Phase Transitions, Vol. 2: Ageing and Dynamical Scaling Far from Equilibrium*. Springer, Heidelberg, 2010.
- [150] C. Becerra, Y. Shapira, N. Oliveira, and T. Chang. Lifshitz Point in MnP. *Physical Review Letters*, 44(25):1692--1695, June 1980.
- [151] Y. Shapira, N. Oliveira, C. Becerra, and S. Foner. Phase Transitions of MnP for a Field Parallel to the Hard-Magnetization Direction: A Possible New Lifshitz Point. *Physical Review B*, 29(1):361--373, January 1984.
- [152] V. Bindilatti, C. Becerra, and N. Oliveira. Specific-Heat Exponent and Critical-Amplitude Ratio at the Lifshitz Multicritical Point. *Physical Review B*, 40(13):9412--9415, November 1989.
- [153] A. Zięba, C. Becerra, H. Fjellvåg, N. Oliveira, and A. Kjekshus. Mn_{0.9}Co_{0.1}P in an External Field: Lifshitz Point and Irreversibility Behavior of Disordered Incommensurate Phases. *Physical Review B*, 46(6):3380--3390, August 1992.
- [154] C. Becerra, H. Brumatto, and N. Oliveira. Line of Multicritical Lifshitz Points in the Phase Diagram of MnP. *Physical Review B*, 54(22):15997--16002, December 1996.

- [155] C. Becerra, V. Bindilatti, and N. Oliveira. Evidence for the Ising-Lifshitz Crossover in MnP. *Physical Review B*, 62(13):8965--8968, October 2000.
- [156] Michel Pleimling and Malte Henkel. Anisotropic Scaling and Generalized Conformal Invariance at Lifshitz Points. *Physical Review Letters*, 87(125702), August 2001.
- [157] S. Rutkevich, Hans Werner Diehl, and Mykola A. Shpot. On Conjectured Local Generalizations of Anisotropic Scale Invariance and their Implications. *Nuclear Physics B*, 843(1):255--301, February 2011.
- [158] David Mukamel. Critical Behaviour Associated with Helical Order Near a Lifshitz Point. *Journal of Physics A: Mathematical and General*, 10(12):L249, 1977.
- [159] R.M. Hornreich and A.D. Bruce. Behaviour of the critical wavevector near a Lifshitz point. *Journal of Physics A: Mathematical and General*, 11(3):595--601, March 1978.
- [160] J. Sak and G.S. Grest. Critical exponents for the Lifshitz point: epsilon-expansion. *Physical Review B*, 17(9):3602--3606, May 1978.
- [161] Mykola A. Shpot and Hans Werner Diehl. Two-Loop Renormalization-Group Analysis of Critical Behavior at m-Axial Lifshitz Points. *Nuclear Physics B*, 612(3):340--372, October 2001.
- [162] C. Mergulhaõ and C. Carneiro. Field-Theoretic Approach to the Lifshitz Point. *Physical Review B*, 58(10):6047--6056, September 1998.
- [163] C. Mergulhaõ and C. Carneiro. Field-Theoretic Calculation of Critical Exponents for the Lifshitz Point. *Physical Review B*, 59(21):13954--13964, June 1999.
- [164] H.W. Diehl and M.A. Shpot. Critical behavior at m-axial Lifshitz points: Field-theory analysis and ϵ -expansion results. *Physical Review B*, 62(18):12338--12349, November 2000.
- [165] Mykola A. Shpot, Hans Werner Diehl, and Yu M. Pis'mak. Compatibility of $1/n$ and epsilon Expansions for Critical Exponents at m -Axial Lifshitz Points. *Journal of Physics A: Mathematical and Theoretical*, 41(13):135003, April 2008.
- [166] Mykola A. Shpot, Yu M. Pis'mak, and Hans Werner Diehl. Large-n Expansion for m-Axial Lifshitz Points. *Journal of Physics: Condensed Matter*, 17(20):S1947--S1972, May 2005.

- [167] Mykola A. Shpot and Yu M. Pis'mak. Lifshitz-Point Correlation Length Exponents from the Large- n Expansion. *Nuclear Physics B*, 862(1):75--106, September 2012.
- [168] G.S. Grest and J. Sak. Low-temperature renormalization group for the Lifshitz point. *Physical Review B*, 17(9):3607--3610, May 1978.
- [169] Marc Mezard, Giorgio Parisi, and Miguel Angel Virasoro. *Spin Glass Theory And Beyond: An Introduction To The Replica Method And Its Applications*. World Scientific Publishing Co Pte Ltd, 1987.
- [170] John Cardy. *Scaling and Renormalization in Statistical Physics*. Cambridge University Press, Cambridge, 1996.
- [171] David C. Morse and Tom C. Lubensky. Curvature disorder in tethered membranes: A new flat phase at $T=0$. *Physical Review A*, 46(4):1751--1768, August 1992.
- [172] David R. Nelson and Leo Radzihovsky. Polymerized Membranes with Quenched Random Internal Disorder. *Europhysics Letters (EPL)*, 16(1):79--84, September 1991.
- [173] Tim R. Morris. The Exact Renormalisation Group and Approximate Solutions. *International Journal of Modern Physics A*, 9(14):2411--2449, August 1994.
- [174] David C. Morse, Tom C. Lubensky, and G.S. Grest. Quenched disorder in tethered membranes. *Physical Review A*, 45(4):R2151--R2154, February 1992.
- [175] Matthieu Tissier, Dominique Mouhanna, Julien Vidal, and Bertrand Delamotte. Randomly Dilute Ising Model: A Nonperturbative Approach. *Physical Review B*, 65(14), March 2002.
- [176] Matthieu Tissier and Gilles Tarjus. Nonperturbative functional renormalization group for random field models and related disordered systems. II. Results for the random field $O(N)$ model. *Physical Review B*, 78(2):024204, July 2008.
- [177] Matthieu Tissier and Gilles Tarjus. Nonperturbative functional renormalization group for random field models and related disordered systems. III. Superfield formalism and ground-state dominance. *Physical Review B*, 85(10):104202, March 2012.
- [178] Matthieu Tissier and Gilles Tarjus. Nonperturbative functional renormalization group for random field models and related disordered systems. IV. Supersymmetry and its spontaneous breaking. *Physical Review B*, 85(10):104203, March 2012.

